Universidad del País Vasco Euskal Herriko Unibertsitatea

NAZIOARTEKO BIKAINTASUN CAMPUSA
CAMPUS DE EXCELENCIA INTERNACIONAL

Brachypodium distachyon as a model for defining the basis of adaptation to ammonium nutrition in grasses

DOCTORAL THESIS

MARLON DE LA PEÑA CUAO

Department of Plant Biology and Ecology

University of the Basque Country (UPV/EHU)

2019

I would like to thank the Plant Physiology laboratory from the Department of Plant Biology and Ecology of the University of Basque Country (UPV/EHU), especially my Thesis supervisors, Dra. Maria Begoña Gonzalez Moro and Dr. Daniel Marino Bilbao for allowing me to complete my Thesis.

I would also like to thank:

Dr. Yves Gibon, leader of the metabolism group at the Fruit Biology and Pathology unit (UMR1332, INRA-Nouvelle-Aquitaine-Bordeaux, Bordeaux University) for the opportunity to enjoy six- months stay research with his team group and his implication and dedication in the analysis of the metabolic profile of 52 accessions of *B. distachyon*.

Dr. Ernesto Igartua, researcher of the Consejo Superior de Investigaciones Científicas (CSIC), Estación Experimental Aula Dei, for his implication in the genome wide association analysis.

Dr. Bruno Contreras, leader of Ensembl Plants Project of European Bioinformatics Institute (EMBL-EBI) for the bioinformatics support in the genome-wide association analysis.

Dra. Pilar Catalan, from Higher Polytechnic School of Huesca at Zaragoza's University for her support and implication in the study of natural variability in *B: distachyon.*

Dr Pedro Aparicio Tejo and **Gustavo Garijo** from the Public University of Navarra, for their support in the analisys of individual amino acids.

Dra. Ana Maria Alvarez, researcher of the CSIC, Estación Experimental Aula Dei, for her technical support in phytosiderophores measurement and interpretation

Dra. Azucena Gonzalez, **Dr. Kerman Aloria** and **Dr. Juan Carlos Raposo** of the Service of the Advanced Research Facilities (SGIKER) for technical and human support.

Dr. Gaétan Glauser from the Neuchâtel Platform of Analytical Chemistry (NPAC) Université de Neuchâtel for his technical support in metabolic measurements.

The author of the doctoral thesis has enjoyed a predoctoral fellowship for the formation of human capital for the Magdalena department granted by COLCIENCIAS (conv. 672) and support for Ph.D. mobility by EPPN2020 (UE H2020 grant agreement No 731013)

This research work has received funding from Basque Government (IT932-16), the Spanish Ministry of Economy and Competitiveness (BIO2017-84035-R co-funded by FEDER) and EPPN2020 (UE H2020 grant agreement No 731013)

Han sido muchas las personas que me han acompañando durante este proceso y me gustaría agradecer.

En primer lugar, quisiera agradecer a mis directores Bego y Dani por la dedicación e implicación en este trabajo. Estoy muy contento con lo aprendido y logrado con vosotros, siempre me brindaron todas las facilidades para realizar este trabajo y la oportunidad de ir a otros centros de investigación especializados a seguir desarrollando la tesis. Bego, aprendí mucho de ti, a siempre a ir con paso firme y entendiendo cada uno de los pasos para no cometer errores y lograr el objetivo. Dani fuiste un hermano mayor para mí, gracias por procupate por mi bienestar y futuro. Muchas gracias a los dos.

Gracias a todos los integrantes del grupo NUMAPs, especialmente a la líder del grupo Carmen que nos ha mantenido como un grupo fuerte. Izargi, gracias por varias veces acompañarme en las cosechas, ayudarme en el laboratorio y trasmitir tu alegría. Miren, fuiste una fiel compañera en el laboratorio, dándome ánimo y acercándome a casa. Inma, fuiste una de las primeras mentoras en el laboratorio, aprendí bastente. Asier y Fernando, me sacaron de varios apuros en el laboratorio y fuera de este, gracias por todos esos momentos. Theo, gracias por tu ayuda en las cosechas y durante la estancia en Burdeos. Adrián, Mario y Agustin, una lástima que solo haya compartido con vosotros mi último año de tesis, pero lo poco compartido ha sido muy agradable. Iraide, de ti aprendí que a pesar de los problemas hay que seguir para adelante. Ximena, mi tocaya colombiana recordándome siempre la tierra. Txema y Teresa, siempre dispuestos en ayudarme en lo que necesitara. Gracias a los exalumnos de TFGs, especialmente a Noemi y Nahia dos grandes amigas con las que he compartido momentos duros de trabajo y me han ayudado en parte importante en el desarrollo de esta tesis, muchas gracias chicas.

Al resto del laboratorio quisiera también agradecer, especialmente a mi mejor amigo Ander con el cual compartí muchos momentos dentro y fuera del laboratorio, gracias por haberme recibido en tu casa como un hermano, gratos momentos pase contigo, Nerea y los de tenis. Marina y Rafa, animo amigos con esa tesis que son los siguientes. A Jon, Unai, Maite, Aitor, Irati, gracias por esos momentos agradables.

Finalmente, pero no menos importante, quiero agradecer a Esther, Iker y Verónica en Pamplona, por ayudarme no solo a conseguir la beca pre-doctoral si no porque la experiencia en la UPNA hizo que quisiera continuar con el doctorado

CONTENT

ABREVIATIONS

A: Accession

AAT: Aspartate aminotransferase

ACD6: Accelerated Cell Death 6

AIC: Akaike's information criterion

AMP: Adenosine monophosphate

AMT: Ammonium transporters

ARD: Acireductone dioxygenase or 2-keto-methylthiobutyric-acid-forming enzyme

AS: Asparagine synthetase

Asn: Asparagine

Asp: Aspartate

BR: Brassinosteroid

C: Control condition Fe

CCoAOMT1: Caffeoyl CoA 3-O-methyltransferase 1

Chl: Clorophyll

CS: Citrate synthase

CSm: Mitochondrial citrate synthase

D: Deficiency Fe

DAP: Differentially abundant proteins

DEP: Methylthioribulose-1-phosphate dehydratase-enolase-phosphatase

DW: Dry weight

FarmCPU: Fixed and random model circulating probability unification model

FDR: False discovery rate

FK: Fructokinase

FW: Fresh weight

GABA: γ-Aminobutyric acid

GAX: Glucuronoarabinoxylans

GDH: Glutamate dehydrogenase

GK: Glucokinase

GLM: General-linear model

Gln: Glutamine

Glu: Glutamate

GOGAT: Glutamate synthase

GS: Glutamine synthetase

GSH: Glutation

GS1: Cytosolic glutamine synthetase

GS2: Chloroplastic glutamine synthetase

GST: Glutathione-S-transferases

GWAS: Genome Wide Association Studies

HRS1: Hypersensitive to low Pi-elicited primary root shortening

ICDH: Isocitrate dehydrogenase

IMP: Inosine monophospahte

IRT: Iron-regulated transporter

L: Leaves

MAs: Mugineic acid compounds

MA: Mugineic acid

MD: Moderate deficiency Fe

MDH: Malate dehydrogenase

ME: Malic enzyme

Met: Methionine

MLM: Mixed-linear models

MLMM: Multi loci linear mixedmodel

MTA: 5-methylthioadenosine

MTI: 5 methylthioribose-1-phosphate isomerase

MTK: 5-methylthioribose kinase

MTN: MTA nucleosidase

MTR: 5-methylthioribose

MTR-P: 5-methylthioribose-1-phosphate

MTRu-P: 5-methylthioribulose-phosphate

NA: Nicotianamine

NAD-ME: NAD-dependent malic enzyme

NADP-GDH: NADP-dependent glutamate dehydrogenase

NADP-ME: NADP-dependent malic enzyme

NADP- ICDH: NADP-dependent isocitrate dehydrogenase

NAS: Nicotianamine synthase

NUE: Nitrogen use efficiency

OAA: Oxaloacetate

OD: absorbance

2-OG: 2-Oxoglutarate

PCA: Principal component analysis

PEPC: Phosphoenolpyruvate carboxylase

PEP: Phosphoenolpyruvate

3-PGA: 3-Phosphoglyceric acid

PHO1: Phosphate 1

PHT: Putrescine hydroxycinnamoyl transferase

PK: Pyruvate kinase

PME: Pectin methylesterase

PS: Phytosiderophores

PSI: Photosystem I

PSII: Photosystem II

Pyr: Pyruvate

Q-Q: Quantile-quantile

QTL: Quantitative trait loci

R: Root

ROS: Reactive oxygen species

RSA1: Root System Architecture 1

SAM: S-adenosylmethionine

SAMS: S-adenosyl-Met synthetase

SNP: Single nucleotide polymorphism

Strategy I: Reduction-based strategy

Strategy II: Chelation-based strategy

T: Toxicity Fe

TCA: Tricarboxylic acid

TOM1: Transporter of mugineic acid family phytosiderophores 1

XTHs: Xyloglucan endotransglucosylase/hydrolases

YS/YSL: Yellow Stripe/Yellow Stripe-Like transporters

ABSTRACT

Nitrogen nutrition in agriculture

Nitrogen (N) is an essential nutrient for plants since is a component of DNA, amino acids, proteins and secondary metabolites. Its availability is decisive for plant growth and productivity. Agricultural soils are often N deficient and maintain crops yield farmers need to apply great amounts of N fertilizers. However, the use of fertilizers entails N losses that provoke detrimental effects for the environment, including the contamination of water resources because of nitrate (NO_3^-) leaching and the emission of nitrogenous gases, such as N_2O, with great impact for global warming. Using of ammonium (NH_4^+)-based fertilizers combined with nitrification inhibitors delays the conversion of ammonium to nitrate, thus maintaining NH_4^+ inputs in the soil for longer periods. This type of enhanced-efficiency fertilizers show promise in mitigating the environmental pollution associated with nitric fertilization from agrosystems. Unfortunately, when NH_4^+ is present in the soil at high concentrations, or as sole source of N, plants may display stress symptoms that commonly imply suppressed growth. The causes of ammonium stress in the plant are still not fully understood but are related to pH deregulation, cation imbalance and to the excessive energetic cost associated with maintaining cytosolic NH_3/NH_4^+ homeostasis. Therefore, understanding the mechanisms underlying ammonium tolerance is of special interest for a proper selection/generation of genotypes adapted to this fertilization management.

Brachypodium distachyon*: a genetic model system to study grasses biology*

Model organisms are vital resources for research, providing a number of advantages respect to non-model organisms. Over the last decade, *Brachypodium distachyon* has gained attention as model plant for C3 grasses. *B. distachyon* is a small grass with short-life cycle, a highly homozygous and small diploid genome and ease to be cultured in growth chambers. Being a model species, a number of tools are available for its study including an increasing number of sequenced accessions, collection of mutants, etc.

The family of grasses (Poaceae) encompasses the world's most important staple, feed, and bioenergy crops. Phylogenetically, *B. distachyon* lies between rice and wheat and possesses high degree of synteny with most grasses. The fact that *B. distachyon* is a non-domesticated make itself of special relevance in the case of ammonium nutrition, since the high nitrification rates common in agricultural soils jointly the huge nitric fertilizer inputs have favoured varieties selection has been nearly exclusively performed in the scenario of nitric nutrition. Besides,

although there is variation in N use efficiency traits among modern cereal varieties, it is clear that a much greater potential of variation exist among the ancient/historical varieties and wild species that may allow identifying alleles that have been lost in the modern germplasm pool. Indeed, probably related to the fact that *B. distachyon* is a wild plant, its pangenome contains nearly twice the number of genes found in an individual genome.

In this context, the general objective of this PhD Thesis was to better decipher the plant response upon ammonium nutrition focusing on the metabolic and molecular basis that may lead to improve ammonium tolerance in cereals, using *Brachypodium distachyon* as a model.

Metabolic and molecular response to ammonia nutrition confirms the role of the root in ammonia tolerance

To first evaluate the suitability of *Brachypodium distachyon* as model plant for the study of ammonium nutrition, plants of Bd21, the reference genotype/accession of *B. distachyon*, were grown hydroponically in 1 or 2.5 mM NO_3^- or NH_4^+. We determined plant performance and the interaction between nitrogen and carbon metabolisms associated with primary NH_4^+ assimilation in root and leaves. Regarding whole-plant performance, the concentration of 1 mM of N represented a condition of ammonium-tolerance for Bd21 since plants grew equally regardless the N-source. In contrast, with 2.5 mM NH_4^+ supply the plants showed lower biomass and symptoms of stress. Overall, *B. distachyon* appeared as a species with moderate tolerance towards ammonium nutrition.

In general, a strong metabolic adaptation of carbon and nitrogen metabolisms was observed when *B. distachyon* faced ammonium nutrition. Notably, the roots behaved as a physiological barrier preventing the translocation of NH_4^+ to aerial parts, as indicated by a sizeable accumulation of NH_4^+, Asn and Gln in the roots. The tuning of the tricarboxylic acid (TCA) cycle and its associated anaplerotic pathways in root cells enabled to match 2-oxoglutarate and oxaloacetate demand for the continuing high NH_4^+ assimilation rate into Gln and Asn synthesis. This metabolic adjustment appears to be a mitigating strategy of ammonium stress as long as imposes an energetic cost for the cell that limits plant growth under toxic ammonium conditions (2.5 mM NH_4^+). These results are completely in line with the response previously reported for cereal crops such as wheat, barley or sorghum. Thus, *B. distachyon* reveals as a highly suitable tool for the study of the physiological, molecular and genetic basis of ammonium nutrition in cereals.

To exploit the benefits of working with *B. distachyon* to gain insight on grasses adaptation to ammonium nutrition, we focused on evaluating the potential intraspecific variability of *B.*

distachyon towards ammonium tolerance. For aim, a large panel of 52 *de novo* sequenced *B. distachyon* natural accessions, already shown as genetically diverse, was selected to be cultured with 2.5 mM NH_4^+ or NO_3^- supply. The ratio between the total plant biomass under NH_4^+ *vs*. NO_3^- conditions was considered to estimate the degree of ammonium tolerance. We observed an extensive natural variability of *B. distachyon* towards ammonium nutrition, with tolerant accessions that grew similarly with NO_3^- or NH_4^+ supply and with accessions that showed high sensitivity experiencing more than 50% of grown reduction under ammonium. In addition, to evaluate whether *B. distachyon* intraspecific variability was related to the metabolic adaptation of leaves and root in function of the N source provided, we analyzed a panel of 22 metabolic markers, including 9 enzyme activities and the content of 13 metabolites in both organs. The overall results highlighted, as it was the case for Bd21, the importance of primary carbon metabolism to sustain NH_4^+ assimilation in the root. We report besides TCA cycle, that the adjustment of the glycolytic pathway, as evidenced by sugars content, fructokinase, glucokinase and pyruvate kinase activities was also of great importance for plant response to ammonium nutrition.

To further explore the biochemical data obtained and to define the relationships between variables we performed different statistical analysis: principal component analysis (PCA), Pearson correlations visualized by clustered matrices, heat map plots that included two-way hierarchical clustering and multiple regression models. Importantly Under ammonium nutrition, genotypes clustering under ammonium nutrition split the 52 accession in two groups, showing that the most tolerant and sensitive accessions segregated in different groups. In contrast, under nitrate nutrition the distribution of tolerant and sensitive accessions was disperse. This observation indicates the importance of the metabolic adaptation under ammonium nutrition in relation with *B. distachyon* natural variability towards ammonium stress.

Finally, data exploration together with stepwise multiple-regression allowed to extract the activity of PEPC and NH_4^+ content in ammonium-fed leaves together with the sucrose content in the root of ammonium-fed plants as key variables to explain *B. distachyon* tolerance to ammonium stress. Besides, glutathione content also appeared closely related to *B. distachyon* performance under ammonium source, suggesting a protective role for this metabolite under ammonium stress.

***A quantitative proteomic study in the root reveals the interaction between ammonium nutrition and iron homeostasis in* B. distachyon**

To deep into the molecular changes occurring in the root, a comparative proteomic approach was carried in plants grown under ammonium or nitrate nutrition with 2.5 mM or 1 mM N supply. Among others, the gene ontology analysis performed with the identified differentially expressed proteins confirmed the adaptation of primary carbon and nitrogen metabolisms, but also identified other processes that potentially participates in the root response to ammonium nutrition, such as cell wall biogenesis and cell redox balance.

Interestingly, a great number of proteins associated with iron homeostasis were more predominant in ammonium compared to nitrate nutrition, notably those participating in methionine cycle and phytosiderophores synthesis. Indeed, the accumulation of phytosiderophores in relation with a concomitant increase in Fe and Zn was confirmed in ammonium-fed roots

Besides, when the impact of the N-source in plant response to changes in Fe availability in the nutrient solution was analyzed, it was evidenced a higher sensitivity of ammonium-fed plants to limited Fe availability respect to nitrate-fed plants. One can hypothesize that this behavior could be related with the huge amounts of NH_4^+ accumulated in the tissues and with impaired Fe translocation to the aerial part. These results in *Brachypodium* differ with a number of previous reports showing a beneficial effect of ammonium under Fe deficiency in both dicots and monocots. The discrepant behavior observed in the literature could be to the fact that in some of these studies NH_4^+ was applied in the presence of NO_3^- or that the plants were not subjected to ammonium stress. On the other hand, the high levels of Zn observed in ammonium-fed plants suffering from Fe-deficiency condition could be also responsible for the higher sensitivity observed in *B. distachyon* Bd21. Future research is indispensable to further understand the mechanistic underlying the interaction between the N-source and the Fe and Zn.

Genome wide association mapping reveals significant genetic association potentially related with the natural adaptation of* B. distachyon *towards ammonium nutrition

Genome-wide association studies (GWAS) are a great means to decipher the genetics underlying of naturally occurring phenotypic variation in populations, in this case with the aim of identifying candidate genes associated to *B. distachyon* natural variation towards ammonium nutrition. Indeed, the combination of GWAS and metabolic analysis has also emerged as an alternative to study the genetic and biochemical bases of plant metabolism with impact in agronomical traits.

Among others, because of the reduced number of genotypes used, we performed GWAS with the data obtained for *B. distachyon* natural accessions using the multiple loci linear mixed model (MLMM) that controls false positives at the same time without compromising true positives. The multi-locus approach ensures that trait variance is associated with the most significant markers, whereas closely similar markers anywhere in the genome will not be selected by this model.

Firstly, we performed GWAs with plant growth parameters, as they are considered the most important and integrative traits indicative of plant performance. No strongly significant marker were found for these traits. In general, the effect of genetic associations with complex, highly polygenic traits are often small and in many cases missing, such as for physical measurements like biomass. However, the use of alternative traits, such as metabolites and enzyme activities that themselves may explain the biomass may be particularly important for studying the GWAS and thus, it may be useful to find loci that ultimately contribute to explain the trait of interest. In this sense, when performing GWAS out of every determined metabolic trait it was found a number of genomic regions where causal genes related to *B. distachyon* ammonium tolerance may be located. Notably, we focused on the most explanatory variables underlined by the multiple regression models, PEPC activity and NH_4^+ content in the leaf and sucrose content in the root of plants grown under ammonium nutrition.

Looking into genomic regions surrounding the significantly associated SNPs (20 kb up- and down-stream each SNP), several genes located in those regions were found. Among them, a number of genes have been previously associated in the literature with carbon and nitrogen metabolism. For instance, associated with the content of sucrose in the root two genes encoding for cysteine synthases were disclosed. Associated to the activity of PEPC in the leaf genes encoding for glutamate carboxypeptidase and for NADP-malic enzyme were found. Finally, a potential association with a gene encoding a probable adenosine monophosphate deaminase was found for leaf NH_4^+ accumulation. Future research will be essential to further identify and validate the causal genes involved in ammonium nutrition.

Concluding remarks

B. distachyon is an emerging genetic model system for C3 grasses. Here, we report that *B. distachyon* responds to ammonium nutrition similarly to important cereal crops and thus it reveals as an excellent model to study the molecular and genetic basis of ammonium tolerance in grasses. Furthermore, we report the key role of the root in plant adaptation to ammonium nutrition, notably revealing an outstanding interaction between NH_4^+ and Fe homeostasis. Finally, the metabolic adaptation to ammonium nutrition appears as a key aspect to understand

B*. distachyon* natural variability towards ammonium stress and an important means to find novel genes associated to the observed variability.

.

RESUMEN

La nutrición nitrogenada en la agricultura

El nitrógeno (N) es un elemento esencial para las plantas ya que es parte estructural de moléculas importantes como el ADN, aminoácidos, proteínas y metabolitos secundarios. No obstante, en la mayoría de los suelos agrícolas el nitrógeno no se encuentra disponible para las plantas, por lo que los agricultores se ven en la necesidad de aplicar grandes cantidades de fertilización nitrogenada. Sin embargo, gran parte de este nitrógeno aplicado se pierde al ambiente, produciendo daños ambientales tales como la contaminación de recursos hídricos debido a la lixiviación de nitratos y la emisión de gases de efecto invernadero, como el N_2O, que incrementan el calentamiento global. Los fertilizantes de base amoniacal (NH_4^+) en combinación con inhibidores de la nitrificación han surgido como estrategia para mantener el nitrógeno en forma de amonio durante mayor tiempo en el suelo, destacando su eficacia para mitigar la contaminación ambiental asociada a las fuentes nítricas. No obstante, cuando el amonio se encuentra en el suelo a altas concentraciones, o como fuente única, las plantas normalmente desarrollan síntomas de estrés que consecuentemente llevarían a una reducción de la produccion. Las causas del estrés, amoniacal aún no están esclarecidas, pero están relacionadas con la desregulación del pH, al desbalance catiónico y el excesivo costo energético asociado con el mantener la citosolica homeostasis del NH_3/NH_4^+. Por lo tanto, entender los mecanismos que regulan la tolerancia al amonio es de especial interés para la selección y generación de genotipos adaptados a este tipo de fertilización.

Brachypodium distachyon: un sistema de modelo genético para el estudio de la biología en gramíneas

Los organismos modelo son una fuente vital de investigación y proveen una gran cantidad de ventajas en comparación con los organismos no modelo. En la última década, *Brachypodium distachyon* ha generado interés como planta modelo de las gramíneas C3. Esta es una planta herbacea con ciclo corto, altamente homocigota, con genoma diploide pequeño y fácil de crecer en condiciones controladas en el laboratorio. Al igual que un gran número de especies modelos existe una gran cantidad de herramientas disponibles para la investigación, de las cuales se destaca un creciente número de accesiones secuenciadas, colección de mutantes, etc.

La familia de las gramíneas (Poaceae) comprende los cultivos más importantes para la alimentación mundial, producción de forraje y biodiesel. Filogenéticamente, *B. distachyon* se

encuentra relacionada estrechamente al arroz y el trigo y posee un alto grado de sintenia con la mayoría de las gramíneas. *B. distachyon* es una especie no domesticada, lo cual es de especial relevancia para el estudio de la nutrición amoniacal ya que las altas tasas de nitrificación en los suelos agrícolas han provocado la selección de cultivares adaptados al nitrato. Además, aunque existe una variabilidad fenotípica en uso eficiente del nitrógeno entre las variedades modernas de cereales, es de destacar que existe un gran potencial de las variedades ancestrales y especies silvestres para identificar alelos que se han perdido en los bancos de germoplasma de los cultivos actuales. De hecho, probablemente debido a que *B. distachyon* es una planta silvestre, su pangenoma contiene aproximadamente dos veces el número de genes encontrado en un genotipo.

En este contexto, el objetivo general de este estudio es mejorar el entendimiento de la respuesta de las plantas sobre la nutrición amoniacal, colocando especial atención a los aspectos metabólicos y moleculares que regulan la tolerancia a la nutrición amoniacal en cereales y usando a *B. distachyon* como planta modelo.

La respuesta metabólica y molecular a la nutrición amoniacal confirma la importancia de la raíz en la tolerancia al amonio.

En primer lugar, para evaluar la idoneidad de *B. distachyon* como modelo de estudio en la nutrición amoniacal, plantas de la accesión Bd21, considerada como el genoma de referencia, se cultivarón hidropónicamente a 1 o 2.5 mM de NO_3^- o NH_4^+, con lo cual se determinó su comportamiento y el metabolismo del carbono y nitrógeno asociados a la asimilación del amonio en hoja y raíz. En función del comportamiento general de las plantas de Bd21, la concentración de 1 mM de N representó una condición de tolerancia al amonio, ya que no se observaron diferencias en el crecimiento en comparación con la nutrición nítrica. En general, las plantas crecidas a 2.5 mM de NH_4^+ redujeron su crecimiento a la vez que mostraron síntomas de estrés amoniacal. Teniendo en cuenta lo anterior, *B. distachyon* se mostra como una especie con tolerancia moderada a la nutrición amoniacal.

En este sentido, se observó una fuerte adaptación metabólica de *B. distachyon* en el metabolismo del carbono y el nitrógeno durante la nutrición amoniacal. En particular, la raíz se comporta como una barrera fisiológica para prevenir la translocación de NH_4^+ hacia la parte aérea, como lo indica los altos contenido de NH_4^+acumulado en este órgano, asi como los niveles de Asn y Gln. El ajuste en el funcionamiento del ciclo de los acidos tricarboxilicos (CAT) y las rutas anapleroticas asociadas permite el aporte continuado de 2 oxoglutarato y oxalacetato y asi mantener la asimilación del amonio en Glu y Asn.

Este ajuste metabólico sería probablemente una estrategia para mitigar el estrés amoniacal, a la vez que impone un coste energético para la célula, lo que limitaría el crecimiento de la planta en condiciones de toxicidad. Esto estaría de acuerdo con lo descrito para otras especies de cereales, como trigo, cebada y sorgo. De esta forma, *B. distachyon* mostraría ser una herramienta idónea para el estudio de los mecanismos fisiológicos, moleculares y genéticos de la nutrición amoniacal en cereales.

Aprovechando los beneficios de trabajar con *B. distachyon* para adquirir información detallada de la adaptación a la nutrición amoniacal, este trabajo se ha centrado en evaluar el potencial de la variabilidad intra-espescifica de *B. distachyon*. Para ello, se creció un panel de 52 accesiones naturales de *B. distachyon* secuenciadas *de novo* y descritas como genéticamente diversas, con 2.5 mM de NH_4^+ o NO_3^- como fuente de nitrógeno. El ratio de la biomasa entre las plantas crecidas con NH_4^+ y NO_3^- (NH_4^+:NO_3^-) se usó como marcador de tolerancia. Los resultados mostraron una extensiva variabilidad natural de *B. distachyon* a la nutrición amoniacal, con accesiones que crecieron de forma similar comparando plantas crecidas con NH_4^+ y NO_3^- y con accesiones que mostraron una alta sensibilidad, reduciendo en más de un 50 % su crecimiento. Además, para evaluar si la variabilidad intra-especifica de *B. distachyon* estaba relacionada con la adaptación metabólica de la hoja y la raíz en función de la fuente de N suministrada, se analizó un panel de 22 marcadores metabólicos incluyendo la actividad de 9 enzimas y el contenido de 13 metabolitos en cada órgano. Los resultados resaltan, como fue el caso para la Bd21, la importancia del metabolismo del carbono en mantener la asimilación de amonio en la raíz. Se observó que además del CAT, el ajuste de la ruta glucolítica, como lo evidencia los contenidos de azúcar, las actividades fructoquinasa, glucoquinasa y piruvato kinasa serían de gran importancia en la respuesta a la nutrición amoniacal.

Con el objetivo de realizar una mayor exploración de los datos obtenidos y entender la relación entre las variables medidas, se llevarón a cabo diferentes análisis estadísticos: análisis de componentes principales (ACP), correlación de Pearson visualizado a través de matrices de asociación, Heat Maps (mapas de colores) que incluyeron 2 jerárquicas agrupaciones y modelos de regresión múltiple. Importantemente, en condiciones de nutrición amoniacal, la agrupación de los genotipos diferenció las 52 accesiones en dos grupos, mostrando que las más tolerantes y sensibles accesiones estaban separadas en ambos grupos. Esta observación indica la importancia de la adaptación metabólica en condiciones de nutrición amoniacal en relación con la variabilidad natural de *B. distachyon* al estrés amoniacal.

Finalmente, el análisis exploratorio de los datos junto con el análisis de regresión lineal por pasos, revelaron la actividad de la PEPC y el contenido de amonio en la hoja, junto con el contenido de sacarosa en la raíz de las plantas crecidas con amonio como las principales variables para explicar la tolerancia de *B. distachyon* al estrés amoniacal. Además, el contenido de glutatión también apareció estrechamente relacionado con el comportamiento de *B. distachyon* en función de la fuente de nitrógeno.

***Estudio de proteomica cuantitativa en la raíz revela la interacción entre la nutrición amoniacal y la homeostasis del hierro en* B. distachyon.**

Profundizando en los cambios moleculares que ocurren en este órgano se realizó un enfoque comparativo de la proteómica en plantas crecidas con nutrición amoniacal o nítrica con 2.5 mM o 1 mM de N. El análisis ontológico de los genes realizó con las proteínas diferencialmente expresadas y sé confirmo el ajuste del metabolismo del carbono y nitrógeno, pero identifico también otros procesos que potencialmente participarían en la respuesta de la raíz a la nutrición amoniacal, tales como la biogénesis de la pared celular y el balance redox en la célula.

Interesantemente, un gran número de proteínas asociadas a la homeostasis del hierro predominaron en nutrición amoniacal en comparación con la nítrica, particularmente aquellas proteínas que participan en el ciclo de la metionina y la síntesis de fitosidoforos. De hecho, se confirmó que la nutrición amoniacal induce la acumulación de fitosidoforos en relación con el incremento concomitante en la acumulación de Fe y Zn en las raíces.

Posteriormente, se analizó el impacto de la fuente nitrogenada en respuesta a la disponibilidad de hierro en la solución nutritiva de las plantas y se evidenció una mayor sensibilidad de las plantas crecidas con nutrición amoniacal a limitada disponibilidad de hierro en comparación con nutrición nítrica. Se plantea la hipótesis de que este comportamiento podría estar asociado a la alticima acumulación de amonio observada en los tejidos y a la translocación interrumpida de Fe a la parte aérea. Estos resultados difieren con una variedad de resultados previos que muestran un efecto beneficioso del amonio bajo condiciones de deficiencia de hierro en dicotiledóneas y monocotiledóneas. Este comportamiento discrepante observado en la literatura podría ser por el hecho de que en algunos de estos estudios el NH_4^+ se aplicó en presencia de NO_3^- o a que las plantas no estuvieran a condiciones de estrés amoniacal. Por otra parte, los altos niveles de Zn observados en las plantas crecidas con nutrición amoniacal en condiciones de deficiencia de hierro podría ser también responsable de la mayor sensibilidad observada en *B. distachyon* Bd21. Futuras investigaciones son necesarias que conduzcan a

entender los mecanismos que gobierna la interacción entre la fuente de nitrógeno y los micronutrientes Fe y Zn

Los estudio de asociación del genoma completo revela asociaciones genéticas significantes potencialmente relacionadas con la adaptación natural de B. distachyon a la nutrición amoniacal

Los estudio de asociaciones del genoma completo (Genome Wide Association Studies GWAS) son una gran herramienta para descifrar los rasgos genéticos de la variación fenotípica que ocurre naturalmente, en este caso con el objetivo de identificar los genes candidatos a la variabilidad natural de *B. distachyon* a la nutrición amoniacal. De hecho, la combinación del GWAS y el análisis metabólico ha emergido también como una alternativa para estudiar las bases genéticas y bioquímicas vegetaly su impacto en caracteres agronómicos de interes.

Entre otras cosas, debido al número reducido de genotipos usados, se desarrolló el GWAS con los datos obtenidos para las accesiones naturales de *B. distachyon* usando el modelo mixto multilocus (MLMM) el cual controla falsos positivos, al mismo tiempo que no compromete verdaderos positivos. El enfoque multilocus asegura que la variabilidad de las características esté asociada con el marcador más significativo, mientras que marcadores estrechamente similares en cualquier parte del genoma no son seleccionados por el modelo.

En primer lugar, se desarrolló el GWAS con los parámetros de crecimiento de las plantas, los más importantes e integradores relacionados con el comportamiento de la planta, aunque no se encontraron marcadores significativos. En general, el efecto de las asociaciones genéticas con caracteres complejos y altamente poligenicos, tales como lo son las medidas físicas como la biomasa, es frecuentemente pequeño y en muchos casos se pierde. Sin embargo, sería particularmente interesante realizar el GWAS con los caracteres alternativos, tales como los metabolitos y las actividades enzimáticas. Estas características por sí mismas podrían determinar la variabilidad de la biomasa y de esta forma, ser útiles para encontrar loci que finalmente contribuyan a explicar la característica de interés. En este sentido, se desarrolló el GWAS para cada uno de los caracteres metabólicos determinados y se encontró un número de regiones genómicas donde los genes causales relacionados a la tolerancia al amonio de *B. distachyon* Bd21 podrían estar localizados. Particularmente, se centró este estudio en las variables más explicativas resaltadas por el modelo de regresión lineal, que fueron la actividad PEPC y el contenido de NH_4^+ en las hojas y el contenido de sacarosa en la raíz de plantas crecidas con nutrición amoniacal.

Buscando asociaciones significativas dentro de las regiones adyacentes a los SNPs (20 kb de ventana), se encontraron un número de genes, que han sido previamente asociados en la

literatura con el metabolismo del carbono y el nitrógeno. Por ejemplo, en asociaciones con el contenido de sacarosa en la raíz se encontraron dos genes que codifican para la cisteína sintasa. En relación a la actividad PEPC en la hoja se encontraron asociados genes que codifican para la glutamato carboxipeptidasa y la enzima málico-NADP. Finalmente, para la acumulación de amonio en la hoja se encontraron potenciales asociaciones con un gen que codifica para una probable adenosina monofosfato desaminasa. Futuras investigaciones serian esenciales para identificar y validar los genes causales involucrados en la nutrición amoniacal.

Conclusiones

B. distachyon es un modelo genético emergente de las gramíneas C3. En el presente estudio se reporta que *B. distachyon* responde a la nutrición amoniacal de forma similar a otras gramíneas consideradas de gran interés agrícola como trigo y cebada. Por lo tanto, esta especie resulta un excelente modelo para estudiar los mecanismos moleculares y genéticos de la tolerancia al amonio en las gramíneas. Además, se destaca el papel esencial de la raíz en la adaptación de las plantas a la nutrición amoniacal, revelando una interacción importante entre la homeostasis del NH_4^+ y del Fe. Finalmente, la adaptación metabólica de la nutrición amoniacal es un aspecto clave para entender la variabilidad natural de *B. distachyon* al estrés amoniacal y esta adaptación resulta prometedora para encontrar genes nuevos asociados a la variabilidad observada.

GENERAL INTRODUCTION

INTRODUCTION

1. NITROGEN REQUIREMENT BY PLANTS

Nitrogen (N) is an essential nutrient for a living organism since it is a component of several organic compounds, such as proteins, nucleic acids, coenzymes, chlorophyll and pyrrole rings, and secondary metabolites (Miller and Cramer, 2005). In plants it represents around 1-7 % of dry matter, being the nutrient required in the largest quantity, after C, H and O. Nitrogen is one of the elements that most likely limits the plant growth and crop productivity. Even though a huge amount of N is present in the Earth´s atmosphere as inorganic gaseous compound (N_2), it is largely unavailable directly for most plants. Plants take N from soil, which content ranges from 0.1 to 0.6 % in 0-15 cm topsoil (Cameron *et al.*, 2013). Inorganic nitrogen (nitrate and ammonium) are the main N forms taken up by plants, but they do not represent more than 10 % of the total N in the soil, what makes that almost all natural soils, except tropical and subtropical ecosystems, are considered as N-limited. Agricultural soils are commonly N-deficient. Therefore, to maintain crops yield farmer need to supplement soils with external N input, mainly in the form of manures, crop residues and synthetic fertilizers in the form of nitrate, ammonium or urea. For instance, according to estimations up to 26 % production increased in the 6-top non-leguminous crops in the US thanks to the use of fertilizers (Cao *et al*., 2018).

Nitrogen fertilizers are derived from the reaction of atmospheric N_2 with H_2 to produce NH_3, using a feedstock source at elevated pressure and temperature (Miller and Cramer, 2005). Fertilizers contain mineral nitrogen as ammonium and nitrate. Uptake of nitrate is rapid due to the high particle mobility (Miller and Cramer, 2005). On the other hand, due to its positive charge ammonium is bound to clay particles in the soil and roots have to reach it. However, most of the ammonium is rapidly oxidized by nitrifiers in few weeks. (Huérfano *et al*., 2015). The more relative presence of nitrate respect to ammonium is the reason that has made most of plants show a preference for nitrate over ammonium. And this is especially evident for crop plants since they have been selected upon nitrate-based fertilization. However, plants are not too much efficient in the use of N applied and is estimated that 30-50 % of N applied as fertilizer is taken up by plants (Cassman *et al*., 2002).

Among all the different kinds of nitrogen fertilizers, urea is the most used in agriculture (Miller and Cramer, 2005). Hydrolysis of urea by soil microorganism converts urea into ammonium and CO_2 a relatively short period of time, depending on the temperature (Sigurdarson *et al.,* 2018). The soil pH around the urea granules strongly increases during this process, leading to ammonium volatilization and consequently to the loss of N. If ammonium volatilization takes

place at the soil surface, the losses are even higher (Al-Kanani *et al*., 1991). In the case of nitrate fertilization, nitrate ion is very soluble in water and easily leached polluting groundwater, rivers and oceans (Paramasivam and Alva, 1997). These are the main causes of why more than half of the N used in agriculture are lost (Kanter and Searchinger, 2018).

The amount of N fertilizer used in agriculture represents as inputs to the agrosystems as 3-fold the natural sources of nitrogen (Bowles *et al.,* 2018). Therefore, a lot of nitrogen could be lost to the environment creating imbalance in the ecosystems. The amount of loses depends on the soil condition, weather and agriculture practice. For instance, leaching of nitrate occurs mainly during rainfall periods when percolating water washes residual and mineralized nitrates bellow the root zone.

Nitrogen loss from agrosystems is an environmental concern, since it contributes to the contamination of soil, water resources and the emission of greenhouse gases. Furthermore, climate change is aggravating these losees due to the changes in precipitation patterns and temperature increases (Bowles *et al.*, 2018). Nitrogen pollution is very disquieting, since affects terrestrial, aquatic and marine biodiversity (Bowles *et al.,* 2018). For example, an elevated concentration of nitrate in drinking water is related to methemoglobinemia and gastric cancer in humans (Fewtrell, 2004). Nitrogen eutrophication provokes loss of seagrasses, blooms of blue-green algae, degradation of recreational opportunities and hypoxia (Chislock *et al*., 2013). In the USA, the damages caused for eutrophication are estimated in approximately $2.2 billion annually (Dodds *et al*., 2008).

The continuous growing in the World´s population will require huge inputs of N in agriculture to supply the food demand, which is projected to increase 50-100 % by 2050 (Kanter and Searchinger, 2018). Therefore, in order to match the N demand by the plant during the vegetative phase and to increase crop yield, but minimizing the environmental impact of the application of fertilizers, it is necessary to increase N use efficiency (NUE) by crops. Strategies to improve N capture and avoid loss by leaching include improving agronomic practice like placement, timing, crop rotation and accurate N source (Robertson and Vitousek, 2009). Placement refers to apply subsurface or incorporated enough nitrogen in the root zone to meet the nutrient demands, which reduces the risk of leaching during the growth and afterward (Bowles *et al.,* 2018). Timing refers to apply N fertilizer when crops have their highest use for nitrogen. For example, nitrogen fertilization after 40 days of sowing and at eight-leaf growth stage is reported to increase biomass and grain yield in sorghum (Khosla *et al*., 2000; Adu-Gyamfi *et al*., 1997). Crop rotation improves NUE in different forms, for example, after the harvest of

one crop, nitrogen will normally be found in deeper soil layers, which could be utilized by placing deep-rooted crops. Finally, among the forms of improving N fertilizers are the enhanced-efficiency fertilizers (Kanter and Searchinger, 2018). In this place, we can find slow and controlled-release fertilizers, which mix traditional fertilizers with polymers that delay the availability of free nitrogen in the soil. Another strategy is the use of urease inhibitors, which reduce the conversion of urea to NH_3 by inhibiting the urease enzyme. Nitrification inhibitors also help to retain the N by delaying the transformation of ammonium to nitrate (Kanter and Searchinger, 2018). NH_4^+-based fertilizers are the second most used after urea. Their low prices and elevated N concentration (46 % of mass) reduce transport and distribution costs (Miller and Cramer, 2005). In this sense, ammonium nutrition with the use of inhibitors of nitrification constitutes a good strategy to mitigate pollution.

2. NITROGEN CYCLE

Nitrogen (N) is the most abundant element in the atmosphere with almost 79 % of dry air in the form of N_2 (Robertson and Vitousek, 2009). However, N_2 consists of a triple bond difficult to break that makes N unavailable for most organisms to metabolize. Fortunately, N_2 gas is converted to more accessible forms thanks to a complex biogeochemical cycle that moves nitrogen through abiotic and biotic parts of ecosystems. From a chemical point-of-view, N is an incredibly versatile element, existing in many oxidation states as well as in many inorganic and organic forms. The N cycle involves successive changes in redox states of atomic N, from +5 in nitrate to -3 in ammonia or organic compounds (Robertson and Vitousek, 2009).

The biogeochemical N cycle could be started with nitrogen fixation, in which electric shocks (lightning), combustion processes, chemical synthesis of fertilizers or microorganisms break the triple bond of N_2 to produce NH_3. The biological nitrogen fixation into nodules of legumes (and non-legume such as *Parasponia* sp.) thanks to a symbiotic relationship with restricted prokaryotes (diazotrophs) play an important input of available nitrogen (Vessey *et al.,* 2005). In this manner, N_2 gas is able to incorporate into the composition of the soil, organisms or converted to other forms very actives (Miller and Cramer, 2005). Besides the nitrogen fixation, there are other three main pathways that reduce the N oxidation state. The denitrification is the reduction of NO_3^- or NO_2^- to produce gaseous nitrogen compounds (N_2, NO and N_2O), carried out by a diverse group of prokaryotes. The other two reduction pathways are assimilatory nitrate reduction and dissimilatory nitrate reduction, both for the conversion of nitrate and nitrite to ammonium (Bernhard, 2010). Both are carried by microorganisms and plants.

On the other hand, there are two oxidation pathways in the cycle, called nitrification and anaerobic ammonium oxidation (anammox). Nitrification is the aerobic oxidation of ammonium (NH_4^+)/ammonia (NH_3) to nitrite NO_2^-, followed by the oxidation of NO_2^- to produce NO_3^-, carried out by microorganisms (Miller and Cramer, 2005). In general, this process takes place from a few days to a few weeks in the soil. The other oxidation pathway is the anammox, acronym of **an**aerobic **am**monium **ox**idation carried out by prokaryotes belonging to Planctomycetes phylum which converts NH_3/NH_4^+ to N_2, using NO_2^- as an acceptor of electrons (Bernhard, 2010). Thus, anammox is comproportionation reaction, where NO_2 and NH_3/NH_4^+ ions are converted directly into diatomic nitrogen and water.

Additionally to the pathways mentioned, there are other factors that determine the availability of nitrogen for most organisms. For instance, since all the living organisms need nitrogen, the immobilization of N by microorganism makes this unable for plants. Nevertheless, mineralization is the reverse process by which microorganisms convert the organic N to ammonium. Leaching is a pathway of loss by which water-soluble N is washed through the profile of the soil due to rain and irrigation. Leaching is a natural environment concern since it can contribute to groundwater contamination. In general, the availability of N in the ecosystems depends on its inputs (e.g. fixation, mineralization and nitrification) and its outputs (e.g. denitrification, volatilization, immobilization, and leaching)

3. NITROGEN AND CARBON METABOLISM

In plants, nitrogen assimilation is the formation of organic nitrogen compounds like amino acids and proteins from nitrate or ammonium. For the absorption of nitrogen forms, plants possess numerous types of transporters of NH_4^+ or NO_3^-, which can be classified into two categories: the systems of transport of high affinity (HATS) and low affinity (LATS) (Glass *et al*., 2002). HATs are characterized by their ability to take up ions when they are present at low concentrations, around ten micromolar. However, these systems are very sensitive to temperature and metabolic inhibitors (Crawford and Glass, 1998). Regarding LATs, they operate at relatively high concentrations nutrient in the media and are less sensitive to the physical and metabolic factors that affect HATs (Crawford and Glass, 1998). In plant tissues, NH_4^+/NH_3 can also enter into the cell by diffusion, via aquaporins, by potassium channels or via non-selective cation channels (Bittsánszky *et al*., 2015). The ammonium absorbed from soil is mostly assimilated in the root and 41 % introduced to the cytoplasm, 20% stored into the vacuole, 19% metabolized and 20 % returned to the environment (Wang *et al*., 1993). Regarding nitrate, after its absorption, it can be stored in vacuoles, reduced, exported to the leaves or returned to the environment. Unlike

ammonium, most of the nitrate is stored into the vacuoles, working as N-pool reserve and participating in the maintenance of the cell turgor (Touraine *et al*., 2001). Contrasting to ammonium, the use of nitrate requires to be reduced previously the incorporation into organic molecules and biomass. The nitrate reduction in most of the plants occurs mainly in photosynthetic parts (Glass *et al*., 2002). The nitrate reduction in the cell is carried out by nitrate reductase (E.C.1.7.1.2), an iron-sulfur molybdoprotein protein that catalyzes the reduction of nitrate (NO_3^-) to nitrite (NO_2^-) using NADP(H) as an electron donor. Then, nitrite is reduced to ammonium by nitrite reductase (E.C.1.7.1.4), a flavoprotein that contains also iron, molybdenum and pterin. This enzyme catalyzes the direct reduction of nitrite to nitrate using reduced ferredoxin (Fd) or NADPH, a step that requires 6 electrons. The form using ferredoxin is characteristic of leaves, meanwhile, the NADP-H isoform is characteristic of roots.

The NH_4^+ derived either from absorption, coming from nitrate reduction, or released by a catabolic process, is incorporated into amino acids by a tandem of two enzymes, the glutamine synthetase and glutamate synthase, in a well-known cycle so-called the GS/GOGAT pathway. This incorporation consists of the amination of glutamate to produce glutamine catalyzed by GS, with consumption of ATP. Subsequently, the amide group of glutamine is transferred to 2-oxoglutarate to produce 2 molecules of glutamate by GOGAT (Miller and Cramer, 2005). In plants, the GS is present as two isoforms, GS1 located in the cytoplasm and GS2, placed in the plastids. In the root GS1 acts in the assimilation of the ammonium taken-up directly from the soil or coming from the reduction of nitrate (Miller and Cramer, 2005) and reassimilation ammonium derived from catabolic processes. The chloroplastic isoform (GS2) assimilates the ammonium from the nitrate reduction and it is the predominant isoform in photosynthetic tissues. For GOGAT, there are two isoforms, one is dependent on NADH and the other dependent on ferredoxin (Fd). The ferredoxin-dependent GOGAT (Fd-GOGAT) is found in chloroplasts and serves in primary nitrogen assimilation and photorespiratory nitrogen metabolism (Miller and Cramer, 2005).

Besides the route GS/GOGAT, the enzymes glutamate dehydrogenase (GDH) and asparagine synthase (AS) also combine NH_4^+ with carbon skeletons (Miller and Cramer, 2005). GDH catalyzes reversibly the oxidative deamination of glutamate and the reductive amination of 2-oxoglutarate. The low affinity for NH_4^+ (K_m of 5.8 mM) showed by this enzyme suggests that it functions as desaminating enzyme at physiological conditions. GDH is located in roots, but although also shows high activities in shoots. An NADH-dependent form of GDH is located in mitochondria, and a NADPH-dependent form is located in the chloroplasts of photosynthetic organs. For decades, a symbolical role has been attributed to this enzyme in the primary nitrate

reduction in plants. In this sense, it is well accepted that primary nitrogen assimilation is mainly incorporated into organic compounds via GS/GOGAT (Miflin and Lea; 1977)

Asparagine synthase (AS) catalyzes the formation of asparagine with ATP consumption. This reaction involves the transfer of the amide group of glutamine to aspartate, rendering asparagine and glutamate with the concomitant ATP consumption. AS and GDH activities are suggested as complementary routes to the GS/GOGAT for ammonium assimilations. Especially relevant is the reported role of both enzymes under environmental stress conditions (Dubois *et al*., 2003; Wang *et al*., 2007).

The nitrogen assimilation pathways are closely interconnected with primary carbon metabolism since carbon skeletons are highly demanded the amino acid synthesis. The glycolysis and more directly tricarboxylic acid (TCA) cycle, provide the carbon skeletons necessary to incorporate the ammonium and produce amino acids. The main carbon skeleton required for glutamine (amide that has 5 C and 2 N) and asparagine (amide that has 4 C and 2 N) are alfa-oxoglutarate and oxaloacetate, respectively. Carbon entrance to TCA cycle occurs mainly in the form of pyruvate and oxaloacetate (OAA) provided via glycolysis but can also enter in the form of malate coming from phosphoenolpyruvate carboxylation (PEP). The TCA cycle is said to be versatile, in such a way that it can operate in cyclic mode providing of energy (NADPH and APT) for the cell metabolism, but it can also operate in non-cyclic mode providing of carbon skeletons for cell anabolic reactions. When ammonium is assimilated, the cycle operates more in non-cyclic mode, since α-cetoglutarate and oxaloacetate are retired from the TCA intermediates pool. Thus, carbon extra is demanded to fuel the continuous functioning of the cycle (Tcherkez *et al*., 2005; Sweetlove *et al*, 2010).

4. AMMONIUM NUTRITION

Ammonium and nitrate are the main N inorganic forms available in soils for plants. Despite ammonium is metabolically cheaper for the cell to be assimilated, plants have generally preference to use nitrate over ammonium. Moreover, elevated concentrations of NH_4^+ in the media are detrimental for plant growth (Britto and Kronzucker, 2002). Ammonium accumulation in the cell happens when the amount of ammonium produced from nitrate reduction and catabolic processes (amino acids deamination proteolysis, phenylpropanoid metabolism) and photorespiration exceeds the ammonium assimilating capacity (Bittsánszky, *et al*., 2015). Above certain thresholds, ammonium results toxic for cell metabolism. This ammonium toxicity is paradoxical because ammonium is a common and ubiquitous metabolite in plant cell pathways, and its assimilation has lower energetic cost. Symptoms of NH_4^+ toxicity include reduction of

growth, leaf chlorosis, decreasing in the root: shoot ratio, and nutrients imbalance, among others (Esteban *et al*., 2016).

Plants response to ammonium toxicity is intra and interspecies-dependent. The causes of ammonium toxicity are still unclear, but some studies related to disorders in pH regulation, deficiency of mineral cations and carbohydrate limitation due to excessive consumption of soluble sugars for NH_4^+ assimilation (Britto *et al.,* 2001; Esteban *et al.,* 2016). In the long term, ammonium nutrition can cause oxidative stress, and consequently cellular damage. This is indicated by the activation of glutathione-ascorbate cycle enzymes, an increase of lipid peroxidation and changes in the redox state of low-mass scavengers (Podgorska *et al* 2013). However, in spinach and pea plant, it was reported that ammonium stress diminishes oxidative damage to proteins (Domínguez-Valdivia *et al*., 2008). Therefore, investigations whether ammonium causes oxidative stress are necessary (Bittsánszky, *et al*., 2015).

Accumulation of NH_4^+ stimulates the synthesis of amino acids and amines with a high N:C ratio (Roosta and Schjoerring, 2007). Although this accumulation of specific amino acids consumes energy and carbohydrates, rarely is inhibited under ammonium nutrition (Roosta and Schjoerring, 2007). Most of the plant accumulate and assimilate ammonium in the root to avoid damage in leaf photosynthesis (Esteban *et al*., 2016). For example, when ammonium assimilation overpasses plant capacity, ammonium is accumulated in leaves of spinach and sunflower, causing damage to the photosynthetic apparatus and consequently, decreasing the growth rate (Lasa *et al.,* 2001). In pea, the tolerance of ammonium stress is associated with decreasing growth potential and increasing respiratory rates and activity of the alternative pathways (Cruz *et al*., 2011). In this manner, ammonium can be rapidly metabolized, producing organic compounds (Loqué *et al*., 2005). Ammonium can also be stored into the vacuoles, by passive and active transporters, to the maintenance of ammonium homeostasis. The pH of the vacuoles can acidify 2 units more than the cytosol, therefore vacuoles can store 100-fold higher concentrations (Bittsánszky *et al*., 2015). Active transport of ammonium into the vacuole depends on membrane-bound ATP-driven pumps. Passive transport is given mainly via aquaporin, which passes NH_4^+ through the membrane in the form of NH_3 and once into the vacuole, this is protonated to NH_4^+, being compartmented (Bittsánszky *et al*., 2015).

Previous studies reported that NH_4^+ and NO_3^- act differently on ions homeostasis (Roosta and Schjoerring, 2007). Every nitrate ion reduced to ammonia produces one OH^- ion, leading to alkalization. Meanwhile, ammonium assimilation results in the production of H^+, leading to acidification. To maintain a pH balance, the plant must either excrete OH^- or H^+ into the

surrounding medium or neutralize it with organic acids (Roosta and Schjoerring, 2007). Ammonium nutrition tends to acidify soil solution since plant expulses ions of H^+ to compensate NH_4^+ uptake. The rate of this pH change is faster than the alkalization produced by nitrate nutrition (Miller and Cramer, 2005). When the accumulation of ammonium in the cell is very high, there is an imbalance of mineral anions that cannot be compensated with the absorption of $H_2PO_4^{-2}$ and SO_4^{-2}, while the absorption of ammonium depolarizes the cell and reduces the absorption of Ca^{+2} and K^+ (Chaillou and Lamaze, 2001).

It is possible to enhance ammonium tolerance by buffering of the external pH (Sarasketa, *et al*., 2016), increasing the supply of cations (Gerendás *et al*., 1997), optimization of the light regime (Setién *et al*., 2013), increasing CO_2 in the atmosphere (Vega-Mas *et al*., 2015) and application of inhibitors of ethylene biosynthesis (Britto and Kronzucker, 2002). Maintenance of carbohydrate synthesis is a major prerequisite for NH_4^+ tolerance. A provision of α-ketoglutarate or bicarbonate ion to roots may in some cases increase NH_4^+ assimilation (Roosta and Schjoerring, 2007). However, these methods are difficult to apply in the field (Esteban *et al*., 2016).

In this sense, a combination of physiological and genomic approaches (genomics, proteomics, metabolomics, genome-wide association and QTLs) may lead to the optimization of the traits and nitrogen use in new crops. For example, it is widely accepted that plants with elevated GS activity are more tolerant when NH_4^+ is accumulated (Magalhäes and Huber, 1989). The identification of orthologue genes responsible for ammonium tolerance in different plant species could allow to clone the most active genes, and been transferred into susceptible traits (Bittsánszky *et al*., 2015). The use of molecular biology tools is a viable option for the selection of enzyme mutants that present a better tolerance to ammonium nutrition.

5. *Brachypodium distachyon* AS MODEL PLANT

The Poaceae family is a group of plants of monocotyledonous that include cereals such as wheat, rice, maize and barley, which are the basis of world food. It is predicted that in 2050 the population will increase by 20-50 % and that the demand for food will exceed current production capacities (Taiz, 2013). As crop fields are limited, grain production must be improved (David *et al*., 2019). Fortunately, scientific advances in molecular biology have allowed characterizing new genes of interest that allow genetic engineers to improve crop yields (Taiz, 2013). In this sense, the improvement of the nitrogen fertilization is one of the most important targets since practically nitrogen drives yield but also produces a lot of pollution. Although the use of ammonium sources with nitrification inhibitors reduces the environmental impact, they produce

stressful condition at high concentrations (Britto and Kronzucker, 2002). Ammonium nutrition response varies among closely related species or even within the same species (Ariz *et al*., 2011). It is known that in general crops are more sensitive to ammonium toxicity than wild species (Cruz *et al.,* 2006), reflecting a loss of natural variability due to the domestication and consequently limiting the discovery of new genes. To elucidate then the genes related to ammonium nutrition in cereal, it desirable to adopt a model that meets the requirements of intraspecific variability, conservation of natural traits and whose metabolic response is similar to cereals. The study of non-domesticated species or native varieties is of special relevance in the case of ammonium nutrition because the high nitrification rates common in agricultural soils have led to a selection of cultivars practically performed under the use of nitrate.

Brachypodium distachyon represents an excellent model plant for the study of cereals physiology and genetics (Brutnell *et al*., 2015; Scholthof *et al*., 2018). *B. distachyon* is a grass native to the Mediterranean region that has been spread by human movement throughout the world. Like *Arabidopsis thaliana*, *B. distachyon* is a model plant without economic importance, which is phylogenetically close to the large-genome cereal crops, especially to wheat. The term model implies that the plant has certain advantages to study the group of cereals that otherwise would be difficult or expensive. In fact, *B. distachyon* is a small plant, easy to grow and use, and has a shorter life cycle and smaller genome than their relatives. For this reason, a set of resources such as genome sequenced and accompanying annotations, a collection of mutants, microarrays, a set of wild accessions, among others, are available to elucidate the molecular biology and genetic basis of agronomic traits (Tyler *et al.,* 2016).

The accession Bd21 was the first line sequenced in 2010. Its genome of 272 Mbp includes, approximately, 25,000 genes (Kellogg, 2015). Over 5.6 % of these genes are specific only for grass. It is notable that the pan-genome of 54 accessions studied by Gordon *et al.,* (2017) is more than twice the size of genes of a particular accession. This is the largest pan-genome found in plants for that number of lines, taking into account that the population of *B. distachyon* is mainly homozygote, showing that possesses a big genetic diversity.

As stated, genetic variability is useful to identify traits of agronomic interest and to elucidate their genetic bases. In this sense, cereals have lost natural diversity since due to domestication processes. Since *B. distachyon* is not a domesticated plant, phenotypic variation in vernalization and flowering among populations has been described (Tyler *et al.,* 2016). In this sense, *B. distachyon* has emerged as a powerful model for studying genetic variability. A new tool of the molecular biology known as genome-wide association (GWAS) correlates allele markers of the

genome of a population with phenotypes of interest (Tyler *et al.,* 2016). The power of this analysis depends on the number of individuals, the variability among individuals and the well-characterized germplasm collections. Around 250 lines of *B. distachyon* are available in the U.S. Department of Agriculture's Germplasm Resources Information Network (GRIN) (https://www.ars-grin.gov/) or from other parts of the world. Although these resources do not represent so many lines by the moment, it is compensated for the big pan-genome. Resources for Brachypodium are publically available in Phytozome (http://phytozome.jgi.doe. gov/), BrachyBio (http://bti.cornell.edu/Brachybio), Brachypodium genome information (http://mips.helmholtzmuenchen.de/plant/brachypodium/ brachypodium/), Brachypodium resources (http://jgi.doe.gov/our-sci ence/science-programs/ plant-genomics/), CoGe (http://synteny.cnr.berke ley.edu/CoGe/), ELEMENT (http://element.cgrb. oregonstate.edu/), Gramene (http://www.gramene.org), PlantGDB (http://www.plantgdb.org/), PlexDB (http://www.plexdb.org/), TILLING database (http://urgv.evry.inra.fr/ UTILLdb), USDA NPGS (http://www.ars-grin.gov/ npgs/).

Taking into account the intraspecific variability in *B. dystachyon*, the characteristics shown as a model for the monocotyledonous in different kind of studies and the genetic resources available we consider appropriate *B. distachyon* to carry out the present project. The aim of the present project is firstly to test the metabolic and physiological response of *B. distachyon* upon ammonium. Secondly, to better understand the root physiology in plants grown with ammonium as the ºsole source of N. Finally, to explore the genetic and metabolic natural intraspecific variability of *B. distachyon.*

GENERAL OBJECTIVES

GENERAL OBJECTIVES

Intensive nitrogen fertilization has an important negative impact on the environment. For instance, the loss of nitrate through leaching causes water eutrophication. Moreover, associated to soil microbial activity, N-fertilization is also responsible for the emission of nitrogenous gases with high contribution to global warming, notably N_2O. The combination of ammonium fertilizers with nitrification inhibitors, which maintains NH_4^+ content in the soil for longer periods, has been extensively proven as efficient strategy to mitigate these N losses. Thus, understanding ammonium nutrition for a proper selection/generation of genotypes adapted to this fertilization management is essential in order to increase crops yield.

In this context, the **general objective** of this PhD thesis is **to better understand plant response upon ammonium nutrition focusing on the metabolic and molecular basis that may lead to ammonium tolerance in cereals, using *Brachypodium distachyon* as a model.**

This general objective is supported in three specific objectives, each one corresponding to a different chapter:

1) To assess the suitability of *B. distachyon* as a model plant for the study of ammonium nutrition in C3 grasses.

2) To gain insight on the molecular mechanisms of *B. distachyon* root response upon ammonium nutrition by means of a proteomic analysis.

3) To decode the genetic basis of the metabolic adaptation underlying ammonium tolerance by the exploitation of *B. distachyon* natural variability towards ammonium nutrition.

CHAPTER 1

Providing carbon skeletons to sustain amide synthesis in roots underlines the suitability of *Brachypodium distachyon* for the study of ammonium stress in cereals

Marlon de la Peña, María Begoña González-Moro, Daniel Marino (2019)

AoB PLANTS 11(3)

1. ABSTRACT

Plants mainly acquire N from the soil in the form of nitrate (NO_3^-) or ammonium (NH_4^+). Ammonium-based nutrition is gaining interest because it helps to avoid the environmental pollution associated with nitrate fertilization. However, in general, plants prefer NO_3^- and indeed, when growing only with NH_4^+ they can encounter so-called ammonium stress. Since *Brachypodium distachyon* is a useful model species for the study of monocot physiology and genetics, we chose it to characterize performance under ammonium nutrition. *Brachypodium distachyon* Bd21 plants were grown hydroponically in 1 or 2.5 mM NO_3^- or NH_4^+. Nitrogen and carbon metabolism associated with NH_4^+ assimilation was evaluated in terms of tissue contents of NO_3^-, NH_4^+, K, Mg, Ca, amino acids and organic acids together with tricarboxylic acid (TCA) cycle and NH_4^+-assimilating enzyme activities and RNA transcript levels. The roots behaved as a physiological barrier preventing NH_4^+ translocation to aerial parts, as indicated by a sizeable accumulation of NH_4^+, Asn and Gln in the roots. A continuing high NH_4^+ assimilation rate was made possible by a tuning of the TCA cycle and its associated anaplerotic pathways to match 2-oxoglutarate and oxaloacetate demand for Gln and Asn synthesis. These results show *B. distachyon* to be a highly suitable tool for the study of the physiological, molecular and genetic basis of ammonium nutrition in cereals.

2. INTRODUCTION

Over the last decade, *Brachypodium distachyon* has gained attention as model plant for C3 grasses. Phylogenetically, it lies between rice and wheat, with a high degree of sequence similarity with wheat, and high degree of synteny with most grasses (Brutnell *et al*., 2015). Given *B. distachyon* is not domesticated, it shows great intra-species diversity; its pan-genome containing nearly twice the number of genes found in any individual genome (Gordon *et al*., 2017). Although many aspects of *Brachypodium* development and responses to biotic and abiotic stresses have been studied, little has been published concerning *Brachypodium* nitrogen (N) signalling and metabolism (Ingram *et al*., 2012; Poiré *et al*., 2014; Barhoumi 2017) and, to our knowledge, no report is available on how *B. distachyon* deals with different N sources. This point is crucial since N is the major mineral nutrient demanded by plants and its availability is yield-limiting in many agronomic soils (Xu *et al.,* 2012). Plants take up N mainly in form of ammonium (NH_3/ NH_4^+) and nitrate (NO_3^-). Nitrate is usually the preferred source but is a source of pollution because anions are readily lost through leaching. Besides, nitrous oxide (N_2O), one of the strongest greenhouse gases, is emitted during bacterial denitrification (Huérfano *et al*., 2015). Ammonium salts, when combined with nitrification inhibitors, are more stable in the soil and have been proved useful in mitigating some of the unwanted effects of nitrate fertilization

(Huérfano *et al*., 2015). Moreover, ammonium nutrition can sometimes confer positive effects on plant performance, for example by increasing sorghum and rice tolerance to osmotic stress (Gao *et al*., 2010; Miranda *et al*., 2016). It has also been suggested that ammonium nutrition may improve the response of some species to high concentrations of atmospheric CO_2 (Bloom *et al*., 2010). In addition, a frequent characteristic associated with ammonium nutrition is an enrichment with N-containing compounds (Marino *et al*., 2016; Coleto *et al*., 2017). However, ammonium nutrition is also known to decrease plant growth. This is the main symptom of ammonium stress, the so-called 'ammonium syndrome' (Liu and Von Wirén, 2017). The energetic cost associated with maintaining cytosolic NH_3/NH_4^+ homeostasis, mainly by pumping NH_3/NH_4^+ out of the cytosol and by increasing NH_4^+assimilation, is considered to be one of the major causes of biomass reduction (Britto and Kronzucker 2002; Esteban *et al*., 2016). If the concentration of NH_3/ NH_4^+ exceeds the capacity for efflux and assimilation, NH_4^+ is, in most species, preferentially accumulated in root cells to avoid damaging the photosynthetic apparatus (Esteban *et al*., 2016). Overall, the study of the metabolic adaptation to ammonium stress is crucial to increase plant N use efficiency while reducing N losses associated with nitrate fertilization.

Ammonium is mainly assimilated via the glutamine synthetase/glutamate synthase (GS/GOGAT) cycle. To sustain GS/GOGAT activity, the tricarboxylic acid (TCA) cycle and its associated routes regulate the continuous supply of carbon skeletons. Indeed, proper management of carbon supply has been shown to be essential for ammonium tolerance (Roosta and Schjoerring, 2008; Vega-Mas *et al*., 2015). Although controlling NH_3/NH_4^+ entry/efflux and its assimilation is crucial for NH_4^+ homeostasis, ammonium stress is also related to other processes such as pH control, ion imbalance and nitrate signalling (Liu and Von Wirén, 2017). The study of the co-ordination and regulation of all these mechanisms is essential to understand fully how they determine the extent of tolerance/sensitivity to ammonium nutrition in a given species or genotype. For instance, there is considerable inter- and intraspecific variability in the extent of ammonium stress amongst grass species such as maize (Schortemeyer *et al*., 1997), rice (Chen *et al*., 2013) and wheat (Wang *et al*., 2016a).

In this work, we undertook a comprehensive physiological and metabolic characterization of *B. distachyon* (reference genotype Bd21) grown with exclusive access to NH_4^+ or NO_3^- as N source. We focused on leaf and root carbon metabolism and on nitrogen assimilatory pathways.

3. EXPERIMENTAL DESIGN AND STATISTICAL ANALYSIS

Brachypodium distachyon Bd21 seeds were sterilized in 100 % ethanol for 1 min, rinsed three times with deionised water and incubated in deionised water for 2 h. Then, seeds were placed in trays filled with a perlite:vermiculite (1:1) mixture moistened with deionised water. After 4 days of stratification at 4°C in the dark, the trays were transferred to a growth chamber (60/70 % of relative humidity, 23 °C day (14 h) with a light intensity of 350 µmol m^{-2} s^{-1} and 18 ºC night (10 h)). Eleven days after sowing, seedlings were transferred to 4.5 L hydroponic tanks (10 plants/tank). The nutrient solution contained 1.15 mM K_2HPO_4, 0.85 mM $MgSO_4$, 0.7 mM $CaSO_4$, 2.68 mM KCl, 0.5 mM $CaCO_3$, 0.07 mM NaFeEDTA, 16.5 µM Na_2MoO_4, 3.7 µM $FeCl_3$, 3.5 µM $ZnSO_4$, 16.2 µM H_3BO_3, 0.47 µM $MnSO_4$, 0.12 µM $CuSO_4$, 0.21 µM $AlCl_3$, 0.126 µM $NiCl_2$ and 0.06 µM KI, pH 6.8. The nitrogen source was $(NH_4)_2SO_4$ for ammonium-fed plants and $Ca(NO_3)_2$ for nitrate-fed ones. Each N source was supplied at 1 or 2.5 mM of total N. To compare both N sources within each concentration, NO_3^--fed plants were supplied with $CaSO_4$ to match the SO_4^{2-} supplied with the NH_4^+. The pH of the solution was checked every two days and the nutrient solution replaced every four days. Four tanks were set up per treatment; thus, a total of 40 plants were grown per condition. Twenty-four days after transfer to hydroponic conditions, plants were harvested. Shoots and roots were separated and individually weighed. For metabolic measurements, plants grown in the same tank were pooled and immediately frozen in liquid nitrogen, homogenized in a Tissue Lyser (Retsch MM 400) and stored at -80 °C until use.

Statistical analysis

All the results presented are given as means with standard errors. Data were analysed with SPSS 17.0 (Chicago, IL, USA). Normality and homogeneity of variance were analysed by Kolmogorov–Smirnov and Levene's tests. The significance of the results was assessed using independent samples t-test or two-way ANOVA.

4. RESULTS

We compared the performance of *B. distachyon* Bd21 growing under the exclusive supply of NH_4^+ as N source with that of plants given an exclusive supply of NO_3^- as the control condition. Concentrations of 1 or 2.5 mM of each N source were given. Statistical analyses indicated that biomass was affected by the N source, its concentration and there was also a significant statistical interaction (Figure 1.1A). Notably, when plants were grown in 1 mM ammonium growth by roots or shoots was closely similar to that by plants in 1 mM nitrate. When NH_4^+ was increased to 2.5 mM, plants showed symptoms of ammonium stress, i.e. a lower biomass compared to plants in 2.5 mM nitrate (Figure 1A). Chlorophyll content was not affected by the

treatment (Figure 1.1B). Therefore, 1 mM ammonium represented a non-toxic supply while 2.5 mM was toxic.

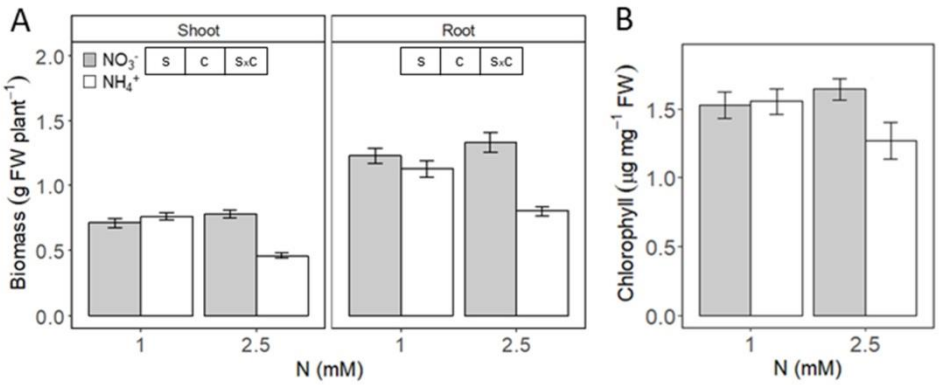

Figure 1.1 Comparison of *B. distachyon* fresh weight and chlorophyll content in response to N source after 24 days. (A) Plant biomass. (B) Chlorophyll content. Plants were grown with nitrate or ammonium as N source at 1 or 2.5 mM. Columns represent mean ± SE (n = 40 for biomass data and n = 4 for chlorophyll). Whenever significant differences according to two-way ANOVA, S indicates N source effect; C indicates N concentration effect and S × C indicates interaction effect ($P < 0.05$).

To analyse N metabolism we determined contents of NH_4^+, NO_3^-, protein, total N, individual amino acids and the activity of enzymes related to N metabolism: GS, GOGAT, AAT and glutamate dehydrogenase (GDH) in both leaf and root (Figures 1.2 and 1.3). The accumulation of ammonium (NH_4^+) is the most common metabolic marker of ammonium stress. In agreement with biomass and chlorophyll content, NH_4^+ content did not accumulate in plants fed with 1 mM ammonium (Figures 1.2 and 1.3). However, with 2.5 mM supply, root tissue accumulated *ca.* 25 times more NH_4^+ compared to equivalent nitrate nutrition (Figure 1.3) whereas in leaf tissue, little NH_4^+ accumulated (Figure 1.2). As expected, NO_3^- content was affected by the N source with NO_3^- levels being much higher for plants grown in nitrate. Indeed, in plants fed with ammonium NO_3^- content was so low it approached the limit of detection of the methodology used (Figure S1.1).

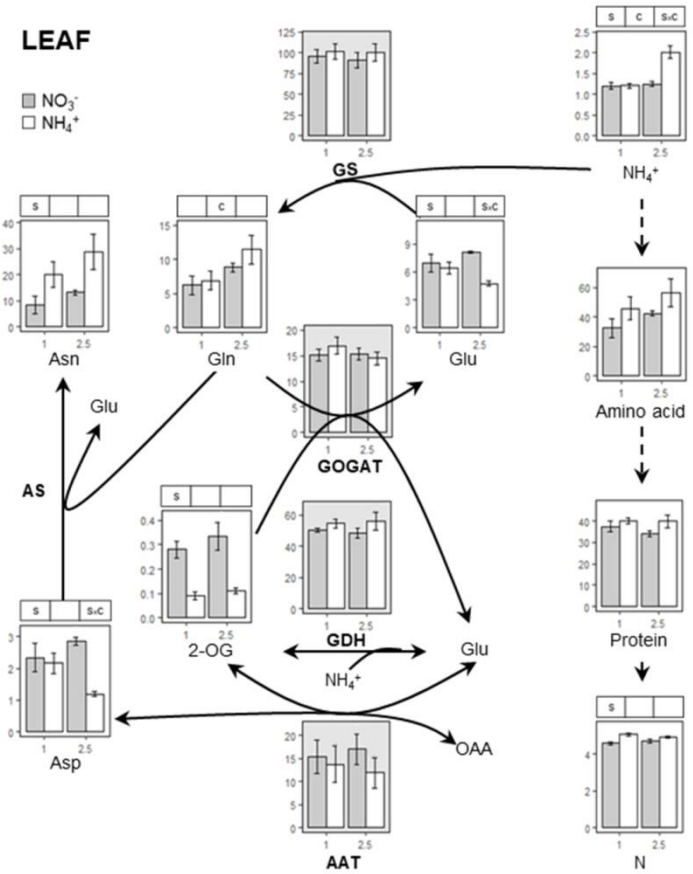

Figure 1.2. Ammonium assimilation in *B. distachyon* leaf tissue. Plants were grown with nitrate or ammonium as N source for 24 days at 1 or 2.5 mM. Ammonium, total amino acids, Asn, Glu, Gln, Asp and 2-OG content are expressed µmol g^{-1} FW. For enzyme activities, GOGAT, GDH and AAT are expressed as µmol NADH g^{-1} FW h^{-1} and GS as µmol γ-GHM g^{-1} FW h^{-1}. Protein content is expressed as mg BSA g^{-1} FW and total N content as % dry wt. Columns represent mean ± SE (n = 3–4). Significant differences according to two-way ANOVA are indicated by S for N source effects, C for N concentration effects and S × C for interactions ($P < 0.05$).

Asn and Gln were the most abundant amino acids in root and leaf under both NO_3^- and NH_4^+, with Glu also being abundant in plants fed with nitrate (Figures 1.2 and 1.3; Tables S1.2 and S1.3). At 1 mM, differences between NO_3^-- and NH_4^+-fed plants were small. Exceptions were Asn and Phe contents which were markedly higher in roots of plants grown with ammonium (Figure 1.3; Table S1.3). With 2.5 mM NH_4^+ supply a large accumulation of NH_4^+ in the roots was associated with much increased levels of amino acids (Table S1.3), mainly in form of Asn and Gln where contents increased *ca.* 17 and 19 times, respectively (Figure 1.3). Overall, total amino acids content was *ca*. 8 times higher compared to nitrate nutrition (Figure 1.3).

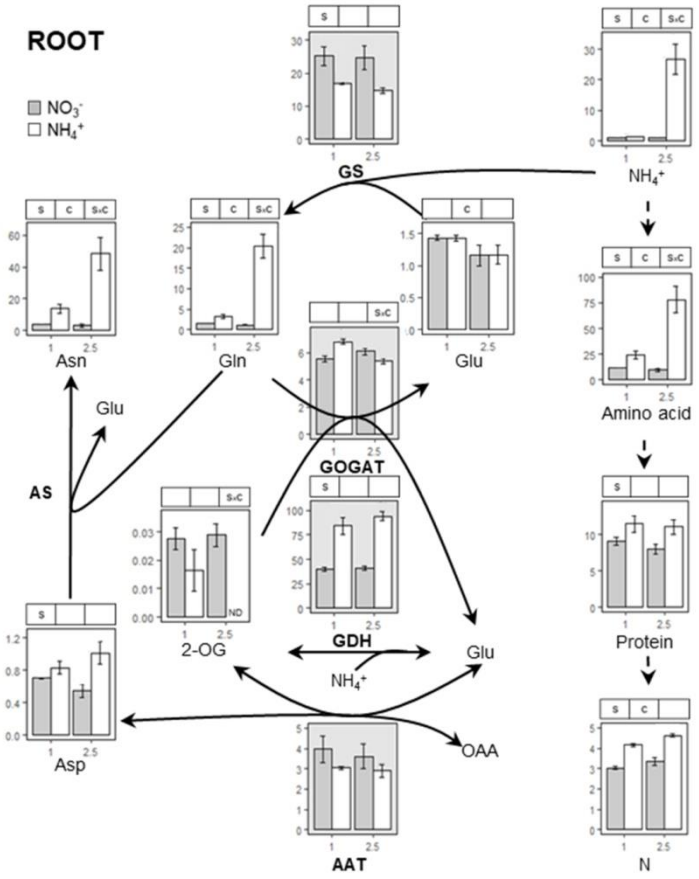

Figure 1.3. Ammonium assimilation in *B. distachyon* root tissue. Plants were grown with nitrate or ammonium as N source at 1 or 2.5 mM for 24 days. Ammonium, total amino acids, Asn, Glu, Gln, Asp and 2-OG content are expressed µmol g^{-1} FW. For enzyme activities, GOGAT, GDH and AAT are expressed as µmol NADH g^{-1} FW h^{-1} and GS as µmol γ-GHM g^{-1} FW h^{-1}. Protein content is expressed as mg BSA g^{-1} FW and total N content as % dry wt. Significant differences according to two-way ANOVA are indicated by S for N source effects, C for N concentration effects and S × C for interactions ($P < 0.05$).

A substantial N source effect was observed in root GDH (NADH- and NADPH-dependent) and GS enzyme activities (Figure 1.3; Figure S1.2A) under both 1 and 2.5 mM. Glutamate dehydrogenase showed high activity in the root of plants fed with ammonium, while the contrary was the case for GS activity (Figure 1.3). The stimulation of N assimilation in plants fed with ammonium was also evident in terms of Gln/ Glu and Asn/Asp ratios (Figure S1.3). Importantly, the increase in Gln/Glu and Asn/Asp ratios in the leaves of plants grown with 2.5 mM of ammonium was not only due to Gln and Asn increase but also to a decrease in Glu and Asp (Figure 1.2).

To evaluate the regulation of ammonium assimilation enzymes, we looked for genes encoding GS, GDH and AS in *B. distachyon* Bd21. We carried out BLAST analysis in GenBank (https://www.ncbi.nlm.nih.gov/genbank/) and Phytozome (https://phytozome.jgi.doe.gov/) databases, using available sequences for *Oryza sativa*, *Triticum aestivum* and *Arabidopsis thaliana* GS, GDH and ASN genes as queries. We found complete sequences for four genes encoding for GS (three GS1 and one GS2), two genes encoding for GDH and one for NADP-GDH and three genes encoding for AS (Table S1.1). We performed a phylogenetic analysis for the

three families including sequences for *A. thaliana*, *T.* aestivum, *O. sativa*, *Hordeum vulgare* and *Aegilops tauschii* (Figs S1.4–S1.6). In general, *B. distachyon* genes lie between Triticeae and rice genes. *Arabidopsis* genes were more difficult to position (Figs S1.4–S1.6). We analysed gene expression by qPCR in leaf and root tissue of plants grown for 24 days with 2.5 mM nitrate or ammonium supply. In roots, expression of *BdGLN1;3* (Figure 1.4A), *BdGDH2* (Figure 1.4B), *BdASN1* and *BdASN3* (Figure 1.4C) was higher in plants under ammonium nutrition. In contrast, the expression of *BdGLN2* was higher in roots of plants fed with nitrate (Figure 1.4A). In leaves, only *BdASN3* expression significantly increased in plants grown with ammonium (Figure 1.4C).

The TCA cycle and its associated pathways are essential to supply carbon skeletons for N assimilation, especially under ammonium nutrition. Thus, we determined the contents of relevant organic acids and the activity of a number of TCA-related enzymes (Figures 1.5 and 1.6; Figure S1.2B). In the leaf, no differences were observed in the activity of TCA-related enzymes, except for NAD-ME (Figure 1.5; Figure S1.2B).

Nevertheless, ammonium nutrition provoked a remarkable decrease in the content of each organic acid (Figure 1.5). In roots, we observed higher activity of NADP-dependent isocitrate dehydrogenase (ICDH), NADP-dependent malic and phosphoenolpyruvate carboxylase (PEPC) enzymes in plants grown with ammonium supply (Figure 1.6; Figure S1.2B). Access to nitrate or ammonium as N source brought about notable alterations in the content and distribution of organic acids in the root. Changes were mostly observed in 2.5 mM ammonium nutrition, where 3-PGA, PEP, 2-OG and malate contents were lower in plants grown with nitrate (Figure 1.6). On the contrary, a significant source × concentration interaction was observed for pyruvate + oxaloacetate (Pyr + OAA) and citrate, whose levels were higher in plants fed with 2.5 mM ammonium compared to those fed with nitrate (Figure 1.6). Finally, since ammonium has been shown by others to provoke an imbalance of essential cations, we assessed whether this was also the case for *B. distachyon*. In roots of plants grown with 2.5 mM of ammonium, Ca, Mg, and K contents were diminished compared to their nitrate counterparts (Table S1.4). In leaves, K also decreased significantly in plants fed with ammonium (Table S1.4).

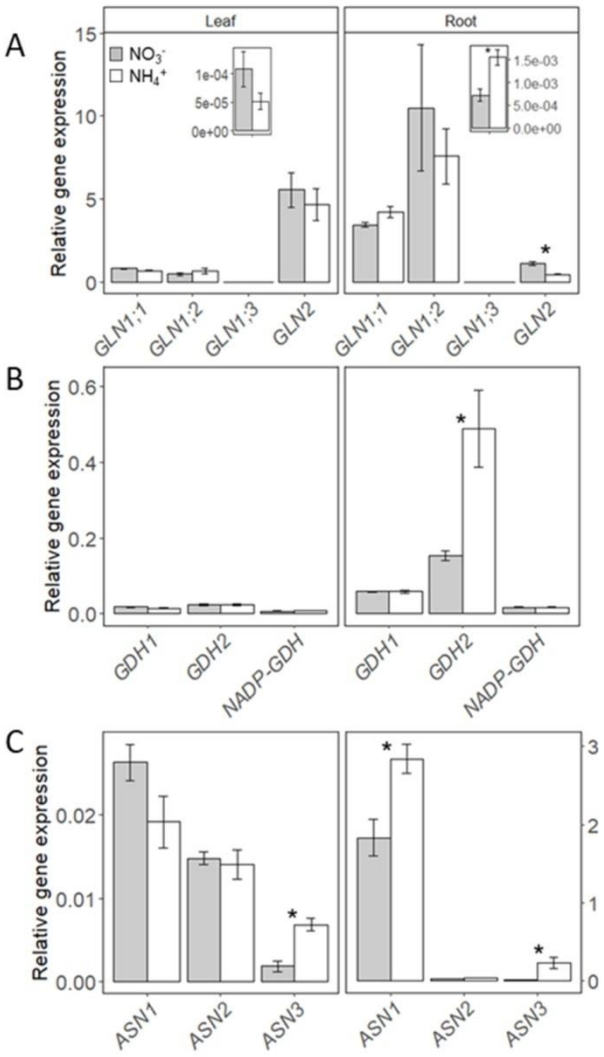

Figure 1.4. GLN, GDH and ASN gene expression pattern in leaves and roots of plants grown for 24 days with 2.5 mM ammonium or nitrate as exclusive source of nitrogen. (A) *GLN* genes expression. (B) *GDH* genes expression. (C) *ASN* genes expression. The insets in panels A and B show the details for *GLN1;3* expression. Columns represent mean ± SE (n = 4). Asterisk (*) indicates significant nitrogen source effect within each nitrogen concentration (t-test, $P < 0.05$).

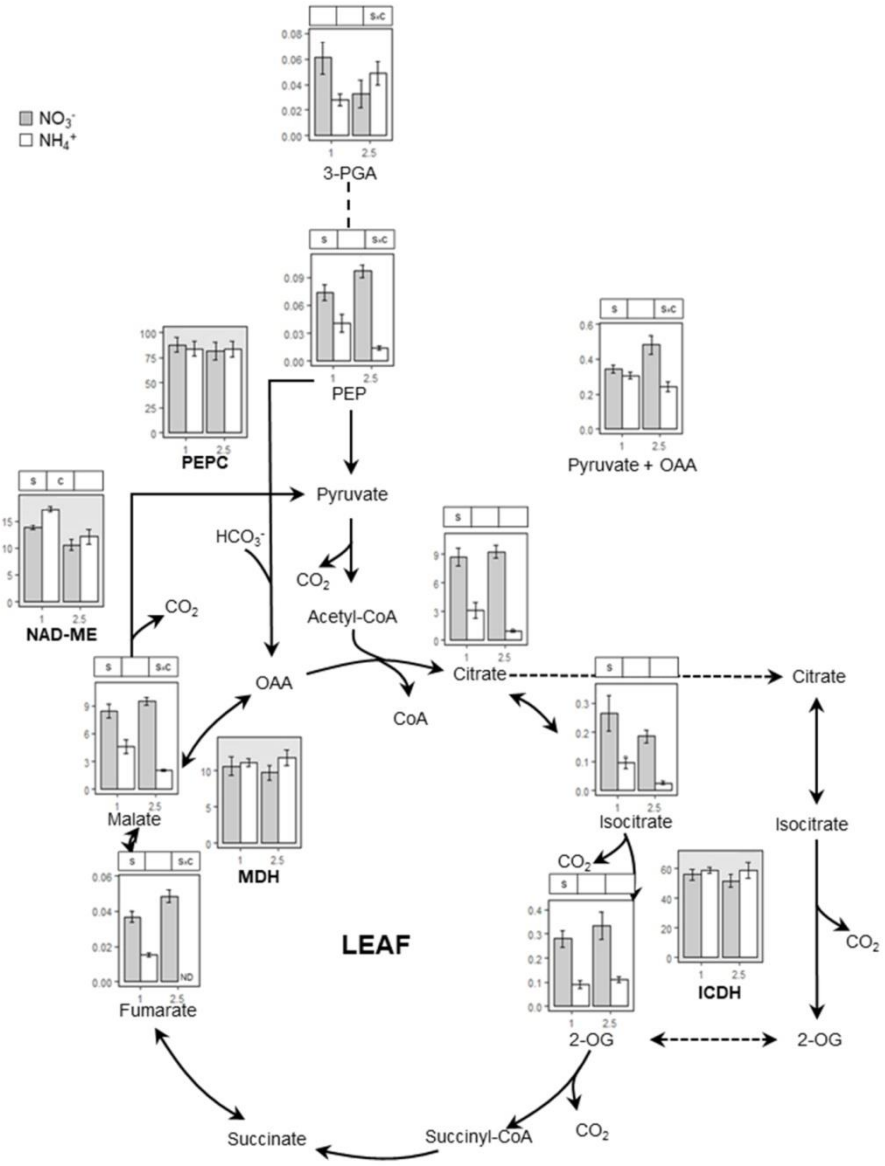

Figure 1.5. Organic acids and enzyme activities associate to TCA cycle in the leaf of *B. distachyon* grown for 24 days with nitrate or ammonium as N source at two different concentrations (1 and 2.5 mM). Organic acids content are given as nmol mg^{-1} FW. ICDH activity is given as µmol NADPH g^{-1} FW h^{-1}, MDH as mmol NADH g^{-1} FW h^{-1} and ME, PEPC as µmol NADH g^{-1} FW h^{-1}. Columns represent mean ± SE (n = 4). Significant differences according to two-way ANOVA are indicated by S for N source effects, C for N concentration effects and S × C for interactions ($P < 0.05$).

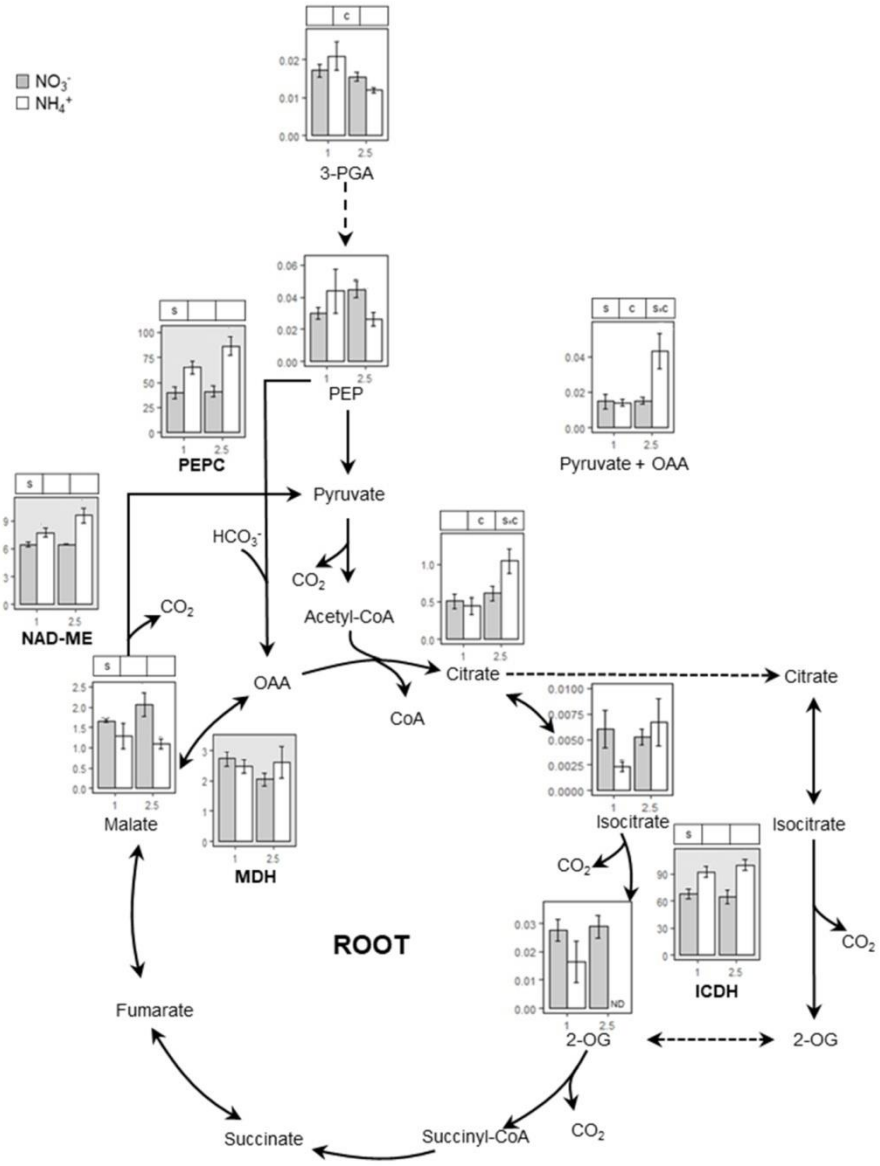

Figure 1.6. Organic acids and enzyme activities associate to TCA cycle in the root of *B. distachyon* grown for 24 days with nitrate or ammonium as N source at two different concentrations (1 and 2.5 mM). Organic acids content are given as nmol mg^{-1} FW. ICDH activity is given as µmol NADPH g^{-1} FW h^{-1}, MDH as mmol NADH g^{-1} FW h^{-1} and ME, PEPC as µmol NADH g^{-1} FW h^{-1}. Columns represent mean ± SE (n = 4). Significant differences according to two-way ANOVA are indicated by S for N source effects, C for N concentration effects and S × C for interactions ($P < 0.05$).

5. DISCUSSION

Ammonium stress is considered universal in most if not all biological systems (Britto and Kronzucker, 2002). However, great variability in ammonium-use efficiency has been reported (Britto and Kronzucker, 2013; Sarasketa *et al*., 2014) and there are plant species and genotypes which display high tolerance of ammonium. Indeed, the Poaceae is considered to be relatively tolerant. For instance, ryegrass (*Lolium perenne*), wheat and notably rice are able to manage adequately the presence of high NH_4^+ concentrations in the external medium (Britto *et al*., 2001; Belastegui-Macadam *et al*., 2007; Setién *et al*., 2013). Additionally, intraspecific variability in

ammonium toxicity has also been reported amongst different species, including cereals (Schortemeyer *et al*., 1997; Chen *et al*., 2013; Wang *et al*., 2016a).

Brachypodium distachyon has emerged as an excellent model species to study different aspects of development in C3 grasses and responses to a number of environmental constraints (Brutnell *et al*., 2015). However, studies of nitrogen metabolism remain scarce. Accordingly, we characterized the performance of Bd21, the reference accession for *B. distachyon*, supplied with nitrate or ammonium as N source with a special focus on interactions between carbon and nitrogen metabolisms. *Brachypodium distachyon* Bd21 appeared to be moderately tolerant to ammonium. Indeed, in hydroponic culture it grew equally in 1 mM N regardless of N source. Importantly, 1 mM represented a N-sufficient condition, since raising NO_3^- supply to 2.5 mM did not further increase plant biomass (Figure 1.1). However, when NH_4^+ was raised to 2.5 mM plants displayed moderate symptoms of ammonium toxicity in terms of slower growth (Figure 1.1).

A high NH_4^+ concentration in the medium is known to affect the homeostasis of essential cations in the cell. For instance, NH_4^+ affects K^+ transport directly by competitive inhibition and indirectly via effects on membrane potential (Coskun *et al*., 2017a). Moreover, NH_4^+ may also stimulate K^+ efflux (Coskun *et al.,* 2017a). Among others, a decrease in K^+ levels has been observed in grasses such as ryegrass (Belastegui-Macadam *et al*., 2007), rice (Balkos *et al*., 2010) or sorghum (Miranda *et al*., 2017). Indeed, when the available concentration of K^+ in the nutrient solution is limiting, the provision of supplementary K^+ improves ammonium tolerance (Balkos *et al*., 2010; Li *et al*., 2012). In contrast, this is not the case when the concentration of K^+ is already sufficient (Balkos *et al*., 2010). In our work, despite the fact that we report a significant decrease in Ca, K and Mg content in the root of plants grown with 2.5 mM NH_4^+ (Table S1.4), the internal concentrations of these elements remained within the limits of an adequate nutrient supply (Marschner 2012). Therefore, under our growth conditions, ion imbalance does not seem to be the primary cause for the growth inhibition observed in *B. distachyon* fed with 2.5 mM NH_4^+. However, further experiments are needed to completely discard the potential role of cationic imbalance in the response of *B. distachyon* to ammonium toxicity.

The main metabolic symptom of ammonium toxicity, and the probable cause of subsequent disorders, is the disruption of cytosolic NH_4^+ homeostasis. Thus, one of the obvious cell strategies for keeping NH_4^+ cytosolic levels under control is to intensify its assimilation into organic molecules. It has already been reported that a prevalent response of many species, including grasses, is an accumulation of free amino acids primarily in the roots, e.g. in wheat and sorghum

(Setién *et al*., 2013; Miranda *et al*., 2016). Alternatively, other species such as rapeseed (Coleto *et al*., 2017) tend to accumulate amino acids in shoot tissues. The amino acids in which NH_4^+ is preferentially stored also vary between species. As in other monocots such as wheat (Setién *et al*., 2013), NH_4^+ is scavenged in *B. distachyon* root systems in the form of amides, mainly Asn followed by Gln (Figure 1.3).

Glutamine synthetase/glutamate synthase is the main NH_4^+ assimilation pathway and its importance during ammonium stress has been highlighted by the fact that mutants such as rice *gln1;1* or *Arabidopsis gln1;2* mutants show hypersensitivity to ammonium nutrition (Kusano *et al*., 2011; Guan *et al*., 2016). In *B. distachyon* Bd21, GS is encoded by four genes (Table S1.1, Figure S1.4). Various studies have revealed that GS is regulated at multiple levels: transcriptional, translational and post-translational. Moreover, GS members are differentially regulated (i) in space, according to cell type and function of the organ; (ii) in time, according to circadian rhythm and phenology; and (iii) in response to growth conditions (Swarbreck *et al.* 2011). Accordingly and in contrast to the decrease of GS activity observed in roots of plants fed with ammonium (Figure 1.3), the expression of *BdGLN1;1* and *BdGLN1;2* did not vary and only *BdGLN1;3* expression was enhanced by NH_4^+ (Figure 1.4A) thereby underlining the probable post-translational regulation of GS. A further and interesting finding is that in roots of barley, *HvGS1.3*, homologue of *BdGLN1;3* was also induced by NH_4^+ nutrition (Goodall *et al*., 2013), indicating that the function and regulation of these isogenes can be similar for both monocot species. Thus, it will be of interest to explore whether the role of *BdGLN1;3* is significant under ammonium stress. The decrease in root GS activity observed in plants fed with ammonium (Figure 1.3) could be related to a feedback regulation by the accumulation of amino acids (Watanabe *et al*., 1997; Oliveira and Coruzzi 1999) as represented by the high Asn/Asp and Gln/Glu ratios (Figure 1.3; Figure S1.3, Table S1.3).

Asparagine synthetase (AS) catalyses the ATP-dependent synthesis of Asn and Glu from Gln and Asp. Asn has a high ratio N:C and plays a key role in nitrogen transport and storage (Lea *et al*., 2007). *BdASN1* and *BdASN3* were induced by ammonium treatment (Figure 1.4C) and thus, probably control Asn synthesis in *B. distachyon* fed with ammonium. Indeed, in plants fed with 2.5 mM NH_4^+, Asn accounted for *ca*. 51 and 70 % of total leaf and root amino acid content, respectively (Tables S1.2 and S1.3). The higher expression of *BdASN1* and its specific up-regulation by ammonium nutrition in roots suggest a prominent role of this gene when ammonium is the only source of N (Figure 1.4C). In support of this, *OsAS1*, a homologue of *BdASN1* (Figure S1.6), was previously shown responsible for Asn accumulation in rice grown under ammonium nutrition (Ohashi *et al*., 2015).

To sustain amino acid synthesis in the root an adequate supply of carbon is essential, necessitating adjustments in carbon metabolism elsewhere. Specifically, TCA cycle adjustment has been shown to be crucial, as well as its associated anaplerotic routes (Setién *et al*., 2014; Sarasketa *et al*., 2016). The significant effect of ammonium nutrition on PEPC activity (Figure 1.6) was presumably essential to guarantee the flux of carbon towards OAA that can yield Asp or follow the Krebs cycle. Moreover, ME activity would also collaborate, through pyruvate entrance in the cycle, in the provision of citrate + isocitrate to generate 2-OG in co-ordination with ICDH (Figure 1.6). Indeed, low malate and PEP contents indicate a higher consumption under ammonium nutrition; therefore, confirming the prioritization of the pathway generating TCA intermediates, mainly OAA and 2-OG. The role of PEPC, ME and ICDH in root response to ammonium nutrition has been highlighted in different species including pea and sorghum (Ariz *et al*., 2013; Arias-Baldrich *et al*., 2017). Moreover, the relevance of PEPC agrees with a report where *Arabidopsis ppc1/ppc2* double mutant was impaired in ammonium assimilation (Shi *et al*., 2015). Complementary evidence that the plant is prioritizing carbon provision to the roots is also evidenced by a general decrease of leaf organic acids (Figure 1.5) and additionally of Glu and Asp (Figure 1.2). As a consequence, we observed a clear N source and concentration effect in total root C content that increased in plants grown with ammonium and provoked a decrease in C:N ratio compared to plants fed only with nitrate (Figure S1.7).

The enhancement of GDH activity in relation with the up-regulation of *GDH2* gene expression is one of the best metabolic markers of ammonium nutrition. Indeed, this GDH response has been reported in different monocots including wheat (Setién *et al*., 2013; Wang *et al*., 2016b), rice (Xuan *et al*., 2013) and *B. distachyon* in the present study (Figs 1.2–1.4). It has been hypothesized that GDH induction could be related to direct NH_4^+ assimilation because of GDH aminating activity and there are published hints for such a role (Skopelitis *et al*., 2006). However, other evidence also supports the idea that the role of GDH is to deaminate glutamate, thus collaborating in 2-OG provision (Labboun *et al*., 2009). We also report higher levels of NADP-GDH activity in *B. distachyon* fed with ammonium (Figure S1.1A). This enzyme is still poorly characterized in plants compared to GDH. Whether NAD(H)- and NADP(H)dependent GDH enzymes possess differential functions in plant metabolism in general and in relation with ammonium nutrition in particular remains to be elucidated.

In conclusion, we report that *B. distachyon* Bd21 is a species with moderate tolerance to ammonium nutrition. We observed a strong metabolic adaptation of *B. distachyon* carbon and nitrogen metabolism when facing ammonium-only N nutrition. The root system is shown as a physiological barrier acting as a reservoir for free NH_4^+ and increasing NH_4^+ assimilation to

amides. This was possible since TCA enzyme activities together with anaplerotic routes were adjusted to increase 2-OG and OAA provision thereby sustaining Gln and Asn synthesis in the root. This metabolic adjustment appears to be a strategy mitigating ammonium stress while imposing an energetic cost for the cell that limits plant growth under 2.5 mM NH_4^+ supply. Overall, these responses of *B. distachyon* to ammonium nutrition are in line with previous studies with cereals crops. Our work underlines the potential of *B. distachyon* as a useful tool for analysing the molecular basis of ammonium tolerance in monocots. Such work is of paramount importance in view of the desirability of increasing the use of ammonium-based fertilizers to lessen environmental pollution associated with nitrate-based nutrition.

6. SUPPLEMENTARY INFORMATION

Table S1.1. *Brachypodium distachyon* Bd21 genes encoding for GLN, AS and GDH enzymes.

Name	Locus name	Gene symbol	Forward	Reverse	E
BdGLN1;1	Bradi3g59970	LOC100845598	aagctgcccaagtggaactacg	tccttgaagatagcctgtgggtag	1.76
BdGLN1;2	Bradi1g69530	LOC100824429	tcgtcgagtacttgtgggttgg	ccattcacggtccttgctttgc	1.80
BdGLN1;3	Bradi1g11450	LOC100837122	caagccatcttcagggatccattc	tgcatagcagtcacacataaccag	1.92
BdGLN2	Bradi5g24550	LOC100842712	tcgcttcacaagtgccatggtatg	agaggccagttcacatctctctgg	1.76
BdASN1	Bradi1g65540	LOC100830770	tgccgaagcatatcctctac	tttcatcatctcatcggtgac	1.93
BdASN2	Bradi2g21050	LOC100830419	tctcttgtctggtggacttg	tcaggagaacccttcaaacc	2.02
BdASN3	Bradi4g45010	LOC100839462	cagtgttcaggatggcattg	gcgacttgatcttgcgtgac	2.05
BdGDH1	Bradi1g05680	LOC100831066	agtttcatggttactcgcctgctg	tcccagagatcctccaaggtcaac	1.89
BdGDH2	Bradi5g17330	LOC100828452	acatgggaactaatgcacagacc	agtggcagcatccctacctaatg	1.91
BdNADP-GDH	Bradi2g41130	LOC100833076	cgatgccgatctacgtcaaagc	tgaaccacctcctggatagactg	1.95
BdSamDC	Bradi5g14640	LOC100821874	tgctaatctgctccaatggc	gacgcagctgaccacctaga	2.04
BdACT3	Bradi4g41850	LOC100834364	cctgaagtccttttccagcc	agggcagtgatctccttgct	2.05

The primers used for qPCR expression together with their efficiencies (E) are shown. *BdSamDC* and *BdACT3* are the genes that served as reference for relative gene expression quantification.

Table S1.2. Individual amino acid content (µmol . g FW^{-1}) of leaf of *B. distachyon* grown for 24 days with nitrate or ammonium as N source.

	Leaf				
	1 mM		2.5 mM		Variance
	NO_3^-	NH_4^+	NO_3^-	NH_4^+	analysis
Ala	3.16 ± 0.21	3.84 ± 0.43	3.6 ± 0.15	3.32 ± 0.17	
Arg	0.15 ± 0.03	0.51 ± 0.17	0.24 ± 0.03	0.91 ± 0.26	S
Asn	8.42 ± 3.3	20.3 ± 4.88	13.17 ± 0.86	28.74 ± 6.84	S
Asp	2.43 ± 0.45	2.17 ± 0.32	2.85 ± 0.13	1.19 ± 0.08	S, SxC
GABA	0.4 ± 0.05	0.61 ± 0.07	0.44 ± 0.03	0.49 ± 0.08	
Gln	6.2 ± 1.41	6.91 ± 1.39	8.82 ± 0.63	11.44 ± 2.17	C
Glu	6.94 ± 1.01	6.44 ± 0.67	8.11 ± 0.13	4.72 ± 0.26	S, SxC
His	0.11 ± 0.01	0.13 ± 0.02	0.12 ± 0.01	0.12 ± 0.02	
Ile	0.06 ± 0.01	0.08 ± 0.01	0.07 ± 0.00	0.10 ± 0.02	S
Leu	0.09 ± 0.01	0.11 ± 0.02	0.10 ± 0.00	0.16 ± 0.03	
Lys	0.09 ± 0.03	0.23 ± 0.07	0.13 ± 0.01	0.46 ± 0.15	S
Met	0.06 ± 0.02	0.07 ± 0.01	0.09 ± 0.01	0.06 ± 0.01	
Phe	0.08 ± 0.01	0.09 ± 0.02	0.10 ± 0.00	0.10 ± 0.02	
Ser-Gly	2.38 ± 0.09	2.67 ± 0.14	2.58 ± 0.06	2.90 ± 0.30	
Thr	1.52 ± 0.14	1.52 ± 0.25	1.71 ± 0.05	1.26 ± 0.10	
Trp	0.01 ± 0.00	0.01 ± 0.00	0.01 ± 0.00	0.03 ± 0.00	S, C, SxC
Tyr	0.12 ± 0.01	0.12 ± 0.03	0.14 ± 0.01	0.16 ± 0.02	
Val	0.23 ± 0.02	0.25 ± 0.02	0.24 ± 0.01	0.35 ± 0.06	

Values represent mean ± SE (n = 3). The column "Variance analysis" shows significant differences according to two-way ANOVA. S indicates N source effects, C N concentration effects and SxC interactions $P < 0.05$).

Table S1.3. Individual amino acid content (µmol . g FW^{-1}) of root of *B. distachyon* grown for 24 days with nitrate or ammonium as N source.

	Root				
	1 mM		2.5 mM		Variance
	NO_3^-	NH_4^+	analysis	NH_4^+	analysis
Ala	1 ± 0.07	1.43 ± 0.16	0.93 ± 0.02	1.64 ± 0.36	S
Arg	0.12 ± 0.01	0.12 ± 0.02	0.1 ± 0.01	0.32 ± 0.07	S, C, SxC
Asn	3.85 ± 0.19	13.89 ± 2.9	2.93 ± 0.76	48.47 ± 10.28	S, C, SxC
Asp	0.7 ± 0.01	0.83 ± 0.08	0.54 ± 0.08	1.01 ± 0.14	S
GABA	0.52 ± 0.06	0.77 ± 0.13	0.42 ± 0.05	0.71 ± 0.04	S
Gln	1.49 ± 0.03	3.23 ± 0.51	1.09 ± 0.14	20.37 ± 2.97	S, C, SxC
Glu	1.44 ± 0.04	1.43 ± 0.05	1.16 ± 0.16	1.17 ± 0.15	C
His	0.06 ± 0.01	0.06 ± 0.01	0.06 ± 0.01	0.2 ± 0.06	SxC
Ile	0.12 ± 0.01	0.12 ± 0.00	0.10 ± 0.00	0.22 ± 0.03	S, C, SxC
Leu	0.16 ± 0.01	0.16 ± 0.01	0.14 ± 0.00	0.3 ± 0.03	S, C, SxC
Lys	0.07 ± 0.00	0.06 ± 0.01	0.06 ± 0.00	0.23 ± 0.08	
Met	0.09 ± 0.00	0.05 ± 0.01	0.07 ± 0.01	0.04 ± 0.01	S
Phe	0.04 ± 0.00	0.05 ± 0.00	0.03 ± 0.00	0.15 ± 0.02	S, C, SxC
Ser-Gly	0.74 ± 0.00	0.8 ± 0.06	0.67 ± 0.04	1.25 ± 0.02	S, C, SxC
Thr	0.69 ± 0.01	0.61 ± 0.04	0.59 ± 0.03	0.92 ± 0.03	S, C, SxC
Trp	0.04 ± 0	0.04 ± 0.01	0.04 ± 0.00	0.1 ± 0.02	S, C, SxC
Tyr	0.08 ± 0.01	0.05 ± 0.01a	0.07 ± 0.00	0.17 ± 0.02	S, C, SxC
Val	0.56 ± 0.03	0.59 ± 0.04	0.41 ± 0.03	0.94 ± 0.1	S, SxC

Values represent mean ± SE (n = 3). The column "Variance analysis" shows significant differences according to two-way ANOVA. S indicates N source effects, C N concentration effects and SxC interactions $P < 0.05$).

Table S1.4. K, Ca, Mg and Na content (mg. g DW^{-1}) of roots and leaves of *B. distachyon* grown for 24 days with 2.5 mM nitrate or ammonium as N source.

	Leaf		Root	
	NO_3^-	NH_4^+	NO_3^-	NH_4^+
Ca	6.80 ± 0.50	6.62±1.15	**21.31 ± 4.66**	**5.62 ± 2.03**
K	**42.23 ± 0.46**	**30.29±3.68**	**58.27 ± 4.53**	**24.24 ± 2.39**
Mg	2.46 ± 0.11	2.81±0.26	**4.65 ± 0.14**	**2.11 ± 0.23**
Na	0.22 ± 0.02	0.21 ± 0.02	0.44 ± 0.04	0.45 ± 0.06

Values represent mean ± SE (n = 4). Significant nitrogen source effect within each dose (t-test, $p < 0.05$) is highlighted in bold.

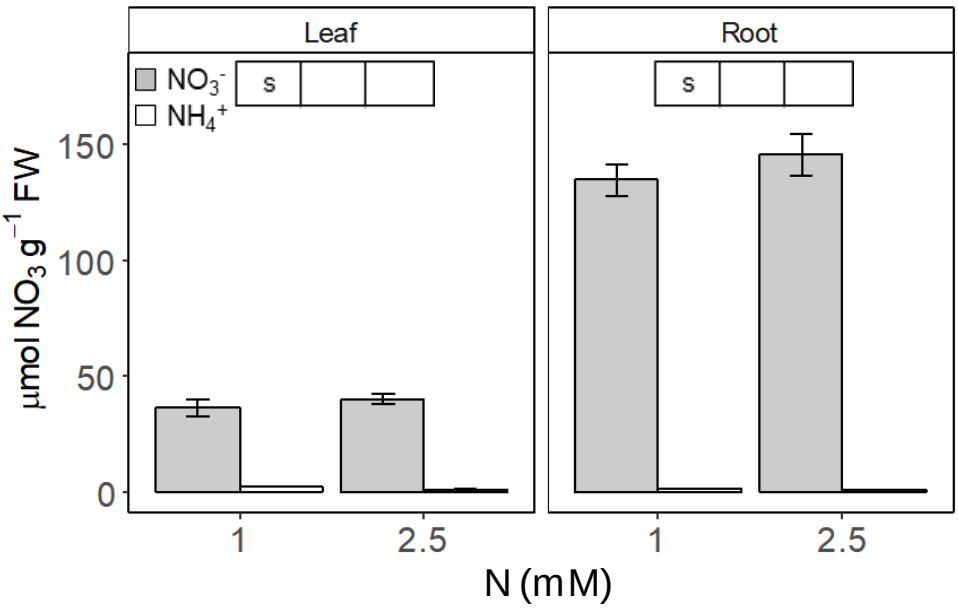

Figure S1.1. Nitrate content in leaf and root of *B. distachyon* Bd21 grown for 24 days with 1 or 2.5 mM of nitrate or ammonium as N source. Values represent mean ± SE (n = 4). Significant differences according to two-way ANOVA are indicated by S for N source effects, C for N concentration effects and SxC for interactions ($P < 0.05$).

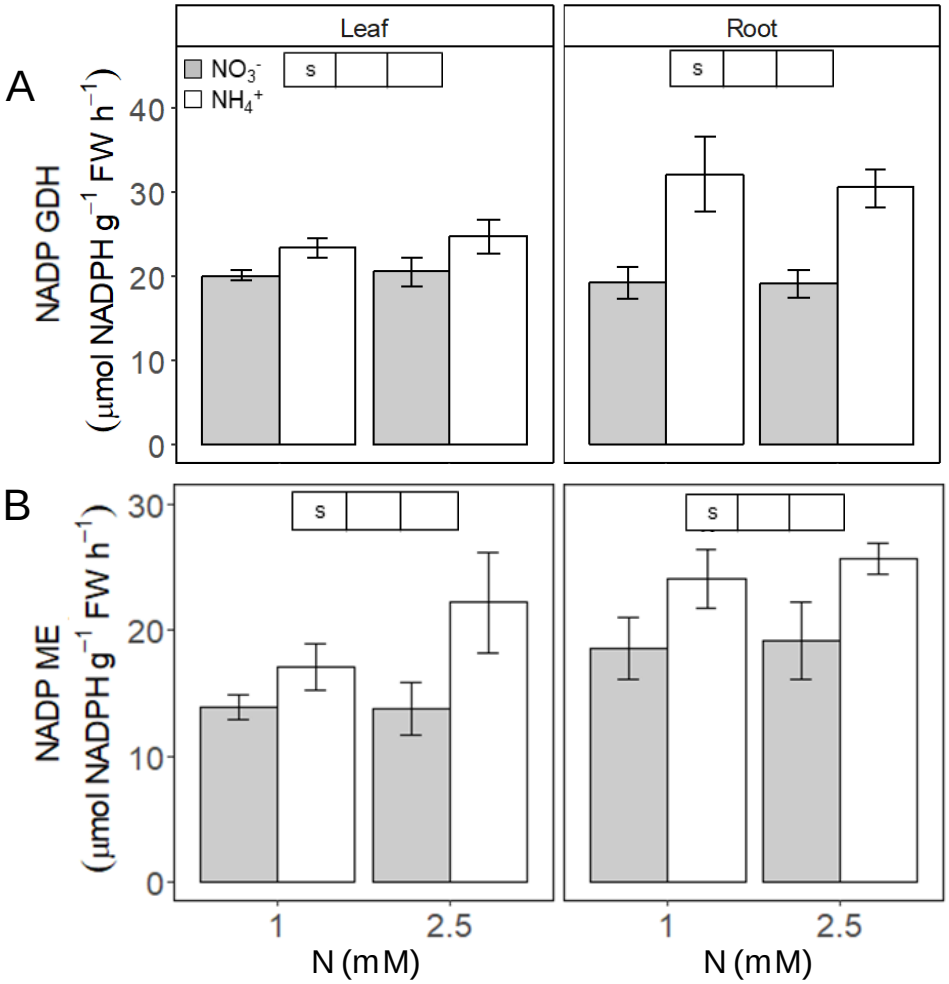

Figure S1.2. NADP-GDH and NADP-dependent ME enzyme activities (B) in leaf and root of *B. distachyon* Bd21 grown for 24 days with 1 or 2.5 mM of nitrate or ammonium as N source. (A) NADP-GDH enzyme activity. (B) NADP-ME enzyme activity. Values represent mean ± SE (n = 4). Significant differences according to two-way ANOVA are indicated by S for N source effects, C for N concentration effects and SxC for interactions ($P < 0.05$).

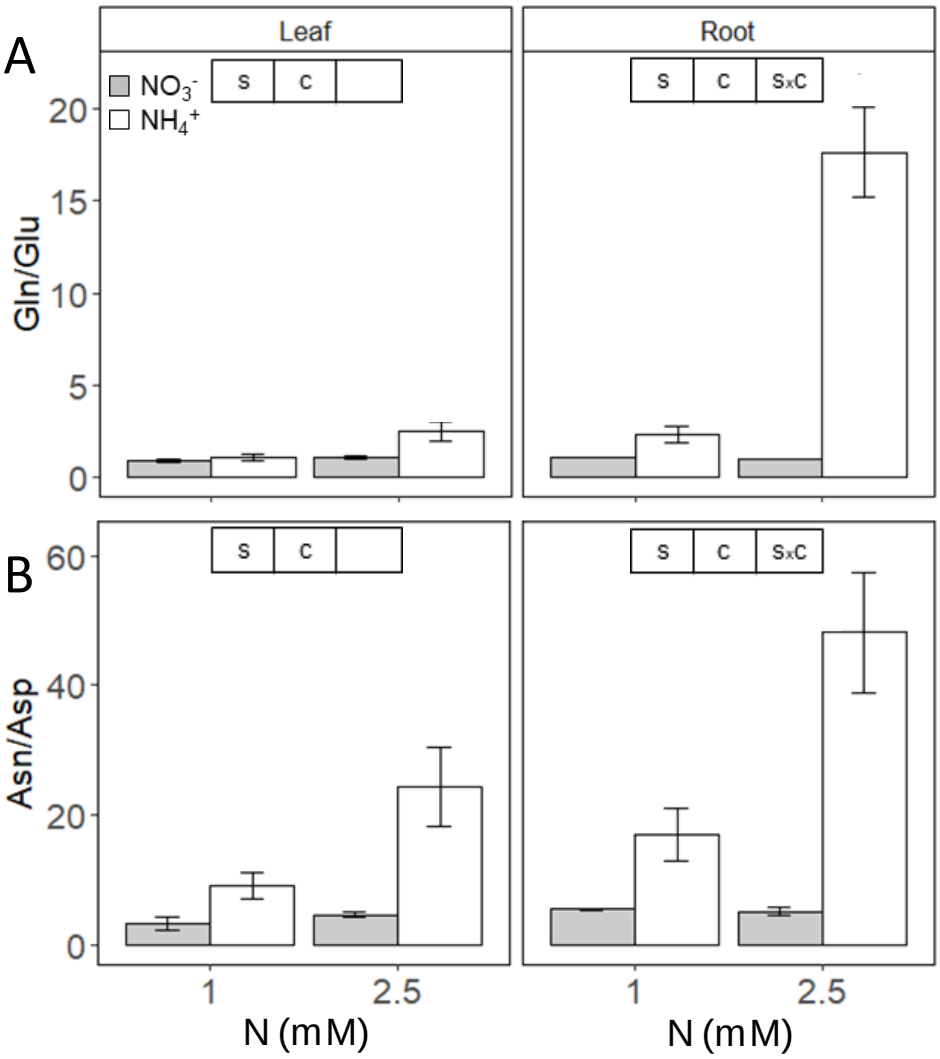

Figure S1.3. Gln/Glu and Asn/Asp ratio of leaf and root of *B. distachyon* grown for 24 days with nitrate or ammonium as N source. (A) Gln/Glu ratio. (B) Asn/Asp ratio. Values represent mean ± SE (n = 3). Significant differences according to two-way ANOVA are indicated by S for N source effects, C for N concentration effects and SxC for interactions ($P < 0.05$).

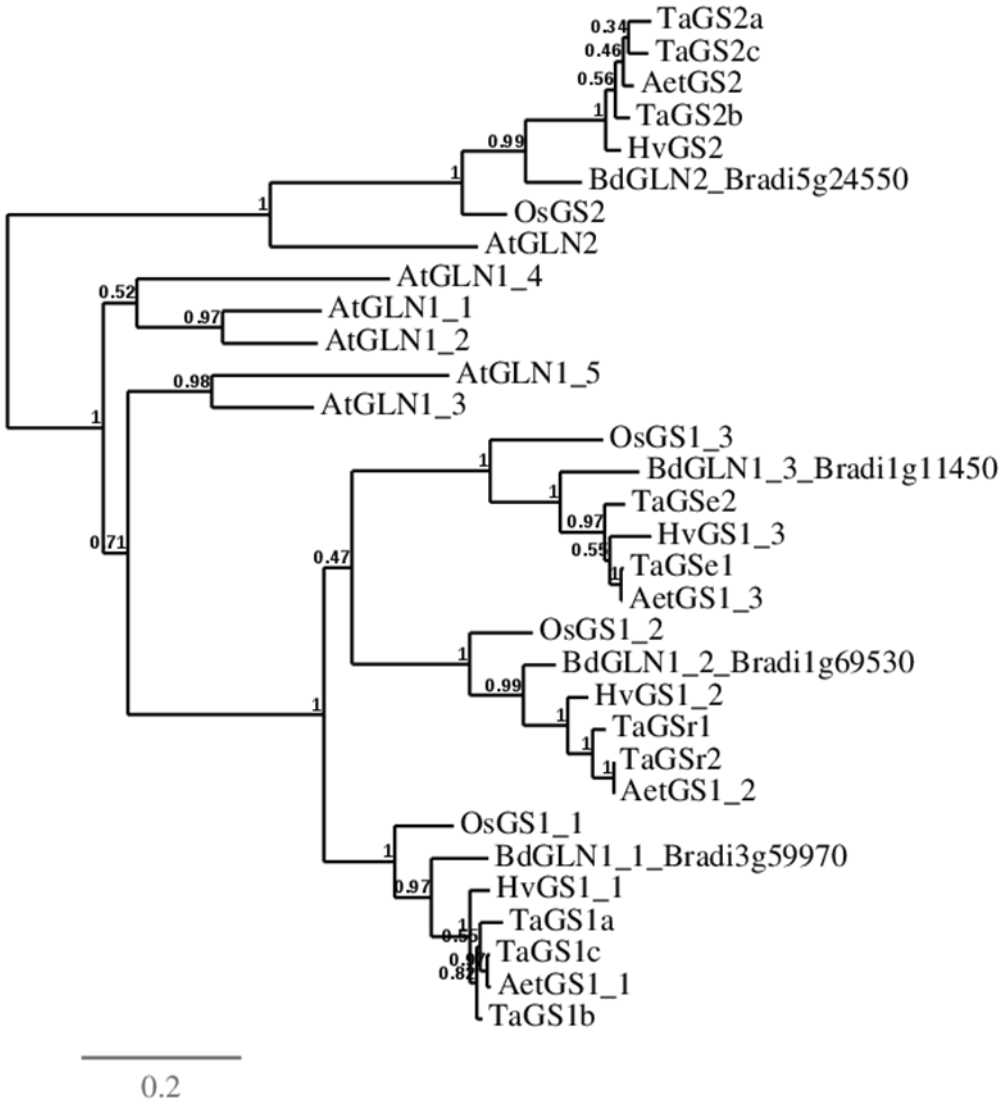

Figure S1.4. Phylogenetic tree of glutamine synthetase genes.

Six plant species were used *Oryza sativa* (Os), *Arabidopsis thaliana* (At), *Aegilops tauchii* (Aet), *Hordeum vulgare* (Hv), *Triticum aestivum* (Ta), and *Brachypodium distachyon* (Bd). The genes used for the analysis are *OsGS1;1* (AB037595), *OsGS1;2* (AB180688), *OsGS1;3* (AB180689), *OsGS2* (X14246), *AtGLN1;1* (At5g37600), *AtGLN1;2* (At1g66200), *AtGLN1;3* (At3g17820), *AtGLN1;4* (At5g16570), *AtGLN1;5* (At1g48470), *AtGLN2* (At5g35630), AetGS1;1 (XM_020314490) AetGS1;2 (XM_020336960), AetGS1;3 (XM_020323172), AetGS2 (XM_020309033), *HvGS1;1* (JX878489), *HvGS1;2* (JX878490), *HvGS1;3* (JX878491), *HvGS2* (AK360336), *TaGS1a* (DQ124209), *TaGS1b* (DQ124210), *TaGS1c* (DQ124211), *TaGSr1* (AY491968), *TaGSr2* (AY491969), *TaGSe1* (AY491970), *TaGSe2* (AY491971), *TaGS2a* (DQ124212), *TaGS2b* (DQ124213), *TaGS2c* (DQ124214). Bd genes are shown in the tree with their respective codes. Numbers indicate branch support values.

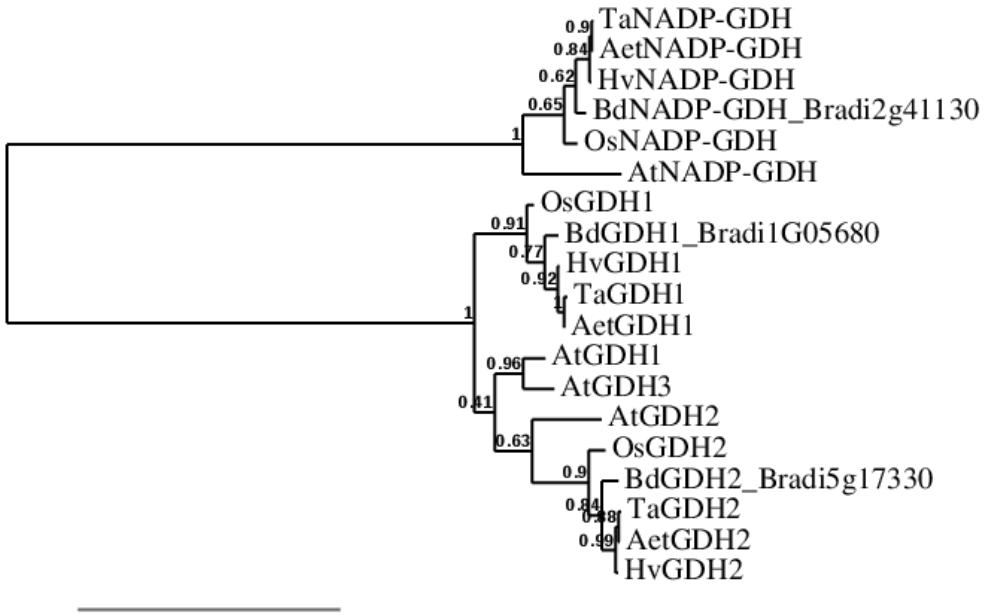

Figure S1.5. Phylogenetic tree of glutamate dehydrogenase genes.

Six plant species were used *Oryza sativa* (Os), *Arabidopsis thaliana* (At), *Aegilops tauchii* (Aet), *Hordeum vulgare* (Hv), *Triticum aestivum* (Ta), and *Brachypodium distachyon* (Bd). The genes used for the analysis are *OsGDH1* (AB024962), *OsGDH2* (AB189166), *OsNADP-GDH* (XM_015764008), *AtGDH1* (At1g51720), *AtGDH2* (At5g07440), *AtGDH3* (At3g03910), *AtNADP-GDH* (At1g51720), *AetGDH1* (XM_020327456), *AetGDH2* (XM_020324446), *AetNADP-GDH* (XM_020298560), *HvGDH1* (AK369720), *HvGDH2* (AK366146), *HvNADP-GDH* (AK369992). For wheat a gene representative of each GDH type was selected *TaGDH1 (*AK449125*)*, *TaGDH2* (AK331666) and *TaNADP-GDH* (AK455316). Bd genes are shown in the tree with their respective codes. Numbers indicate branch support values.

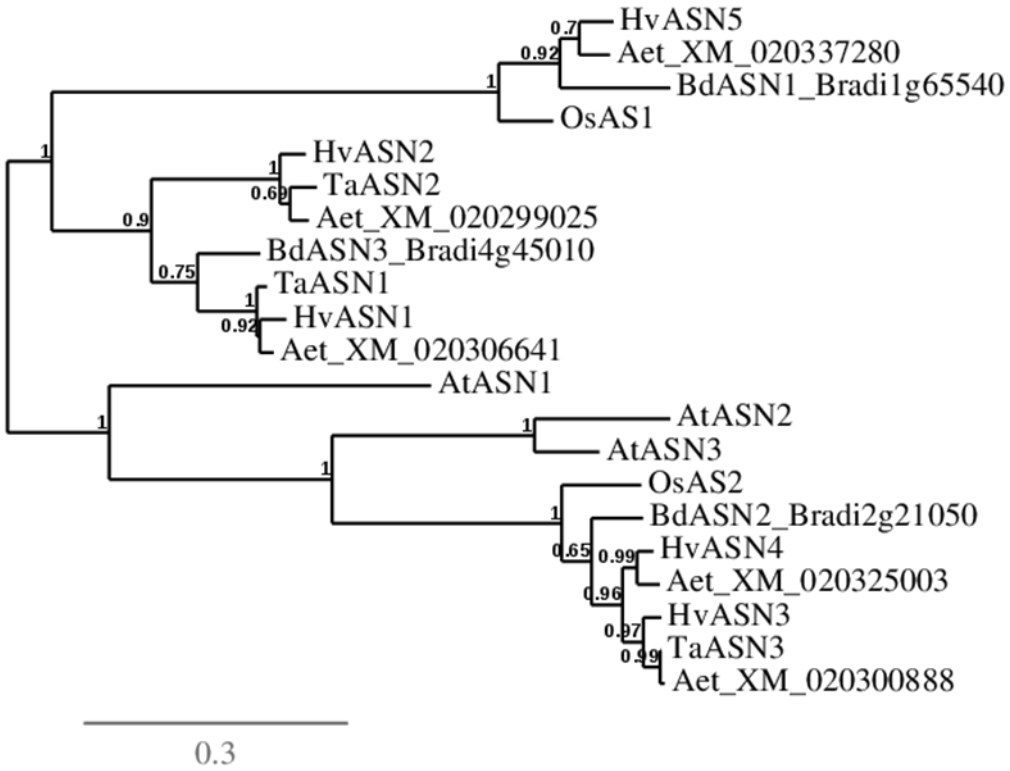

Figure S1.6. Phylogenetic tree of asparagine synthetase genes.

Six plant species were used *Oryza sativa* (Os), *Arabidopsis thaliana* (At), *Aegilops tauchii* (Aet), *Hordeum vulgare* (Hv), *Triticum aestivum* (Ta), and *Brachypodium distachyon* (Bd). The genes used for the analysis are *OsAS1* (XM_015776603), *OsAS2* (XM_015787697), *AtASN1* (At3g47340), *AtASN2* (At5g65010), *AtASN3* (At5g10240), *HvASN1* (AK359770), *HvASN2* (AK357350), *HvASN3* (AK353762), *HvASN4* (AK363899), *HvASN5* (AK361923), *TaASN2* (KY937996), *TaASN1* (KY937995), *TaASN3* (KY937997), the five *AetASN* genes found in the databases are shown with their gene codes in the tree. Bd genes are shown in the tree with their respective codes. Numbers indicate branch support values.

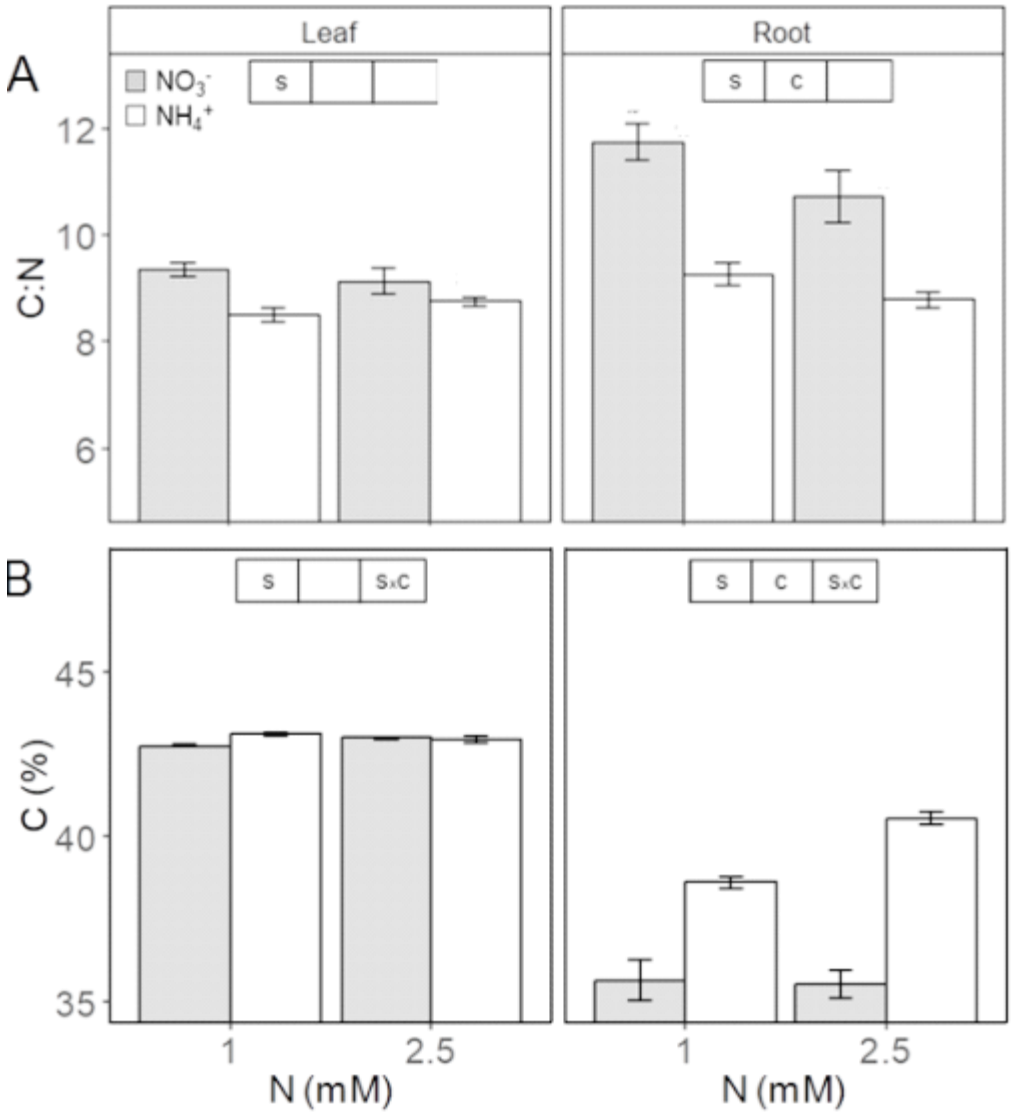

Figure S1.7. C:N ratio and carbon content of leaf and root of *B. distachyon* grown for 24 days with nitrate or ammonium as N source. (A) C:N ratio. (B) Carbon content. Values represent mean ± SE (n = 4). Significant differences according to two-way ANOVA are indicated by S for N source effects, C for N concentration effects and SxC for interactions ($P < 0.05$).

CHAPTER 2

Root proteomics reveal that ammonium nutrition influences *Brachypodium distachyon* response to iron availability

1. ABSTRACT

B. distachyon has revealed as a highly suitable tool for the study of the physiological, molecular and genetic basis of ammonium nutrition in cereals. The root behaves as a physiological barrier preventing ammonium translocation to aerial parts. To do so, key metabolic adaptations occur, among others, to sustain ammonium (NH_4^+) assimilation into organic compounds. To deep into the molecular changes occurring in this organ, a comparative proteomic approach was carried in roots of plants grown under ammonium or nitrate nutrition with 2.5 mM or 1 mM N supply. Among others, the proteome data confirmed the adjustment of carbon and nitrogen metabolisms, but identified other processes potentially participating in root response to ammonium nutrition such as cell wall biogenesis and cell redox balance. Interestingly, a great number of proteins associated with iron homeostasis were predominant in ammonium compared to nitrate nutrition, notably those participating in methionine cycle and phytosiderophores synthesis. Indeed, we confirmed that ammonium nutrition induced de accumulation of phytosiderophores in relation with a concomitant increase in Fe and Zn accumulation in the roots. Besides, we analyzed the impact of the N-source in plant response to changes in Fe availability in the nutrient solution and evidenced a higher sensitivity of ammonium-fed plants to limited Fe availability respect to nitrate-fed plants. This behavior could be related with an increased NH_4^+ accumulation in the tissues and with impaired Fe translocation to the aerial part. Future research are necessary to further understand the mechanistic underlying the interaction between the N-source and the Fe and Zn. Notably, both micronutrients are key for the quality of cereal grains.

2. INTRODUCTION

B. distachyon has been described as a highly suitable tool for the study of the physiological, molecular and genetic basis of ammonium nutrition in cereals, as shown in chapter 1 (De la Peña *et al*., 2019). The metabolic response of *B. distachyon* to ammonium nutrition occurred mostly in the root, as also shown in other monocot species like wheat (Setién *et al*., 2013) or sorghum (Miranda *et al*., 2016). The root behaves as a physiological barrier preventing NH_4^+ translocation to aerial parts, as indicated by a sizeable NH_4^+ accumulation and assimilation increase. The continuous high NH_4^+ assimilation rate required the tuning of the TCA cycle and its associated anaplerotic pathways to match the demand of ketoacids for Gln and Asn synthesis (Chapter 1; De la Peña *et al*., 2019).

To further study *B. distachyon* root adaptation to ammonium nutrition in this chapter a proteomic analysis was conducted to identify molecular players helpful to gain insight on the

molecular mechanism of *B. distachyon* ammonium response. Recent studies have explored root proteome response to ammonium nutrition in different species such as *Medicago truncatula* (Royo *et al*., 2019), *Arabidopsis thaliana* (Coleto *et al*., 2019; Menz *et al*., 2016) or maize (Prinsi and Espen, 2018). Although important differences appear among species, as expected, these proteomic studies found that nitrogen assimilation and carbon metabolism were regulated by the nitrogen source. Common responses in these studies also include alterations in proteins involved in cell redox and the phenylpropanoid metabolism associated to cell wall biogenesis.

B. distachyon cell wall content and vascular anatomy are similar to economically important C3 grasses (Bouvier d'Yvoire *et al*., 2013, Matos *et al*., 2013). For instance, *B. distachyon* has been used to model the transcriptional regulation of the cell wall in grasses (Handakumbura and Hazen, 2012). The fact that under ammonium nutrition plants are reported to alter the cell wall deserves further studies since it may represent a nutritional strategy to enhance bioenergy-related traits in grasses.

Apart from N, plants need 15 other essential nutrients to complete their life-cycle. These nutrients interact between each other and genetic, physiological and biochemical interactions among elements have been reported (Bouain *et al*., 2019). In particular, the N source is known to interact with the acquisition and homeostasis of other macronutrients and also micronutrients. For instance, it has been extensively reported that plants grown under ammonium nutrition display lower content of cations such as K^+, Ca^{2+} and Mg^+ respect to nitrate nutrition because of their direct competition with the uptake of NH_4^+ (Van Beusichem *et al*., 1988; Serna *et al*., 1992; Roosta and Schjoerring, 2007). As shown in chapter 1, this is also the case for *B. distachyon,* since under ammonium nutrition presented a diminished content of these cations compared to nitrate nutrition (Chapter 1; De la Peña *et al*., 2019). Notably, when K^+ availability is limiting the exogenous application of K^+ has been shown to greatly mitigate ammonium stress symptoms (Balkos *et al*., 2010; Li *et al*., 2012). As another example of N source interaction with other nutrients, molecular players that connect nitrate signaling to P deficiency have been identified, such as the NO_3^- transporter NPF7.3/NRT1.5 (Cui *et al*., 2018) or the transcription factor HRS1 (hypersensitive to low Pi-elicited primary root shortening (Medici *et al*., 2015) an, at the same time NH_4^+ promotes P remobilization of the cell wall (Zhu *et al*., 2016). The N source also interacts with S, for instance, ammonium nutrition enhances sulphate assimilation and uptake (Van Beusichem *et al*., 1998; Gerendás *et al*., 1997; Coleto *et al*., 2017). Overall, the N source interaction with macronutrients is clear and their study has attracted important interest. However, less attention has been paid to the interaction between the N source and micronutrients homeostasis.

In another line of evidence of N source interaction with other nutrients, H^+ production during NH_4^+ assimilation leads to enhanced net extrusion of H^+ and thus to the acidification of the rhizosphere (Van Beusichem *et al*., 1988). Particularly in neutral and alkaline soils, this acidification may increase the availability of some macronutrients, such as phosphate (Gahoonia *et al*., 1992) or micronutrients such as Fe or Mn (Thomson *et al*., 1993). Regarding Fe, recent works have provided support for the interaction between NH_4^+ and Fe homeostasis in rice (Zhu *et al*., 2018) and Arabidopsis (Zhu *et al*., 2019), suggesting that NH_4^+ somehow promotes the release of Fe bound to the cell wall, notably hemicellulose.

Fe is an essential micronutrient for plant growth as well as for human nutrition. Fe is an important determinant in building prosthetic groups of proteins such as Fe-S clusters and hemo groups, which makes Fe participate in many essential plant functions (e.g. chlorophyll synthesis, electron transfer between PSI and PSII). Thus, any defect in Fe availability has a great impact in plant growth and quality (Briat *et al*., 2015). Although Fe is one of the most abundant micronutrients in soils, often it cannot be used by plants because it is present as insoluble complexes with low bioavailability, particularly in calcareous/alkaline soils since Fe is hardly soluble at pH higher than 7.4 (Lindsay and Schwab, 1982; Briat *et al*., 2015). To face this limitation, plants have developed two strategies to make Fe soluble. Most flowering plants display the named Strategy I or reduction-based strategy. However, only graminaceous species, and thus *B. distachyon*, display the so-called Strategy II or chelation-based strategy. Exceptionally, rice has acquired a combined strategy (Ricachenevsky and Sperotto, 2014). Strategy I is a three-step process that starts with proton release from the roots to increase local Fe^{3+} solubility. Ferric form (Fe^{3+}) is reduced to ferrous ion (Fe^{2+}) by a plasma membrane-bound ferric reductase and then Fe^{2+} is taken up by the root via IRT transporters (iron-regulated transporter) (Hindt and Guerinot, 2012; Kobayashi *et al*., 2019). In Strategy II, graminaceous plants synthesize compounds of the mugineic acid family called phytosiderophores (PS) that are released into the rhizosphere via TOM1 (transporter of mugineic acid family phytosiderophores 1). Mugineic acid compounds (MAs) derive from nicotianamine (NA) and bind Fe^{3+} with high affinity forming Fe^{3+}-PS complexes that enter into root cells by a Yellow Stripe/Yellow Stripe-Like (YS/YSL) transporters. Once inside the plant, Fe^{3+} binds other compounds to be translocated to the rest of the plant. Carboxylates (notably citric acids), NA, MAs and phenolic compounds are involved in Fe^{3+} translocation (Kobayashi *et al*., 2019).

Both Fe uptake strategies are induced upon iron deficiency (Hindt and Guerinot, 2012; Kobayashi *et al*., 2019). In Strategy II, Fe deficiency stimulates the synthesis of NA and MAs. NA is synthesized by NA synthase (NAS) from the combination of three units of S-

adenosylmethionine (SAM). SAM is an abundant co-factor in plant metabolism and is the precursor of many other biomolecules such as polyamines and ethylene. In these reactions, e.g. NA synthesis, 5-methylthioadenosine (MTA) is released and can be recycled again to Met or SAM thanks to the Met cycle, also known as Met salvage cycle or Yang cycle in plants (Kobayashi *et al*., 2005; Sauter *et al*., 2013). The increase of SAM synthesis leads, among others, to increased synthesis of ethylene and NA (Li and Lan, 2017). Indeed, Met cycle is highly active in the root and it is also induced under Fe deficiency to enable this organ to meet the increased demand of SAM required for the synthesis of MAs (Ma *et al*., 1995; Kobayashi *et al*., 2005; Li and Lan, 2017).

In the present chapter we aimed to better understand the root physiology in plants grown with ammonium as a sole source of N. To do so, we engaged a proteomic approach that revealed several processes potentially involved in root adaptation to ammonium nutrition respect to plants fed with nitrate. Among others, cell wall biogenesis, carbon and nitrogen metabolism and cell redox balance were affected by the nutrition type. Importantly, we found a great number of proteins associated to iron homeostasis, notably in relation with Met cycle and PS synthesis. In this sense, we hypothesized that NH_4^+ could be playing a role in the control of Fe homeostasis in *B. distachyon* and thus, we focused on the study of the interaction between ammonium nutrition and Fe homeostasis.

3. EXPERIMENTAL DESIGN AND STATISTICAL ANALYSIS

Growth conditions for the proteome analysis were as described in section 3 of chapter 1. To study the interaction between ammonium nutrition and Fe homeostasis *B. distachyon* Bd21 seeds were treated following the methodology described in Tyler *et al*. (2016). Seeds were peeled by removing the lemma, washed for 4 min in a solution containing 15 % bleach plus 0.1 % Triton-X 100 (Sigma-Aldrich) and thoroughly rinsed with sterile deionised water. To synchronise germination, seeds were placed in Petri dishes on damp paper towels and stratified in the dark at 4°C for 7 days. After stratification, the plates covered with aluminum foil were transferred into a growing chamber for 3 days. Germinated seeds were then sowed in trays filled with perlite:vermiculite (1:1) misted with deionised water. After 7 days, seedlings with a uniform appearance were transferred to hydroponic tanks filled with 4.5 L of nutrient solution (10 plants/tanks) with a 2.5 mM N provision in the form of NO_3^- or NH_4^+. Plants grew in hydroponic conditions during 19 days. The interaction between nitrogen and Fe nutrition was studied supplying different Fe(III)EDTA-treatments to the nutrient solutions either with ammonium or nitrate. Fe(III)EDTA-treatment consisted of free-NaFe(III)-EDTA or 0.01 mM NaFe(III)-EDTA for deficiency (D) or moderate Fe deficiency (MD), respectively 0.1 mM NaFe(III)-EDTA for Fe control

conditions, and 2.5 mM NaFe(III)-EDTA for Fe toxicity (T). During the first 7 days, treatments of Fe deficiency were grown in the same nutritional regime with optimal Fe supply (0.1 mM NaFe(III)-EDTA). At 7th day, Fe control plants were kept under the same conditions, but Fe was removed for deficiency treatments (D) or supplied at 0.01 mM for moderate deficiency (MD). For Fe toxicity treatment the plants were provided with 2.5 mM Fe since the transfer of seedlings to hydroponic tanks. As in chapter 1, to maintain the pH and the concentration of mineral elements of the hydroponic medium constant, the nutrient solution was replaced three times on days 7, 11 and 15. After every change, the stability of pH in the nutrient solution was confirmed. The plants were harvested between 10 and 12 a.m. Shoots and roots were separated and individually weighed. Plants grown within the same tank were pooled, immediately frozen in liquid nitrogen, homogenized in a Tissue Lyser (Retsch MM 400) and stored at -80 °C until use. Three tanks were set up per treatment, 10 plants/tank, thus a total of 30 plants were grown for each condition.

Statistical analysis

All the results presented are given as means with standard errors. Data were analysed with SPSS 17.0 (Chicago, IL, USA) or R software v. 3.4.4. Normality and homogeneity of variance were analysed by Kolmogorov–Smirnov and Levene's tests. Statistical analysis for proteomics analysis was performed as described in general materials and methods section. For the rest of data two-way ANOVA was used for multiple comparisons, while for paired comparison of independent samples t-student test was performed.

4. RESULTS

A label-free quantitative proteomic analysis was used to analyze the relative abundance of proteins in *B. distachyon* roots grown under four different conditions, with ammonium or nitrate supplied at 1 or 2.5 mM concentration. A total of 4506 distinct proteins were identified with a false discovery rate (FDR) < 1 % (Table S2.1). For quantification, only proteins identified in the three replicates of, at least, one condition were selected. Following these criteria, 4109 were quantified (Table S2.1). Principal component analysis (PCA) and hierarchical clustering demonstrated a strong correlation among the replicates within each N treatments, with greater homogeneity among replicates for 1 mM N treatments (Figure S2.1 and S2.2). N source treatments were separated along PC1 and N concentration along PC2. Besides, the effect of the source was more evident at 2.5 mM N dose, these two treatments being more distant to 1 mM N concentration (Figure S2.1). Four comparisons were made to analyze, on one hand, the effect of the N source and, on the other hand, that of the N concentration. Volcano plots resume the

proteins quantified for each comparison and highlight the differentially abundant proteins (DAP) between groups with a significant level of $p < 0.05$ and 1.5-fold change (FC) cut-off (Figure S2.3).

When comparing the effect of the N concentration within each N source we found that under nitrate nutrition 128 proteins were affected by the N dose with 48 DAPs showing higher abundance at 2.5 mM and 80 proteins at 1 mM. The N dose had greater effect under ammonium nutrition and 243 DAPs were found, 126 DAPs with higher abundance at 2.5 mM and 117 more abundant at 1 mM. Only, 19 proteins were significantly regulated by the N dose regardless the N source (Figure 2.1; Table S2.1).

Regarding the N source effect, and in agreement with the PCA, the number of DAPs is much higher with 2.5 mM N supply compared with 1 mM N. With 2.5 mM, 475 proteins showed differential abundance. Among them, 243 showed higher abundance in roots of ammonium-grown plants, whereas 232 showed a higher abundance in roots of nitrate-grown ones (Figure 2.1B, Table S2.1). With 1mM, 195 DAPs were found, 142 being more abundant in ammonium condition and 53 in nitrate condition. Regarding proteins commonly regulated in both comparison (72 DAPs), 47 DAPs were always more abundant under ammonium nutrition and 25 under nitrate nutrition (Figure 2.1; Table S2.1, Table S2.2).

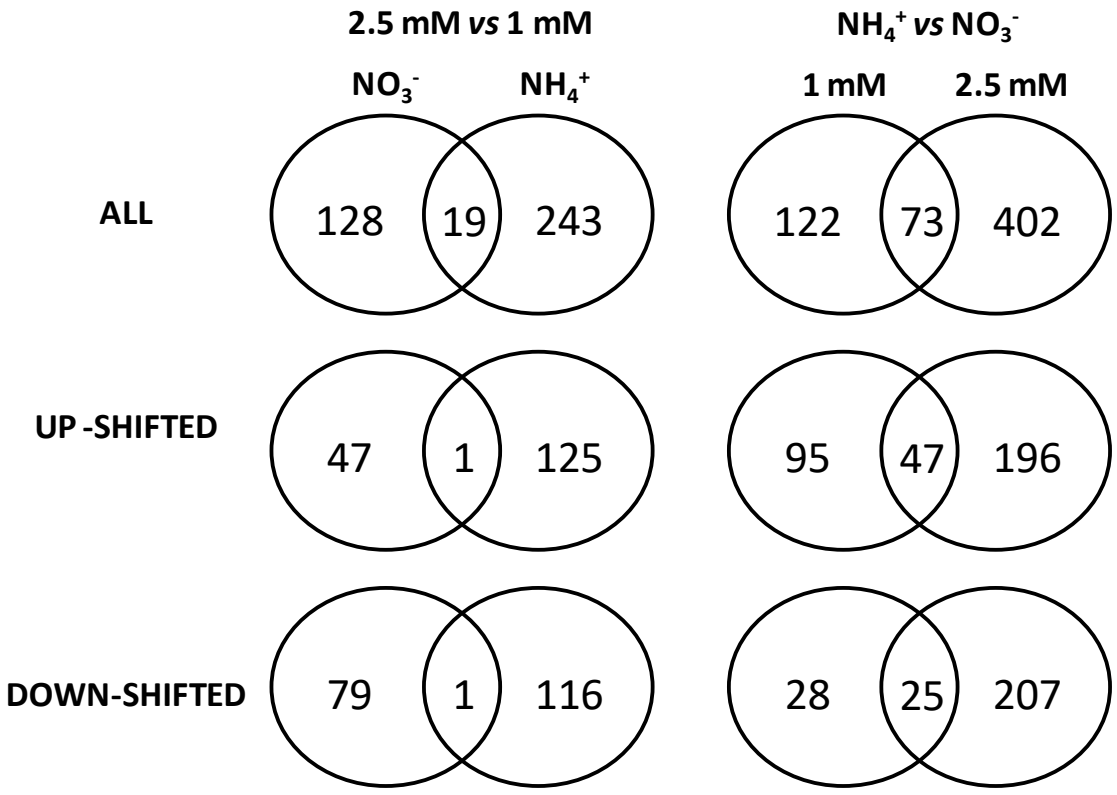

Figure 2.1. Venn diagrams showing the number of differentially abundant proteins identified for the comparison of different nutritional conditions in roots of *B. distachyon*.

Gene ontology functional classification of the differentially abundant proteins

As a first exploratory approach of the data obtained with the proteomic study, we analysed the DAPs of the four comparisons using the PANTHER classification system (PANTHER 14.1; www.pantherdb.org) and classified them following the three classic ontologies: biological process, cellular component and molecular function. The more general categories/terms are shown in Figures 2.2 and 2.3 and the more specific ones are described in Table S2.3. Regarding biological process, the greatest number of proteins was classified into "metabolic process", category, followed by "cellular process", "biological regulation" and "localization". As ammonium nutrition is considered a stressful situation also an important number of DAPs were associated to "response to stimulus" notably when comparing ammonium at 2.5 mM concentration (Figures 2.2, 2.3). Molecular component ontology revealed a great number of enzymes (category "catalytic activity") among the DAPs discovered together with an important amount of proteins associated to "binding" and "transporter activity" (Figures 2.2, 2.3).

To further understand the proteome changes observed, we performed a gene ontology enrichment analysis focused on biological process ontogeny across the four comparisons between N treatments (Figures 2.4, 2.5, S2.4, S2.5; Table S2.4). In agreement with the fact that 2.5 mM NH_4^+ represents a stressful situation for *B. distachyon* (Chapter 1, De la Peña *et al*., 2019) most of the enriched categories were found when comparing NH_4^+ vs. NO_3^- at 2.5 mM N and 2.5 mM vs. 1 mM for NH_4^+ nutrition, finding 139 (68 with the up-shifted and 71 with the down-shifted DAPs) and 103 enriched processes/terms (59 with the up-shifted and 44 with the down-shifted DAPs), respectively (Table S2.4). Among the significantly enriched processes/terms found some are very general and often comprise more specific, and also enriched, processes that form groups of processes/terms (Table S2.4). In general, most of the information is obtained from the more specific terms rather than with higher-level terms. Thus, we concentrated in the most specific terms within each group (Figures 2.4, 2.5, S2.4, S2.5; Table S2.4). Importantly, many similarities were found between both comparisons at 2.5 mM NH_4^+ vs. NO_3^- and NH_4^+ 2.5 mM vs. 1 mM because in both cases we are comparing a situation where ammonium stress is taking place (2.5 mM NH_4^+) vs. a non-stressful situation (2.5 mM NO_3^- or 1 mM NH_4^+). Indeed, both comparisons shared an important number of DAPs (167) (Figure S2.5, S2.6, Table S2.3).

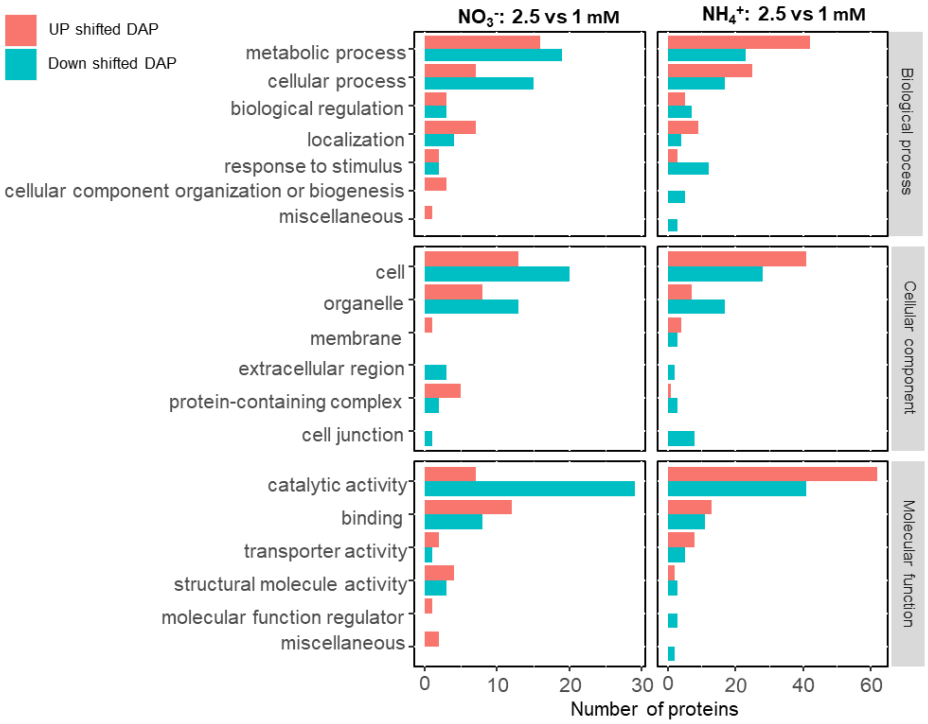

Figure 2.2. Gene ontology classification of the DAPs found when comparing N concentration within each N source. Classification was done based on three ontologies: biological process, cellular component and molecular function.

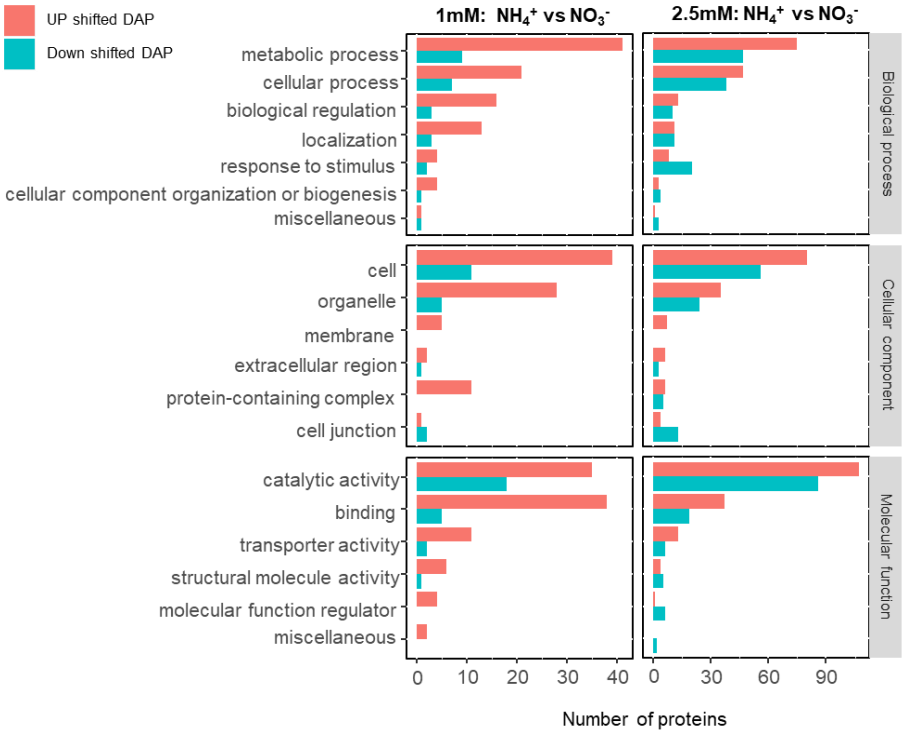

Figure 2.3. Gene ontology classification of the DAPs found when comparing N source within each N concentration. Classification was done based on three ontologies: biological process, cellular component and molecular function.

Gene ontology enrichment analysis of the differentially abundant proteins

Most of the enriched categories were related to carbon and nitrogen metabolism, sulphur/Met metabolism, cell redox balance, cell wall biogenesis and metabolism and ion homeostasis, notably iron. Ammonium nutrition is known to stimulate NH_4^+ assimilation supported by the TCA cycle (Chapter 1); in agreement, the categories related to carbon and nitrogen metabolism (e.g. glycolytic process, glutamine metabolic process or carboxylic acid catabolic process) were mostly found when analyzing the DAPs with higher abundance in 2.5 mM NH_4^+ (Figures 2.4, 2.5). Specifically looking for example to classic enzymes related to NH_4^+ assimilation in 2.5 mM: NH_4^+ vs NO_3^- comparison, we found that chloroplastic glutamine synthetase (I1J2T4) showed lower abundance in 2.5 mM NH_4^+. In contrast, an asparagine synthetase isoform (I1IV86) and a glutamate dehydrogenase 2 (I1J084) were more abundant in 2.5 mM NH_4^+. Regarding enzymes connected to C metabolism, among others, pyruvate kinase (I1HEH4), a cytosolic triose phosphate isomerase (I1HC04), hexokinase (A0A0Q3IMN1) and citrate synthase (I1HYA2) were up-shifted in 2.5 mM NH_4^+ (Tables S2.1, S2.3)

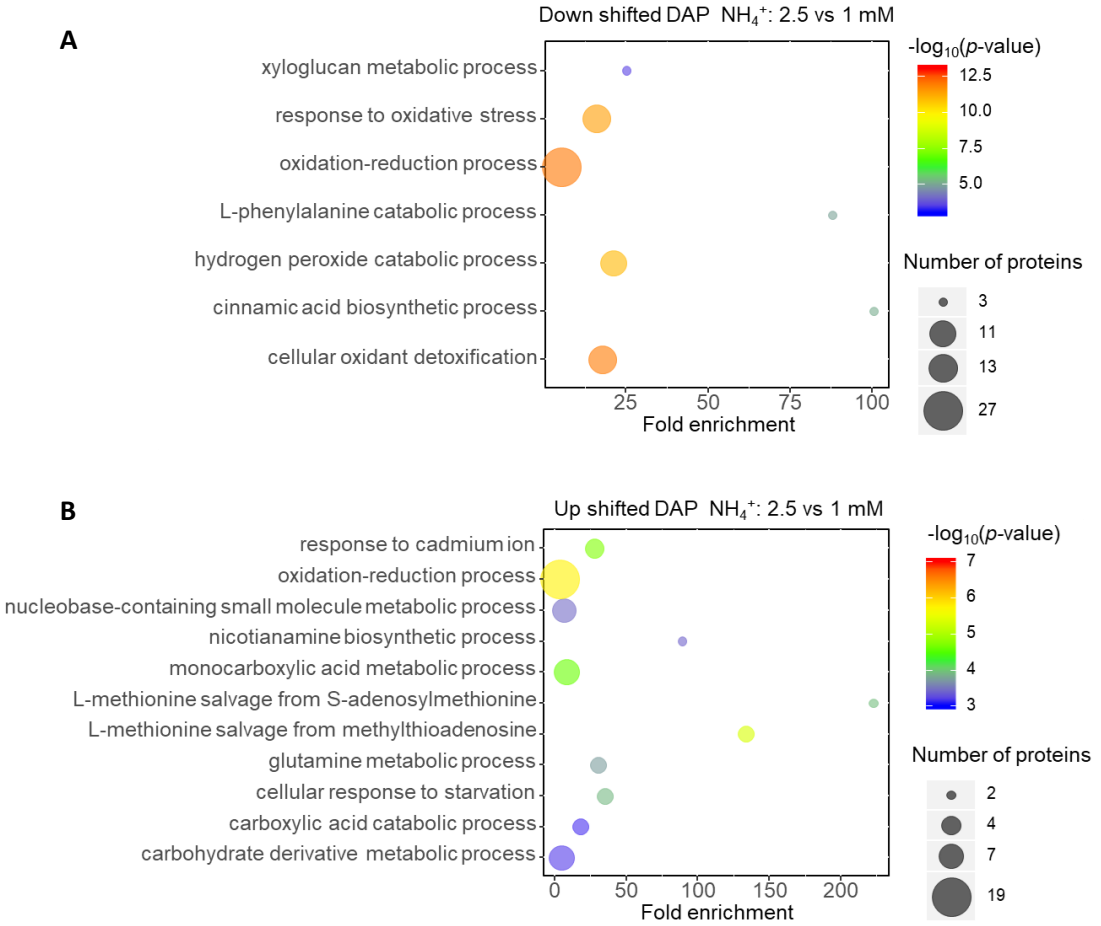

Figure 2.4. Gene ontology enrichment analysis of down-shifted (A) and up-shifted (B) DAPs in 2.5 vs. 1 mM NH_4^+ comparison in *B. distachyon* roots. The fold enrichment is the ratio of the number of DAPs observed over the expected number of proteins associated to a particular category/term based in the reference proteome. Only the more significant specific categories/terms are represented. The full list is available in the Table S2.4.

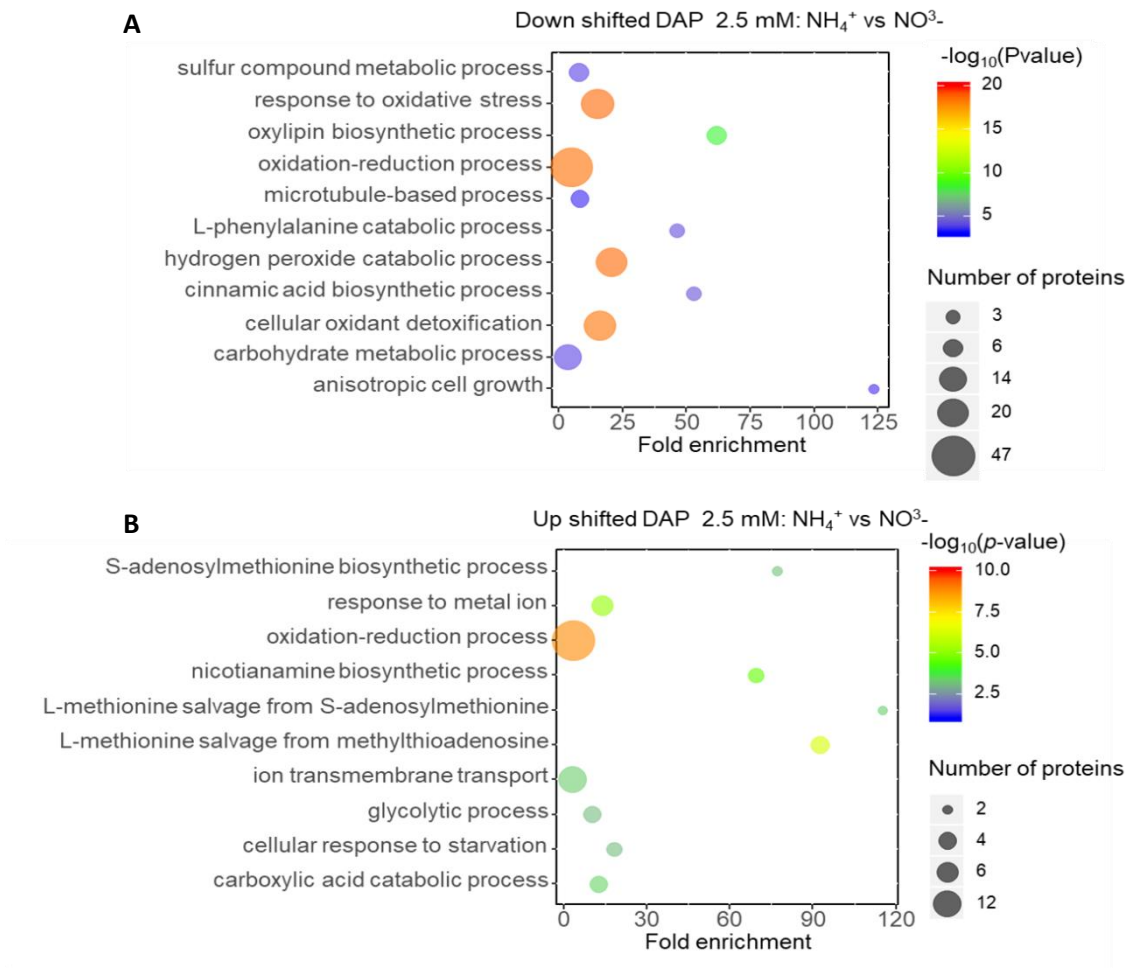

Figure 2.5. Gene ontology enrichment analysis of down-shifted (A) and up-shifted (B) DAPs in 2.5 mM, comparing ammonium *vs.* nitrate nutrition in *B. distachyon* roots. The fold enrichment is the ratio of the number of DAPs observed over the expected number of proteins associated to a particular category/term based in the reference proteome. Only the more significant specific categories/terms are represented. The full list is available in the Table S2.4.

Categories related to the cell wall metabolism and biogenesis were found in the enrichment test performed with the down-shifted DAPs, comparing 2.5 mM NH_4^+ vs. 2.5 mM NO_3^- and also 2.5 mM NH_4^+ vs 1mM NH_4^+ (e.g. xyloglucan metabolic process, cinnamic acid biosynthetic process) (Figures 2.4, 2.5). For instance, three phenylalanine ammonia-lyase involved in the biosynthesis of lignin were found down-shifted in both comparisons (I1IZQ0, I1IBR8, I1IBR6) (Tables S2.1, S2.3). Besides, three xyloglucan endotransglucosylase/hydrolases were down-shifted in 2.5 mM NH_4^+ respect to 1 mM NH_4^+ (I1I257, I1GTU3, I1I258). Cell wall peroxidases play an active role in the polymerization of lignin and redox processes are also associated with cell wall loosening (Tenhaken, 2015). In this line, this could be in relation with the categories related to cell redox balance (e.g. oxidation-reduction process, response to oxidative stress or cellular oxidant detoxification) that were mostly found with the DAPs showing lower abundance in 2.5 mM NH_4^+ (Figures 2.4, 2.5). For instance, an important number of peroxidases, mostly including non-specific peroxidases but also an ascorbate peroxidase (I1H6P1), appeared as less abundant in

2.5 mM NH_4^+ respect to 2.5 mM NO_3^- (Tables S2.1, S2.3). Also a number of DAPs related with glutathione were found; in particular, several glutathione-S-transferases were found more abundant in 2.5 mM NH_4^+ condition, as it has also been highlighted in previous proteomic analysis of plants grown under ammonium nutrition (Prinsi and Espen, 2018; Coleto *et al*., 2019; Royo *et al*., 2019).

Ion transport was affected by ammonium stress since among the DAPs a number of ion transporters appeared. In agreement with the nutrition type, high-affinity nitrate transporters (I1IB70, I1HW98) were down-shifted in 2.5 mM ammonium-fed plants, while ammonium transporter 1;2 was up-shifted (I1IBN3). In contrast, two NRT1/PTR family transporters were also up–shifted in ammonium-fed plants. This could be related to the reported nitrate-independent function of Arabidopsis NRT1;1 in the alleviation of ammonium toxicity (Hachiya and Noguchi, 2011; Jian *et al*., 2018). The higher abundance of potassium transporter 1-like (A0A0Q3P0Y8), homolog to barley HvHAK1 also reported as induced upon ammonium nutrition (Fulgenzi *et al*., 2008), may be trying to compensate the lower tissue K content (Chapter 1). In addition, among others, a Mg transporter (A0A0Q3EIQ9), two Cu transporters (copper transporter 5.1, I1IQG8; probable copper-transporting ATPase HMA5, I1HYC6), and a metal transporter Nramp2 (I1H8C0) were also more abundant with 2.5 mM NH_4^+ supply respect to 2.5 mN NO_3^- supply.

When the highest ammonium concentration in the nutrient solution was considered in the comparisons, this is both in 2.5 mM NH_4^+ vs 2.5 mM NO_3^- and 2.5 mM NH_4^+ vs 1mM NH_4^+, the up-shifted categories with the highest fold enrichment were related to the Met cycle and nicotianamine biosynthesis ("L-methionine salvage from methylthioadenosine", "S-adenosylmethionine biosynthetic process" and "nicotianamine biosynthetic process" categories). Notably, as shown in Figure 2.6, almost every protein of the Met cycle was up-shifted in the ammonium stress condition. Met cycle and nicotianamine biosynthesis are related with the uptake of metals, notably Fe and Zn (Kobayashi *et al*., 2005). Looking deeper into the full list of DAPs (Table S2.1) an important number of proteins related to Fe homeostasis were found regulated (Table 2.1). Besides, "sulfur compound metabolic process" category was highlighted in 2.5 mM NH_4^+ vs. 2.5 mM NO_3^- comparison (Figure 2.5A). S-adenosylmethionine (SAM), in addition of being the precursor of mugineic acids (MAs), it is also the precursor of ethylene; indeed, 1-aminocyclopropane-1-carboxylate oxidase (I1IMV2), in charge of ethylene synthesis, was also up-shifted under ammonium nutrition. Interestingly, ethylene is also an important signal of Fe deficiency and PS synthesis (Divte *et al*., 2019).

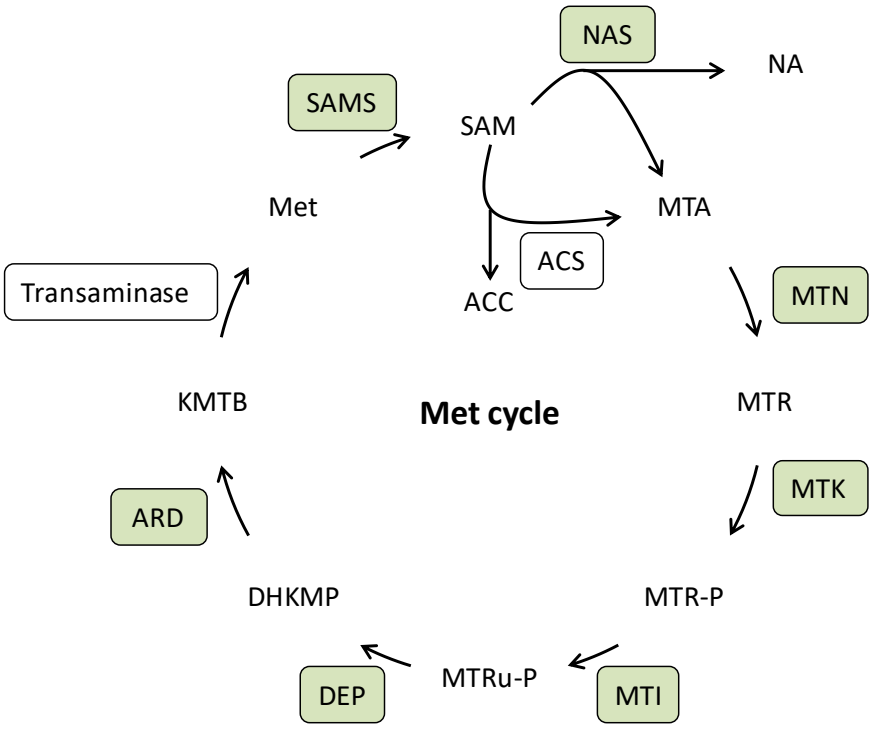

Figure 2.6. The methionine cycle in graminaceous plants. Enzymes are shown in boxes and those found among the DAPs identified in 2.5 mM NH_4^+ vs 2.5 mM NO_3^- in *B. distachyon* roots are shown in green color. Met, methionine; SAM, S-adenosyl-Met; SAMS, S-adenosyl-Met synthetase; NA, nicotianamine; NAS, nicotianamine synthase; MTA, 5-methylthioadenosine; MTN, MTA nucleosidase; MTR, 5-methylthioribose; MTK, 5-methylthioribose kinase; MTR-P, 5-methylthioribose-1-phosphate; MTI, 5 methylthioribose-1-phosphate isomerase; MTRu-P, 5-methylthioribulose-phosphate; DEP, methylthioribulose-1-phosphate dehydratase-enolase-phosphatase; DHKMP, 1,2-dihydro-3-keto-5-methylthiopentene; ARD, acireductone dioxygenase or 2-keto-methylthiobutyric-acid-forming enzyme; KMTB, 2-oxo-4-methylthiobutyrate; Transaminase, putative aminotransferase catalysing the synthesis of Met from 2-keto-methylthiobutyric acid.

Table 2.1. DAPs related to the Met cycle, phytosiderophores synthesis and iron homeostasis found in 2.5 mM NH_4+ vs 2.5 mM NO_3^- and 2.5 mM NH_4^+ vs 1 mM NH_4^+ comparisons in *B. distachyon* roots. The log_2FC values shown in red were not significantly regulated ($p < 0.05$).

			2.5 mM NH_4+ vs 2.5 mM NO_3-	2.5 mM NH_4^+ vs 1 mM NH_4^+
Uniprot ID	**Gene ID**	**Description**	**log_2FC**	**log_2FC**
I1HF18	LOC100843457	S-adenosylmethionine synthase 1	1.22	0.86
I1HF17	LOC100844978	S-adenosylmethionine synthase 3-like	0.99	0.88
I1H1W0	LOC100839737	5'-methylthioadenosine/S-adenosylhomocysteine nucleosidase 2-like	1.00	0.52
I1IMJ2	LOC100834960	methylthioribose-1-phosphate isomerase	1.60	0.68
I1IES2	LOC100828599	probable bifunctional methylthioribulose-1-phosphate dehydratase	1.87	1.03
I1J366	LOC100837535	methylthioribose kinase 2	1.93	1.00
I1GTE3	LOC100837759	1,2-dihydroxy-3-keto-5-methylthiopentene dioxygenase 2	2.15	1.50
I1IAD2	LOC100829217	nicotianamine synthase-like 5 protein	2.50	1.70
I1HZL5	LOC100822873	nicotianamine synthase 2-like	2.52	0.95
I1H680	LOC100832895	probable nicotianamine synthase 2	1.18	0.08
I1HZX5	LOC100831451	nicotianamine aminotransferase A-like	3.60	1.15
I1GYH1	LOC100822209	nicotianamine aminotransferase A-like	0.74	0.41
I1IL44	LOC100841166	nicotianamine aminotransferase A-like	0.68	0.63
I1IUR4	LOC100823408	2'-deoxymugineic-acid 2'-dioxygenase-like	2.67	0.79
I1J071	LOC100826305	probable metal-nicotianamine transporter YSL9-like	3.52	0.26
I1IP67	LOC100837011	ferrochelatase-2, chloroplastic	0.95	0.87
I1H8C0	LOC100845842	metal transporter Nramp2	1.40	0.47
I1IV67	LOC100837024	ferritin-1, chloroplastic	-4.67	-3.60
I1GUN7	LOC100837457	CDGSH iron-sulfur domain-containing protein NEET	-2.41	-2.43
I1HBL2	LOC100825497	Uncharacterized protein (SUF_FeS_clus_asmbl_SufBD)	-1.07	-0.66

Ammonium nutrition enhances the synthesis of phytosiderophores and leads to higher Fe and Zn accumulation

In view of the great amount of up-shifted DAPs found in ammonium stressed plants (2.5 mM NH_4^+) in relation with Met cycle and Fe homeostasis we aimed to further study the potential relationship between ammonium stress and Fe homeostasis in *B. distachyon*. To do so, firstly we decided to confirm the proteome data that suggested the stimulation of the synthesis of MAs analyzing the PS content in roots. We focused on 2.5 mM concentration (NH_4^+ vs NO_3^-) and we measured the content of NA and MAs: avenic acid, mugineic acid, 2´-deoxymugineic acid, 3 -hydroxymugineic acid, distichonic acid A and deoxydistichonic acid A. In addition, we determined glutathione (GSH) content because some studies reported a key role for glutathione in iron metabolism, notably for Fe-S clusters assembly (Kumar *et al*., 2011; Couturier *et al*., 2013). In agreement with the proteome profile, 5 out 6 of the MAs were higher in ammonium nutrition (Figure 2.7). Among them, the content of MA, which represented around 90 % of total MAs content, was 7.6-fold higher upon ammonium nutrition. Moreover, the accumulation of NA was 13.5-fold higher under ammonium respect to nitrate nutrition. Similarly, the content of citrate, Fe chelator, nearly doubled under ammonium nutrition (Figure 2.7). However, the content of Met was significantly lower in ammonium nutrition, meanwhile the content of total glutathione was not affected by the N source (Figure 2.7).

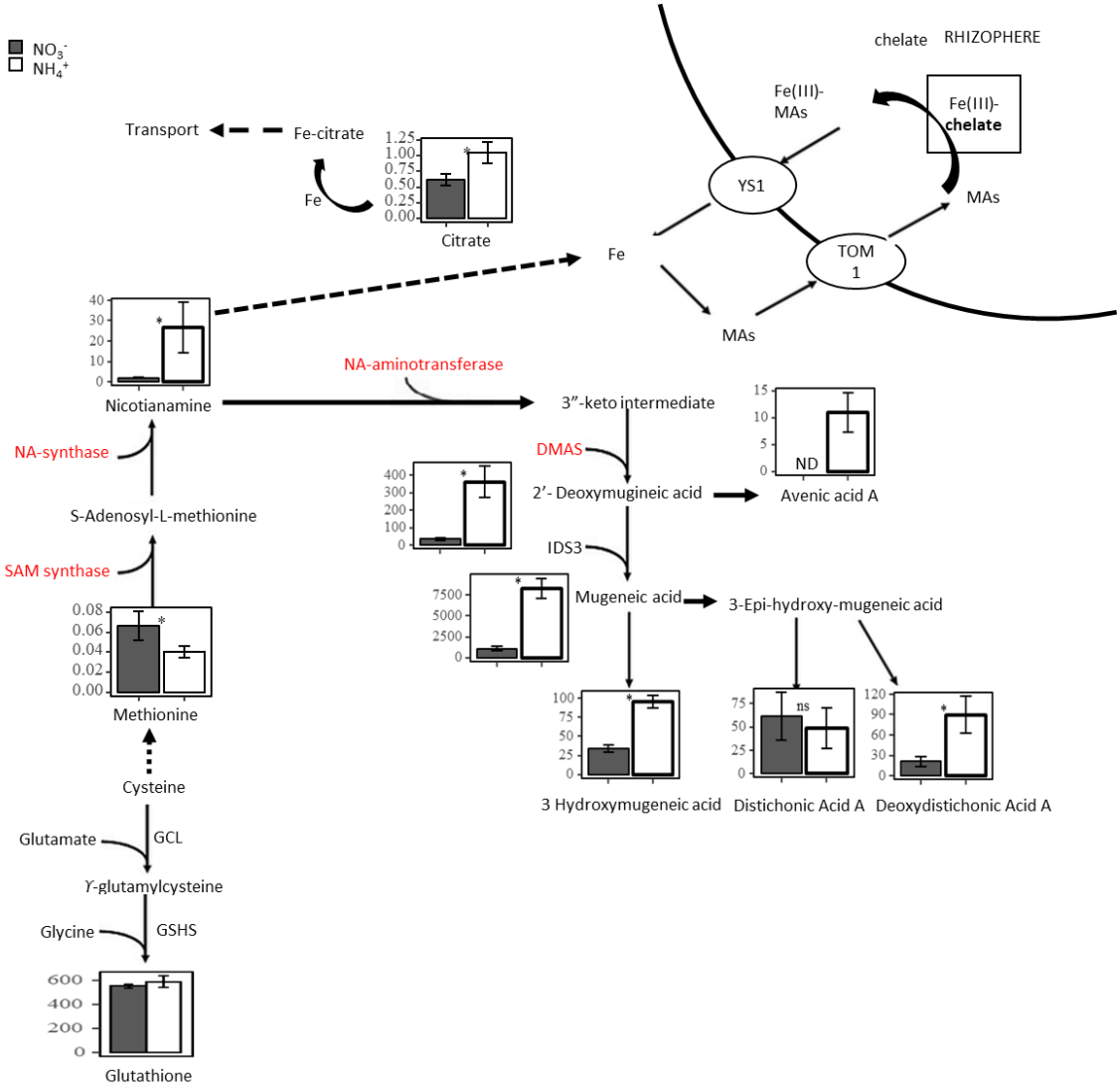

Figure 2.7. Phytosiderophores and metabolites involved in Fe uptake and transport in roots of *B. distachyon* Phytosiderophores (nicotianamine, mugineic acid 2´-deoxymugineic acid, 3-Hydroxymugineic acid, distichonic acid A, deoxydistichonic acid A, and avenic acid), citrate, and total glutathione (expressed as GSSG equivalents) are given as nmol g^{-1} FW. Met is given as µmol g^{-1} FW. Proteins shown in red represent the up-shifted DAPs related to MAs synthesis in the proteomic comparison between 2.5 mM NH_4^+ *vs* 2.5 mM NO_3^-. Met and citrate data correspond to those already presented in chapter 1. Values are the mean ± SE (n = 4). The statistical significance was assessed by t student ($p<0.05$).

Both the proteome data and the PS analysis suggest a potential capacity to increase of Fe uptake under ammonium nutrition. Thus, we determined Fe content in roots and leaves. Moreover, because MAs are also chelators of Zn, we also determined its content. Accordingly, both the content of Fe and Zn was higher in the root of plants grown with 2.5 mM NH_4^+ respect to those grown with NO_3^- (Figure 2.8). In leaves Zn was also accumulated in ammonium-fed plants while no differences were found for Fe (Figure 2.8). MAs synthesis requires an active sulphur assimilation machinery to provide their precursor SAM. In this sense, the content of sulphur and sulphate was increased under ammonium nutrition both at the root and aerial part level (Figure 2.8).

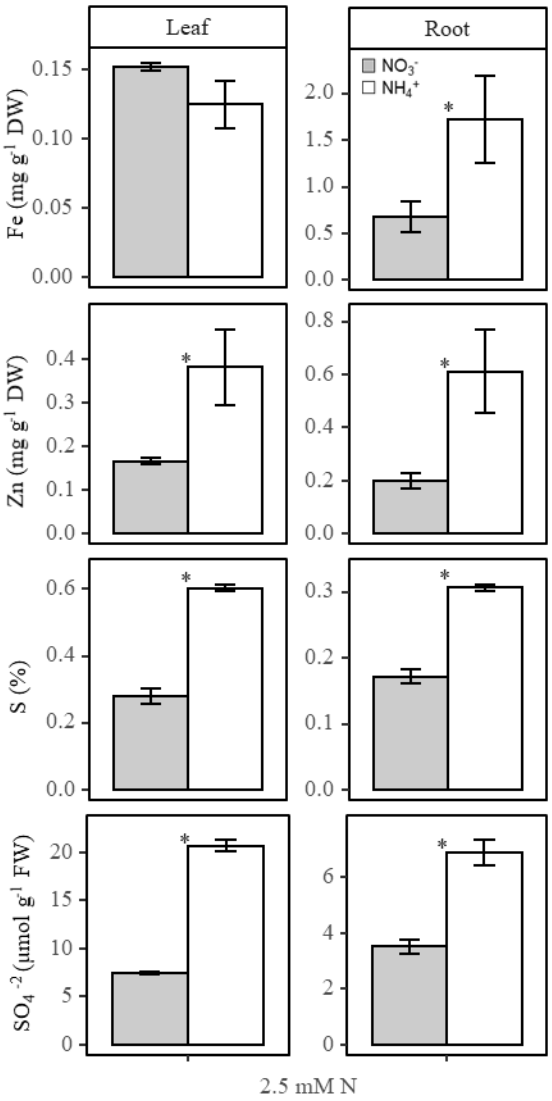

Figure 2.8. Contents of Fe, Zn, sulphur and sulphate in leaves and roots of *B. distachyon* grown with 2.5 mM NH_4^+ (white bars) and 2.5 mM NO_3^- (grey bars). Values are the mean ± SE (n = 4). The statistical significance was assessed by t student ($p<0.05$).

The nitrogen source influences the plant response to Fe availability

Following the higher Fe and MAs content in *B. distachyon* root under ammonium nutrition, we hypothesized that NH_4^+ may affect the plant response to changes in Fe availability. To test this hypothesis, we performed an experiment growing the plants under Fe deficiency (D) and also under Fe toxicity (T) and determined plant growth, chlorophyll, NH_4^+ and total amino acids content together with Fe and Zn accumulation (Figure 2.9).

As expected, we found that D condition provoked a substantial decrease in plant growth in chlorophyll content independently of the N source provided (Figure 2.9). However, the growth inhibition provoked by ammonium nutrition in the root was more evident in Fe deficiency compared to C, suggesting a synergistic effect of both nutrients, Fe and NH_4^+ (Figure 2.9). Interestingly, this higher sensitivity to combined Fe deficiency and ammonium nutrition was correlated with higher NH_4^+ accumulation in the tissues (Figure 2.9), which is indicative of a higher ammonium stress. As commonly happens under ammonium nutrition amino acids level followed the same trend as NH_4^+ content (Figure 2.9).

As previously observed, Fe and Zn contents in root were higher in C condition under ammonium nutrition and this higher Fe content was observed both in D and T treatments (Figure 2.9). Regarding Zn levels, the accumulation observed in ammonium nutrition in C was promoted under Fe deficiency but was absent under Fe toxicity (Figure 2.9). Overall, ammonium-fed plants appeared more sensitive to Fe deficiency at the root level regardless the Fe accumulation. As suggested by the proteomic study, physiological data and micronutrient analysis confirm the interaction between Fe homeostasis and ammonium nutrition in *B. distachyon*.

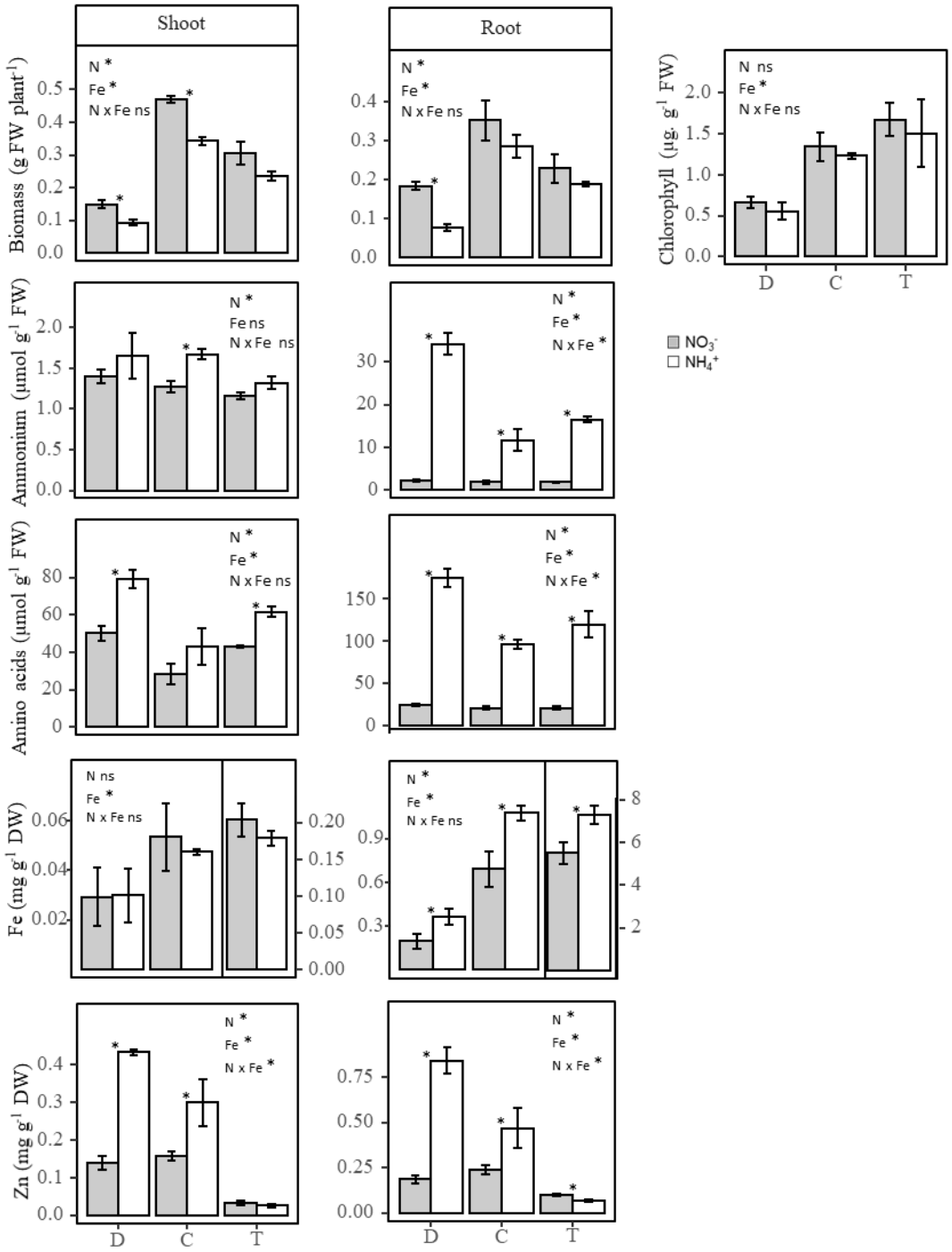

Figure 2.9. Biomass and content of chlorophyll, NH_4^+, total amino acids, Fe and Zn in response to the interaction between the N source (2.5 mM NH_4^+ represented in white bars and 2.5 mM NO_3^- in grey bars) and Fe supply (Fe^{3+} Deficiency, D in X-axis; Fe^{3+} Control condition, C; Fe^{3+} toxicity, T) in *B. distachyon*. Columns represent the mean values ± SE (n = 3). Asterisk (*) indicates either significance of the two-way ANOVA (N for nitrogen source, Fe for iron condition) or significance between nitrogen source at the same iron condition analysed by the t-student test ($p<0.05$).

Finally, we decided to perform a last experiment again growing *B. distachyon* plants in C and D conditions but adding a new condition that we called Fe moderate deficiency or MD. In MD condition plants were grown with 10 µM Fe^{3+}, which corresponds to 10% of the Fe^{3+} supplied in C condition. The results found in D condition confirm the previous experiment with a higher sensitivity of the root under ammonium nutrition in association with NH_4^+ accumulation in the

root. Interestingly, in view of the biomass and chlorophyll data, MD treatment represented a Fe-sufficient condition for nitrate-fed plants that performed as in C condition. In contrast, for ammonium-fed plants MD represented an important stress evidenced by a lower biomass and an important decrease in the chlorophyll content.

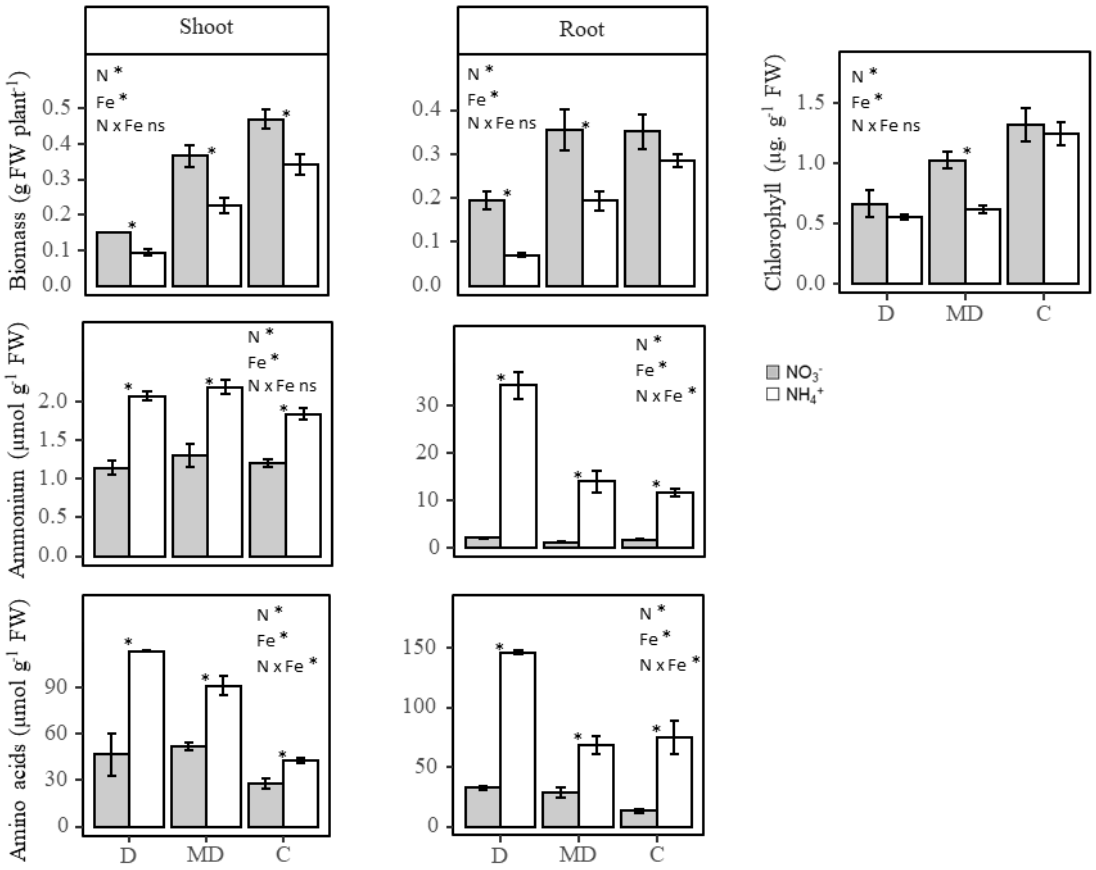

Figure 2.10. Biomass, and content of chlorophyll, NH_4^+ and total amino acids in response to the interaction between the N source (2.5 mM NH_4^+ represented in white bars and 2.5 mM NO_3^- in grey bars) and Fe supply (Fe^{3+} Deficiency, D in X-axis; Moderate Fe^{3+} Deficiency, MD; and Fe^{3+} Control condition, C) in *B. distachyon*. Columns represent the mean values ± SE (n = 3). Asterisk (*) indicates either significance of the two-way ANOVA (N for nitrogen source, Fe for iron condition) or significance between the N sources at the same iron condition analysed by the t-student test ($p<0.05$).

5. DISCUSSION

Proteomic analyses in roots of B. distachyon *exposed to ammonium nutrition indicates adaptation of carbon and nitrogen metabolism and changes in the cell wall.*

Proteome analysis offers one of the best options for the functional analysis of translated regions of the genome and generates detailed information about the essential mechanisms of plant stress response. Previous studies have already used proteomics to study root adaptation to ammonium nutrition in different species (Menz *et al*., 2016; Prinsi and Espen, 2018; Coleto *et al*., 2019; Royo, *et al*., 2019). The proteome analysis carried out in *B. distachyon* confirmed a number of processes already shown relevant in plant response to ammonium nutrition such as redox homeostasis control or the adaptation of root carbon and nitrogen metabolism. The major differences were found when comparing NH_4^+ vs NO_3^- at high N concentration (2.5 mM). Thus, proteomic data are in agreement with the physiological characterization performed in Chapter 1 (De la Peña *et al*., 2019), since most changes occurred with the 2.5 mM NH_4^+, which represented a stressful situation, compared for instance to 1 mM NH_4^+, which meant a situation of ammonium tolerance.

Among others, the proteome data corroborated the down-regulation of GS2 ("glutamine synthetase chloroplastic" I1J2T4) already observed in ammonium-fed *B. distachyon* (Chapter 1) at the gene expression level and in other species, such as Arabidopsis (Sarasketa *et al*., 2016). The stimulation of asparagine synthetase (I1IV86) is also in agreement with the huge accumulation of Asn reported in chapter 1. Besides, the induction of GDH is a classical marker of plant response to ammonium nutrition (Loulakakis and Roubelakis-Angelakis, 1991; De la Peña *et al*., 2019) and accordingly GDH2 (I1J084) was up-shifted in root of ammonium-fed plants. Although long-studied, the physiological role of GDH under ammonium nutrition remains still controversial, notably regarding its working sense. Notably with the use of labeling techniques, a number or works advocate for its function deaminating Glu for 2-OG provision, e.g. in tobacco and wheat (Labboun *et al*., 2009; Vega-Mas *et al*., 2019a). This skeleton-supplier role is in agreement with its low affinity for NH_4^+, which suggests its function to be linked to compensate carbon depletion in the cell under stressful conditions (Robinson *et al*, 1991; Fontaine *et al*., 2012). However, other studies have provided evidence for GDH function in NH_4^+ assimilation, e.g. in tomato (Ferraro *et al*., 2015; Vega-Mas *et al*., 2019b).

The cell wall is key for cell expansion; loosening of the wall allows the cell to expand, whereas crosslinking between their polymers inhibits cell expansion. Several reports have shown a relationship between ammonium nutrition and cell wall biogenesis and organization.

Transcriptomic and proteomic studies have shown that ammonium treatment down-regulates the expression of genes encoding cell wall-modifying enzymes that contribute to cell expansion (Patterson *et al*., 2010). In this line, Prinsi and Espen *et al*. (2018) and Royo *et al*. (2019) also identified a number of cell wall-related proteins, notably associated to the lignification and suberization of the secondary cell wall. Xyloglucan is a major hemicellulosic structural component of the cell-wall matrix of dicotyledons and non-commelinid monocotyledons and xyloglucan endotransglucosylase/hydrolases (XTHs) have a double catalytic activity mediating both the splitting and the reconnection of the xyloglucan crosslinks in the cell wall, what stiffen and loose the cell wall respectively (Hara *et al*., 2014). Xyloglucan is not a major component of the cell wall of Poales, including *B. distachyon*, which is characterized by increased amount of glucuronoarabinoxylans (GAX) and (1,3;1,4)-β-D-glucans. However, the importance of xyloglucan and XTHs has been reported even in commelinoid monocots, which include Poales (Hara *et al*., 2014). In our work we found decrease abundance of three XTHs in ammonium-fed roots (I1I257, I1I258, I1GTU3). We also report a decreased abundance in a number of proteins associated to phenylpropanoid biosynthesis including lignin; among others, three PAL enzymes, a probable 4-coumarate-CoA ligase 3 (I1HXV5) and a caffeoyl-CoA O-methyltransferase 1 (I1H0Q2). These results are in line with the proteome changes of *Medicago truncatula* root under ammonium nutrition reported by Royo *et al*., (2019). In addition, it is known that ROS are involved in cell wall loosening and stiffening (Gapper and Dolan, 2006). In particular, Class III peroxidases are a source of ROS to form lignified tissues and strengthen cell walls (Yan *et al.*, 2019). Podgórska *et al*. (2017a) and Royo *et al*. (2019) reported higher peroxidase activity in ammonium-grown *A. thaliana* and *M. truncatula* plants, respectively. Indeed, Royo *et al*., (2019) showed increased lignin production and Podgórska *et al*. (2017a) reported a higher cell wall stiffness under ammonium nutrition, overall suggesting that NH_4^+-mediated growth inhibition could be related to a more rigid cell wall structure. In our proteome, we also identified several peroxidases but most of them were down-shifted in ammonium-grown plants (Table S2.1, S2.3). Future studies will be helpful to further go into depth in the cell wall dynamics in *B. distachyon* depending on the N source provided, which may be important to better exploit bioenergy production in grasses.

Phytosiderophores synthesis, Fe and Zn uptake are promoted in B. distachyon *roots under ammonium nutrition*

Graminaceous species, including *B. distachyon*, acquire Fe using a chelation-based strategy. To do so, PS are secreted and chelate Fe(III) in the rhizosphere that becomes soluble as Fe(III)–PS complexes, which are then taken up by YS/YSL transporters (Hindt and Guerinot, 2012;

Kobayashi *et al*., 2019). Proteome data showed a higher abundance of proteins involved in the synthesis of PS, thus suggesting the higher capacity of plants grown under ammonium nutrition to acquire metals (Table 2.1). This was confirmed both by the quantification of PSs and Fe in plant tissues, that were higher under ammonium nutrition (Figures 2.7, 2.8). Indeed, MAs are also chelators of Zn and notably this metal was also accumulated at the whole-plant level under ammonium nutrition. SAM is the precursor for the synthesis of PSs, therefore to sustain PS synthesis a proper SAM availability is needed, which in turn demands sulphate uptake and assimilation. Ammonium nutrition has been suggested to enhance sulphate uptake probably to provide anionic equivalents and charge balance to ammonium-fed plants, which contain less low-molecular weight anions such as NO_3^- or carboxylates (Van Beusichem *et al*., 1988; Gerendas *et al*., 1997; Zhang *et al*., 2005). Furthermore, Coleto *et al*., (2017) observed enhanced sulphur assimilation under ammonium nutrition in *Brassica napus*. In this line of evidence, we reported higher levels of S and sulphate (Figure 2.8) and higher abundance of ATP sulfurylase 1 (I1GNF6) and other sulfur-related proteins under ammonium nutrition (Tables S2.1, S2.3). Moreover, almost all the enzymes taking part in the Met cycle, in charge of recycling Met derivatives for SAM replenishment, were up-regulated under ammonium nutrition (Figure 2.6; Table 2.1). This activation of the Met cycle would explain the diminished content of Met in 2.5 mM NH_4^+ and could indicate that Met Cycle would be diverted towards SAM recycling (Figure 2.7). Overall, present results suggest a coordination between sulphur metabolism and PS synthesis, potentially to enhance Fe uptake under ammonium nutrition.

Fe uptake stimulation under ammonium nutrition has been already observed in the context of the acidification of apoplastic/rhizosphere pH that increases the solubility of Fe^{3+} and in the case of Strategy I plant also activating ferric reductase enzyme (Mengel and Geurtzen, 1988; Alloush *et al*., 1990; Kosegarten *et al*., 1998, 1999). In our work the nutrient solution was buffered and often replaced thus, the medium pH remained quite stable (6.9-7.4) during the whole experiment regardless the treatment. Indeed, several reports indicate that pH acidification of the rhizophere is unlikely the sole reason for the Fe uptake stimulation observed under ammonium nutrition (Zhu *et al*., 2018; Zhu *et al*., 2019). In agreement, Zhu *et al*. (2018) reported a higher expression of genes for Fe transporters in ammonium-fed rice. In our work, although a pH effect cannot be completely discarded the differences found in Fe levels seem mainly related to enhanced MAs synthesis rather than to an increase of Fe solubility related to pH in the rhizosphere.

The N source modifies B. distachyon *response to Fe availability*

Following the higher capacity of ammonium-fed roots to take up Fe, we hypothesized that NH_4^+ might affect the Brachypodium´s response to changes in Fe availability. To test this hypothesis, we performed experiments combining the N source with altered Fe availability.

Fe is an essential micronutrient for plants and both its deficiency and excess represent stressful situations for the plant. Among others, the excess of Fe provokes leaf bronzing, poor root growth, suppression of cations levels and induction of ROS levels (Becker and Asch, 2005). Tolerance mechanisms to Fe toxicity include, among others, formation of Fe plaques in the rhizosphere, limitation of Fe acquisition regulating PS synthesis, Fe confinement at the root level, sequestering Fe in the vacuole or joined to ferritins, and increasing the plant antioxidant defence (Briat *et al*., 2010; Kabir *et al*., 2016; Siqueira-Silva *et al*., 2019).

In our study, T treatment produced an important accumulation of Fe, mainly at the root level accompanied by a sharp decrease in Zn levels, suggesting a high competition for the uptake of both microelements. Notably under ammonium nutrition the uptake of Fe was still higher with 30% more Fe being accumulated in the root. However, since at the leaf level no differences were found in Fe accumulation, it appears that ammonium-induced growth decrease respect to nitrate nutrition was partially mitigated in T treatment. The underlying reasons for this difference remain to be elucidated in future studies but one could hypothesize a higher Fe-chelating or compartmentalization capacity of ammonium-fed plants. Indeed, NA avoids Fe precipitation and minimizes Fe toxicity as the chelation of Fe prevents ROS production via the Fenton reaction (Hell and Stephan, 2003). In Brachypodium roots fed with ammonium, the clear promotion of NA synthesis could act in this sense, shielding the cell machinery from the Fe excess stress (Figure 2.7). Besides, ammonium is known to sometimes induce the plant antioxidant-machinery (Dominguez-Valdivia *et al*., 2008; Podgórska *et al*., 2017b), that could be helping to prevent from the excess of Fe. Overall, our proteome data do not highlight an induction of the antioxidant machinery at the root level, although, for example monodehydroascorbate reductase (I1I9F4) was accumulated.

Because of Fe involvement in chlorophyll synthesis, leaf chlorosis is one of the most common symptoms of Fe deficiency. In our work we detected almost no-interaction between Fe deficiency and N source at the shoot level since the behavior of ammonium-fed plants respect to nitrate-fed ones in D was similar as observed in C conditions (Figures 2.9, 2.10). At the root level we observed a lower biomass of ammonium-fed plants, suggesting higher sensitivity to D. Moreover, NH_4^+ content in the root notably increased in D respect to C. The excessive

accumulation of NH_4^+ in tissues is an undesirable effect of ammonium nutrition and is considered one of the main factors governing plants sensitivity towards ammonium nutrition (Britto and Kronzucker, 2002; Esteban *et al*., 2016). Thus, despite the root enhances the ammonium assimilation into amino acids (Figure 2.9, 2.10) in D, the observed huge NH_4^+ accumulation could be responsible for the strongly impaired growth of *B. distachyon* roots. In this line, Zhu *et al*. (2019) recently reported an increase NH_4^+ uptake in *Arabidopsis thaliana* under Fe deficiency, that was correlated with the induction of *AMT1;1* and *AMT1;3* NH_4^+ transporters. Moreover, *amt1;3* mutant displayed increased sensitivity to Fe deficiency respect to wild type plants (Zhu *et al*., 2019).

In a second experiment, in MD condition we observed again the negative effect of ammonium nutrition in root physiology when Fe availability is limiting. Interestingly, we also observed this effect at the shoot level, notably in chlorophyll content that decreased respect to C condition in ammonium-fed plants, whereas, in nitrate-fed ones the chlorophyll contents remained constant despite the lower Fe availability (Figure 10B). These results differ with a number of previous results showing a beneficial effect of ammonium under Fe deficiency in both dicots and monocots (Alloush *et al*., 1990; Kosegarten and Englisch, 1994; Kosegarten *et al*., 1998; Zhu *et al*., 2018; Zhu *et al*., 2019; Zou *et al*., 2001).

To our knowledge, the present work is the first one studying Fe-NH_4^+ interaction in *B. distachyon* and thus, to explain the contrasting behavior found a potentially different physiology of *B. distachyon* respect to other species cannot be discarded. Additionally, the discrepant behavior observed could be also to the fact that in some of these studies ammonium was applied in the presence of nitrate (Kosegarten *et al*., 1998; Zhu *et al*., 2019; Kosegarten and Englisch, 1994). Besides, in our study *B. distachyon* plants grown with the supply of 2.5 mM NH_4^+ were clearly subjected to ammonium stress, which differs from other studies where exclusive ammonium nutrition did not provoke a stressful situation because of the NH_4^+ concentration used, the timing of exposure to NH_4^+ or the species of study, such as rice that is highly tolerant to ammonium nutrition (Alloush *et al*., 1990; Zou *et al*., 2001; Zhu *et al*., 2018). The reported beneficial effect of NH_4^+ on Fe deficiency would be supported by the increased Fe uptake of ammonium-fed plants and by the capacity of NH_4^+ to make soluble the Fe bound to hemicelluloses in the cell wall (Zou *et al*., 2001; Zhu *et al*., 2018; Zhu *et al*., 2019). In addition, NH_4^+ has also been shown to promote remobilization of the P from the cell wall (Zhu *et al*., 2016). Both in the case of Fe and P, the release of these nutrients from the cell wall appears to be dependent on NH_4^+-triggered production of nitric oxide (NO) (Zhu *et al*., 2018; Zhu *et al*., 2016).

In our study, ammonium nutrition also promoted Fe uptake independently of the Fe supply (Figures 2.8, 2.9), however we observed a higher sensitivity of ammonium-fed plants to limiting Fe availability, in particular in MD, compared to nitrate-fed plants (Figures 2.9, 2.10). As stated, this could be due to higher tissue NH_4^+ content (Figures 2.9, 2.10). Alternatively, the capacity of plants to properly utilize the available Fe could be compromised, thus provoking leaf chlorosis (Figure 2.10). Indeed, a number of works have observed that the alteration of Fe utilization capacity yields chlorotic symptoms without affecting total tissue Fe content (Kosegarten *et al*., 1998; Haydon *et al*., 2012). Among others, this can be due to an improper loading of the Fe from the xylem/apoplast into the cells or to perturbations in subcellular partitioning of Fe (Haydon *et al*., 2012). Supporting the idea of an impaired Fe utilization capacity, we found for instance that a CDGSH iron-sulfur domain-containing protein (I1GUN7) and notably ferritin-1 (I1IV67) were less abundant under ammonium nutrition (Table 2.1; Table S2.1). In this line of evidence, citrate is a key Fe chelator for its transport from the root to the leaf. Under ammonium nutrition it is known that citrate pool in the root is mainly diverted to 2-OG supply for NH_4^+ assimilation (Setién *et al*., 2013; Vega-Mas *et al*., 2019a), as also s discussed in *B. distachyon* in chapter 1 (De la Peña *et al*., 2019). Thus, we may hypothesize that the withdrawal of citrate for NH_4^+ assimilation would suppose a trade-off for proper Fe transport within the plant. Indeed, in view of low Fe-content shoot/root ratio (Figure S2.8), the long-distance transport appears compromised under ammonium nutrition.

On the other hand, the high levels of Zn observed in ammonium-fed plants in Fe deficiency condition could be also responsible for the higher sensitivity observed in Brachypodium. Changes in gene expression to facilitate the availability of Fe are known to promote the uptake of other essential and non-essential metals (Li and Lan, 2017). To avoid toxicity of these micronutrients, genes encoding transporters to sequester these metals into vacuoles are also commonly induced, including Zn (Haydon *et al*., 2012), but also Cu (Perea-García *et al*., 2013) or Mn transporters (Arrivault *et al*., 2006). As Zn is strongly accumulated both in root and leaf, Zn stress cannot be discarded.

Concluding remarks

The proteome analysis revealed important root adaptation to ammonium nutrition involving among others: carbon and nitrogen metabolism, cell wall metabolism, redox homeostasis and interaction with other ions. In particular, ammonium-nutrition induced MAs synthesis and Fe and Zn uptake. Besides, the interaction between ammonium nutrition and Fe metabolism was evidenced by the increased sensitivity of ammonium-fed plants to suboptimal Fe availability.

The overall results suggest that impaired Fe transport to shoots and utilization would be responsible for the observed phenotype. Future research is needed to further elucidate the mechanisms underlying the interaction between these nutrients. Studying the partitioning of Fe, Zn and its chelators, in different tissues and subcellular compartments will be of especial interest. Besides, further integrating the metabolism of other nutrients, notably Zn, is also necessary to get the whole picture of Fe-NH_4^+ interaction and the potential applications of ammonium nutrition, since both micronutrients Fe and Zn are key in the grain cereal quality and also essential for animal nutrition.

SUPPLEMENTARY TABLES LEGENDS (available in attached USB flash drive)

Table S2.1. List of proteins identified, quantified, and differentially expressed in roots of *B. distachyon* grown under nitrate or ammonium nutrition.

Table S2.2. Proteins significantly regulated in common way in different comparisons in roots of *B. distachyon*.

Table S2.3. Functional categorization in three ontologies: biological process, cellular component and molecular function of differentially abundant proteins in every comparison in roots of *B. distachyon*.

Table S2.4. Full list of enriched GO categories/terms in every comparison in roots of *B. distachyon*.

6. SUPPLEMENTARY INFORMATION

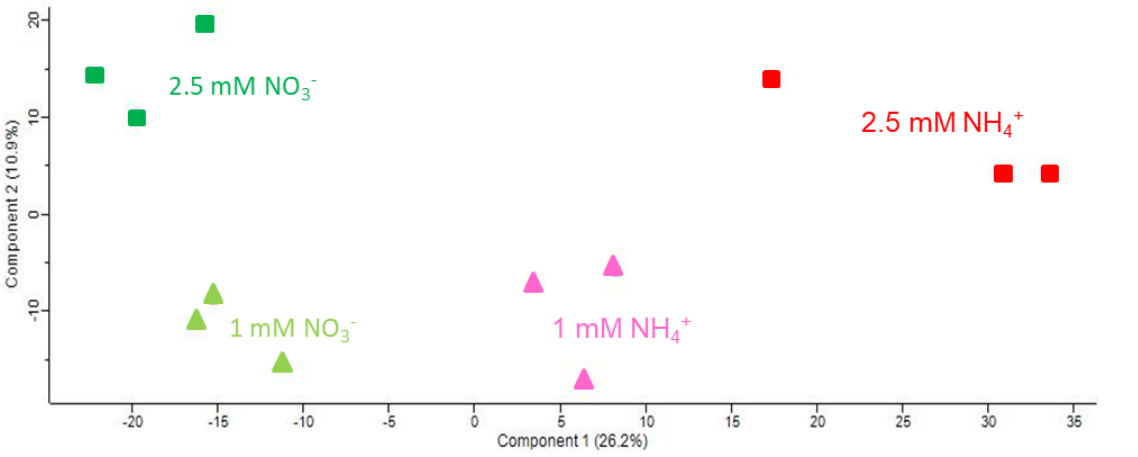

Figure S2.1. Principal component analysis (PCA) of protein expression profiles of the 12 samples analyzed (three biological replicates per N condition) in *Brachypodium distachyon* roots.

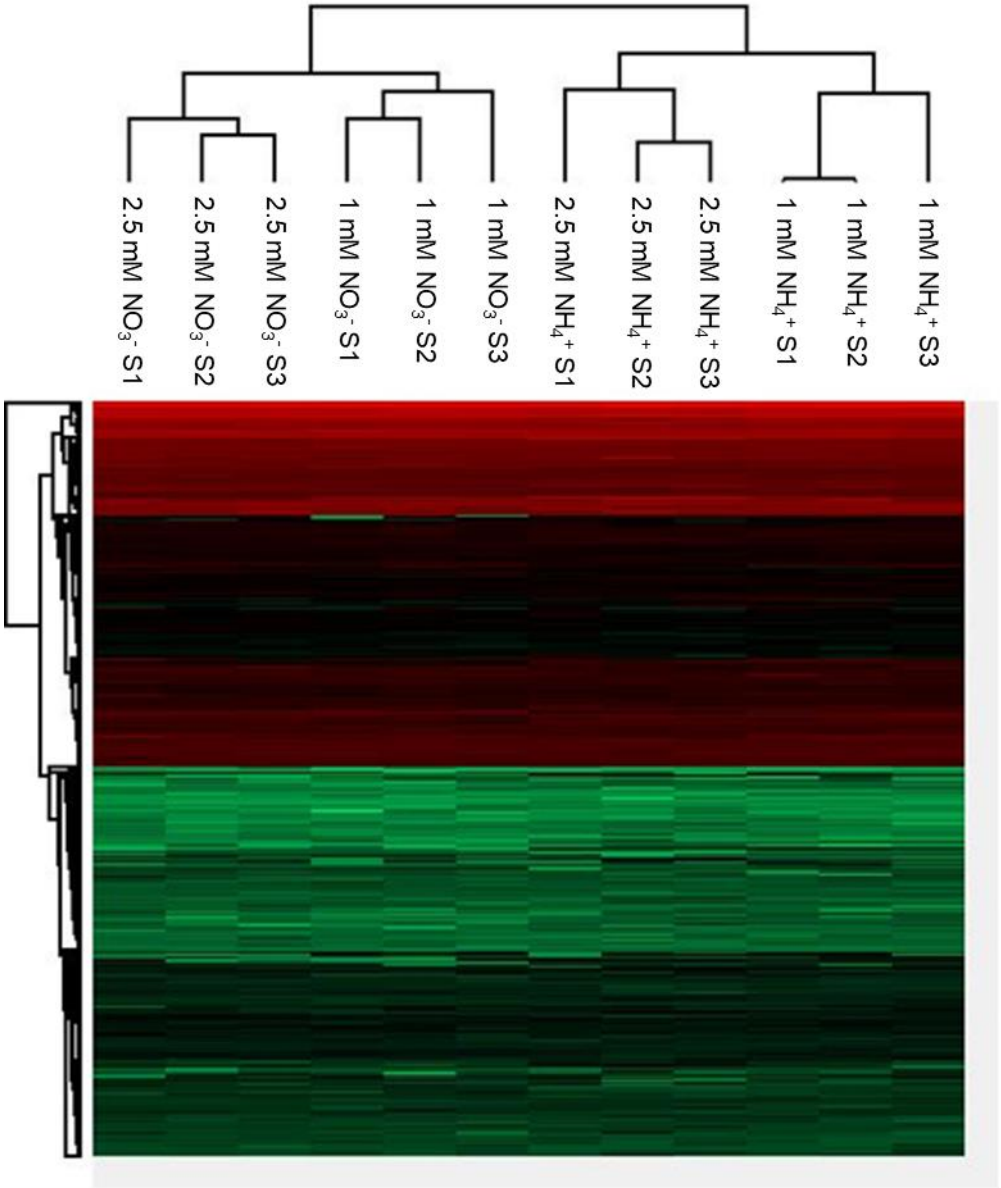

Figure S2.2. Hierarchical clustering of protein expression profiles of the 12 samples analyzed (three biological replicates per N condition) in *Brachypodium distachyon* roots.

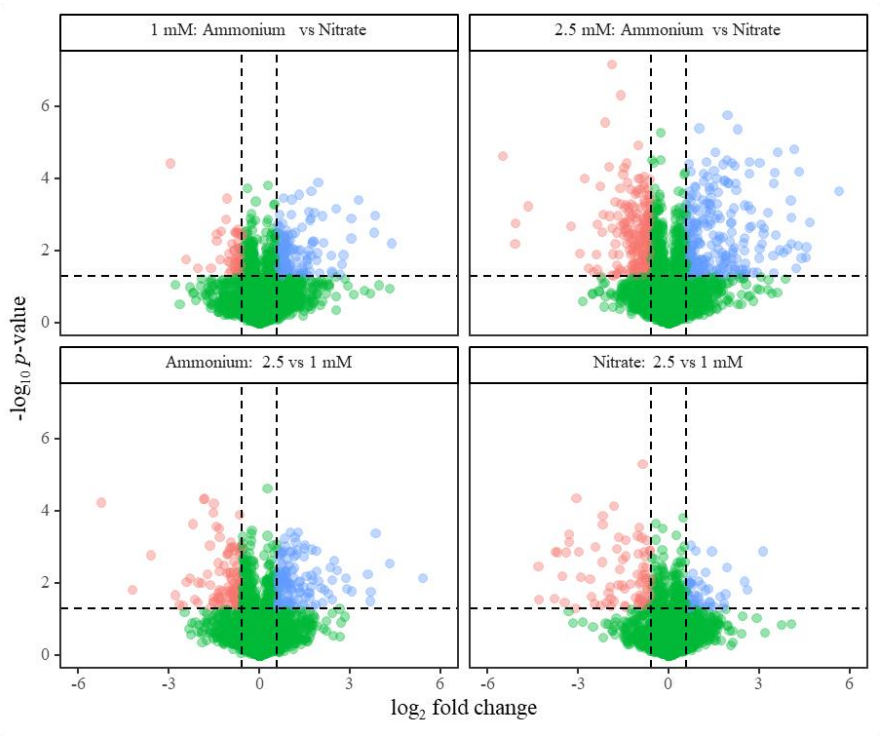

Figure S2.3. Volcano plots representing the proteins quantified in the four nitrogen nutritional comparisons analysed in *Brachypodium distachyon* roots. Proteins are ranked according to their statistical $-\log_{10}$ (*p*-value) (y-axis) and their relative abundance ratio ($\log_2$ fold change). Red and blue dots represent differentially abundant proteins (DAPs) with a fold-change greater than 1.5 and a p-value < 0.05.

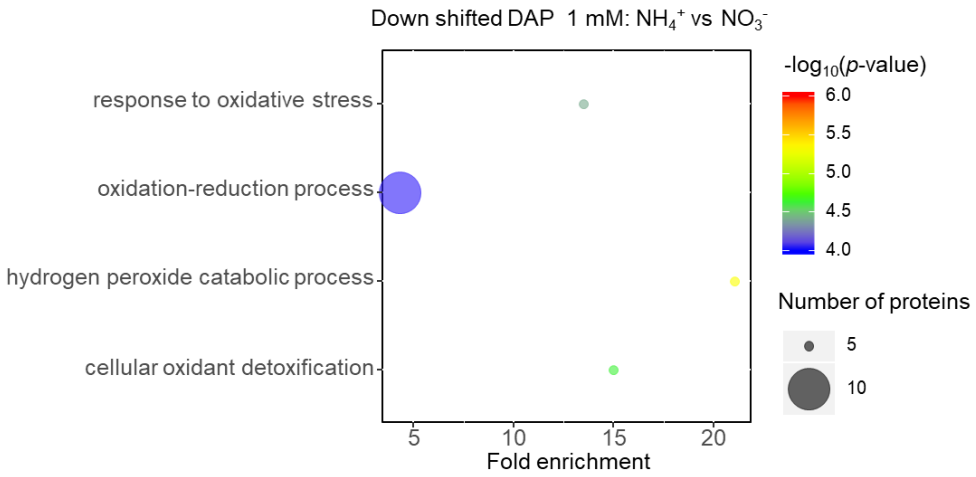

Figure S2.4. Gene ontology enrichment analysis of down-shifted DAPs in 1 mM NH_4^+ vs 1 mM NO_3^- comparison (No significant enrichment was found for up-shifted DAPs) in roots of *B. distachyon*. The fold enrichment is the ratio of the number of DAPs observed over the expected number of proteins associated to a particular category/term based in the reference proteome. Only the more significant specific categories/terms are represented. The full list is available in the Table S2.4.

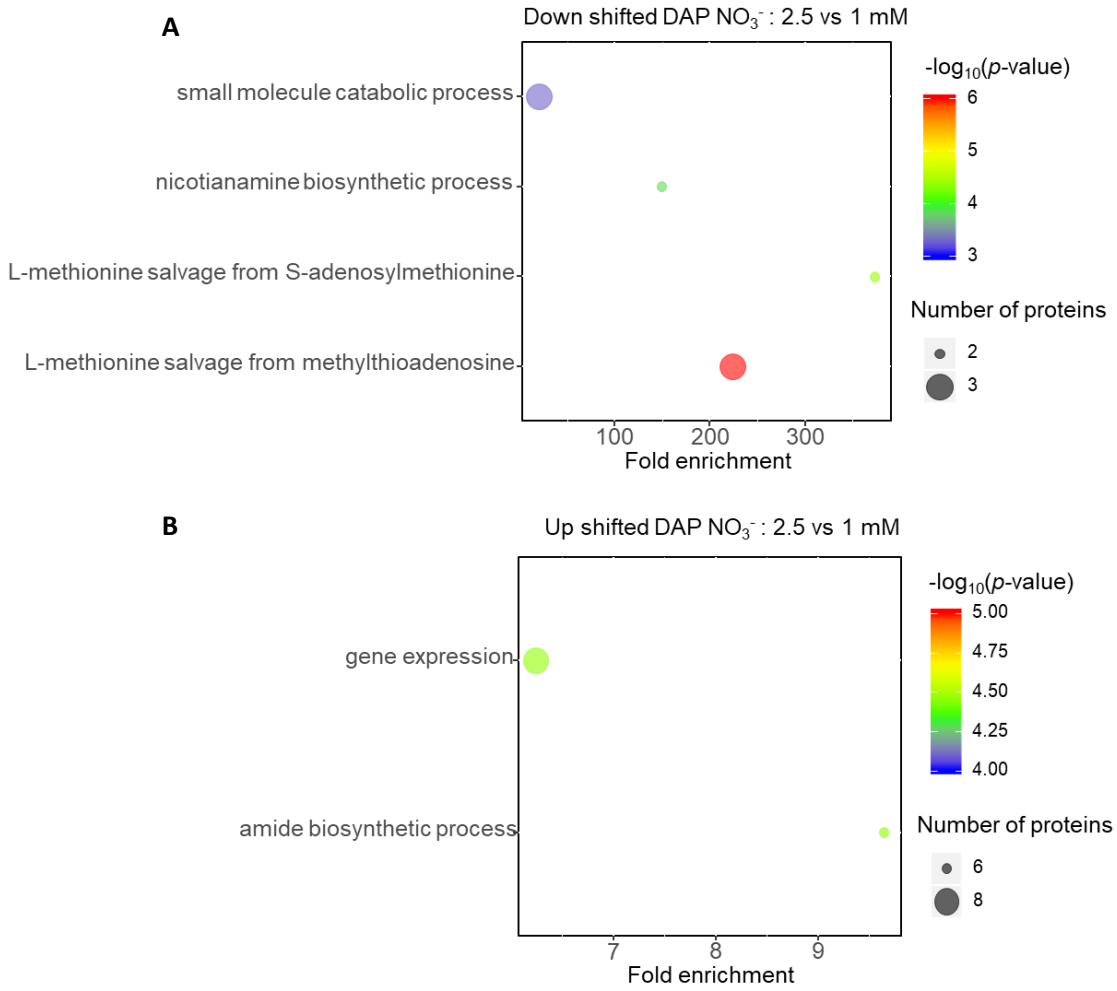

Figure S2.5. Gene ontology enrichment analysis of down-shifted (A) and up-shifted (B) DAPs in 2.5 mM NO_3^- vs 1 mM NO_3^- comparison in roots of *B. distachyon*. The fold enrichment is the ratio of the number of DAPs observed over the expected number of proteins associated to a particular category/term based in the reference proteome. Only the more significant specific categories/terms are represented. The full list is available in the Table S2.4.

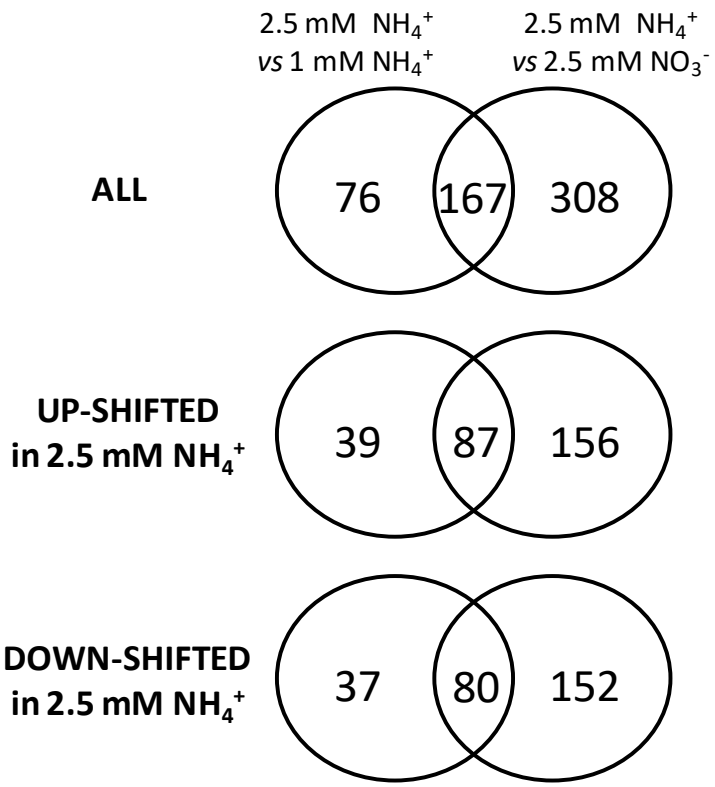

Figure S2.6. Venn diagram showing the number of common differentially abundant proteins (DAP) identified between 2.5 mM NH_4^+ *vs* 1 mM NH_4^+ , and 2.5 mM NH_4^+ *vs* 2.5 mM NO_3^- comparisons in *Brachypodium distachyon* roots.

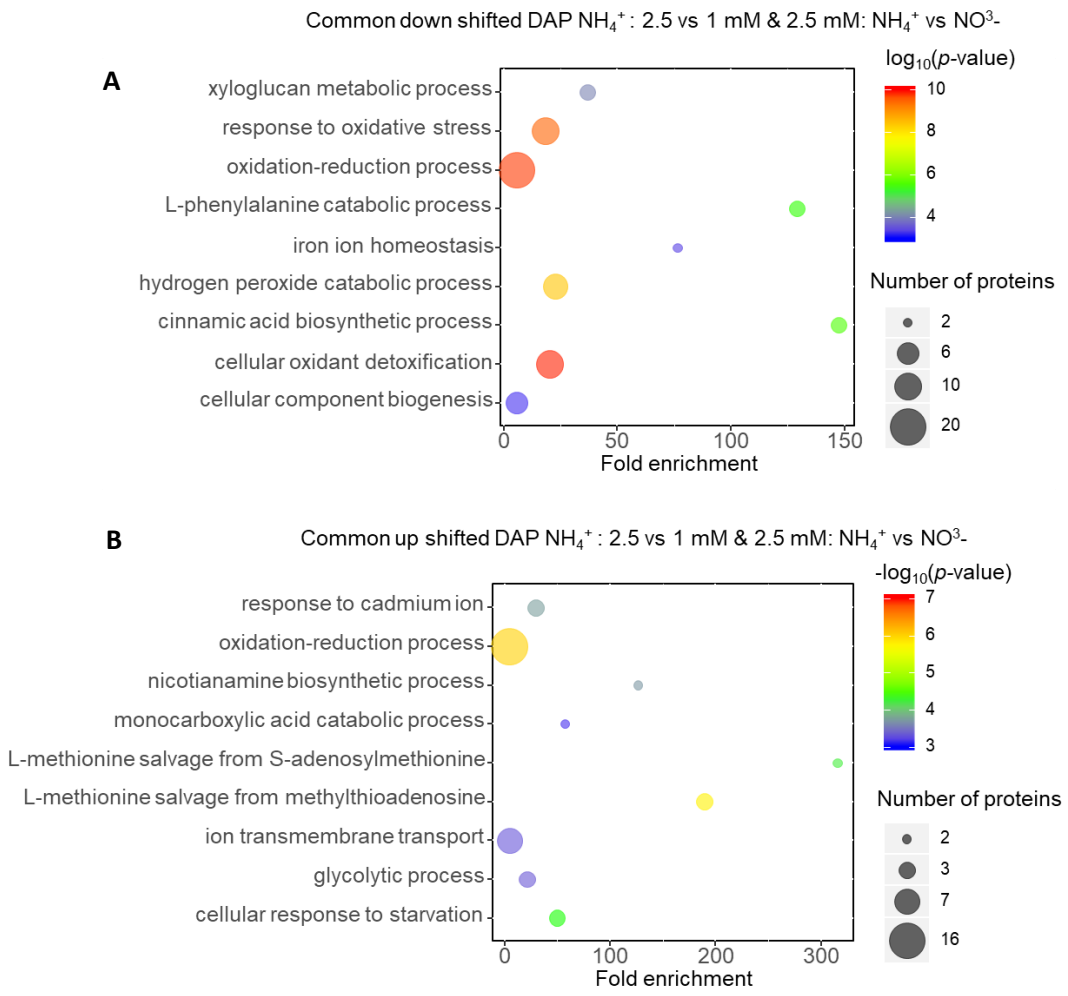

Figure S2.7. Gene ontology enrichment analysis performed with the down-shifted (A) and up-shifted (B) DAPs commonly identified both in 2.5 mM NH_4^+ vs 1 mM NH_4^+ and 2.5 mM NH_4^+ vs 2.5 mM NO_3^- comparisons in *B. distachyon* roots. The fold enrichment is the ratio of the number of DAPs observed over the expected number of proteins associated to a particular category/term based in the reference proteome. Only the more significant specific categories/terms are represented. The full list is available in the Table S2.4.

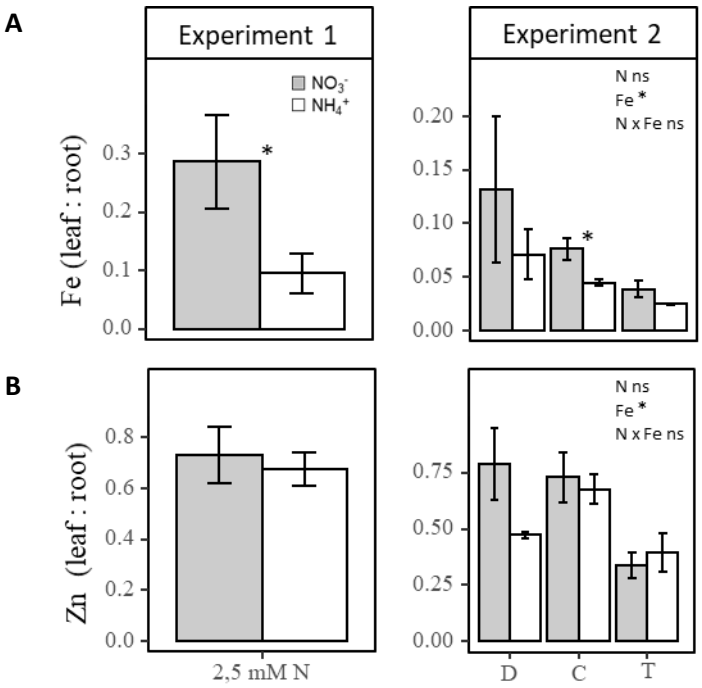

Figure S2.8. Shoot-to-root Fe (A) and Zn (B) contents (Figure S10), for the experiments 1 and 2. Values are the mean ± SE (n = 3-4). Asterisk (*) indicates either significance of the two-way ANOVA (N for nitrogen source, Fe for iron condition) or significance between nitrogen source at the same iron condition analysed by the t-student test ($p<0.05$).

CHAPTER 3

Exploiting natural metabolic variability in *Brachypodium distachyon* to define the genetic basis of adaptation to ammonium nutrition

1. ABSTRACT

Ammonium (NH_4^+) is a fundamental substrate for the synthesis of many biomolecules. However, when present in excess it results toxic for most species develop symptoms of stress although a great inter- and intraspecific variability in ammonium tolerance has been reported. Today, the causal genes underlying the observed variability are far of being discovered. In this work, we explored the genetic and metabolic natural intraspecific variability of the model grass *Brachypodium distachyon*. To do so, we characterized a panel of 52 sequenced *B. distachyon* natural accessions, shown as genetically diverse, when growing under ammonium or nitrate nutrition. We determined plant growth and depicted the metabolic adaption to the N source of every genotype determining a panel of 22 metabolic markers, including enzyme activities and metabolite content. In general, we observed extensive natural variation in *B. distachyon* response to ammonium nutrition, which was closely related to plant metabolic adaptation. Statistical and exploratory data analysis highlighted, among others, PEPC activity and NH_4^+ content in the leaves, sucrose content in the root and glutathione levels as important traits explaining the observed variability in ammonium tolerance. Genome-wide association studies using multi-locus mixed models for every trait determined revealed an important number of significant SNPs, highlighting genomic regions where key genes related to *B. distachyon* ammonium tolerance may be located. Overall, this work represents a significant advance to unmask the complex networks that link metabolism with natural variability under ammonium nutrition.

2. INTRODUCTION

Cereals are the major source of calories for human nutrition and essential for animal feed and also for the production of biofuel. To maximize yields the application of fertilizer is required. Although plants require a balance of all mineral nutrients for optimal growth, nitrogen (N) is generally the main driver of yield. Thus, over 100 million tons of N fertilizers are globally applied per year (Garnett *et al*., 2015; Swarbreck *et al*., 2019). Unfortunately, cereal nitrogen use efficiency (NUE), defined, as the amount of applied fertilizer that is recovered by grain, is very low and it is estimated that only 33 % of the applied N is recovered at harvest, which represents a huge loss of N to the environment and consequently a great threat for the environment (Raun, and Johnson, 1999). These N losses, on average 50 kg N ha^{-1} $year^{-1}$, leads to pollution of groundwater and the emission of greenhouse gases (Lassaletta *et al*., 2014). These losses make agriculture unsustainable, even more in the context of a growing world population. Thus, decreasing crop N requirement while maintaining high yield is necessary. Increasing NUE can be achieved by improving fertilization management and increasing plant potential for higher NUE

(Garnett *et al*., 2015; Hawkesford and Griffiths, 2019). Very recently, it has been proposed to consider N responsiveness as an alternative selection trait to NUE, a concept defined as the capacity of plants to induce physiological and morphological changes according to N availability that may increase N uptake and assimilation (Swarbreck *et al*., 2019).

The use of ammonium fertilizers, in combination with nitrification inhibitors, has been demonstrated efficient to mitigate N losses to the environment and therefore a good approach to increase NUE (Ruser and Schulz, 2015; Coskun *et al*., 2017b). This is because the use of inhibitors of nitrification delays the conversion of ammonium to nitrate, allowing ammonium to stay bonded to the soil profile for longer, but yet available for the plant to uptake. Nevertheless, when NH_4^+ is present in the soil at high concentrations may lead to reduced growth respect to nitrate nutrition, therefore it makes necessary to improve crops performance under ammonium nutrition.

When plants directly take up NH_4^+, the metabolic energy needed for NO_3^- reduction is saved. However, although NH_4^+ is a fundamental substrate for many biomolecules synthesis, when it is present in excess many species develop toxic symptoms. The adverse effects of ammonium stress range from visible symptoms such as leaf chlorosis to physiological disorders such as oxidative stress, alteration in intracellular pH or mineral nutrition imbalance (Britto and Kronzucker, 2002; Liu and von Wirén, 2017). In general, it is considered that these physiological disorders are the result of excessive NH_4^+ uptake and accumulation in tissues (Britto and Kronzucker, 2002; Sarasketa *et al*. 2014). In fact, the main strategies plants have evolved to avoid ammonium toxicity are the increase of NH_4^+ efflux outside, and its capture inside the vacuole. Alternatively, enhancing NH_4^+ assimilation, which demands an important adaptation of primary metabolism, is essential to restrain the unwanted effects of ammonium stress. The energetic cost of these processes is considered as a cause of the growth impairment often observed under ammonium nutrition. Although considered as universal (Britto and Kronzucker, 2002), different species display great variation in ammonium tolerance or sensitivity and indeed intraspecific variability in ammonium tolerance has also been reported in different species such as *Arabidopsis thaliana* (Rauh *et al*., 2002; Sarasketa *et al*., 2014.) or rice (Di *et al*., 2018.). Today, the causal genes underlying the observed variability are far of being discovered.

Indeed, NUE and ammonium tolerance are highly complex polygenic traits that involve biochemistry, phenology, architecture and responses to the environment. Indeed, there is great variation in NUE traits among different genotypes and thus, the exploitation the genetic variation, in particular with quantitative genetic approaches such as quantitative trait loci (QTL)

mapping of bi-parental populations or the use of association genetics, is a great means for the identification of genes controlling NUE (Garnett *et al*., 2015; Han *et al*., 2015; Hawkesford and Griffiths, 2019). Although there is variation in NUE traits among modern cereal varieties, it is clear that a much greater potential of variation exists with the study of ancient/historical varieties and wild species that may allow identifying alleles which have been lost in the modern germplasm pool (Hawkesford and Griffiths, 2019). Indeed, it appears at a global scale that cereals yield increase is plateauing and that modern varieties are not improving in their NUE (Han *et al*., 2015). In this line, a functional allele of the NAC transcription factor NAM-B1 that influences nutrients remobilization was identified in wild wheat populations and was absent in most modern hexaploid wheat varieties (Uauy *et al*., 2006). The study of non-domesticated species or varieties may be of special relevance in the case of ammonium nutrition, since the high nitrification rates common in agricultural soils have made that varieties selection has been nearly exclusively performed in the use of nitrate as N source.

Brachypodium distachyon represents an excellent model plant for the study of cereals physiology and genetics (Brutnell *et al*., 2015; Scholthof *et al*., 2018). Moreover, as evidenced in chapter 1 its behavior under ammonium nutrition is very similar to that of cereal crops such as wheat or barley (De la Peña *et al*., 2019). *B. distachyon* is a diploid grass with a highly homozygous and small genome (272 Mbp) and there is an increasing number of sequenced natural accessions available, which are geographically, genetically and phenotypically diverse (Vogel *et al*. 2009; Tyler *et al*., 2016; Gordon *et al*., 2017). Interestingly, probably related to the fact that *B. distachyon* is a wild plant that has not experienced domestication, the pangenome of *B. distachyon* contains nearly twice the number of genes found in an individual genome (Gordon *et al*., 2017).

In this context, the general objective of this chapter was to explore the genetic and metabolic natural intraspecific variability of *B. distachyon*. To do so, we characterized a large panel of 52 *de novo* sequenced *B. distachyon* natural accessions, already shown as genetically diverse (Gordon *et al*., 2017), grown under ammonium and using nitrate as nutritional control. We determined the plant biomass and we depicted the metabolic adaption to the N source of every genotype determining a panel of 22 metabolic markers including enzyme activities and metabolites content. The obtained phenotypes were then used to identify genomic regions associated with the different traits by the use of Genome-Wide Association Studies (GWAS).

3. EXPERIMENTAL DESIGN AND STATISTICAL ANALYSIS

To characterize the metabolic adaptation of *B. distachyon* natural accessions grown under nitrate or ammonium nutrition, we studied 52 diverse *B. distachyon* inbred lines that have been recently *de novo* assembled and annotated (Gordon *et al*., 2017; https://brachypan.jgi.doe.gov/). Seeds for the different accessions were obtained from different laboratories working in *B. distachyon*: Pilar Catalán (University of Zaragoza, Spain), Luis Mur (Aberystwyth University, UK), Ludmila Tyler (University of Massachusetts, USA), Amy Cartwright (Joint Genome Institute) and from the National Plant Germplasm System of the United States (https://www.ars-grin.gov/npgs/).

Seeds were treated were treated following the methodology described in Tyler *et al*. (2016). Seeds were peeled by removing the lemma, washed for 4 min in a solution containing 15 % bleach plus 0.1 % Triton-X 100 (Sigma-Aldrich) and thoroughly rinsed with sterile deionised water. To synchronise germination, seeds were placed in Petri dishes on damp paper towels and stratified in the dark at 4°C for 7 days. After stratification, the plates covered with aluminum foil were transferred into a growing chamber for 3 days. Germinated seeds were then sowed on trays filled with perlite:vermiculite (1:1, v:v) misted with deionised water. After 7 days, seedlings with a uniform appearance were finally transferred to hydroponic tanks filled with 4.5 L of nutrient solution. 12 seedlings were placed per tank corresponding to 3 individuals of four different genotypes. With a 2.5 mM N provision in the form of NO_3^- or NH_4^+ during 19 days. Growth chamber conditions and medium composition were as described in chapter 1 and after the renewed to maintain the pH and the concentration of mineral elements of the hydroponic medium constant, the nutrient solution was replaced every 4 days. After every change, the stability of pH in the nutrient solution was confirmed. The plants were harvested between 10 and 12 am. (Two hours after the onset of the photoperiod). Shoots and roots were separated and individually weighed. Accession plants grown within the same tank were pooled, immediately frozen in liquid nitrogen, homogenized in a Tissue Lyser (Retsch MM 400) and stored at -80 °C until use. Three tanks were set up per condition and accession. 12 seedling were placed per tank. The three individuals of the same accession growing in the same tank were considered as a biological replicate.

Statistical analysis

Statistical analyses were performed with IBP SPSS ver.22 (IBM Corp., Armonk, USA). Normality and homogeneity of variance were analyzed by Kolmogorov–Smirnov and Levene's tests. Analysis of variance (ANOVA) was carried out to assess the effects of accession (A), nitrogen

source (S), and A × S interactions using the general linear model procedure. T-student test was performed between ammonium and nitrate condition into each genotype for total biomass. Multiple linear regression analysis (stepwise) was used to analyse the relationship between the studied variables and the biomass. In this analysis, some traits were excluded to avoid collinearity based on multi-collinearity test.

For PCA analysis, data was standardized with Vegan package and the PCAs runned with FactoMineR and Factoextra packages. To deepen into the correlation among the variables, correlation matrixes (p<0.01) and a hierarchical clustering using Euclidian distance and average linkage were performed using Hmisc and corrplot packages. Heatmaps were visualized with heatmap.plus package. Statistical analysis corresponding to Genome Wide Association study is available in materials and methods section.

4. RESULTS

B. distachyon *accessions display extensive intraspecific natural variation in their response to growing with ammonium or nitrate as N source.*

To evaluate *B. distachyon* intraspecific variability when growing with ammonium as sole N-source we compared the total biomass of 52 *B. distachyon* natural accessions (Table S3.1) after 19 days of growth with 2.5 mM NH_4^+ supply and we used 2.5 mM NO_3^- as control condition (Figure 3.1, S3.1). To estimate the degree of ammonium tolerance, we used the ratio between the plant total biomass under NH_4^+ versus NO_3^- conditions, as it has been previously used in other works (Cruz *et al*., 2006; Ariz *et al.,* 2011; Sarasketa *et al*., 2014). We observed highly significant genetic variation regarding ammonium tolerance (SxA) (Figure 3.1, Table S3.2). As reported in previous chapters with Bd21 genotype, the results confirm *B. distachyon* as a sensitive species towards ammonium nutrition when 2.5 mM NH_4^+ is provided. Indeed, every accession except BdTR1i (ratio 1.0) displayed an ammonium/nitrate biomass ratio lower than 1, with the lowest ratio reported for Foz1 (0.40). Bd21 displayed an intermediate phenotype, with a ratio of 0.68 (Figure 3.1). Overall, 31 accession showed significant differences when comparing plant biomass sunder ammonium and nitrate nutrition, notably for the accessions that have a ratio lower than that of BdTR11I (less than 0.77). Regarding shoot and root biomass separately, they showed a similar pattern to that of total biomass, with a significant SxA interaction in both organs (Figure S3.1).

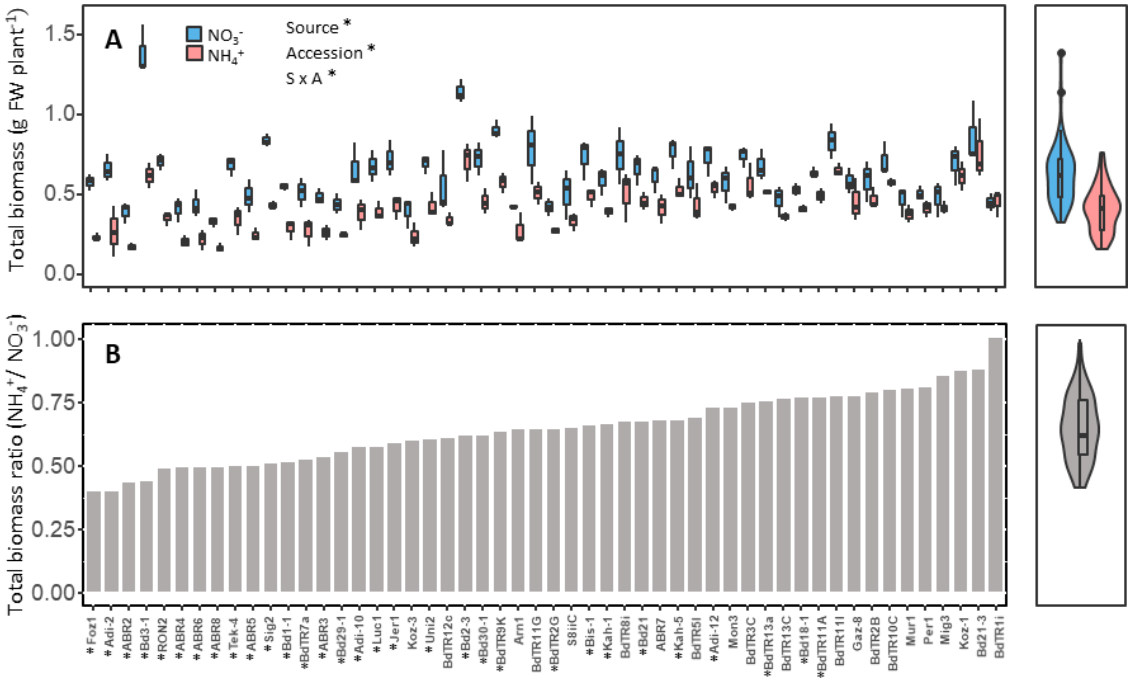

Figure 3.1. Natural variation of *B. distachyon* grown under nitrate or ammonium as N source in 52 accessions of *B. distachyon*. (A) Total plant biomass, (B) Ratio between total biomass under NH_4^+ and NO_3^- nutrition. Values in left graphs are the mean ± SE (n = 3). Asterisk (*) indicates either significant of the two-way ANOVA (S for nitrogen source, A for accession) or significant difference between total biomass under ammonium compared with nitrate for each accession (p<0.05). The violin plots on the right side show the distribution of the traits.

The metabolic adaptation of B. distachyon *to the N-source is essential to explain its intraspecific natural variability in growing under ammonium nutrition*

To evaluate whether *B. distachyon* intraspecific variability, highlighted by the significant SxA interaction of growth parameters, is related to the metabolic adaptation of leaf and root in function of the N source provided, we analyzed a panel of metabolic markers in both organs. We analyzed the content of 13 metabolites (chlorophyll, glucose, fructose, sucrose, starch, malate, citrate, NH_4^+, NO_3^-, glutamate, total amino acids, protein and glutathione) and 10 enzyme activities (glucokinase, GK; fructokinase, FK; glutamate dehydrogenase, GDH; glutamine synthetase, GS; phosphoenolpyruvate carboxylase, PEPC; malate dehydrogenase, MDH; pyruvate kinase, PK; total citrate synthase, CS; mitochondrial citrate synthase (CSm) and NADP-dependent isocitrate dehydrogenase, ICDH). The whole dataset is available in Table S3.2 and represented in boxplots available in supplementary material (Figures S3.2, S3.3, S3.4 and S3.5).

Overall, we observed significant SxA interaction effect for the content of NH_4, NO_3^-, amino acids, glucose, malate and citrate and for the activity GDH activity in both leaf and root. Besides, in leaf a significant interaction was also observed for the content for chlorophyll, sucrose and glutamate and for CS and CSm activities. In root, we report significant A x S effect for the content of fructose and total glutathione and for PEPC activity (Figure S3.2, S3.3, S3.4 and S3.5).

To explore the dataset and to understand the relationships between variables we performed different statistical analysis: principal component analysis (PCA), Pearson correlations visualized by clustered correlograms and heat map plots that included two-way hierarchical clustering. Firstly, PCA was performed with the whole dataset (Figure 3.2) taking into consideration 11 metabolites and 9 enzymes measured in leaf and root and using the organ biomass as supplementary variable. Since root has no value of chlorophyll and starch they were not considered for this PCA analysis. GS activity was discarded for every analysis because of the low-quality of the data obtained. PC1 and PC2 accounted for 76 % of the total variation (Figure 3.2). Indeed all the metabolic markers were represented in the PC1-PC2 biplot, except fructose that is almost exclusively represented in PC4 (Figure 3C) and citrate and malate, whose variations are explained by PC1 but also by PC3. Organ biomass was placed in PC1 and negatively correlated with most enzymes. Looking to individuals plot, the metabolic data allowed to clearly differente root and leaf data and also a clear differentiation between nitrate and ammonium-grown plants. The N-source appeared to have a higher impact on the root metabolism since the leaf data overlap while the root-data are clearly separated (Figure 3.1A). Besides, the highest variability appears to take place in the root of ammonium-fed plants.

In view of the expected clear separation between root and leaf we next performed PCAs and heat map visualization with hierarchical clustering for each organ separately, both showing again a clear separation in function of the N-source supplied (Figures S3.6, S3.7, S3.8 and S3.9). In leaf tissue, the heat map highlighted on the one hand the tendency of ammonium-fed plants for having a higher content of NH_4^+, total amino acids and glutathione together with higher GDH, CSm, CS, ICDH, MDH, GK and FK enzyme activities. On the other hand, nitrate-fed plants nutrition showed the tendency to accumulate more NO_3^-, citrate and malate. On the other hand, roots under ammonium nutrition showed the tendency for having a higher content of NH_4^+, total amino acids and a higher activity of all the enzymes determined. Similar information can be extracted from the root-PCA and leaf-PCA (Figures S3.6, S3.7). For instance, in the leaf PCA, ammonium-fed accessions were placed in the positive side of the PC1 in agreement with the metabolic markers with higher values shown for this nutrition (Figure S3.6).

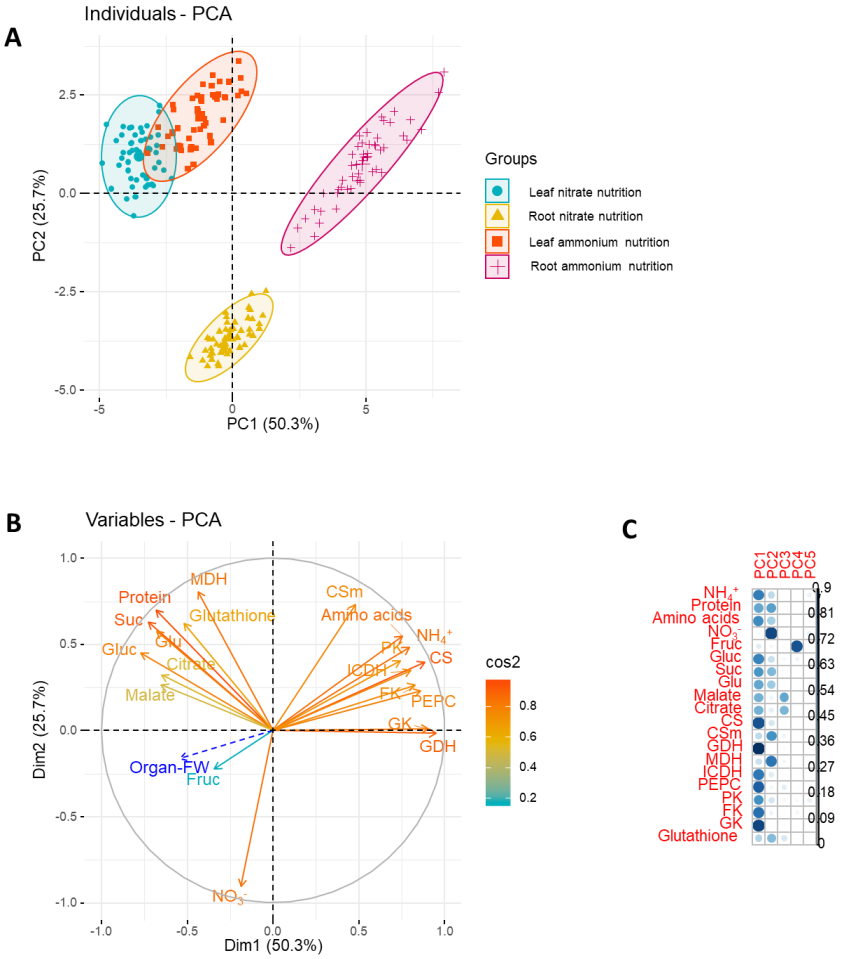

Figure 3.2. Principal component analysis (PCA) of metabolic data set for leaf and root of 52 *B. distachyon* accessions grown under ammonium or nitrate nutrition. (A) Individuals PCA score plot. (B) Variables loading plot represent cos2 as the square loadings for variables shows the quality of the representation for metabolites traits included in the plot. (C) Correlation plot showing the PCs where the variables are represented.

To further narrow down the exploratory analysis, we performed new heat maps analyzing separately not only the organ but also the nutrition type (Figures 3.3, 3.4, S3.10, S3.11). In leaves, variables were split into two groups, one including biomass in close relation with the content of sugars for both ammonium and nitrate nutrition. In the case of ammonium nutrition, leaf biomass was also closely associated to NH_4^+ content type (Figure 3.3). For roots, the split of variables was more disperse with biomass closely related to soluble carbohydrates in the case of ammonium-fed plants and to amino acids (figure 3.3), malate and sucrose in the case of nitrate-fed ones (Figure 3.4). Regarding the distribution of the accessions, the clustering revealed two groups, in the case of leaves the groups formed contain a similar number of accessions (Figures 3.3 S3.10)while for roots one of the groups was smaller and contained 21 for ammonium-fed and 13 accessions for nitrate-fed plants (Figures 3.3, 3.4, S3.10, S3.11). Looking to the localization of the 10 accessions showing the highest (FOZ1, Adi-2, ABR2, Bd3-1, RON2, ABR4, ABR6, ABR8, Tek 4, ABR5) and the lowest (BDTR1i, Bd21-3, Koz-1, Mig3, Per1, Mur1, BdTR10C, BdTR2B, Gaz8, BDTR11I) sensitivities to ammonium stress, in both leaf and root

tissue of nitrate-fed plants their distribution was scattered (Figures S3.10, S3.11). Interestingly, under ammonium nutrition, these accessions were distributed in the two groups of the cladogram in function of their tolerance degree. In particular, in roots every tolerant accession was located in the upper group while 8 out of the 10 most sensitives located in the lower group (Figure 3.4). Similarly in leaves 9 out of 10 tolerant genotypes were placed in the upper group while also 9 of the 10 more sensitive accessions were located in the lower group (Figure 3.3). This observation highlights the relevance of the metabolic adaptation under ammonium nutrition in relation with *B. distachyon* natural variability towards ammonium stress.

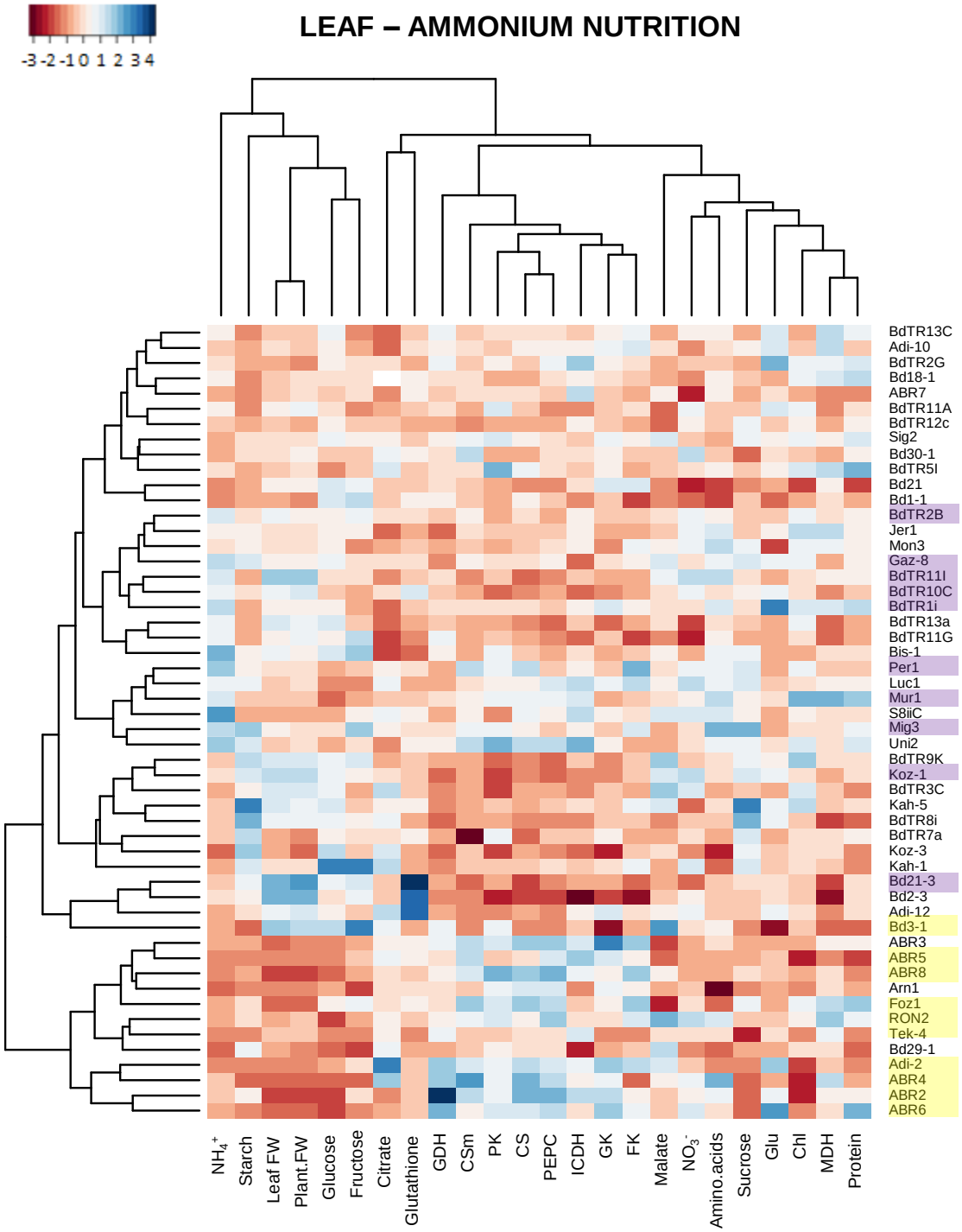

Figure 3.3. Leaf heat map visualization with two-way clustering of 13 metabolites and 9 enzymatic activities determined plants grown under ammonium-nutrition including also biomass data against 52 accessions of *B. distachyon*. Chl means chlorophyll, CS citrate synthase, CSm mitochondrial citrate synthase, FK fructokinase, FW fresh weight, GDH NAD-dependent glutamate dehydrogenase, GK glucokinase, Glu glutamate, ICDH NADP-dependent isocitrate dehydrogenase, MDH malate dehydrogenase, PEPC phosphoenolpyruvate carboxylase and PK pyruvate kinase. The 10 accession displaying the highest tolerance and the highest sensitivity to ammonium nutrition in Figure 3.1 are shown in purple and yellow, respectively.

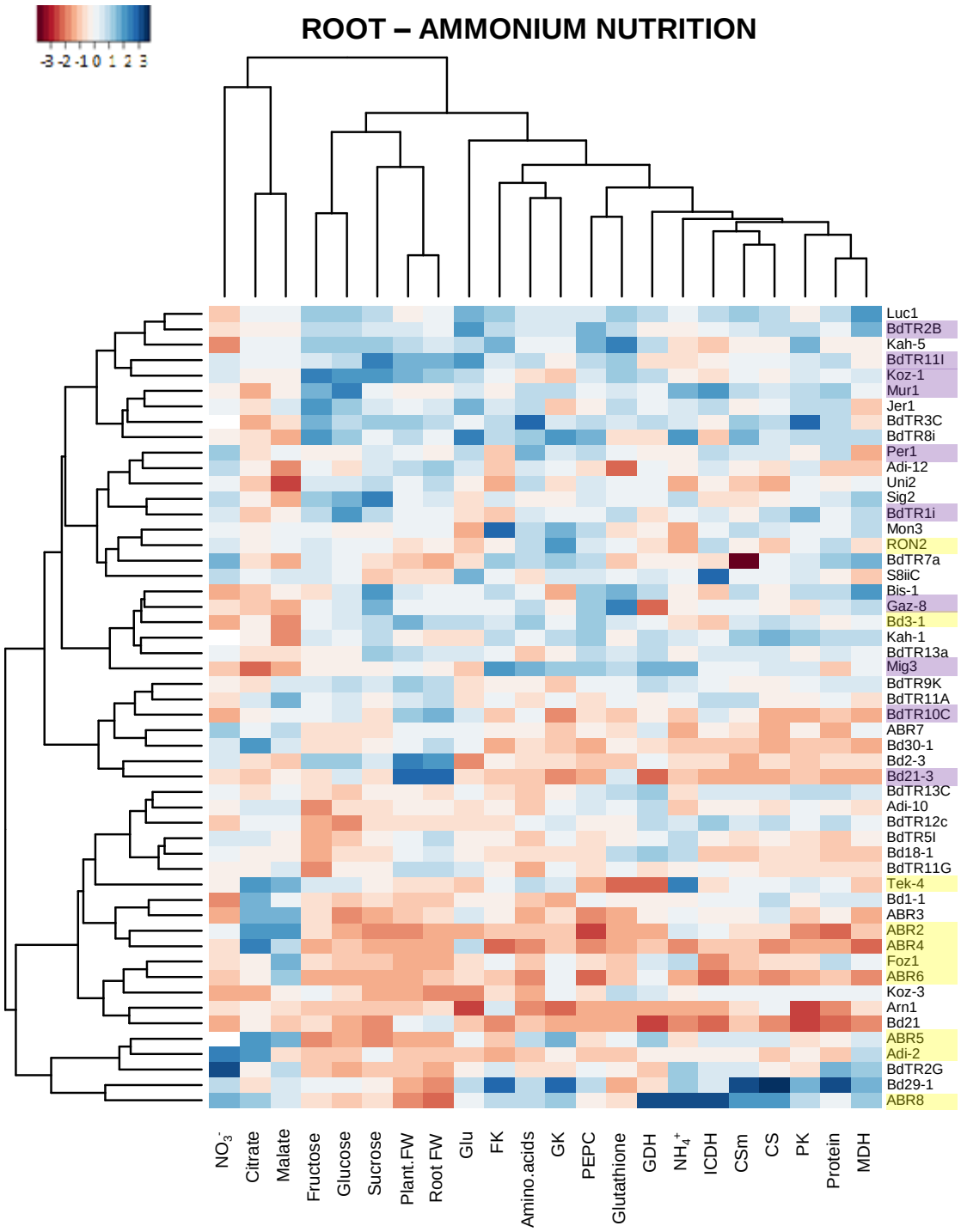

Figure 3.4. Root heat map visualization with two-way clustering of 13 metabolites and 9 enzymatic activities determined in plants grown under ammonium-nutrition including also biomass data against 52 accessions of *B. distachyon*. Abbreviations are in Figure 3.3. The 10 accession displaying the highest tolerance and the highest sensitivity to ammonium nutrition in Figure 3.1 are shown in purple and yellow, respectively.

To test the connectivity between paired variables, we tested their linear dependence using Pearson's correlation coefficient was calculated for P≤0.01 that were then clustered in correlograms (Figure 3.5). Under ammonium nutrition shoot biomass showed to be positively correlated with glucose (r=0.59), fructose (r=0.41) and chlorophyll (r=0.36) content and negatively correlated with all the enzymatic activities, notably with CS (r=-0.77) and PEPC (r=-0.83) (Figure 3.5). Under nitrate nutrition leaf biomass was only negatively correlated with protein content (r=-0.68) and the activity of ICDH (r=-0.45) and PEPC (r=-0.50) (Figure 3.3b). In the case of root biomass under ammonium nutrition, it was positively correlated with the content of sucrose (r=0.49) and glucose (r=0.52) (Figure 3.5). Under nitrate nutrition root biomass was positively correlated with the content of citrate (r=0.43), malate (r=0.53), glucose (r=0.53) and fructose (r=0.44) and negatively correlated with the content of proteins (-0.40) and NO_3^- (r=-0.40) and with the activity of many of the determined enzyme activities (GK, r=-0.48; GDH, r=-0.46; MDH, r=-0.43; CSm, r=-0.41; ICDH, r=-0.38; CS, r=-0.37) (Figure 3.3d). Regarding the total plant biomass ratio ammonium and nitrate-fed plants we only observed was significant correlation with the metabolic markers determined under ammonium nutrition. In particular, with leaf PEPC (r=-0.54), GDH (r=-0.46), CS (r=-0.43) and PK (r=-0.36) enzyme activities and, with root citrate (r=-0.55), glutathione (r=0.48) and glucose (r=0.44) content (Figure 3.5).

Finally, we analyzed the connectivity between the metabolic variables but regarding their ratios under ammonium vs. nitrate nutrition, again considering leaf and root data separately (Figures S3.12 and S3.13). In this context, the both total and root biomass ratios were strongly associated with the ratio of glutathione content. This association, is also apparent observing the glutathione boxplot (Figure S3.4), notably in the root, where the difference in the content of glutathione tends to diminish when moving from the most sensitive accession (on left side of the figure) to the most tolerant (on right side of the figure). Interestingly this difference does not appear to be due to a decrease of glutathione in nitrate nutrition but to an increase of the glutathione content of those accessions more tolerant to ammonium. Indeed, both leaf and root glutathione content under ammonium nutrition were significantly correlated with biomass parameters, while no correlation was observed under nitrate nutrition (Figure 3.5). In this sense, this points out that glutathione may play an important role in *B. distachyon* variability versus the tolerance to ammonium.

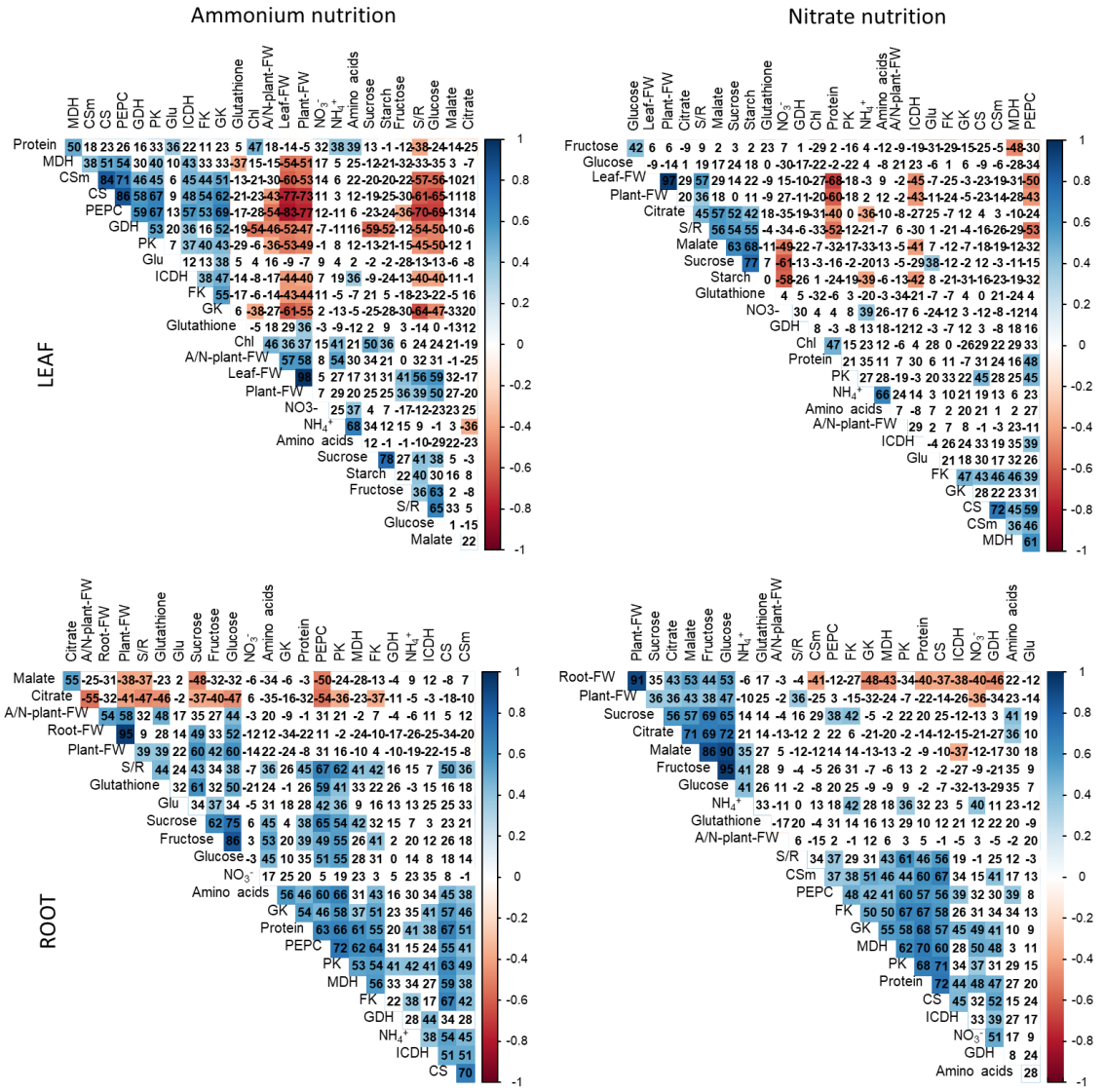

Figure 3.5. Correlation matrixes of the 13 metabolites and 9 enzymatic activities, including also biomass data determined in the in leaf and root of 52 *B. distachyon* accession grown under ammonium or nitrate nutrition. Numbers inside the boxes indicate Pearson r correlation coefficient (x100). Significant positive and negative correlations ($P < 0.01$) are highlighted in blue and red, respectively following the scale shown in the right-side of the plots. Abbreviations are shown in Figure 3.3.

Multiple regression analysis is a helpful tool to select the most explanatory metabolic variables regarding B. distachyon *response to growing under ammonium or nitrate nutrition.*

To try to make a hierarchy of the most explanatory variables related with plant growth. We performed multiple regression models with a sequential methods using Akaike's information criterion (AIC) to determine the 'best' model by rewarding the variables that add explanatory power but penalizing the inclusion of additional variables. This provides the simplest model with the least collinearity and, thus, supposedly, the best estimation (Shaw and Geyer, 2010).

We analyzed eight different scenarios considering the organ biomass (Tables 3.1, 3.2, S3.3 and S3.4) and total plant biomass (Table 3.3, S3.5) as dependent variables. Besides, we also made two additional models using ammonium vs. nitrate total biomass ratio as dependent variable (Table 3.4).The standardized coefficient shows the strength of the independent variables to explain the corresponding dependent variable. Under ammonium nutrition, the regression models explained 82.5 % and 52.6 % of the variability for shoot and root biomass respectively (Tables 3.1, 3.2). For shoot biomass, PEPC activity was the variable with the highest contribution to the model and showed a negative effect on shoot biomass. PEPC contribution was followed by the content of amino acids, glucose, malate, glutathione and MDH activity (Table 3.1). For root biomass, sucrose was the most explanatory variable showing a positive effect and was followed by the activity of MDH activity, glucose content and CS activity (Table 3.2).

Table 3.1. Stepwise-multiple-regression analysis of the metabolic measurements (independent variables) in leaves of *B. distachyon* fed with ammonium- associated with shoot biomass (dependent variable).

	SHOOT BIOMASS – AMMONIUM NUTRITION	
INDEPENDENT VARIABLE	STANDARDIZED COEFFICIENT	*P*- value
PEPC ACTIVITY	-0.512	0.000
AMINO ACIDS	0.295	0.000
GLUCOSE	0.261	0.005
MALATE	0.213	0.001
GLUTATHIONE	0.204	0.003
MDH ACTIVITY	-0.171	0.031
R^2	0.846	
ADJUSTED R^2	0.825	
ESTIMATE SE	0.036	

Table 3.2. Stepwise-multiple-regression analysis of the metabolic measurements (independent variables) in root of *B. distachyon* fed with ammonium associated with shoot biomass (dependent variable)

	ROOT BIOMASS – AMMONIUM NUTRITION	
INDEPENDENT VARIABLE	STANDARDIZED COEFFICIENT	*P*- value
SUCROSE	0.484	0.004
MDH ACTIVITY	-0.373	0.009
GLUCOSE	0.312	0.039
CS ACTIVITY	-0.282	0.029
R^2	0.565	
ADJUSTED R^2	0.526	
ESTIMATE SE	0.040	

Under nitrate nutrition, for shoot biomass, protein content followed by ICDH activity and NH_4^+ content explained 55.6 % of the total variability (Table S3.3). For root biomass glucose showed

the highest contribution to the model, followed by the activity of GK and FK, overall explaining the 48.7 % of the variability (Table S3.4).

Regarding total plant biomass, under ammonium nutrition root-sucrose and leaf-PEPC were the most explanatory variables, which together with root PK and leaf CS activity, glutathione and total amino acids content explained 86.5 % of the variability (Table 3.3). Under nitrate nutrition leaf-protein and GDH activity in combination with root-malate and glucose content explained 63.9 % of the variability (Table S3.5). In the next scenario, the ratio of ammonium vs. nitrate total plant biomass leaf PEPC activity and NH_4^+ content under ammonium nutrition, together with leaf nitrate and starch content under nitrate nutrition where the variable with the highest contribution to the model, which in total explained 76.9 % of the variability (Table 3.4).

Table 3.3. Stepwise-multiple-regression analysis of the metabolic measurements (independent variables) in leaf and root of ammonium-fed plants associated with whole-plant biomass (dependent variable). AR and AL are used to differentiate the variable determined respectively in roots and leaves of ammonium-fed plants.

	TOTAL BIOMASS – AMMONIUM NUTRITION	
INDEPENDENT VARIABLE	STANDARDIZED COEFFICIENT	*P*- value
AR - SUCROSE	0.445	0.000
AL – PEPC ACTIVITY	-0.348	0.003
AL - CS	-0.303	0.009
AL - GLUTATHIONE	0.280	0.000
AL – AMINO ACIDS	0.242	0.000
AR – PK ACTIVITY	-0.242	0.001
R^2	0.882	
ADJUSTED R^2	0.865	
ESTIMATE SE	0.051	

Table 3.4. Stepwise-multiple-regression analysis of the metabolic measurements (independent variables) in leaf and root of ammonium- and nitrate-fed plants associated with whole-plant biomass ratio of ammonium- vs. nitrate-fed plants (dependent variable) AR and AL are used to differentiate the variable determined respectively in roots and leaves of ammonium-fed plants. Accordingly, NR and NL are used to differentiate the variable determined respectively in roots and leaves of nitrate-fed plants.

	RATIO AMMONIUM BIOMASS/NITRATE BIOMASS	
INDEPENDENT VARIABLE	STANDARDIZED COEFFICIENT	*P*- value
AL – PEPC ACTIVITY	-0.565	0.000
NL - NITRATE	-0.513	0.000
NL - STARCH	-0.507	0.000
AL - NH_4^+	0.469	0.000
AL - FRUCTOSE	-0.368	0.000
AL - STARCH	0.360	0.001
NR – MDH ACTIVITY	-0.250	0.010
R^2	0.803	
ADJUSTED R^2	0.769	
ESTIMATE SE	0.066	

GWA mapping of the different traits reveals significant genetic association potentially related with the natural adaptation of B. distachyon *towards ammonium nutrition*

One strategy to decipher the underlying genetics of naturally occurring phenotypic variation is the use of genome-wide association studies (GWAS). The power of GWAS has been demonstrated by multiple plant studies in different species that mapped and validated individual genes associated to many traits like pathogen resistance, Cd content (Atwell *et al*., 2010; Chao *et al*., 2012; Rosas *et al*., 2013; Yan *et al*., 2019), complex traits such as flowering or root architecture (Rosas *et al*., 2013; Romero-Navarro *et al*., 2017) or even metabolites and enzyme activities (Angelovici *et al*., 2013; Luo, 2015; Fusari *et al*., 2017).

Complex agricultural traits are controlled by complex genetic architectures that may include thousands of genes controlling the variation in the trait of interest (Boyle *et al*., 2017; Miao *et al*., 2019). Most GWAS carried out in crops use single-locus linear models, such as mixed-linear models (MLM) including EMMAX. However, mainly because these models do not take into account the background genome possess a reduced statistical power, which is of great importance for the study of complex traits (Jaiswal *et al*., 2016; Miao *et al*., 2019). In this sense, in this study we gave importance to the multi-locus models such as multi-locus mixed-model (MLMM) and fixed and random model circulating probability unification model (FarmCPU) which take the background genome into account for the analysis using a multiple regression approach (Wang *et al*., 2012; Jaiswal, *et al* 2016). We select MLMM model over FarmCPU, because the last

one uses a reduced kinship matrix, which is a less restrictive way to control false positives. Indeed, using MLMM more markers passed the significance thresholds, demonstrating that the power of association mapping improved due to the MLMM. This is a rather conservative approach, as we are aware of the possible multicollinearity that can arise as a result of testing a reduced number of genotypes with a very large number of markers. The multi-locus approach ensures that trait variance is associated with the most significant markers, whereas closely similar markers anywhere in the genome will not be selected by this model. Nevertheless, general-linear model (GLM) and MLM, single-locus models, were performed (data not shown). Overall, MLMM model showed the best level of confidence and seemed to perform well in controlling false positives, as revealed by the closeness of the expected vs. observed probabilities points to the 1:1 line in the quantile-quantile (Q-Q) plots for all traits.

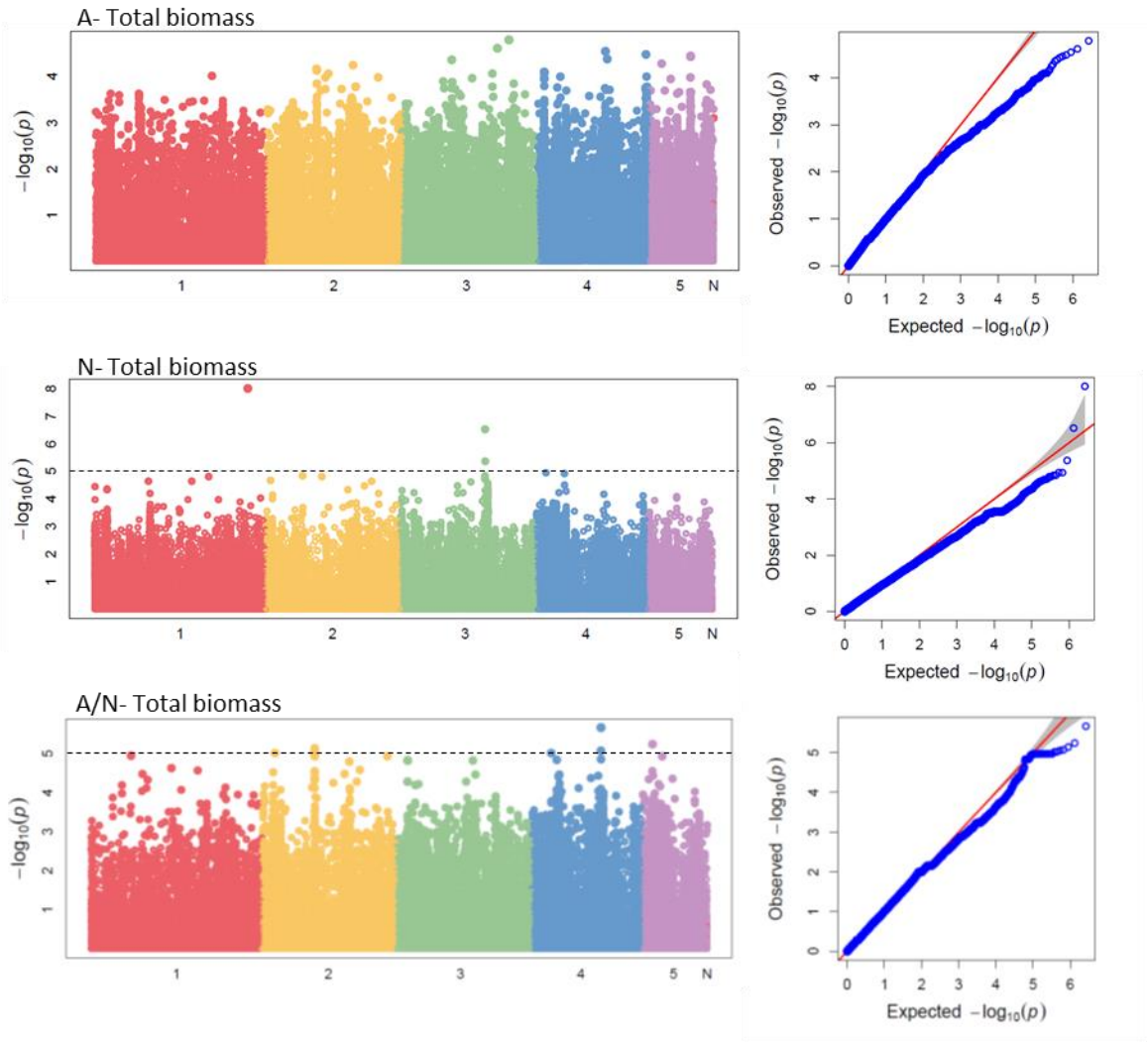

Figure 3.6. Manhattan plots (left side) showing the marker-trait associations and Q-Q plots (right side) showing distribution of observed and expected *p*-values for the total biomass of plants grown under ammonium (A) or nitrate (N) nutrition and for the whole-plant biomass ratio of ammonium vs nitrate-fed plants. When SNPs over –log10(p)>5 threshold the threshold is shown with a black dashed line

First, we performed GWAs with the most important and integrative trait related to plant performance, which is plant biomass. Besides, we also performed a GWAS with the total plant biomass ratio of ammonium vs. nitrate grown plants (Figure 3.6) together with leaf and root biomass separately (Figure S3.14). According to Bonferroni-corrected threshold we did not find any significant marker for these traits. In general, the effect sizes of genetic associations with complex, highly polygenic traits are often small and in many cases missing (Huang *et al*., 2012; Luo, 2015) For instance, it is common to find that GWAS does not have enough power to find associations for physical measurements such as biomass (Burghard *et al*., 2017). In this line, we performed GWAS for all the metabolic markers analyzed in both leaf and root tissue under both nutritions (Figures S3.15-S3.18). We found highly significant associations for 15 of 80 of the metabolic markers analyzed (Table S3.6). For ammonium nutrition, highly significant associations were found for 6 traits: leaf NH_4^+, glucose, and glutathione content, leaf CS and CSm

activities and root GK activity. For nitrate nutrition, highly significant associations appeared for 9 traits: leaf NH_4^+, NO_3^-, malate and fructose content and root malate content and CS, GDH, MDH and PK activities (Table S3.6). We look for the genomic regions (20kb up- and down-stream surrounding the significant SNPs) and extracted the genes encoded, which are also available in Table S3.6. Although for biomass parameters and many metabolites we did not find significant SNPs with the Bonferroni-corrected threshold, it must be noted that this statistical analysis is very restrictive and sometimes hides SNPs that might be also relevant. In this sense, we also extracted the SNPs with a significance higher than $-\log_{10}(p)=5$, which are all available in Table S3.7.

For biomass, taking $-\log_{10}(p)=5$ as threshold, under nitrate nutrition we found 1 SNP associated to leaf biomass , 3 SNPs to root biomass and 3 SNPS to whole plant biomass. Under ammonium nutrition we found only 1 SNP for leaf biomass. Besides, 2 SNPS were found associated with whole plant biomass ratio under both nutritions (Table S3.7). The genes encoded in the genomic regions surrounding the significant SNPs (20 kb up- and down-stream each SNP) are shown in Table S3.8.

The exploration of the data, notably with the clustering of genotypes in the heat maps, revealed that *B. distachyon* natural variation in ammonium stress degree, quantified as the ratio of the plant biomass under ammonium vs. nitrate nutrition, was mainly influenced by the metabolic performance under ammonium nutrition. Thus, we focused on the variables with the highest contribution to the multiple regression models performed using as dependent biomass parameters of ammonium-fed plants (Table S3.9) and the ratio of total plant biomass (Table S3.9). In particular, we focused on PEPC activity and NH_4^+ content in the leaves and in sucrose content in the root. For PEPC activity and sucrose content no significant SNPs were found with Bonferroni-corrected threshold, but 12 and 2 SNPS were associated, respectively with a $-\log_{10}(p)>5$ significance. For NH_4^+ content in the leaves 1 SNP in chromosome 1 was found associated with Bonferroni-corrected threshold together with 8 SNPS with $\log_{10}(p)>5$ significance.

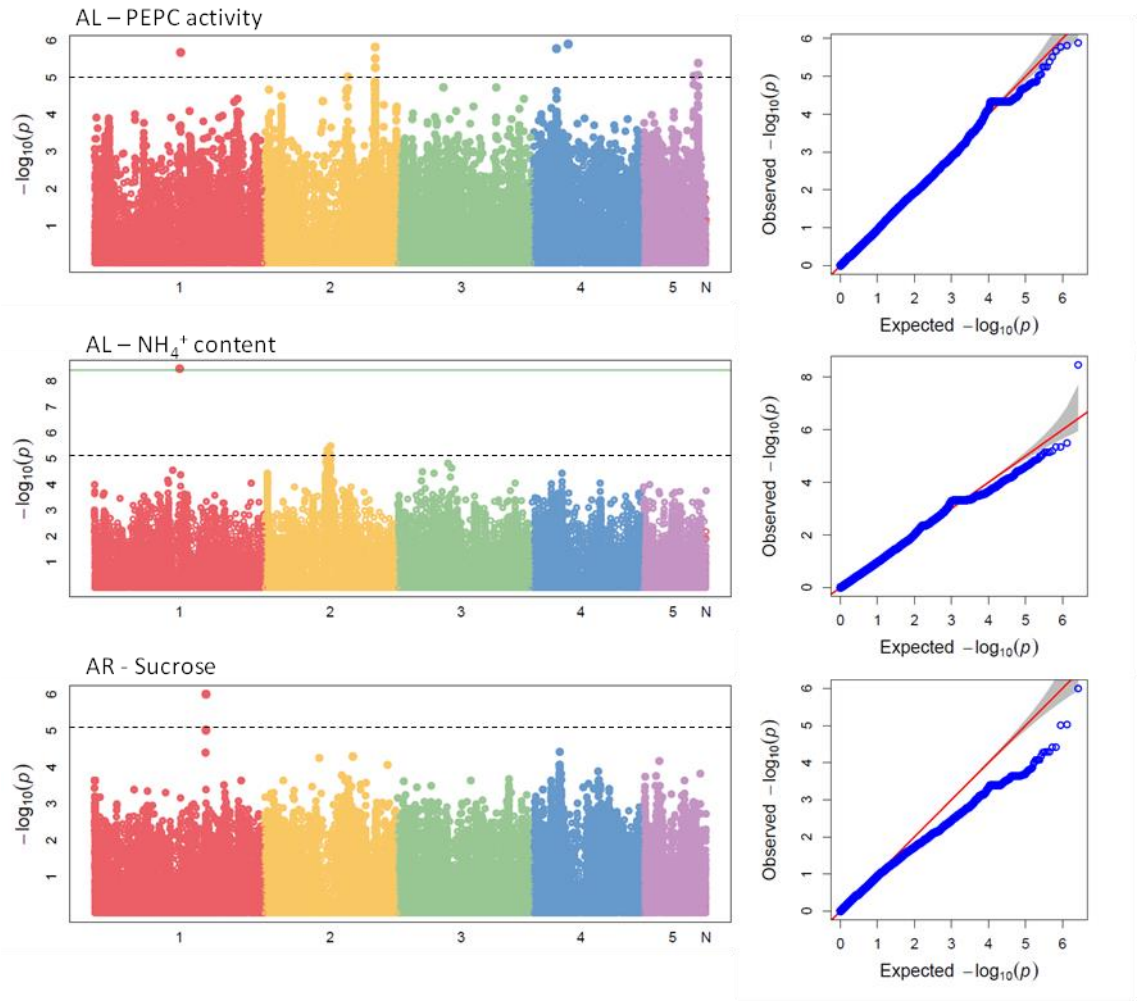

Figure 3.6. Manhattan plots (left side) showing the marker-trait associations and Q-Q plots (right side) showing distribution of observed and expected *p*-values for PEPC activity and NH_4^+ content in leaves and sucrose content in roots of ammonium-fed plants. When SNPs over Bonferroni-corrected threshold are found the threshold is shown with a green line within the Manhattan plot and the threshold for –log10(*p*)>5 is shown with a black dashed line.

Looking into genomic regions surrounding the significant SNPs (20 kb up- and down-stream each SNP) we found 13 genes for the content sucrose in the root, 10 for leaf NH_4^+ content and 39 genes for leaf PEPC activity (Table S3.9). Out of the 13 genes in the sucrose associated genomic regions, 9 were uncharacterized or unknown genes and 4 were encoding for a rosmarinate synthase (BRADI_1g50770), a protease (BRADI_1g50760) and two cysteine synthases (BRADI_1g50826, BRADI_1g50832). For leaf NH_4^+ content only 2 of the genes had a function associated: BRADI_2g28450 that encodes for a probable AMP deaminase and BRADI_2g28427 for anaphase-promoting complex subunit 1. Interestingly for PEPC, out of the 12 SNPs with $-\log_{10}(p)>5$ significance, 5 were located in a 10 kb region of Chromosome 2 and among the genes in that region we found that they encoded a probable pectinesterase (BRADI_2g49500), a probable glutamate carboxypeptidase (BRADI_2g49510) and interestingly a NADP-malic enzyme (BRADI_2g49540), an enzyme that is closely related to PEPC as anaplerotic enzyme of the TCA cycle (Table S3.9)

Finally, since the overall data exploration also suggested an role for glutathione content under ammonium nutrition, we further look to the SNPs associated to this trait (Table S3.7; S3.8) and found in leaf under ammonium nutrition 3 SNPS with a significance lower than $-\log_{10}(p)>5$, one SNP being significant with Bonferroni-corrected threshold while no significant SNPS were found in the root. Sixteen genes were located in the surrounding regions of these SNPS, with an assigned function for 12 of them (Table S3.9). Among them, associated to the SNP with the highest significance we found a MYB transcription factor (BRADI_4g09490), a threonine kinase (BRADI_4g09498) and a probable LRR receptor-like kinase (BRADI_4g09481) that may be involved in the regulation of glutathione homeostasis.

5. DISCUSSION

Brachypodium distachyon *displays extensive natural variation to growing with* NH_4^+ *as sole N source*

Ammonium stress is considered as universal, virtually affecting every species. However, great variation in ammonium tolerance or sensitivity has been reported in different species (Monselise and Kost, 1993). For instance, there are species that even display ammonium preference such as late-successional conifers, probably because of the adaptation of boreal forests to low nitrification soils (Britto and Kronzcuker, 2013). Besides, two of the species with high tolerance to ammonium belong to the Poaceae family such the halophyte C4 grass *Spartina alterniflora* (Hessini *et al*., 2013) and notably rice, likely because its adaptation to paddy fields were the limited oxygen availability restraints nitrification.

Within the same species great variability towards ammonium stress has also been reported in different species such as pea (Cruz *et al*., 2011), *Arabidopsis thaliana* (Rauh *et al*., 2002; Sarasketa *et al*., 2014) and a number of graminaceous species like maize (Schortemeyer *et al*. 1997), rice (Chen *et al*., 2013; Di *et al*., 2018) or wheat (Wang *et al*., 2016a). In agreement, in this study carried out with a panel of 52 natural accessions of *Brachypodium distachyon* model grass, we report extensive variability in ammonium tolerance with accessions that grew similarly with NO_3^- or NH_4^+ supply and with accessions that showed high sensitivity experiencing more than 50 % of grown reduction under ammonium respect to nitrate nutrition (Figure 3.1). We considered biomass as the main marker to evaluate the performance of plants under each N-supplied since biomass integrates all the metabolism changes, nutrient uptake and assimilation. Overall, we observed a similar degree of intraspecific variability as previously reported by Sarasketa *et al*. (2014) studying 47 *A. thaliana* accessions or by Di *et al*. (2018), who phenotyped the response of 25 rice genotypes upon ammonium stress. Previous works with *A. thaliana* have

tried to take advantage of intraspecies variability to map quantitative trait loci (QTL) in relation with ammonium tolerance. For instance, Rauh *et al.* (2002) and Sasaki and Kojima (2018) identified, respectively, 5 and 6 QTLs analyzing a RIL population of *A. thaliana* derived from the cross between Columbia-4 × Landsberg erecta (Ler). However, the identified QTLs covered big genomic regions and no positional cloning or candidate gene analysis was performed (Rauh *et al*., 2002; Sasaki and Kojima, 2018).

Brachypodium distachyon *displays a natural variation in metabolic adaptation under ammonium nutrition*

Metabolite composition and concentration, together with enzyme activity, reflect the metabolic adaptation of organisms to a particular nutrient environment or stressing conditions and may obviously impact plant growth. The advantage of taking natural genetic diversity into account is that it represents a powerful tool to unmask the complex networks that link metabolism with biomass because it allows the study of thousands of genetic perturbations that vary independently between different genotypes (Sulpice *et al*., 2013). In the present study, whole-plant metabolic data gives light about the strategy of Brachypodium as species to face up ammonium stress and could potentially reveal genetic clues regarding the extent of the growth response in sensitive and tolerant genotypes. In view of genotypes distribution (Figures 3.3, 3.4) it is clear that the metabolic adaptation to ammonium nutrition has great impact in the observed natural variability towards ammonium stress (Figure 3.1).

In many species, including cereals, primary nitrate assimilation occurs mainly in the photosynthetic organs and ammonium assimilation mainly in the root and this has been reported in many species including wheat, sorghum (Setien *et al*., 2013; Miranda *et al*., 2016; Wang *et al*., 2016a) and *B. distachyon* in chapter 1 (De la Peña *et al*., 2019). This fact had a huge impact on the metabolic behaviour of virtually every accession and indeed, the metabolic profiling of the 52 accessions clearly segregated the dataset in four groups separating organs (leaves and roots) and N-nutrition (ammonium and nitrate) (Figure 3.2). In agreement, we mostly focused on the behaviour on each plant organ under a given specific nutrition, looking for specific features in their metabolic response.

One of the most common markers of ammonium stress is the accumulation of free NH_4^+ and amino acids (Sarasketa *et al*., 2014; Esteban *et al*., 2016). In agreement, and as reported in chapters 1 and 2 for Bd21, ammonium nutrition provoked in every accession the accumulation of NH_4^+, mostly in roots, accompanied by parallel increments in the contents of amino acids and proteins. Disproportionate amino acid synthesis in the root entails the using of most of the 2-

OG available for NH_4^+ assimilation, thus making TCA-cycle to work in a non-cyclic mode (Setién *et al*., 2013; Vega-Mas *et al*., 2019a). Moreover, there is a need to increase the flux of carbon towards NH_4^+ assimilation. This functioning requires a coordinated regulation of TCA cycle enzymes together with its associated anaplerotic enzymes as evidenced in the present study with the generalized induction in the root of CS, mCS, MDH, NADP-ICDH and PEPC (Figure S3.9). Besides, TCA cycle was also coordinated with glycolytic pathway, as evidenced by sugars content, FK, GK and PK activities. In agreement with this mode of action ammonium-fed leaves were almost depleted of citrate and malate levels.

Genotypes clustering evidenced that the metabolic adaptation to ammonium nutrition (Figures 3.3, 3.4) rather than to nitrate nutrition (Figures S3.10, S3.11) was responsible of *B. distachyon* variability in ammonium stress degree taking the biomass ratio when growing in ammonium vs. nitrate nutrition as a marker. After data exploration together with stepwise multiple-regression, the activity of PEPC and NH_4^+ content in ammonium-fed leaves together with the sucrose content in the root of ammonium-fed plants revealed as key variables explaining *B. distachyon* tolerance to ammonium stress. Besides, glutathione content also appeared closely related to *B. distachyon* performance in function of the N source provided.

Interestingly, in agreement with the underlined importance of NH_4^+ content in leaves of ammonium-fed *B. distachyon*, Sarasketa *et al*. (2014) observed that the accumulation of free NH_4^+ in the leaves was correlated with *A. thaliana* natural variability to ammonium tolerance. In fact, the excessive accumulation of NH_4^+ in cells´ cytosol has been put forward as the most probable cause of the biomass reduction typically observed in plants subjected to ammonium stress. Suggesting that growth reduction could be a trade-off of the energy consumed by the cell to deal with free NH_4^+, through its assimilation into organic molecules, its efflux outside the cell or its confinement inside the vacuole (Coskun *et al*., 2013; Kirscht *et al*., 2016). Similarly, Schortemeyer *et al*. (1997) studying 4 maize cultivars with contrasted ammonium-tolerance observed that growth reduction in Helga variety, which displayed the highest sensitivity to ammonium nutrition, was correlated with the accumulation of twice the concentration of free NH_4^+ in the shoot.

Regarding soluble sugars, and particularly sucrose, paired correlations with growth parameters support the idea that the availability of soluble sugars (Gluc, Fru and Suc; Figure 3.5) in roots is essential to fuel the capacity to assimilate ammonium and key to explain *B. distachyon* natural variation towards ammonium stress. Schortemeyer *et al*. (1997) also reported decreased concentration in root soluble carbohydrates in the maize cultivars that displayed higher

sensitivity to ammonium nutrition. Wang *et al*. (2016a) also observed that soluble sugar content in the root decreased with ammonium respect to nitrate nutrition notably in the sensitive wheat ecotype AK58, while this reduction was less pronounced in the tolerant Xumai25. Besides, ratio of shoot to root in soluble sugar was higher in AK58 respect to Xumai25 (Wang *et al*., 2016a). Interestingly, in our study shoot-to-root sucrose ratio was negatively correlated with plant biomass under ammonium nutrition (Figure S3.19), overall indicating perturbed sucrose transport toward the root together with sugars content in this organ may explain the observed *B. distachyon* variability in ammonium tolerance.

The role of PEPC upon ammonium nutrition has been addressed in several works from different experimental approaches. In non-photosynthetis tissues, the enzyme has a primary role functioning as anaplerotic route to refill the TCA cycle, mainly when intermediates of the cycle are removed to maintain different biosynthetic pathways as, it is the case for ammonium nutrition (Lasa *et al*., 2002; Setién *et al*., 2013 and 2014; Arias-Baldrich *et al*., 2017; Vega-Mas *et al*., 2019a). Moreover, studies using PEPC-deficient or knockdown mutants demonstrated that this enzyme would be key for the provision of citrate and malate (Shi *et al*., 2011; Matsumoto *et al*., 2010). PK is also another enzyme that uses PEP to provide pyruvate to the TCA cycle. Therefore, PK and PEPC are key enzymes to branch the channelling of PEP pool either towards pyruvate or OAA. In *B. distachyon* there was also induction of PK in roots under ammonium, which agrees with evidences described in other works, for instance in sunflower (Lasa *et al*. 2002), wheat (Liu *et al*., 2017) and *A. thaliana* (Coleto *et al*., 2019). In spinach plants, considered a sensitive species, PK was the main way to provide carbon skeletons while the induction of PEPC was prioritized in pea plants, considered as an ammonium tolerant species (Ariz *et al*., 2011; Cruz *et al*., 2011). Thus PEP seems a crucial checkpoint in the capacity of the root cell to assimilate NH_4^+. However, root PEPC activity was not underlined as metabolic trait contributing to explain the natural variability of *B. distachyon* root. In contrast, the activity of PEPC in the leaf, negatively correlated with growth parameters, showed a relevant contribution to explain the variability of *B. distachyon* growing with exclusive NH_4^+ supply.

Glutathione is an essential molecule for plants that possess a myriad of functions (Noctor *et al.*, 2012). It is a potent non-enzymatic antioxidant, with a central role in Foyer-Halliwell-Asada cycle, it participates in the regulation of cell redox homeostasis. Indeed, one of the symptoms of ammonium nutrition may be ROS overproduction and thus ammonium is known to sometimes induce the plant antioxidant-machinery (Domínguez-Valdivia *et al*., 2008; Podgórska *et al*., 2017b). GSH also acts as regulator of cellular sulphur homeostasis, storage and transport. Indeed, in chapter 2 the proteome analysis showed a link between sulphur metabolism and

ammonium nutrition that could be related with the increasing GSH content observed in roots under ammonium-nutrition in relation with the promotion of ammonium tolerance. In the same line of evidence, Coleto *et al*., (2017) reported that ammonium nutrition enhanced sulphur assimilation, supported among others by an increase in the synthesis of GSH in *Brassica napus*. Alternatively, since GSH is a tripeptide formed by Glu, Cys and Gly, it seems logical that its content could be favored when the overall synthesis of amino acids is also promoted. Besides GSH is the substrate of glutathione-S-transferases (GSTs) and several transcriptomic and proteomic studies, including *B. distachyon* (chapter 2), observed the up-regulation of GSTs under ammonium nutrition (Patterson *et al*., 2010; Vega-Mas *et al*., 2017; Prinsi and Espen, 2018; Coleto *et al*., 2019; Royo *et al*., 2019). One explanation could be that GSTs would be contributing to sequester ammonium-derived compounds into non-toxic metabolites (Vega-Mas *et al*., 2017). Overall, GSH seems to accomplish several protective functions under ammonium nutrition and its content seems to be an important trait related to the natural variation in the response of *B. distachyon* to ammonium stress.

Genome-wide association analysis reveals new candidate loci associated to B. distachyon *ammonium tolerance.*

Genome-wide association studies (GWAS) are a relatively new way for scientists to identify potential genes that are responsible for the phenotypic variation in populations. Although GWAS were originally developed in humans (Hirschhorn and Daly. 2005), they have been even more successful in plants (Brachi *et al.,* 2011) and now this technique constitutes one of the tools of the so-called "Gene Revolution" aimed to identify and alter genes that may increase crops performance (Taiz, 2013). In the case of *B. distachyon*, studies of GWAS have been conducted to find genes related to flowering time (Tyler *et al.,* 2016), seed metabolite levels (Onda *et al.,* 2019), environmental adaptation using climatic data (Dell'Acqua *et al.,* 2019) or agronomic traits such as flowering time, early vigor, and energy traits in response to climate (Wilson *et al*., 2018), among others. These studies in Brachypodium have been successful identifying candidate genes/genomics regions associated to traits of interest in *B. distachyon* but to date the functional validation of these genes has not been completed. However, other works have demonstrated the soundness of GWAS to identify and validate new genes related to a certain trait. For instance, in relation to nitrogen nutrition, Rosas *et al*., (2013) in *A. thaliana* identified Phosphate 1 (PHO1) and Root System Architecture 1 (RSA1) genes associated to root plasticity, among others, in response to nitrate availability. Similarly, Jia *et al.,* (2019) identified the brassinosteroid (BR) signaling kinase BSK3 as a modulator of *Arabidopsis thaliana* root elongation under mild N deficiency. The combination of GWAS and metabolic analysis has also

emerged as an alternative to study the genetic and biochemical bases of plants metabolism with impact in agronomical traits (Luo, 2015). For instance, Wen *et al.* (2014) identified five potential genes associated with metabolites of interest in maize kernel and validate the function of putrescine hydroxycinnamoyl transferase (PHT) and a caffeoyl CoA 3-O-methyltransferase 1(CCoAOMT1). Fusari *et al*. (2017) used GWAS to map QTLs for biomass, 9 metabolites and 24 enzyme activities and validated a number of candidate genes by the use of T-DNA insertional knocked-out and found, among others, that the leucine-rich repeat immune receptor Accelerated Cell Death 6 (ACD6) modulates central metabolism in a pleiotropic manner pointing to a trade-off between defense and metabolism. Overall, the power of GWAS to study the genetics underlying the natural variability of complex traits is unquestionable.

However, GWAS have some limitations. False positives are not rare and are usually generated due to the population structure and kinship among individuals. Most of the studies in crops have used single-locus models such as MLM that control very well false positives, however the adjustment of the model also compromises false negatives because of the confounding between population structure, kinship, and quantitative trait nucleotides (Liu *et al*., 2016). In this context, the Multiple Loci Linear Mixed Model (MLMM) used in this study, has been recently created to control false positives at the same time without compromising true positives by incorporating multiple markers simultaneously as covariates in a stepwise MLM to partially remove the confounding between testing markers and kinship (Liu *et al*., 2016). Allelic heterogeneity is another limitation because GWAS assumes that common (biallelic) genetic variation explains quantitative trait variation (Brachi *et al.,* 2011). Fortunately, the genome of *B. distachyon* is mostly homozygous but with a large diversity population. The size of the population is another limitation that affects the power of GWAS. Although in comparison with the usually recommended over 100 to 300 individuals (Vogel, 2016), in the present study we used a relatively small number of accessions (51) but we increased the efforts in the amount and quality of phenotypes, which is reported to be more relevant for finding associations in complex traits than increasing the amount of individuals (Han *et al.,* 2015). Another weakness of GWAS is its lack of power to detect rare alleles that are involved in natural variation, for this reason, researchers increase artificially the *P*-value threshold in tests of association to be sensitive to SNPs that have low minor-allele frequencies (Brachi *et al.,* 2011). A suggestive threshold of –log(*P*-value)>5 has been used in several studies of GWAS (Matsuda *et al.,* 2015; Yano *et al.,* 2016; Montaez *et al*., 2018) even in *B. distachyon* this threshold was used to study flowering time (Vogel, 2016). Nevertheless, the most stringent control of false positives is to apply a Bonferroni correction that divides the threshold for statistical significance (for example, $P = 0.05$)

by the number of markers. In general, individual *P* values of monogenic traits are higher compared with the *P-values* obtained for highly polygenic traits. (Sánchez-Vallet *et al.,* 2018). Although, for polygenic traits the identification of causal SNPs is of great difficulty, association mapping analysis allows finding markers to make phenotypic predictions out of individual genomic information (Gondro *et al.,* 2013).

In this study, we combined metabolic profiling trying to explain the growth of a diverse panel of *B. distachyon* accessions under ammonium and nitrate nutrition. For traits like biomass is normal that the GWAS do not provide strong signals because of its complex multigenic nature (Luo *et al.,* 2015; Burghardt *et al.,* 2017). However, it may be particularly important to study the GWAS of alternative traits such as metabolites and enzyme activities that themselves may explain the biomass and thus, may be useful to find loci that ultimately contribute to explain the trait of interest. In this sense the content of sucrose in root and the activity of PEPC activity and the content NH_4^+ content in leaf of ammonium-fed plants stood above the other determined variables affecting *B. distachyon* ammonium tolerance.

Among the genes harboring the significant SNPS associated with the content of sucrose in the root, we highlight a rosmarinate synthase (BRADI_1g50770; Table S3.8). Rosmarinic acid is a phenolic compound with diverse biological function. It is derived from caffeic acid which is provided by the general phenylpropanoid pathway that starts with the transformation of Phe to cinammic acid by PAL enzyme (Bulgakov *et al*., 2012; Pezeshki and Petersen, 2018). . Interestingly, the proteome analysis in Chapter 2 underlined the modulation of phenylpropanoid pathway in ammonium-fed plants. The synthesis of rosmarinic acid has been shown dependent on the availability of sucrose (Xiao and Wang, 2015). However, rosmarinic acid is mostly present in Lamiacea and Boraginaceae and its interest in Poaceae has been mostly related as a marker for botanical and evolutionary relationships (Míka *et al*., 2005) and thus, it is difficult to establish a potential relationship with ammonium nutrition. Besides, two genes encoding for cysteine synthases (BRADI_1g50826, BRADI_1g50832; Table S3.8) were found close to the significant SNPs. Previous works have shown the interaction between sulfur metabolism and the N source. For instance, ammonium nutrition enhances sulphate uptake and assimilation (Van Beusichem *et al.,* 1998; Gerendas *et al.,*, 1997; Coleto *et al.,* 2017). Moreover, in Chapter 2 an important link between ammonium nutrition and sulfur metabolism was observed in *B. distachyon*, notably in relation with Met homeostasis and recycling.

For leaf NH_4^+ accumulation we found encoded a probable adenosine monophosphate deaminase (AMPD; BRADI_2g28450; Table S3.8) harbouring the SNP ss.31153022. AMDP

catalyzes the hydrolytic removal of the 6- amino group of adenosine monophosphate (AMP) to yield inosine monophospahte (IMP). AMPD is the first step in the degradation of purine compounds that leads, by multiple pathways, to the production of oxypurines such as xanthine and hypoxanthine (Yoshino and Murakami, 1980). Further xanthine degradation yields ureides, which are also nitrogenous compounds that contribute to nitrogen recycling in plants. Accumulation of ureide compounds has been reported in a number of plant species under stress conditions, suggesting their involvement in plants' response to stress (Irani and Todd, 2016). Indeed, during the sequential hydrolysis of purines four NH_4^+ molecules are released, which then need to be reassimilated (Werner *et al.,* 2010). Besides, purine catabolism has been shown to contribute to N balance in *Arabidopsis thaliana*, for instance regulating leaf senescence (Soltabayeva *et al.,* 2018). Overall, the interaction between AMPD and ammonium nutrition cannot be precluded and deserves further investigation.

For leaf PEPC activity significant, among the genes in the region of chromosome 2 were we found 5 significant SNPs, a gene encoding a pectin methylesterase (PME; BRADI_2g49500; Table S3.8) is present. PMEs are enzymes that modify the degree of methyl-esterification of pectins, a major component of plant cell wall. PMEs play role in major processes including plant growth, defence and reproduction (Pelloux *et al*., 2007). For instance, PMEs are involved in cell wall extension and stiffening. In Chapter 2 the one of the findings derived from the proteome analysis was the relationship between ammonium nutrition and cell wall biogenesis. Importantly, Zhu *et al*. (2006) reported that NH_4^+ positively regulates the pectin content and activity of PME in cell walls. In the associated genomic region, a probable glutamate carboxypeptidase LAMP1 was encoded (BRADI_2g49510; Table S3.8). Arabidopsis AMP1 has been suggested to AMP1 modulate abscisic acid, oxidative and abiotic stress responses. Interestingly, AMP1 has been related to carbon and amino acid metabolism since Arabidopsis *amp1* mutant presents lower levels of amino acids and its overexpressor accumulates several amino acids, notably Asn (Shi *et al.,* 2013). Indeed, considering AMP1 peptidase activity it has been speculated that AMP1 may be a regulator of the activity of metabolic enzymes related with C/N metabolism (Shi *et al.* 2013). Finally, in this region in chromosome 2, a gene encoding NADP-dependent malic enzyme (NADP-ME; BRADI_2g49540) was also present. This fact is of great interesting, considering the close link between NADP-ME and PEPC. Both enzymes are key in the "biochemical pH-stat" known important for the pH regulation according to the N-form absorbed (Raven, 1986; Schubert and Yan, 1997; Coleto *et al.,* 2019). Besides, as anaplerotic enzymes associated to TCA cycle, both enzymes contribute to sustain the supply of carbon skeletons for NH_4^+ assimilation, as described

in Chapter 1. Overall, the relation of these two enzymes seems more important when plants are subjected to stressful conditions (Doubnerová and Ryšlavá; 2011).

Summarizing, *B. distachyon* is an emerging model system with extensive genetic, genomic, and natural variation resources. Here we report extensive natural variation in *B. distachyon* response to ammonium nutrition, which is related to plant metabolic adaptation. Statistical and exploratory analysis of the data highlighted, among others, PEPC activity and NH_4^+ content in the leaves, sucrose content in the root and glutathione levels as important variables explaining the observed variability in ammonium tolerance. GWAS using Multi Locus Mixed Model (MLMM) for every trait determined a panel of 51 accessions revealed an important number of significant SNPs, highlighting genomic regions where causal genes related to *B. distachyon* ammonium tolerance may be located. A better understanding of natural variation in *B. distachyon* especially at the molecular level will provide a unique opportunity for gaining insight into plant adaptation to ammonium tolerance as well as novel avenues for improving nitrogen fertilization. Future research to further identify the causal genes involved in ammonium nutrition include transcriptomic analysis of tolerant vs. sensitive accessions and phenotyping of mutant lines publicly available, such as the BRACHYTIL TILLING platform for functional genomics developed in Bd21-3 genetic background (Dalmais *et al*., 2013) and the T-DNA lines collection in Bd21 genetic background (Hsia *et al*., 2017).

6. SUPPLEMENTARY INFORMATION

Table S3.1. List of *B. distachyon* accessions studied and their associated metadata. Available in attached USB flash drive.

Table S3.2. Data of biomass and metabolic profile of 52 accessions of *B. distachyon* under ammonium or nitrate nutrition. Available in attached USB flash drive.

Table S3.3. Stepwise-multiple-regression analysis of the metabolic measurements (independent variables) in leaves of nitrate-fed plants associated with shoot biomass (dependent variable).

	SHOOT BIOMASS – NITRATE NUTRITION	
INDEPENDENT VARIABLE	STANDARDIZED COEFFICIENT	*P*- value
PROTEIN	-0.683	0.000
ICDH ACTIVITY	-0.278	0.007
NH_4^+	0.244	0.018
R^2	0.582	
ADJUSTED R^2	0.556	
ESTIMATE SE	0.083	

Table S3.4. Stepwise-multiple-regression analysis of the metabolic measurements (independent variables) in root of nitrate-fed plants associated with root biomass (dependent variable).

	ROOT BIOMASS – NITRATE NUTRITION	
INDEPENDENT VARIABLE	STANDARDIZED COEFFICIENT	*P*- value
GLUCOSE	0.573	0.000
GK ACTIVITY	-0.294	0.018
FK ACTIVITY	-0.266	0.036
R^2	0.517	
ADJUSTED R^2	0.487	
ESTIMATE SE	0.053	

Table S3.5. Stepwise-multiple-regression analysis of the metabolic measurements in leaf and root of NO_3^-fed plants (independent variable) affecting the NO_3^- total biomass (dependent variable)

	TOTAL BIOMASS – NITRATE NUTRITION	
INDEPENDENT VARIABLE	STANDARDIZED COEFFICIENT	*P*- value
NL - PROTEIN	-0.618	0.000
NR - MALATE	0.546	0.000
NL – GDH ACTIVITY	-0.266	0.004
NR - GLU	-0.212	0.017
R^2	0.667	
ADJUSTED R^2	0.639	
ESTIMATE SE	0.114	

Table S3.6. Selected SNPs by the significance of their statistical association with a trait. Available in attached USB flash drive.

Table S3.7. Selected SNPs by the $-\log_{10}(p)>5$ of their statistical association with a trait. Available in attached USB flash drive.

Table S3.8. Genes associated to the selected SNPs ($-\log_{10}(p)>5$) of the selected variables PEPC activity and NH_4^+ content in leaf and sucrose content in root under ammonium nutrition. Available in attached USB flash drive.

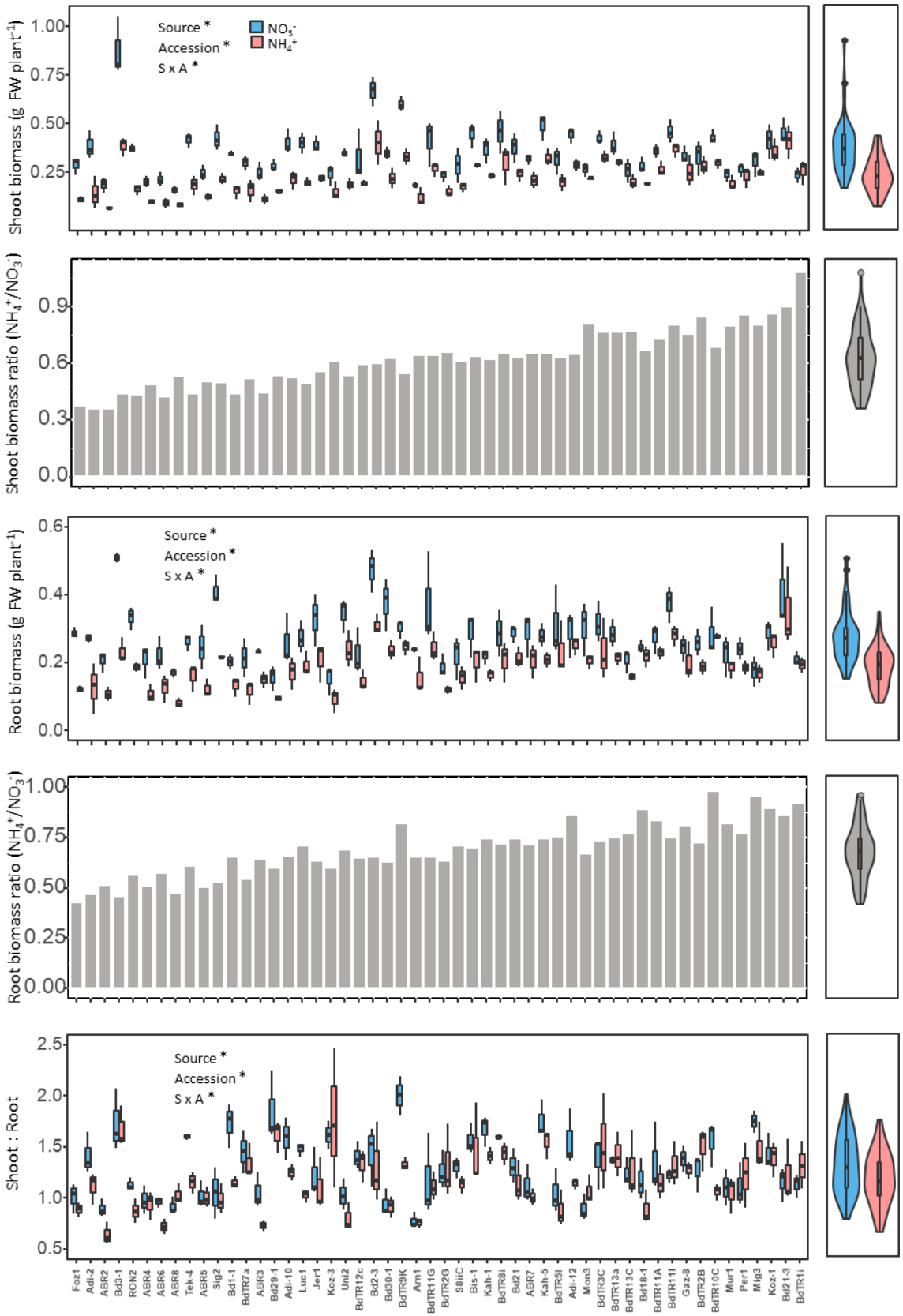

Figure S3.1. Natural variation in shoot and root biomass of 52 *B. distachyon* accessions grown under nitrate or ammonium as N source. Values in left graphs are the mean ± SE (n = 3). Asterisk (*) indicates significant (p<0.05) of the two-way ANOVA (S for nitrogen source, A for accession). The violin plots on the right side show the distribution of the traits.

Values in left graphs are the mean ± SE (n = 3). Asterisk (*) indicates either significant of the two-way ANOVA (S for nitrogen source, A for accession) or significant difference between total biomass under ammonium compared with nitrate for each accession (p<0.05). The violin plots on the right side show the distribution of the traits.

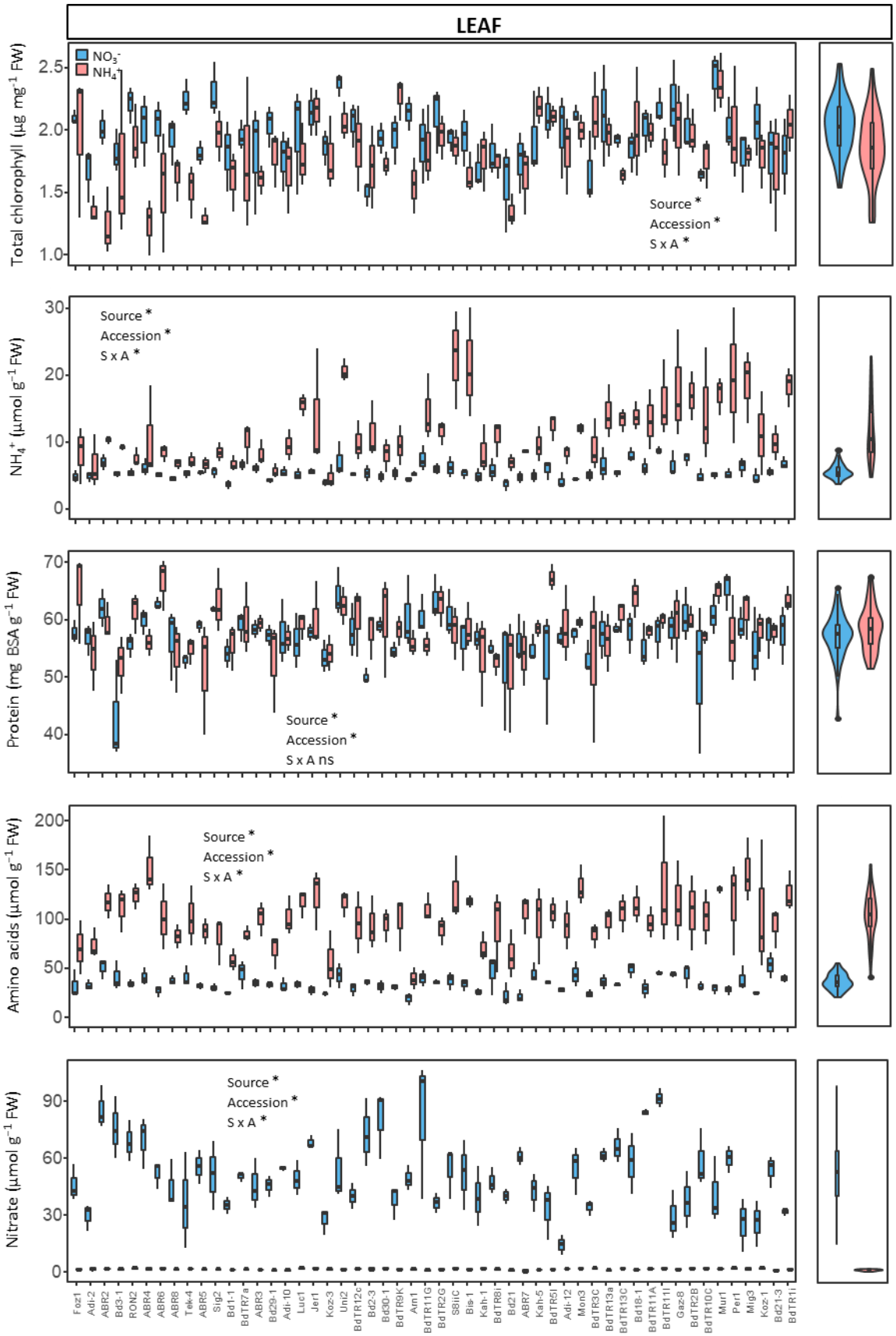

Figure S3.2. Natural variation in leaf metabolites of 52 *B. distachyon* accessions grown under nitrate or ammonium as N source. Values in left graphs are the mean ± SE (n = 3). Asterisk (*) indicates significant (p<0.05) of the two-way ANOVA (S for nitrogen source, A for accession). The violin plots on the right side show the distribution of the traits.

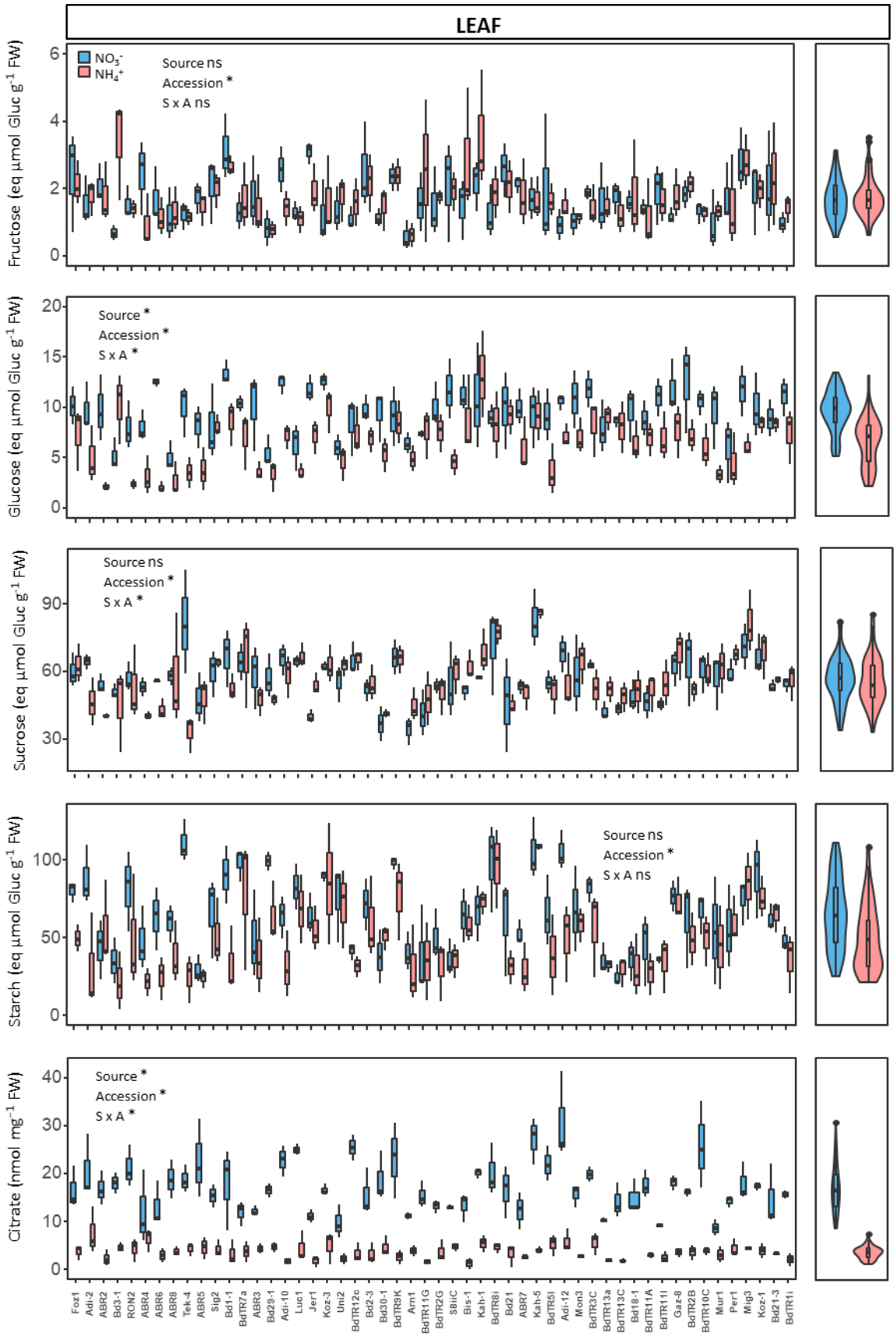

Figure S3.2. Continuation

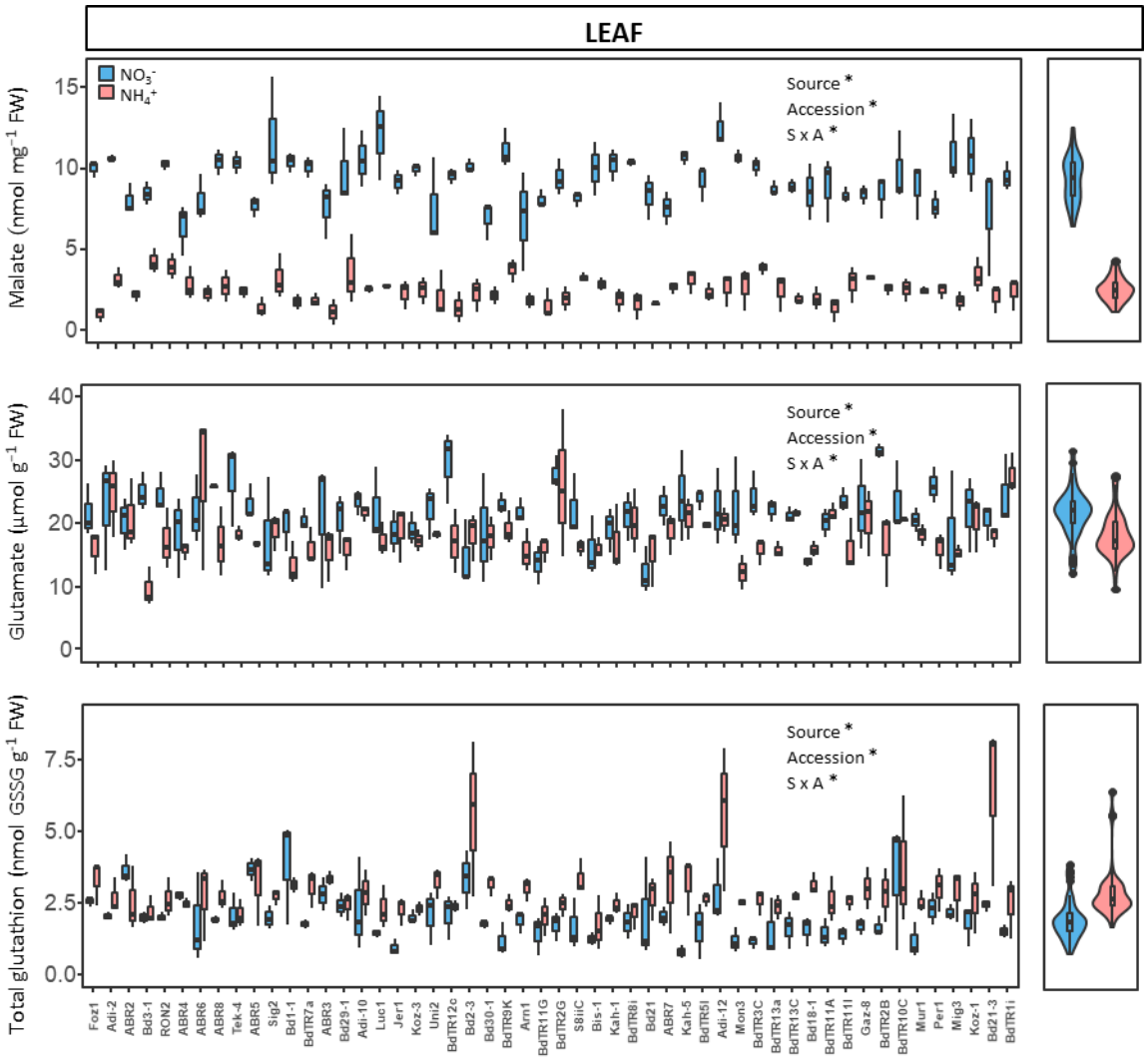

Figure S3.2. Continuation.

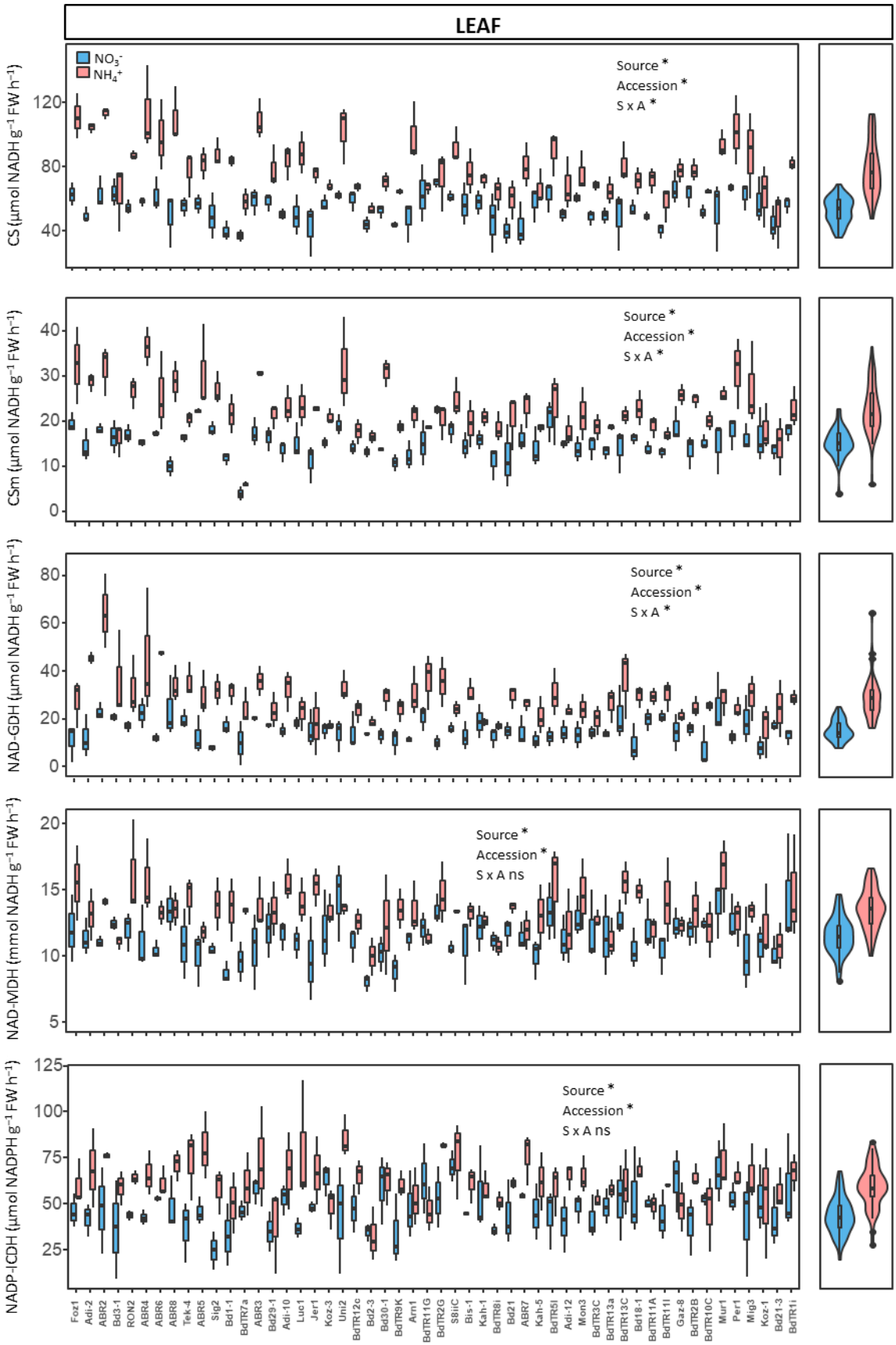

Figure S3.3. Natural variation in leaf enzymes activities of *B. distachyon* grown under nitrate or ammonium as N source. Values in left graphs are the mean ± SE (n = 3). Asterisk (*) indicates significant ($p<0.05$) of the two-way ANOVA (S for nitrogen source, A for accession). The violin plots on the right side show the distribution of the traits.

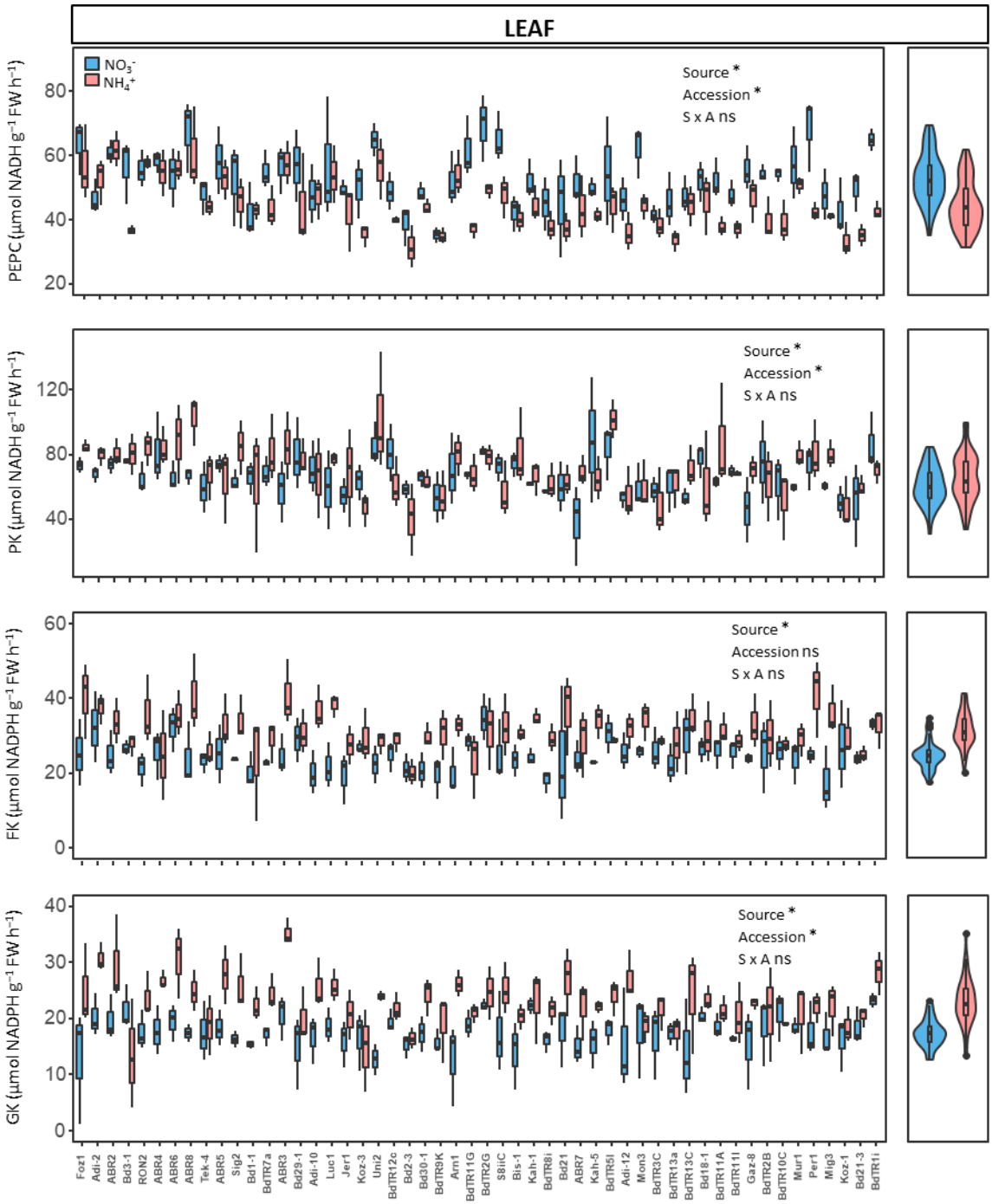

Figure S3.3. Continuation.

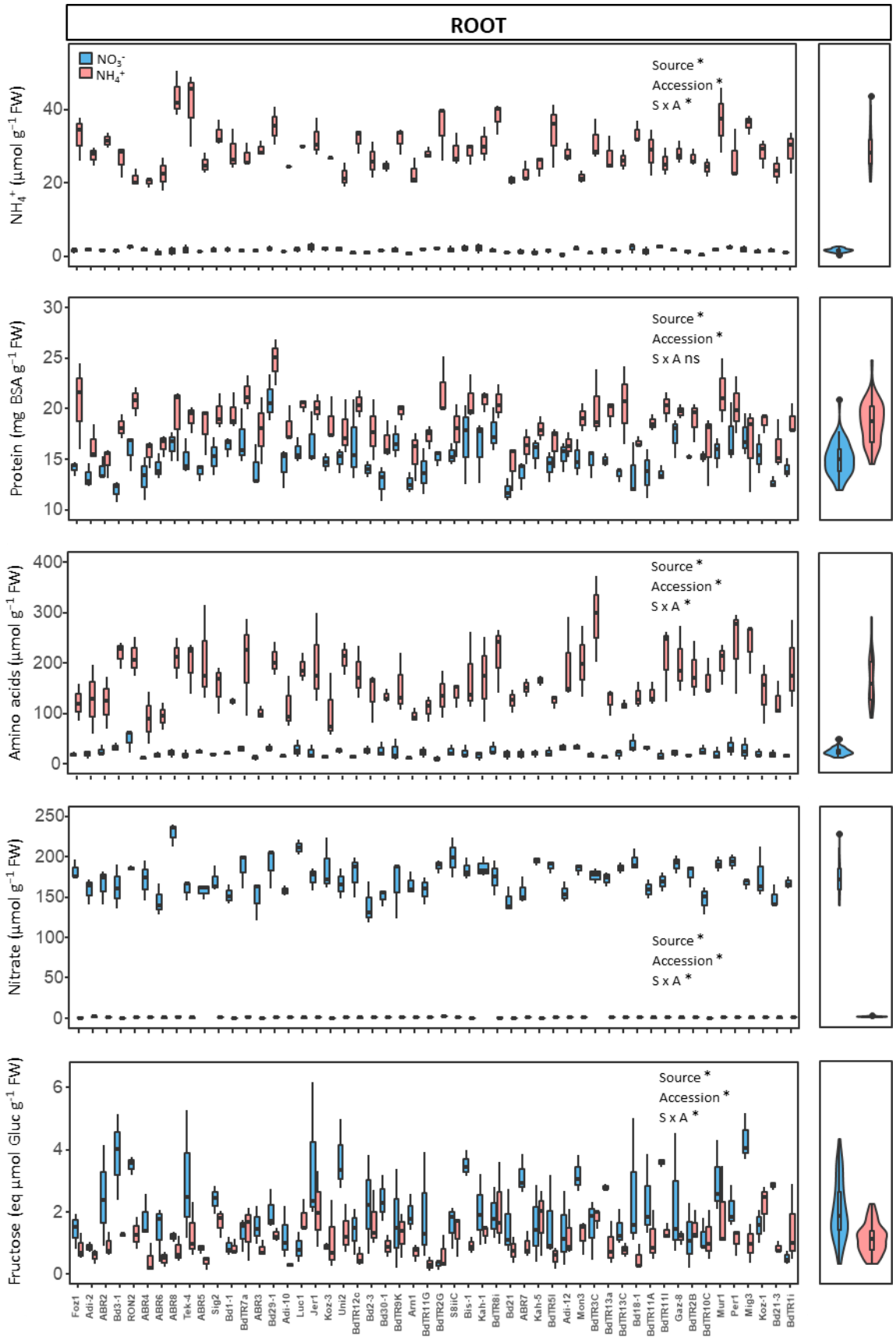

Figure S3.4. Natural variation in root metabolites of 52 *B. distachyon* accessions grown under nitrate or ammonium as N source. Values in left graphs are the mean ± SE (n = 3). Asterisk (*) indicates significant ($p<0.05$) of the two-way ANOVA (S for nitrogen source, A for accession). The violin plots on the right side show the distribution of the traits.

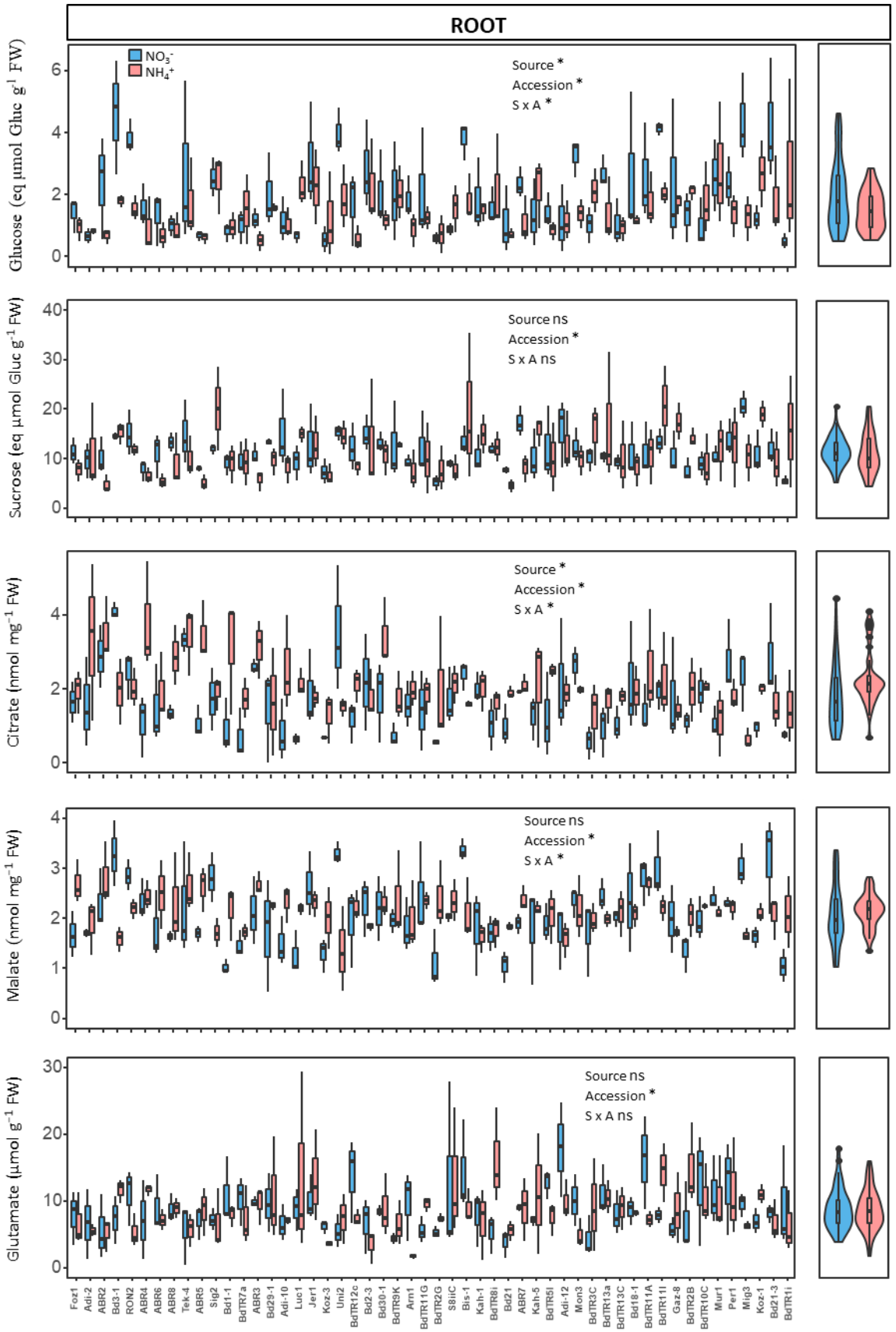

Figure S3.4. Continuation

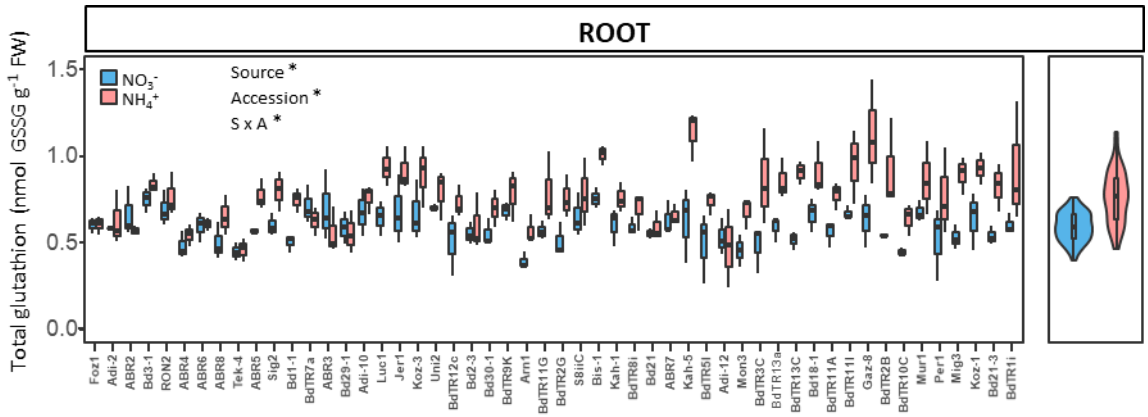

Figure S3.4. Continuation

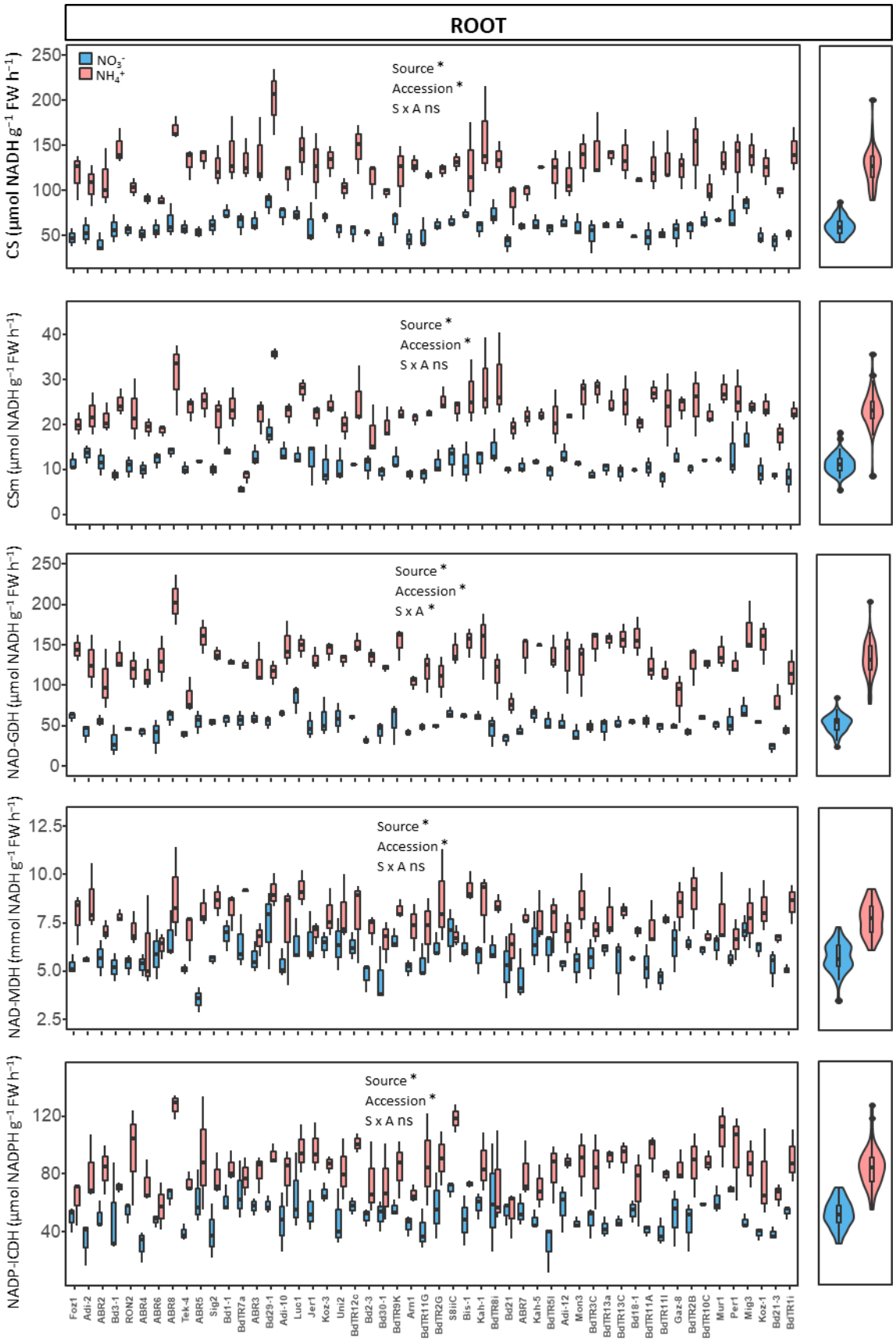

Figure S3.5. Natural variation in root enzymes activity of 52 *B. distachyon* accessions grown under nitrate or ammonium as N source. Values in left graphs are the mean ± SE (n = 3). Asterisk (*) indicates significant ($p<0.05$) of the two-way ANOVA (S for nitrogen source, A for accession). The violin plots on the right side show the distribution of the traits.

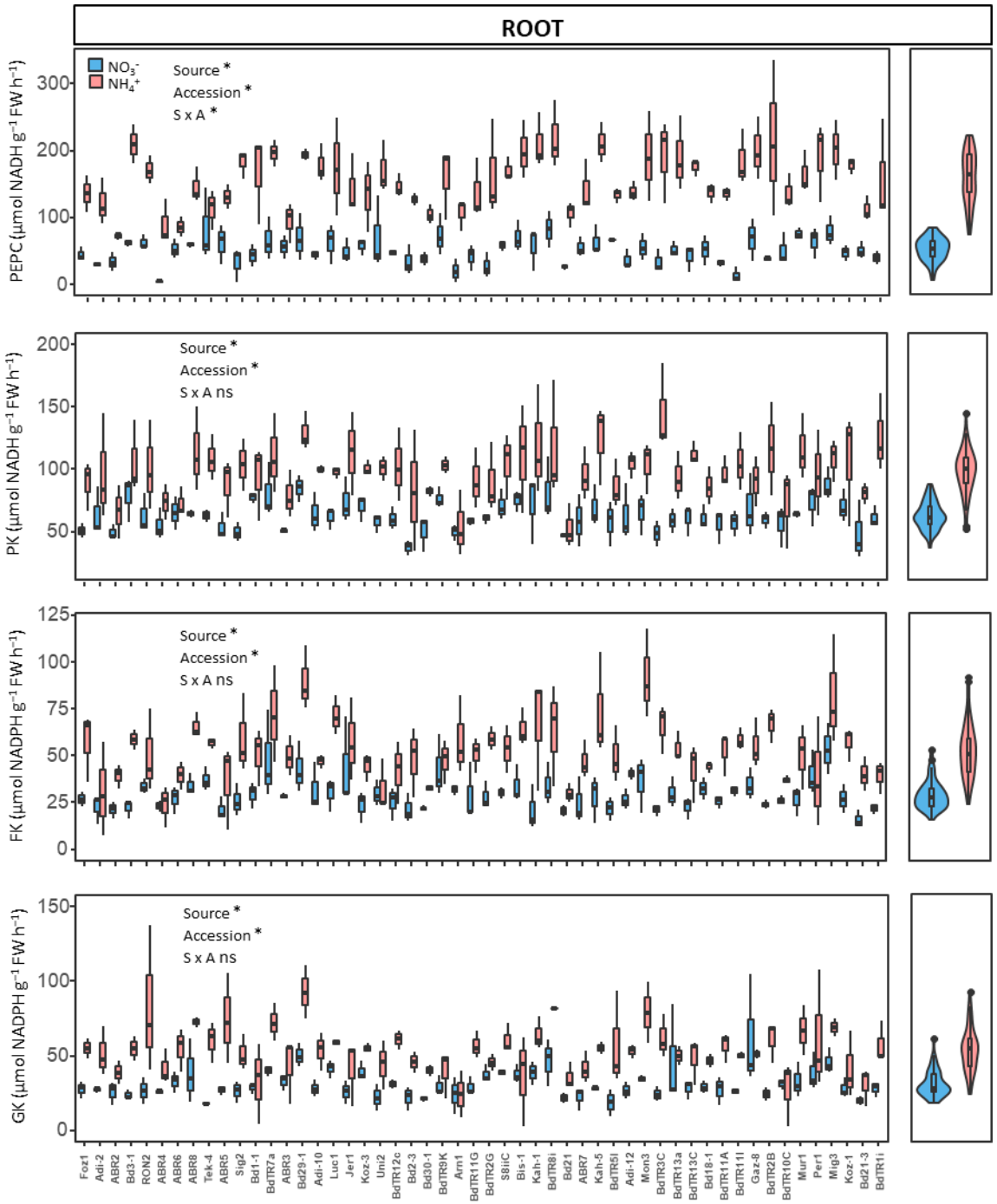

Figure S3.5. Continuation

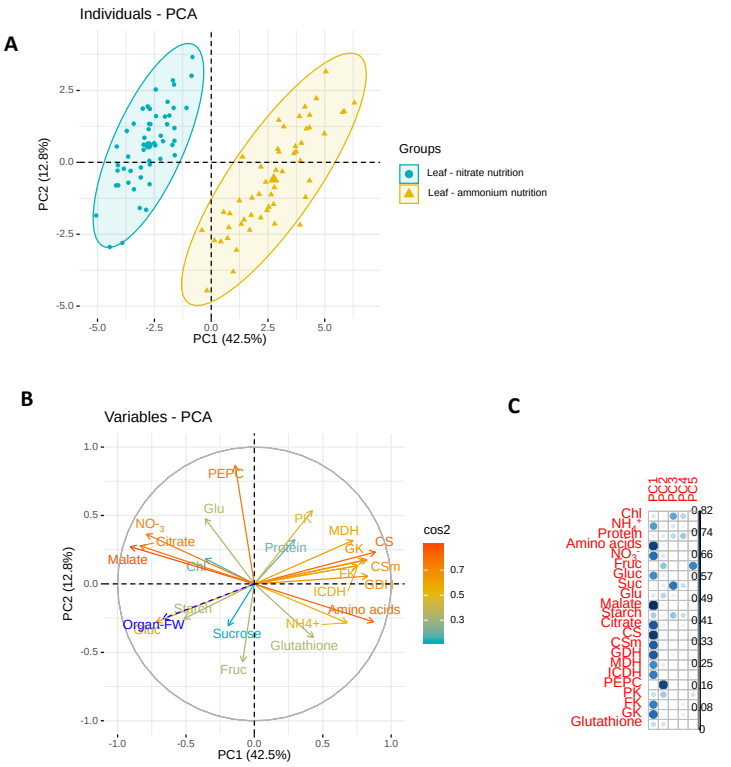

Figure S3.6. Principal component analysis (PCA) of leaf metabolic data of of 52 *B. distachyon* accessions grown under ammonium or nitrate nutrition. (A) Individuals PCA score plot. (B) Variables loading plot where cos2 is the square loadings for variables and shows the quality of the representation for variables on the plot. (C) Correlation plot showing the PCs where the variables are represented.

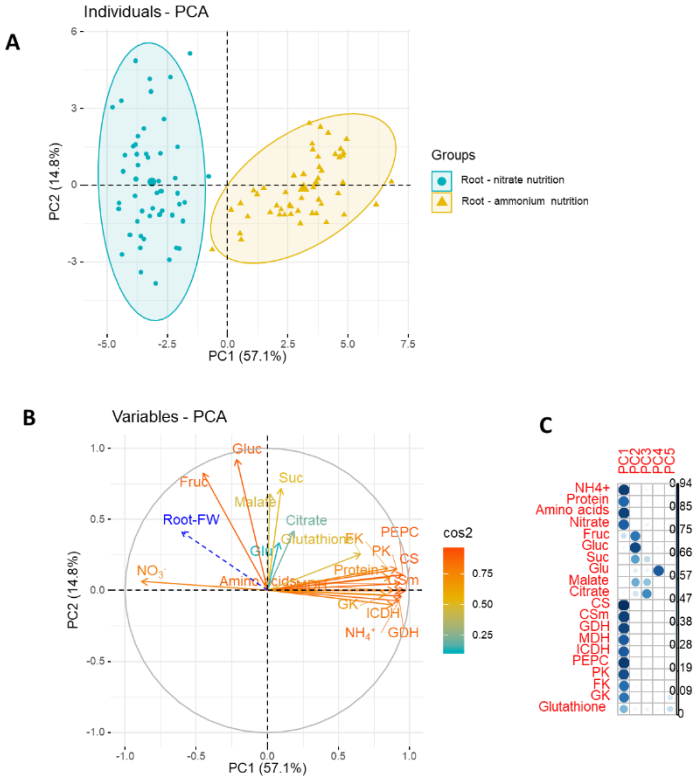

Figure S3.7. Principal component analysis (PCA) of root metabolic data of 52 *B. distachyon* accessions grown under ammonium or nitrate nutrition. (A) Individuals PCA score plot. (B) Variables loading plot where cos2 is the square loadings for variables and shows the quality of the representation for variables on the plot. (C) Correlation plot showing the PCs where the variables are represented.

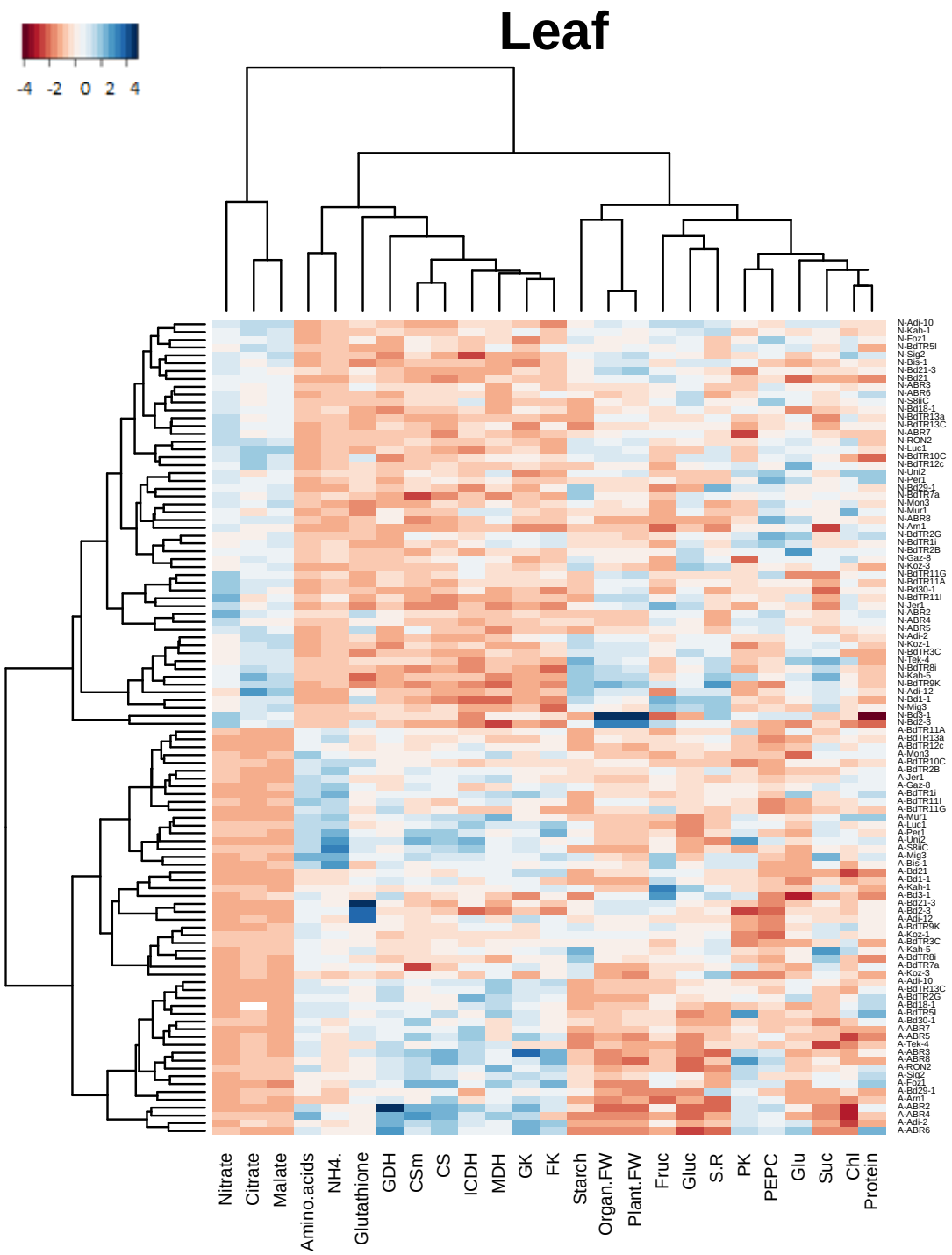

Figure S3.8. Leaf heat map visualization with two-way clustering of 13 metabolites and 9 enzymatic activities determined in plants grown under ammonium and nitrate-nutrition including also biomass data against 52 accessions of *B. distachyon*. Chl means chlorophyll, CS citrate synthase, CSm mitochondrial citrate synthase, FK fructokinase, FW fresh weight, GDH NAD- dependent glutamate dehydrogenase, GK glucokinase, Glu glutamate, ICDH NADP-dependent isocitrate dehydrogenase, MDH malate dehydrogenase, PEPC phosphoenolpyruvate carboxylase and PK pyruvate kinase.

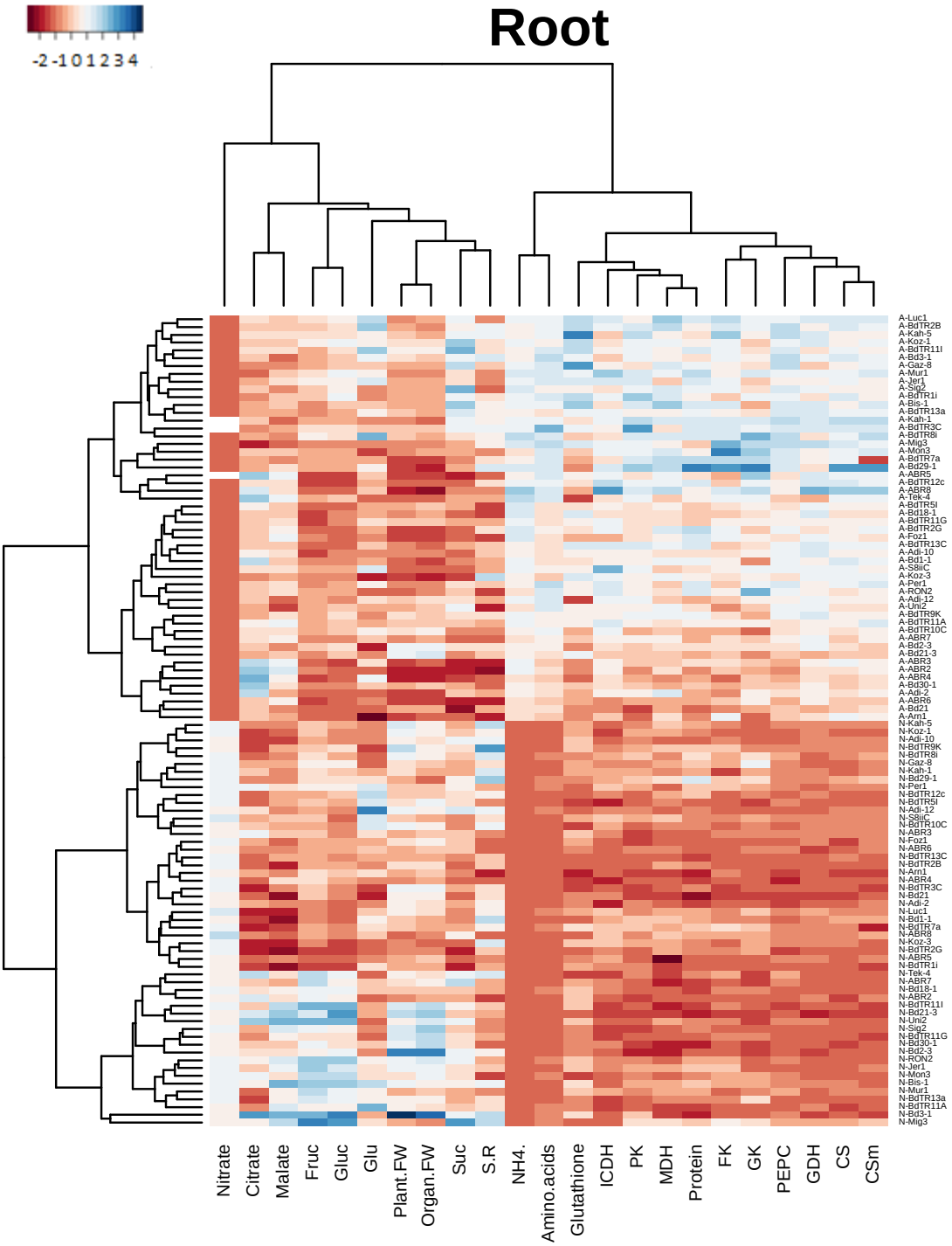

Figure S3.9. Root heat map visualization with two-way clustering of 13 metabolites and 9 enzymatic activities determined in plants grown under ammonium and nitrate-nutrition including also biomass data against 52 accessions of *B. distachyon*. Abbreviations as in Figure S3.8.

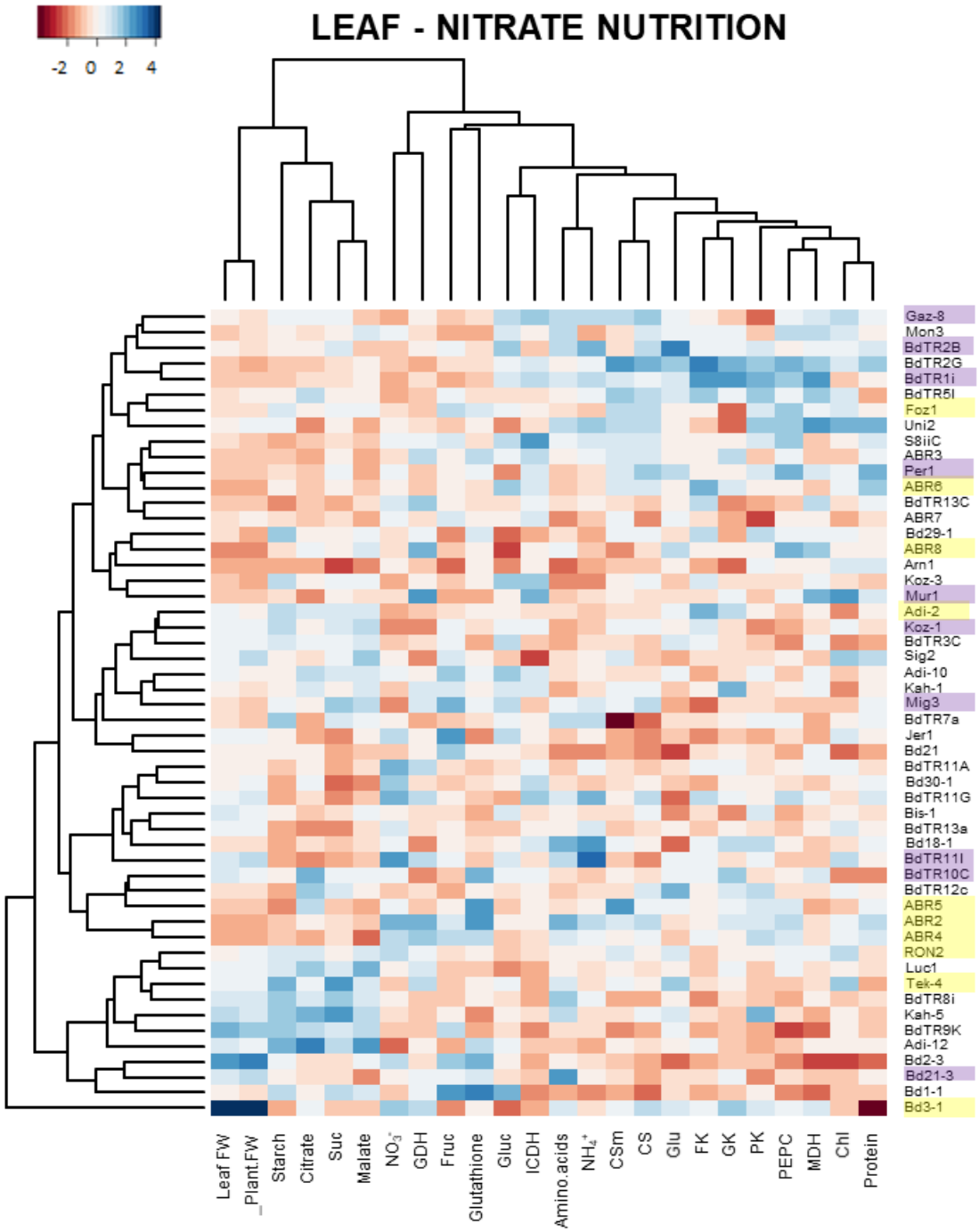

Figure S3.10. Leaf heat map visualization with two-way clustering of 13 metabolites and 9 enzymatic activities determined in plants grown under nitrate-nutrition including also biomass data against 52 accessions of *B. distachyon.* Abbreviations as in Figure S3.8. The 10 accessions displaying the highest tolerance and the highest sensitivity to ammonium nutrition in Figure 1 are highlighted in purple and yellow, respectively.

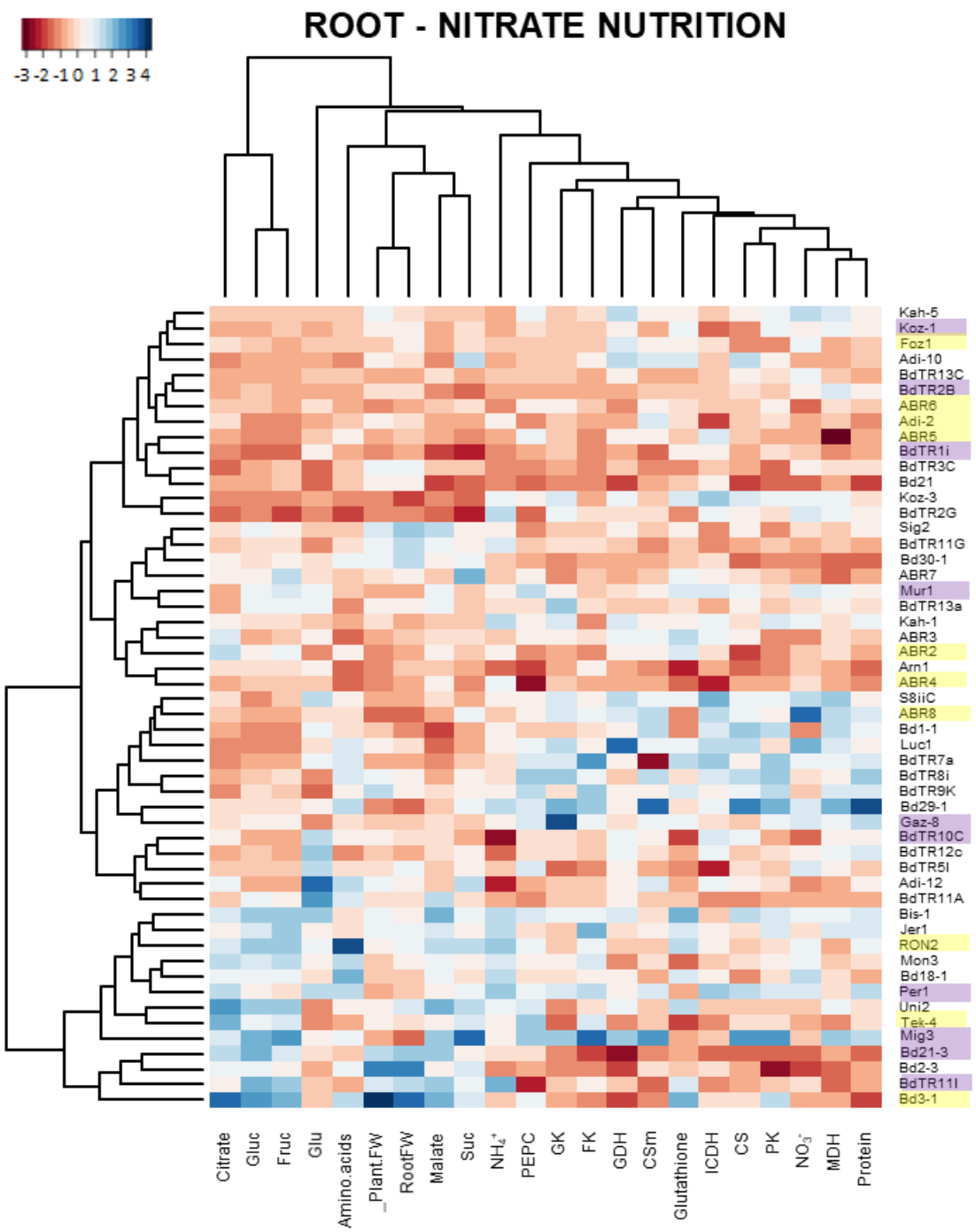

Figure S3.11. Root heat map visualization with two-way clustering of 13 metabolites and 9 enzymatic activities determined in plants grown under ammonium-nutrition including also biomass data against 52 accessions of *B. distachyon*. Abbreviations as in Figure S3.8. The 10 accessions displaying the highest tolerance and the highest sensitivity to ammonium nutrition in Figure 1 are highlighted in purple and yellow, respectively.

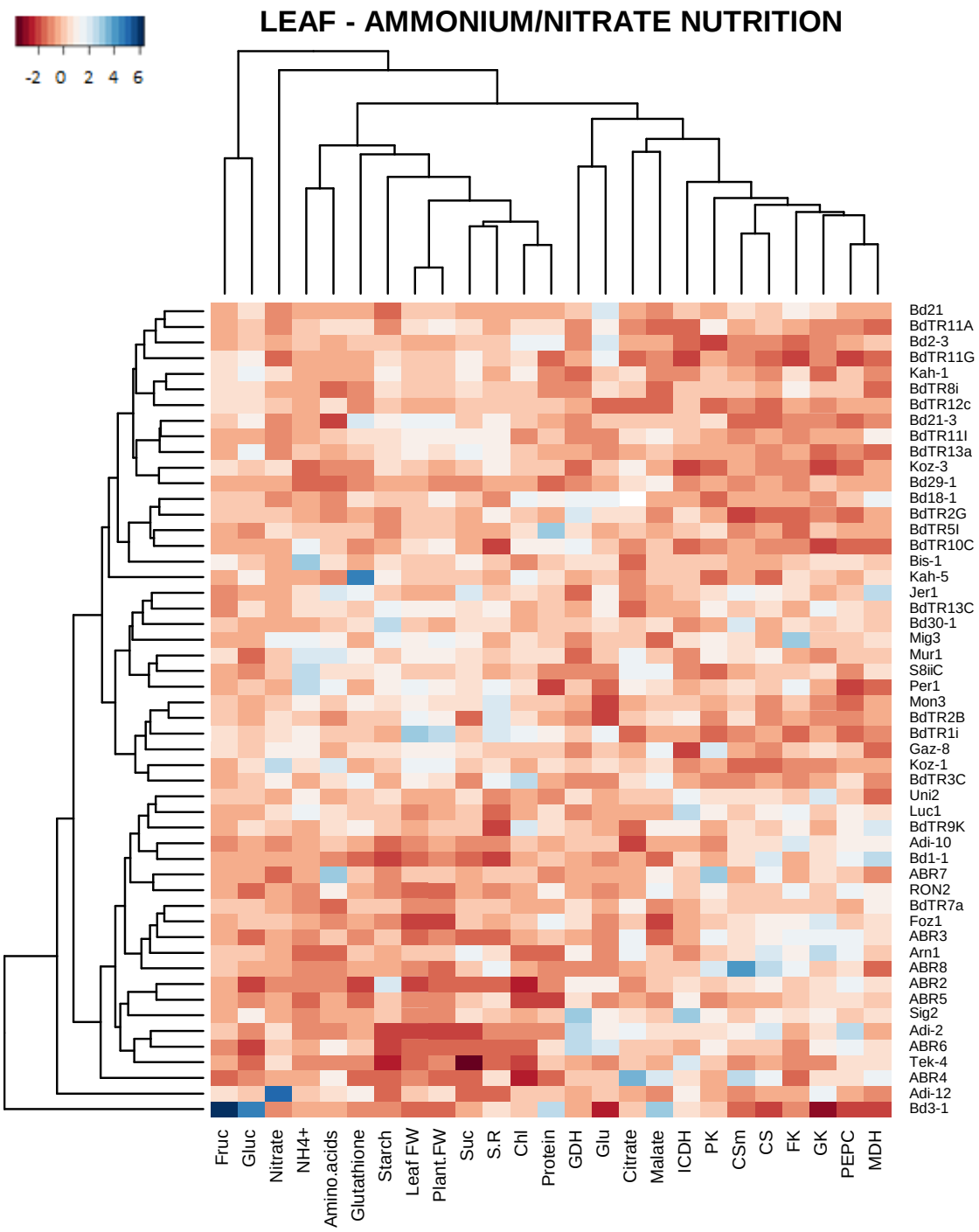

Figure S3.12. Leaf heat map visualization with two-way clustering of the ratio ammonium/nitrate nutrition of 13 metabolites and 9 enzymatic activities determined in plants grown under ammonium-nutrition or nitrate nutrition including also biomass data against 52 accessions of *B. distachyon*. Abbreviations as in Figure S3.8.

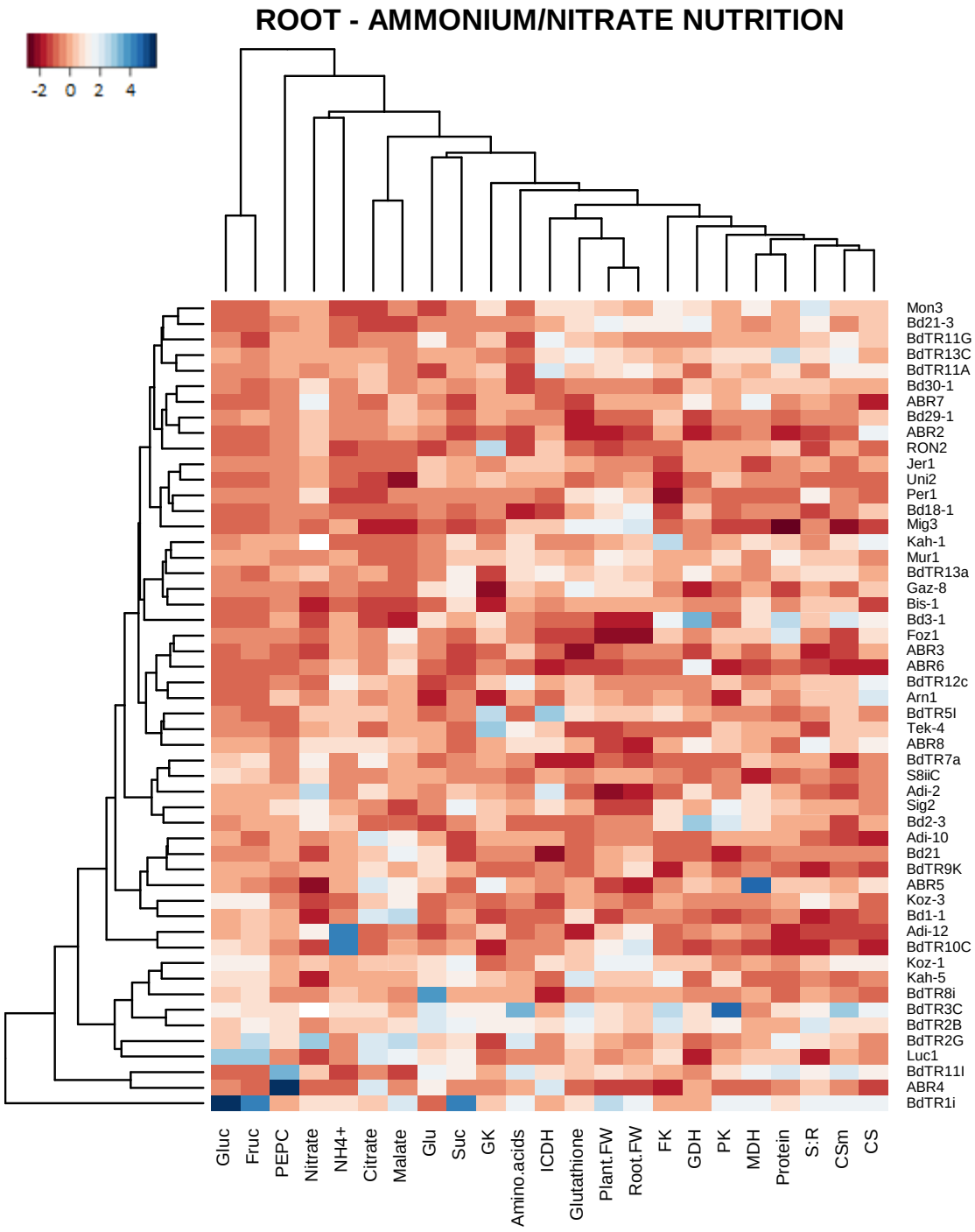

Figure S3.13. Root heat map visualization with two-way clustering of the ratio ammonium/nitrate nutrition of 13 metabolites and 9 enzymatic activities determined in root of plants grown under ammonium-nutrition or nitrate nutrition including also biomass data against 52 accessions of *B. distachyon*. Abbreviations as in Figure S3.8.

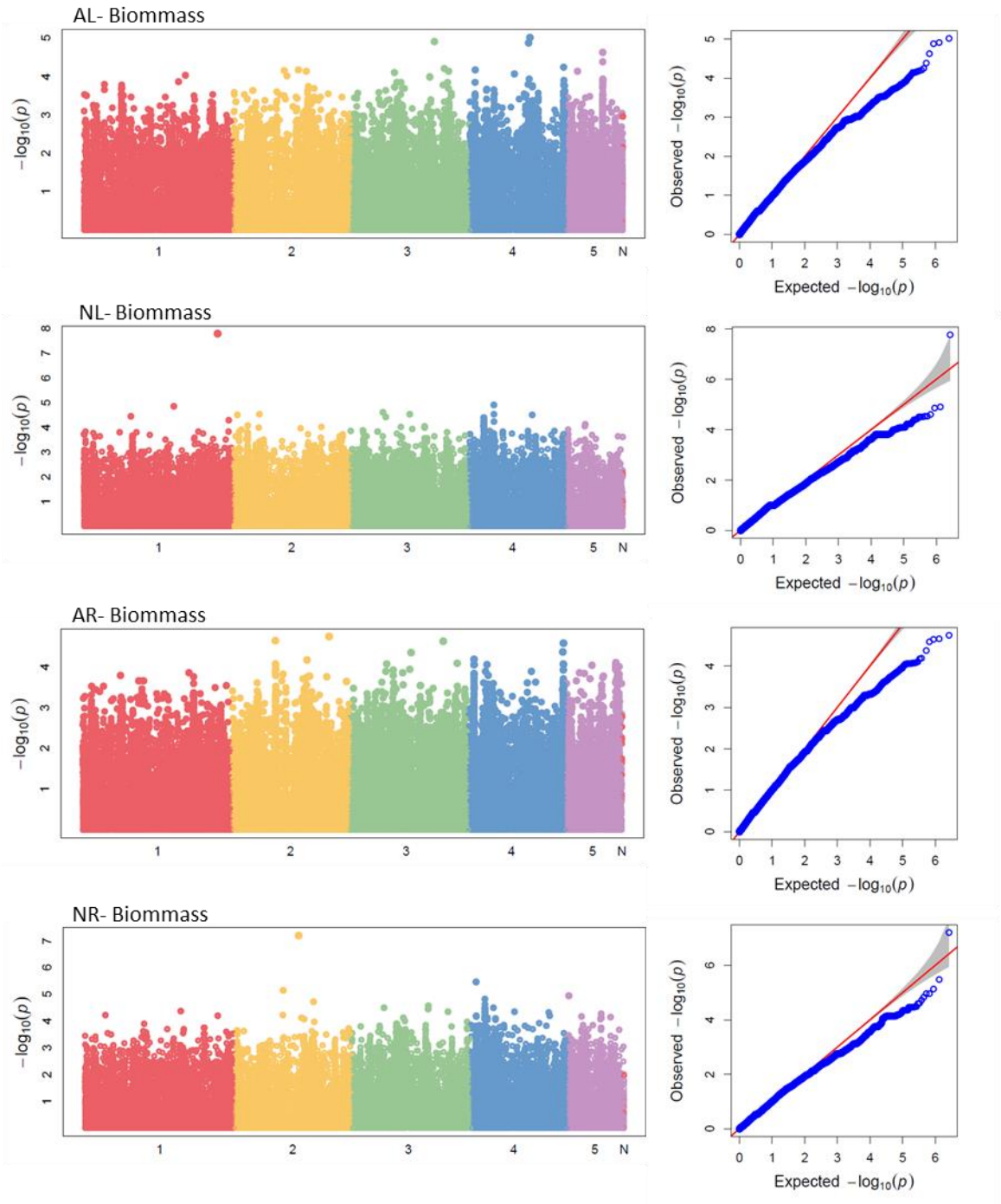

Figure S3.14.Manhattan plots (left side) showing the marker-trait associations and QQ plots (right side) showing the distribution of observed and expected *p*-values for leaf and root biomass of ammonium and nitrate nutrition of *B. distachyon*.

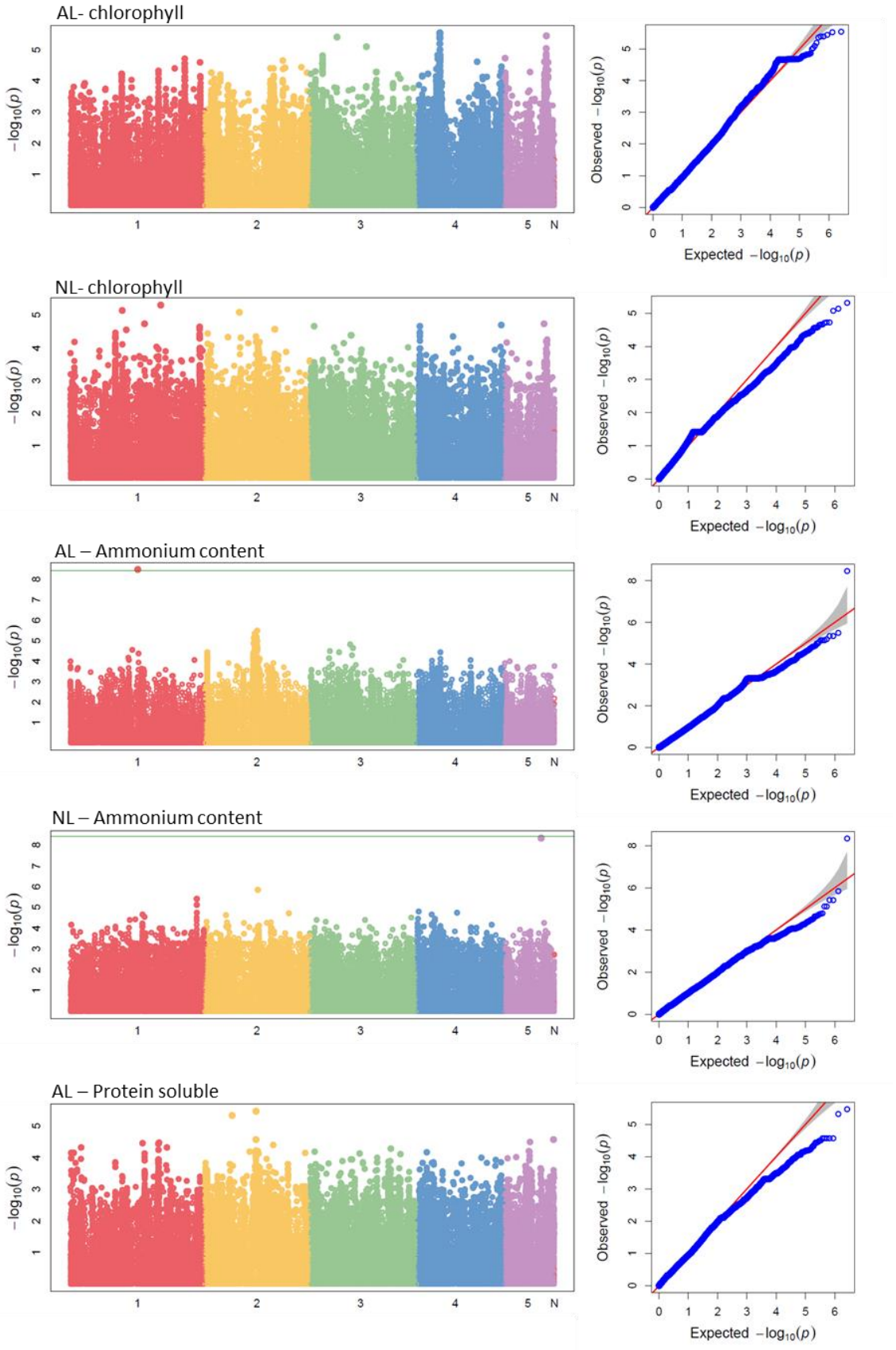

Figure S3.15. Manhattan plots (left side) showing the marker-trait associations and QQ plots (right side) showing distribution of observed and expected *p*-values for metabolites measured in leaf of ammonium and nitrate nutrition of *B. distachyon*. When SNPs over Bonferroni-corrected threshold are found the threshold is shown with a green line within the Manhattan plot.

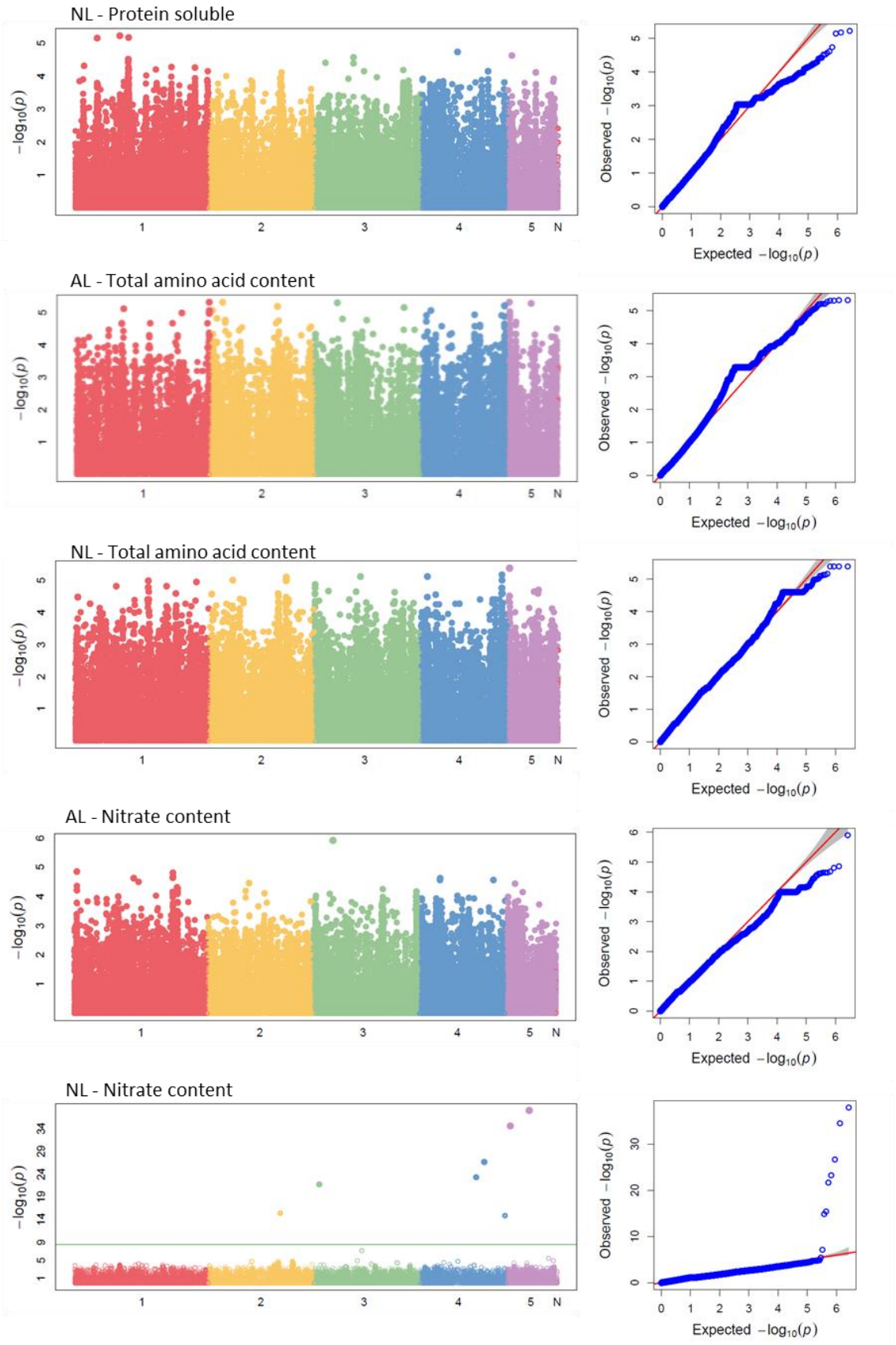

Figure S3.15. Continuation.

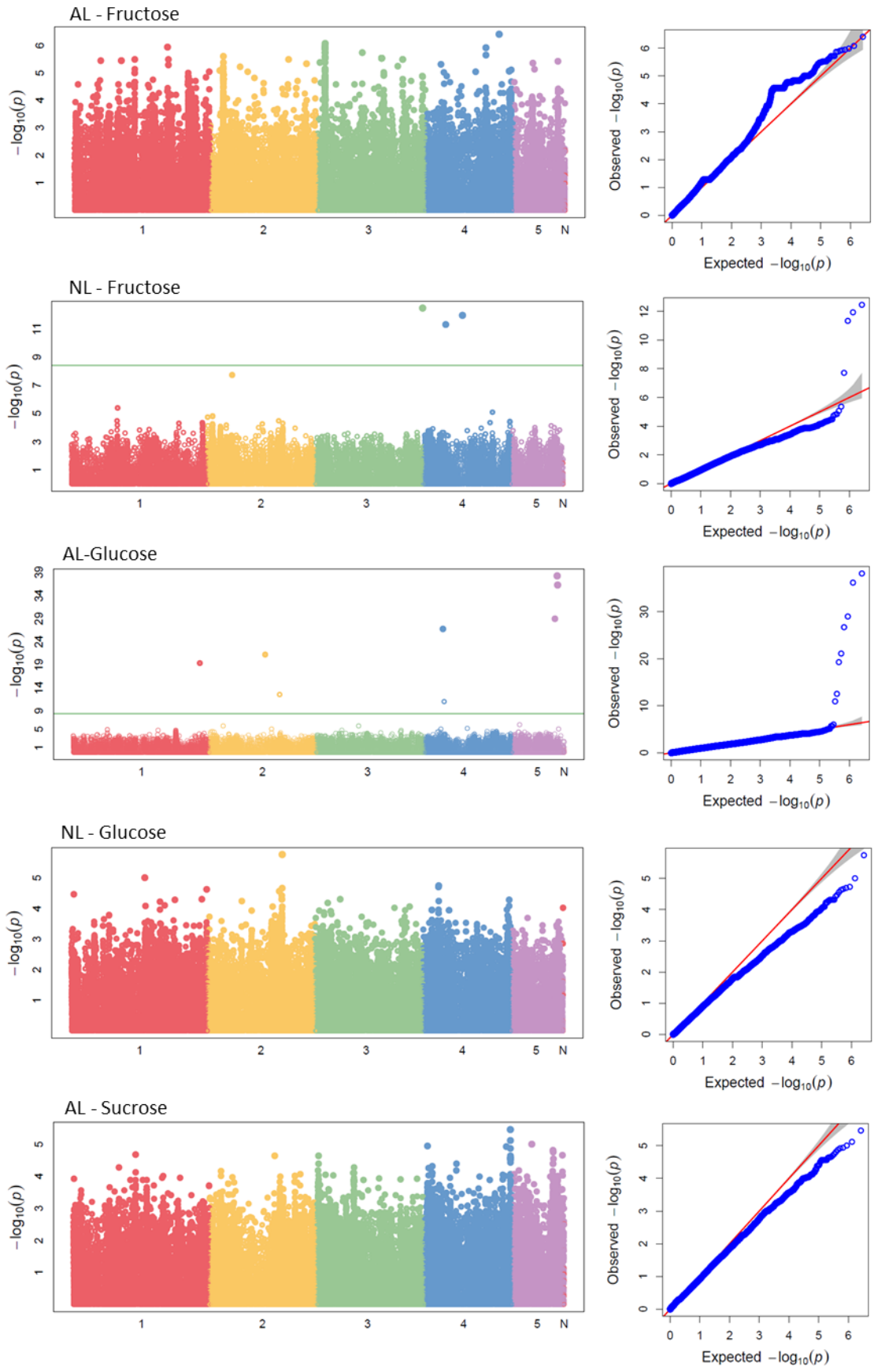

Figure S3.15. Continuation.

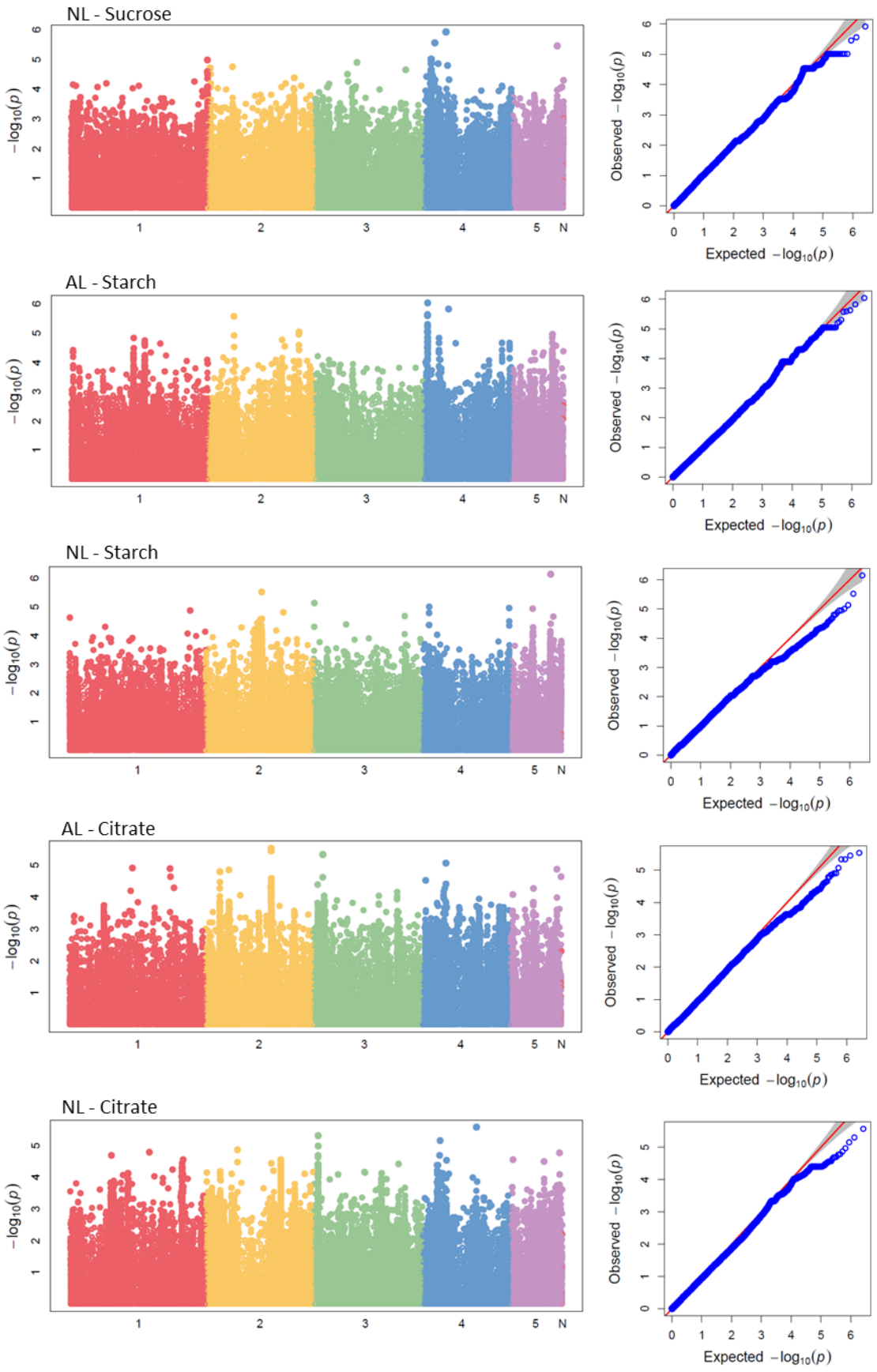

Figure S3.15. Continuation.

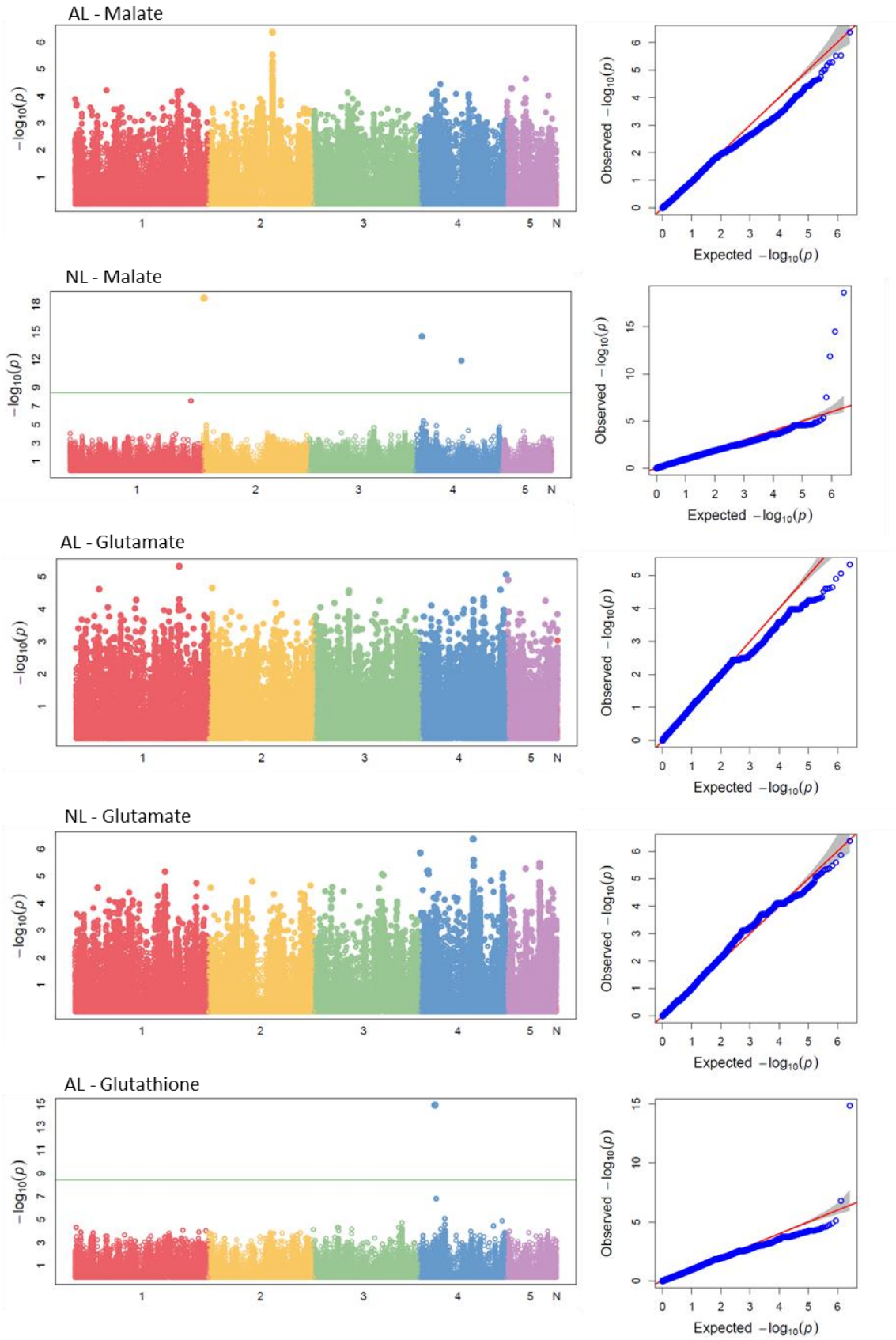

Figure S3.15. Continuation.

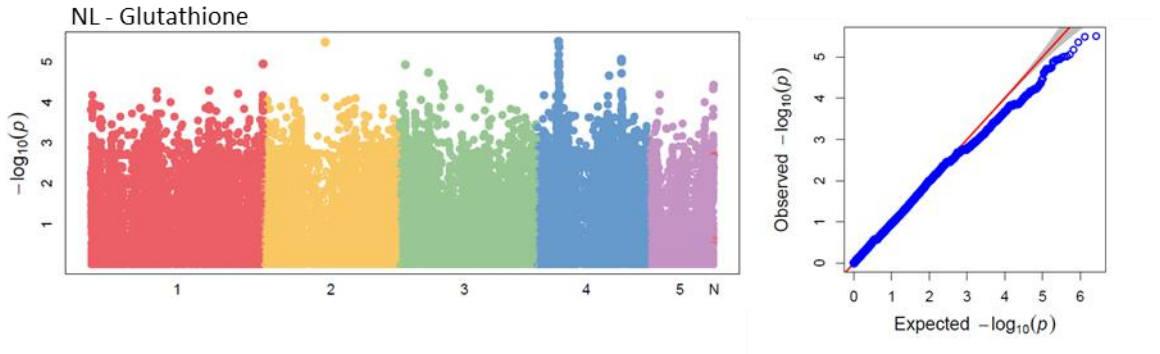

Figure S3.15. Continuation.

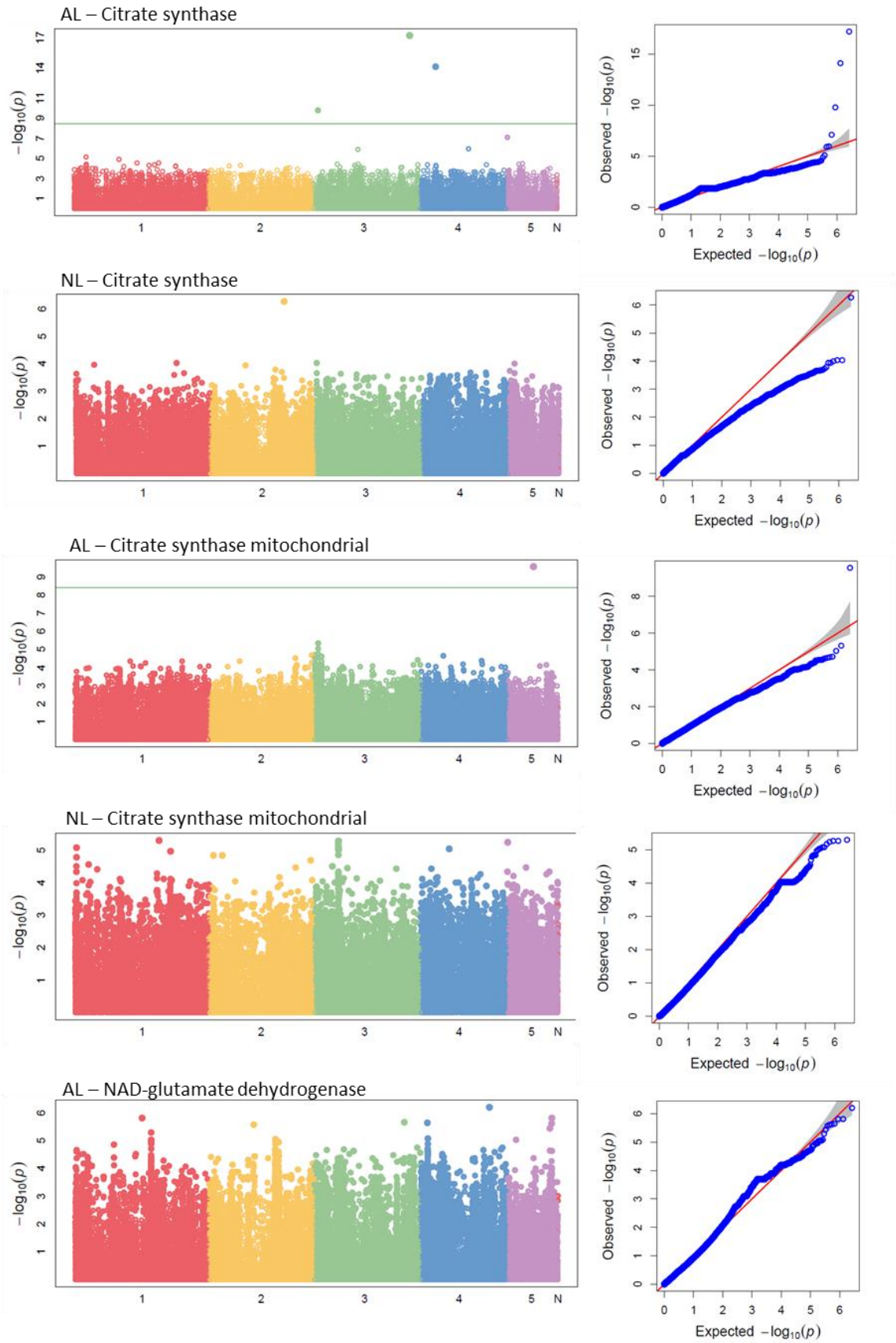

Figure S3.16. Manhattan plots (left side) showing the marker-trait associations and QQ plots (right side) showing distribution of observed and expected *p*-values for enzymatic activity in leaf of ammonium and nitrate nutrition of *B. distachyon*. When SNPs over Bonferroni-corrected threshold are found the threshold is shown with a green line within the Manhattan plot.

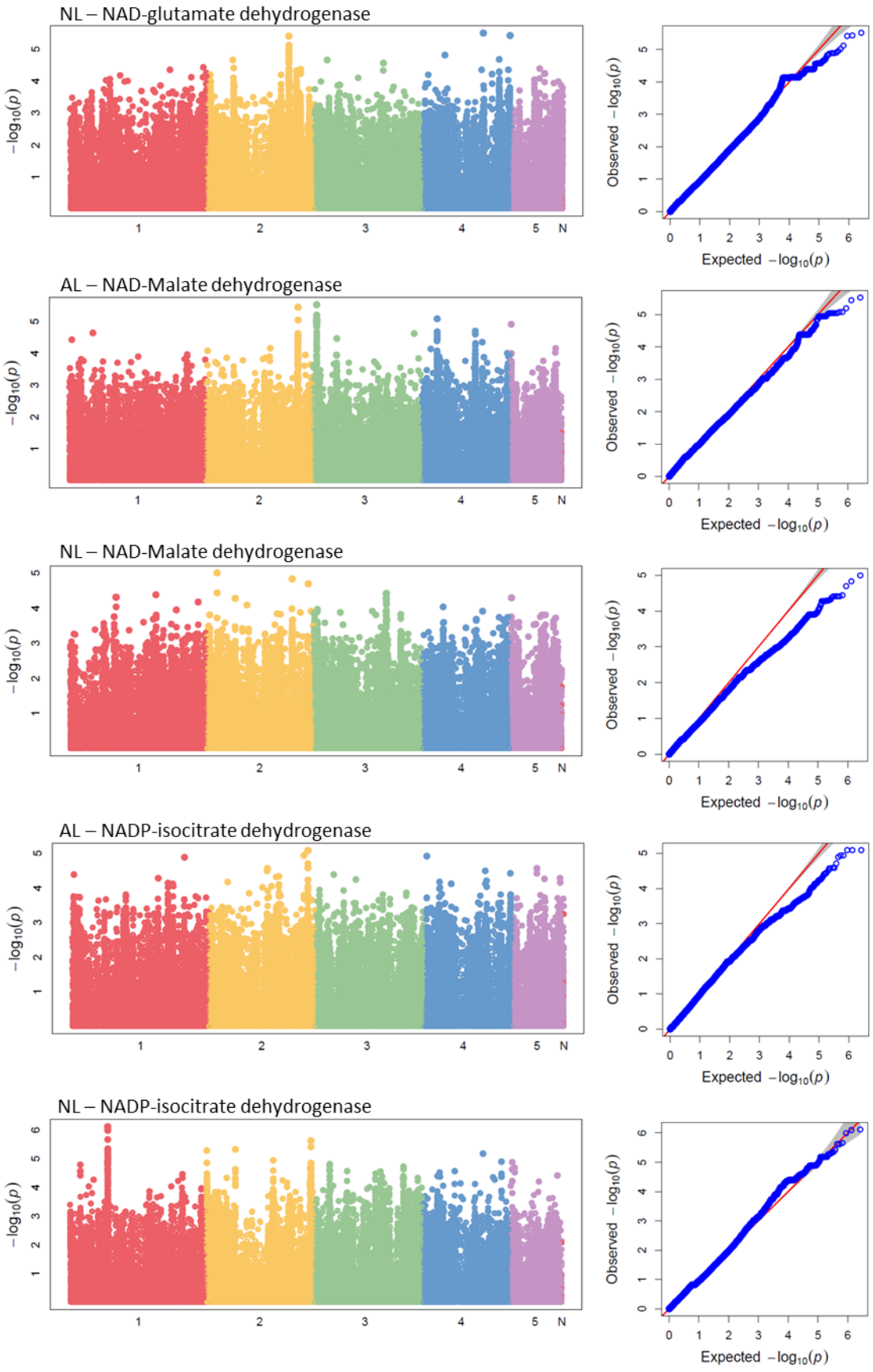

Figure S3.16. Continuation

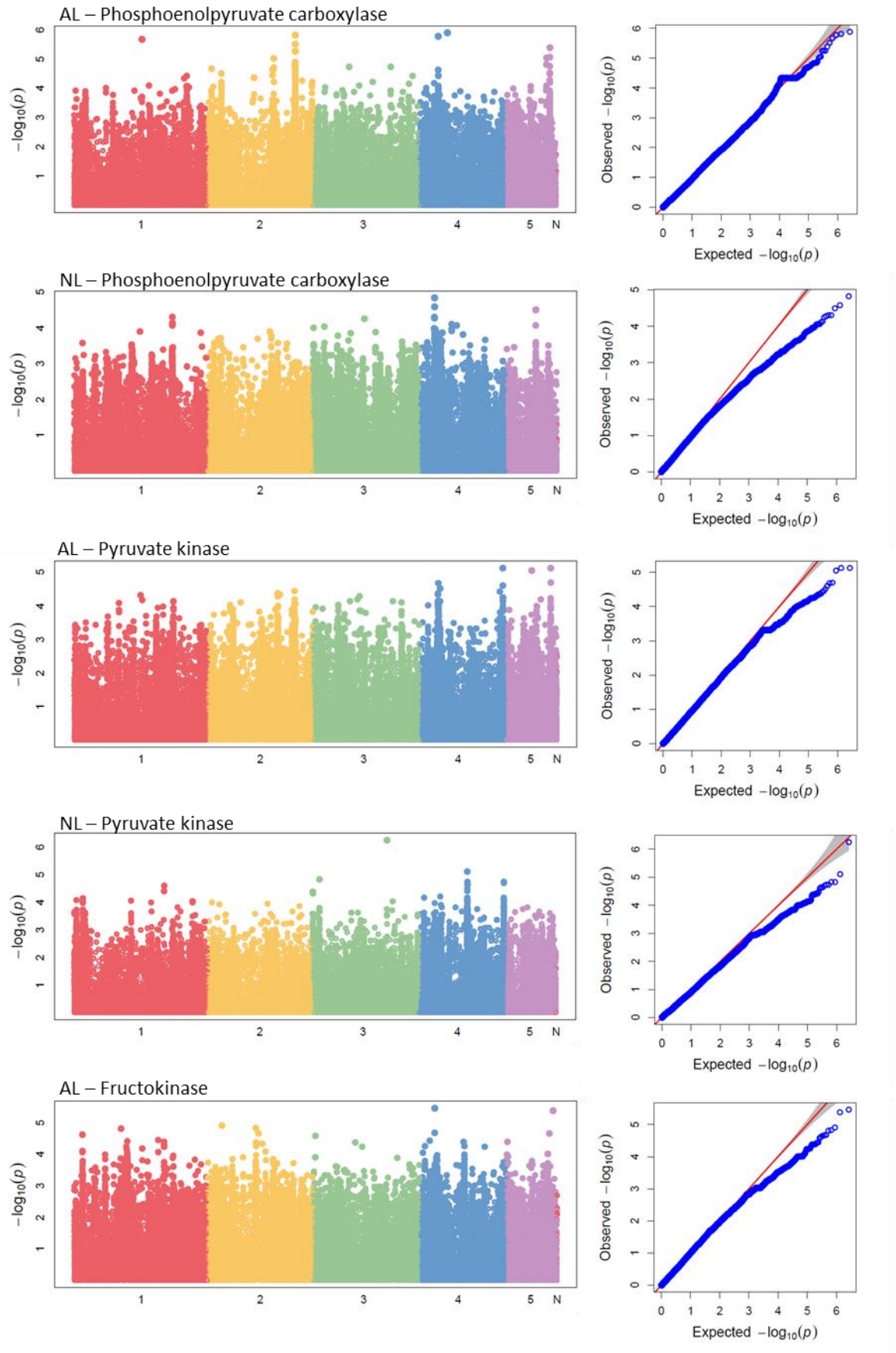

Figure S3.16. Continuation

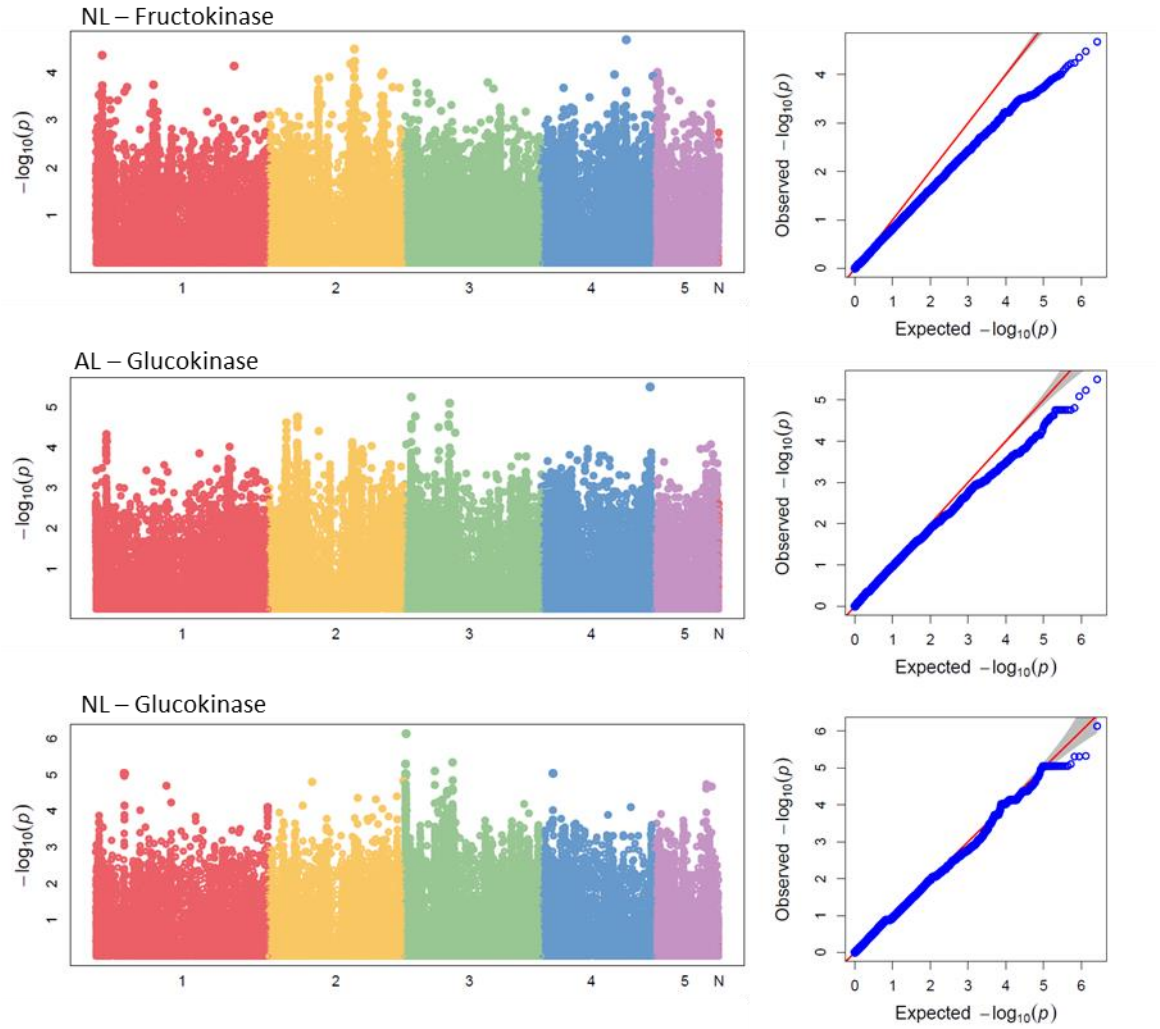

Figure S3.16. Continuation

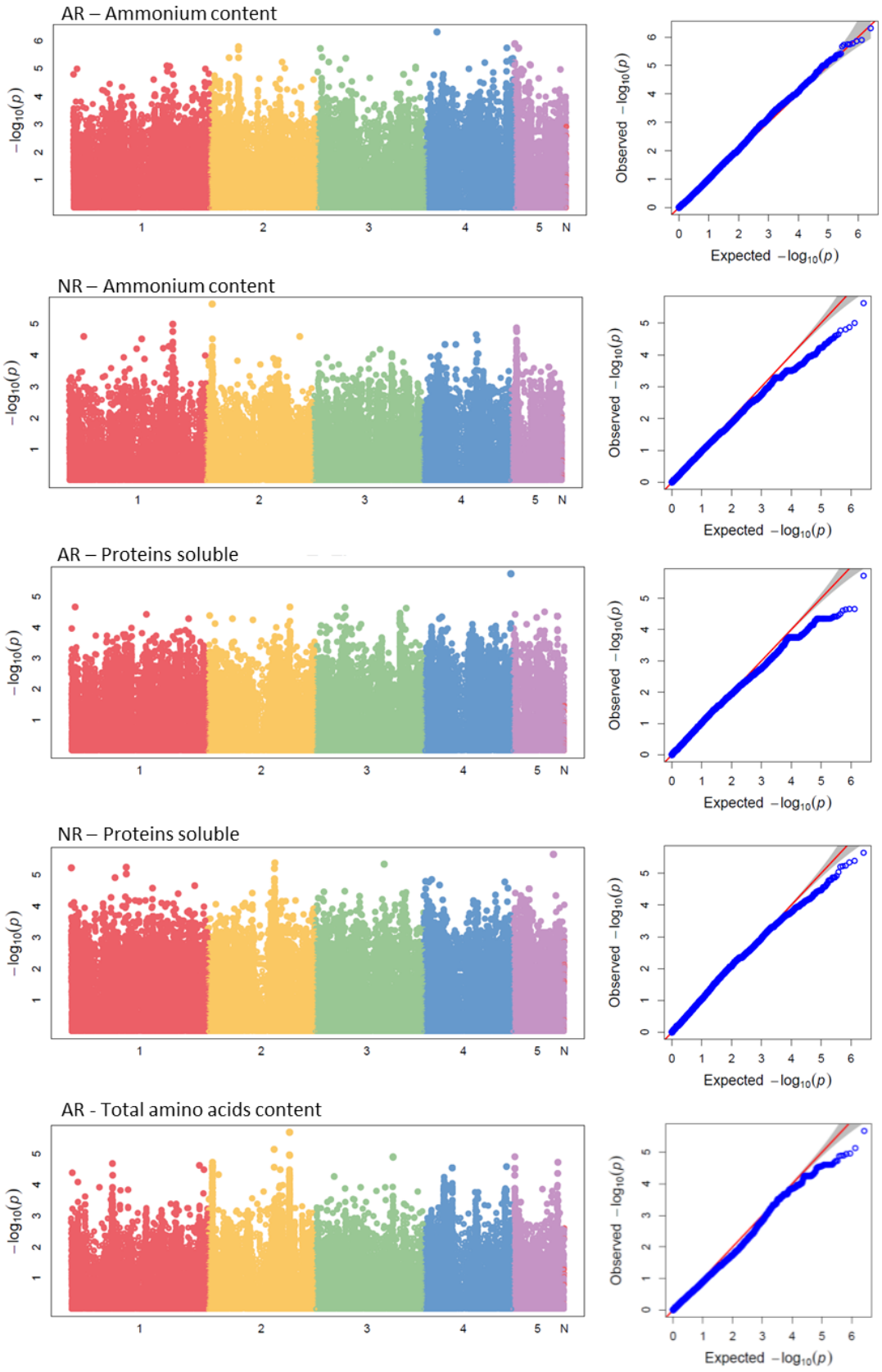

Figure S3.17. Manhattan plots (left side) showing the marker-trait associations and QQ plots (right side) showing distribution of observed and expected *p*-values for metabolites measured in root of ammonium and nitrate nutrition of *B. distachyon*. When SNPs over Bonferroni-corrected threshold are found the threshold is shown with a green line within the Manhattan plot.

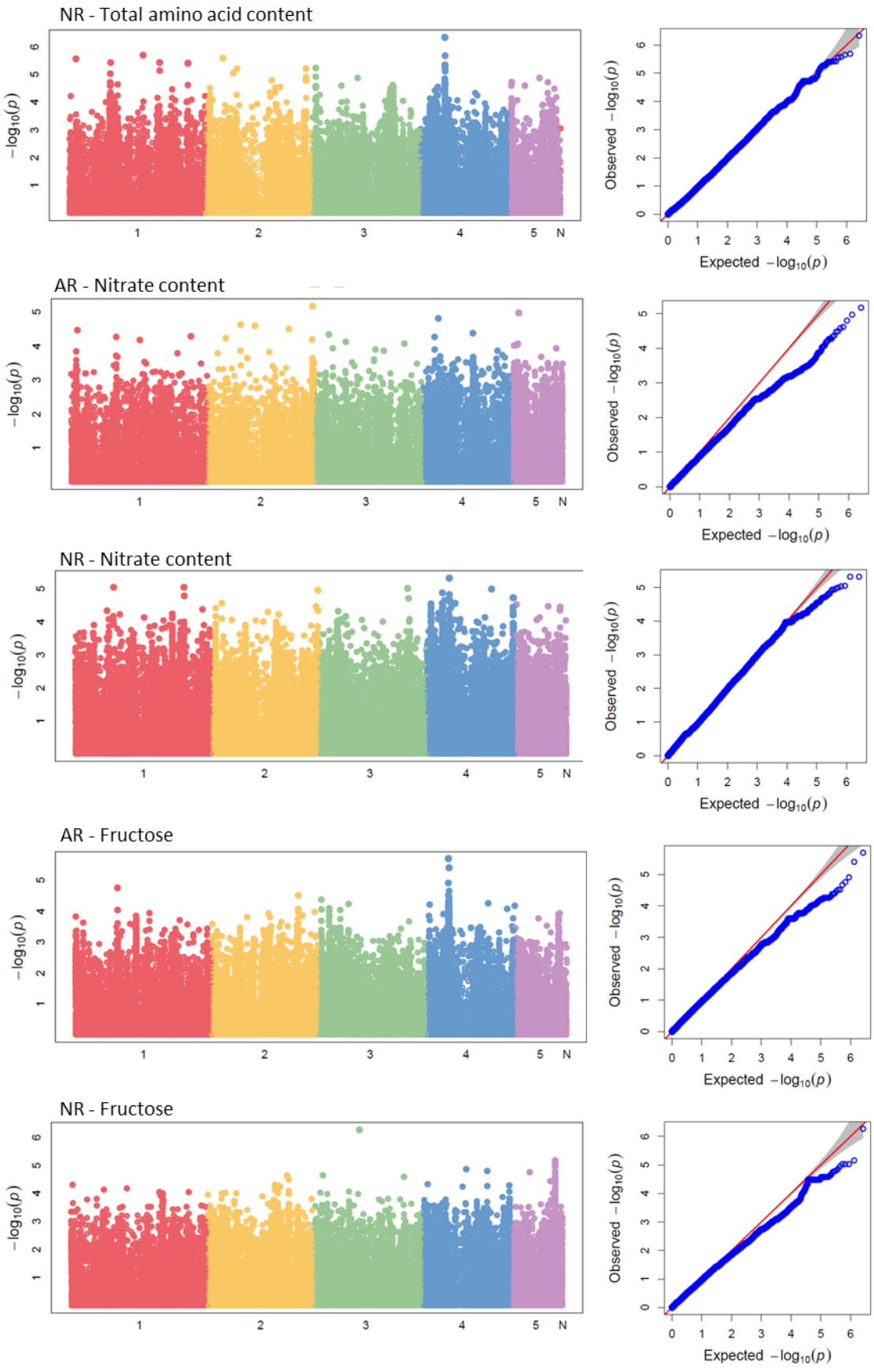

Figure S3.17. Continuation

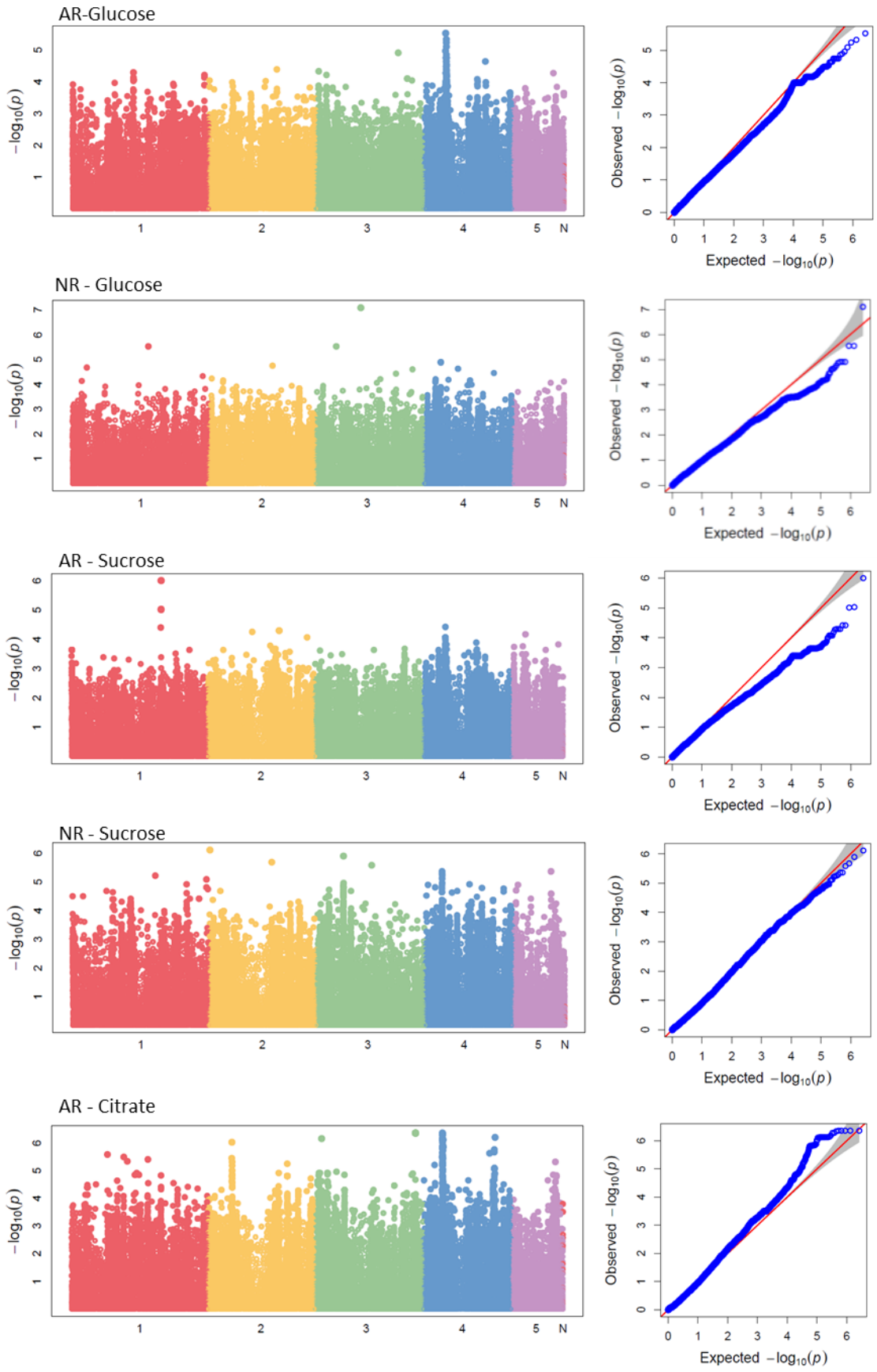

Figure S3.17. Continuation

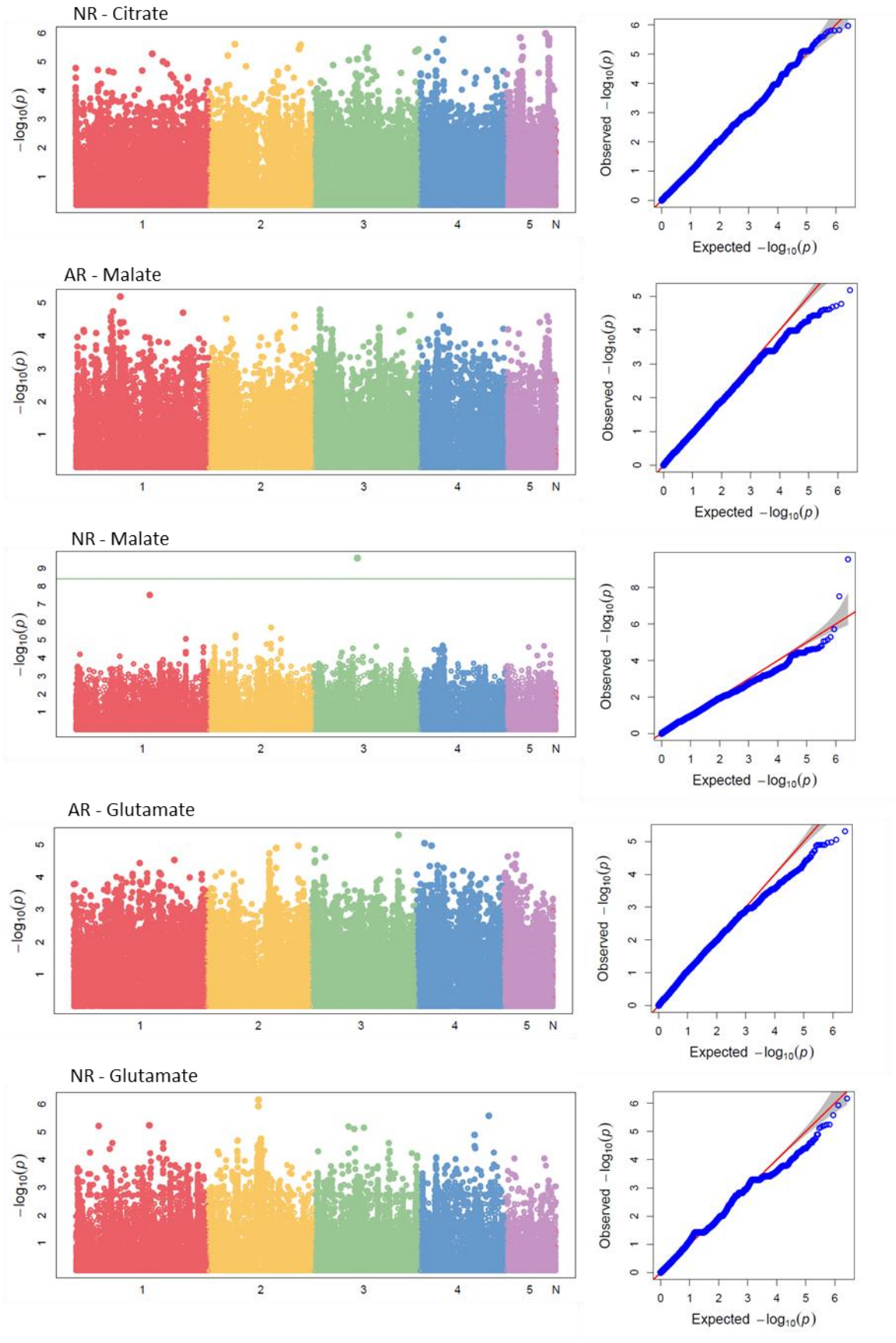

Figure S3.17. Continuation

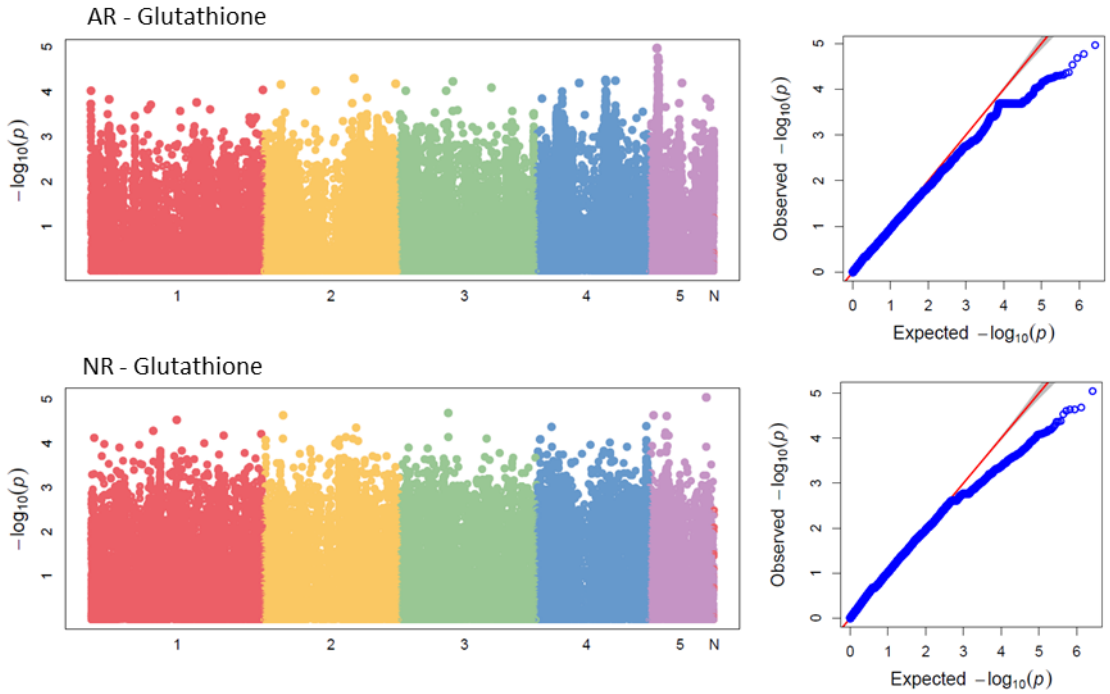

Figure S3.17. Continuation

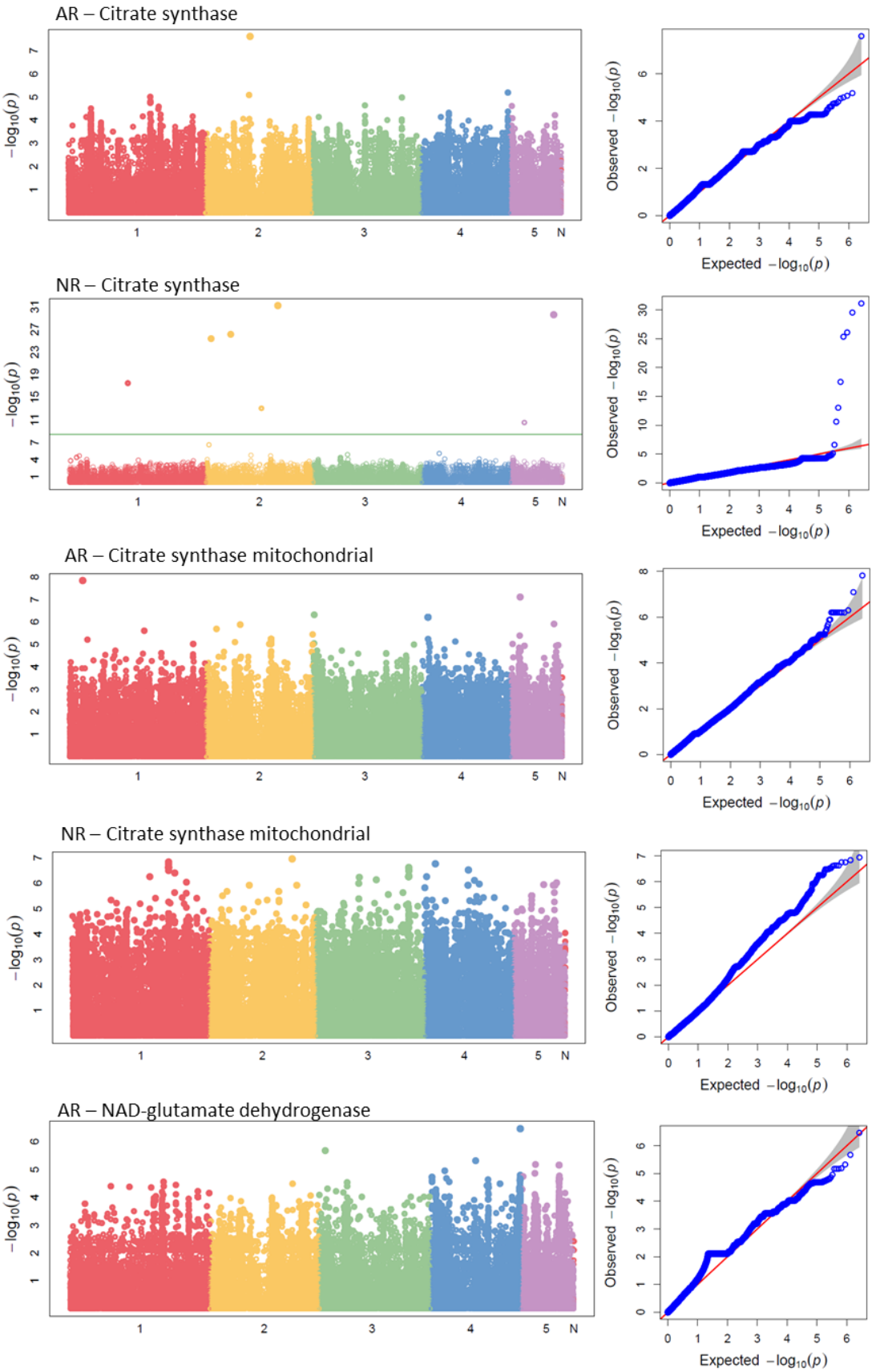

Figure S3.18. Manhattan plots (left side) showing the marker-trait associations and QQ plots (right side) showing distribution of observed and expected *p*-values for enzymatic activity in root of ammonium and nitrate nutrition of *B. distachyon*. When SNPs over Bonferroni-corrected threshold are found the threshold is shown with a green line within the Manhattan plot.

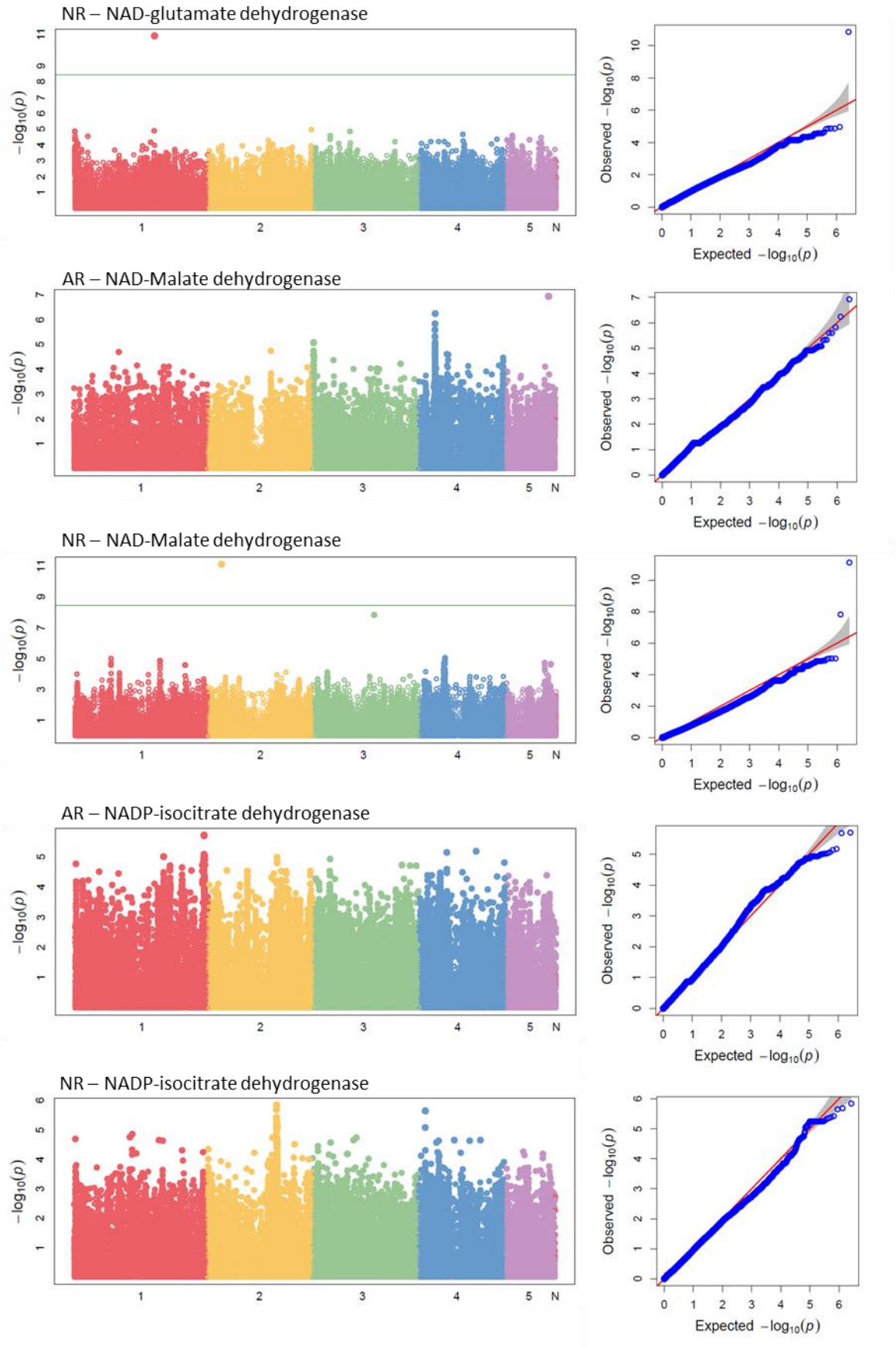

Figure S3.18. Continuation

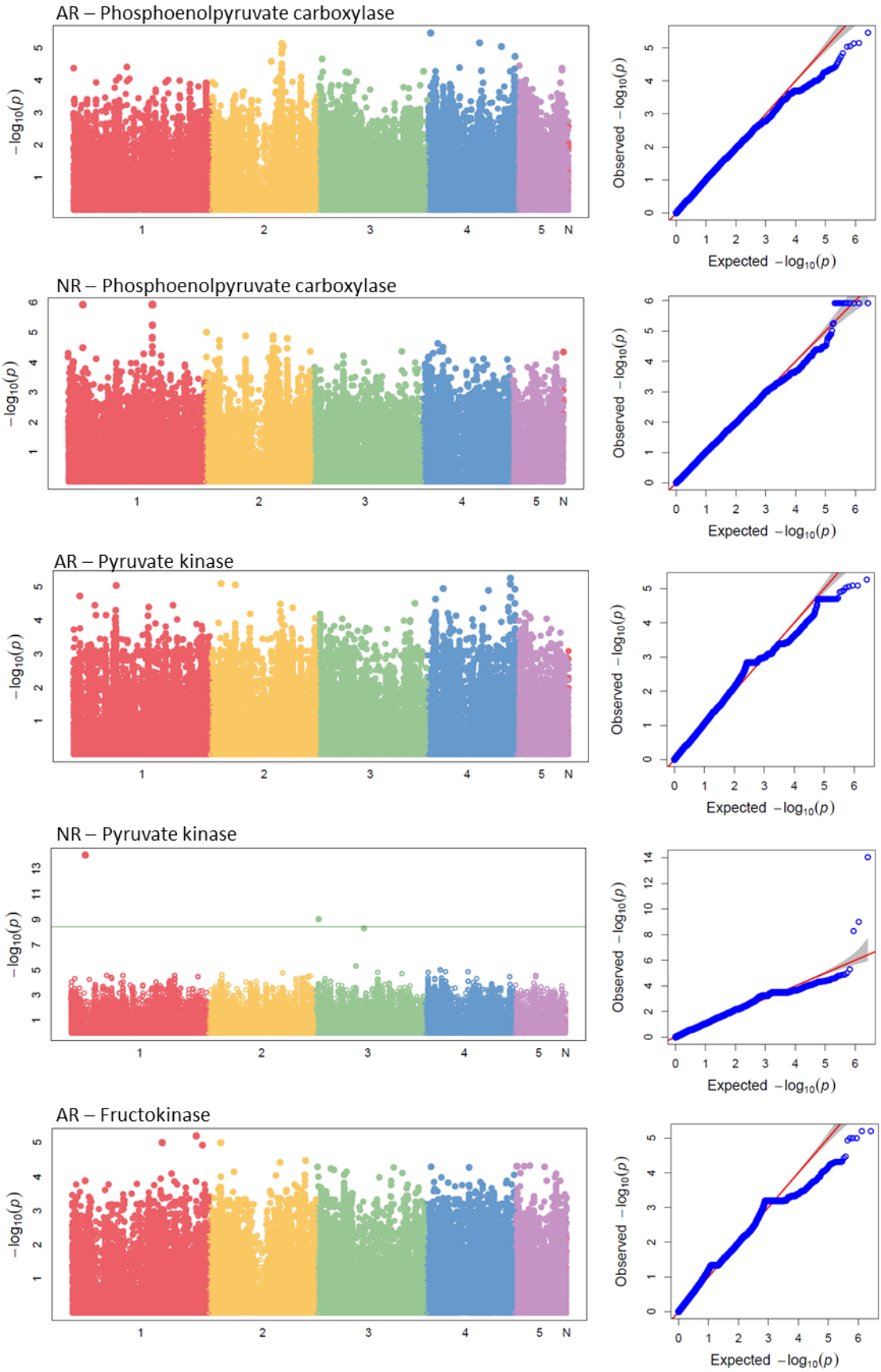

Figure S3.18. Continuation

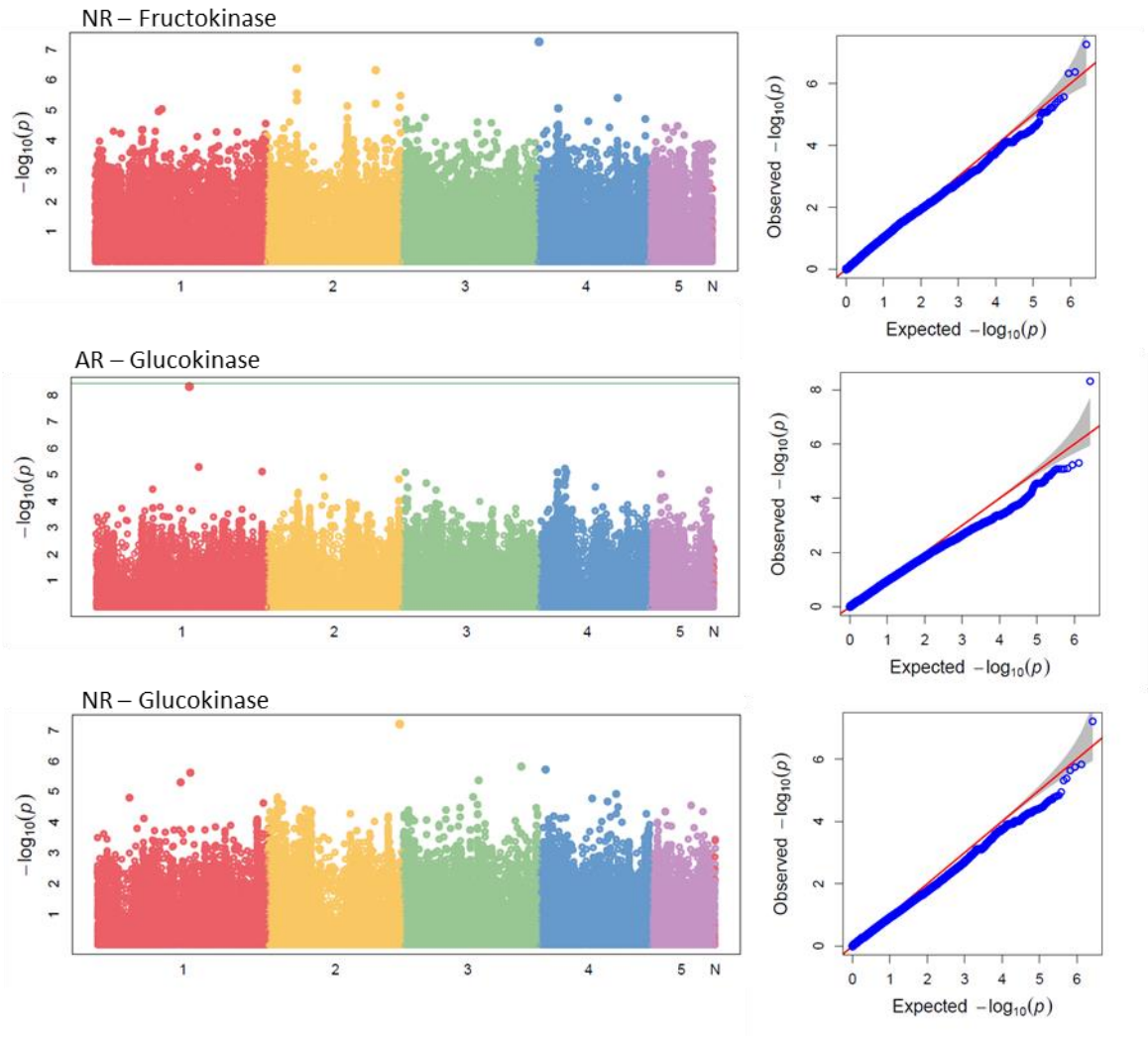

Figure S3.18. Continuation

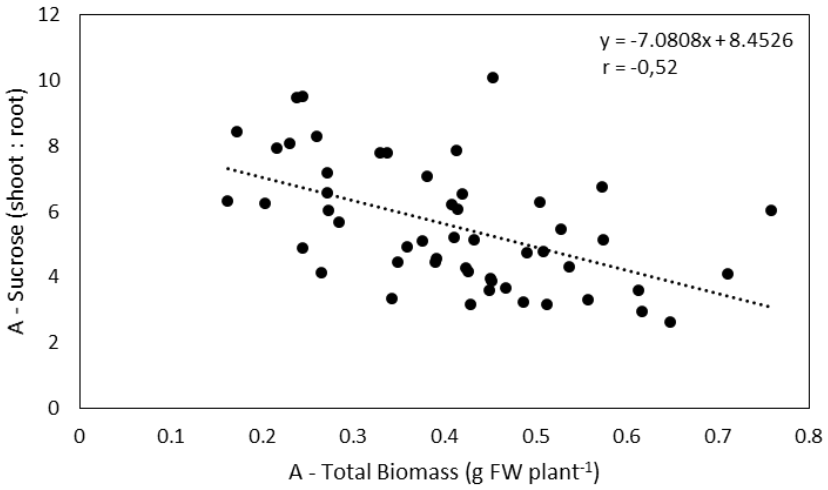

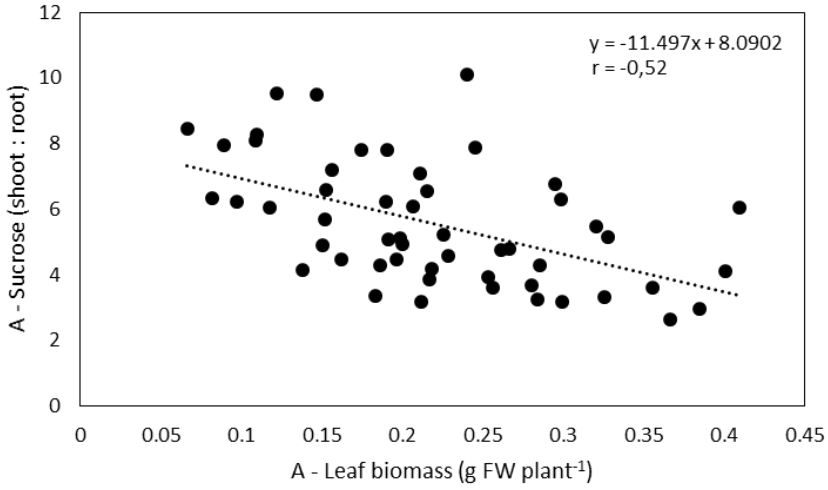

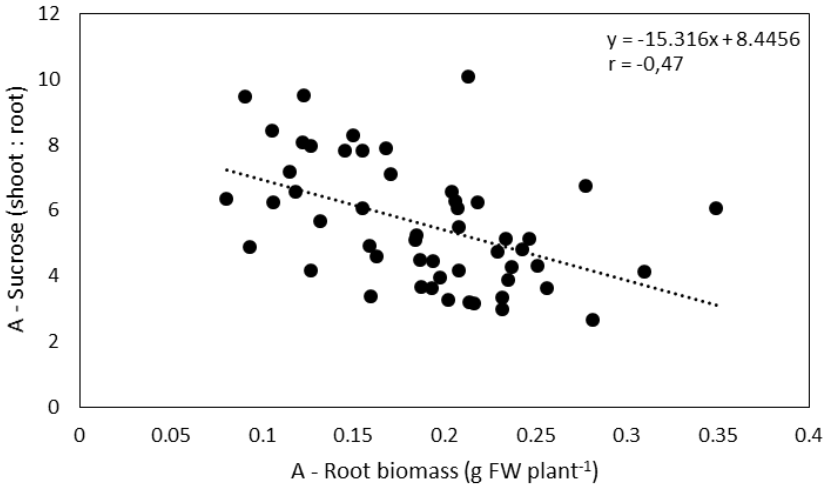

Figure S3.19. Linear regression of sucrose ratio (leaf : root) vs total, leaf and root bioamas. r represents the Pearson correlation coefficient significant for p <0.01.

GENERAL CONCLUSIONS

GENERAL CONCLUSIONS

1. The physiological and metabolic response of *Brachypodium distachyon* Bd21 to ammonium nutrition is in line with previous studies with cereal crops, such as wheat, ryegrass and sorghum. Thus, *B. distachyon* emerges as a suitable tool for defining the physiological, molecular and genetic basis of ammonium nutrition in cereals.

2. Under ammonium nutrition, the root behaves as a physiological barrier preventing NH_4^+ translocation to aerial parts, as indicated by a sizeable accumulation of NH_4^+, Asn and Gln in this organ. A continuing high NH_4^+ assimilation rate was made possible by a tuning of the TCA cycle and its associated anaplerotic pathways in order to match carbon skeletons demand, mainly 2-oxoglutarate and oxaloacetate for Gln and Asn synthesis.

3. Proteome analysis reveals an important root adaptation to ammonium nutrition, involving carbon and nitrogen metabolism, but also among others cell wall metabolism, redox homeostasis and interaction for the acquisition of essential mineral nutrients.

4. Ammonium nutrition induces the accumulation of Fe and Zn in the root, probably due to a higher uptake of these elements in relation with the activation of methionine cycle and the synthesis of phytosiderophores observed in this organ.

5. There exists an interaction between the N-source and *B. distachyon* response to Fe availability. Indeed, ammonium-fed plants displayed higher sensitivity to limiting Fe availability respect to nitrate-fed plants. This behavior could be related with increased NH_4^+ accumulation in the tissues and with impaired Fe transport and utilization.

6. The use of a panel of 52 natural accessions of *B. distachyon* reveals great intraspecific variability in response to ammonium stress using growth as a marker of plant performance.

7. The metabolic variability observed through the analyses of 13 metabolites and 9 enzyme activities of carbon and nitrogen metabolism in root and leaf tissue of 52 accessions grown under ammonium and nitrate nutrition highlighted the importance of the metabolic adjustment to explain the observed natural variability *in B. distachyon* growth upon ammonium stress.

8. Multiple regression analysis underlined the accumulation of NH_4^+ and activity of PEPC in leaves of ammonium-fed plants, together with the content of sucrose in the root as key variables explaining *B. distachyon* intraspecific variability in ammonium tolerance.

9. GWAS using Multi Locus Mixed Model (MLMM) for every trait determined in the panel of 51 accessions reveals an important number of significant SNPs, highlighting genomic regions where causal genes related to *B. distachyon* ammonium tolerance may be located.

MATERIALS AND METHODS

MATERIALS AND METHODS

Brachypodium distachyon *lines*

Brachypodium distachyon Bd21, considered as reference inbred line, was used to define the strategies of the species to ammonium nutrition. *Brachypodim distachyon* Bd21 seeds were provided by Elena Benavente, from the Polytechnic University of Madrid.

A total of 52 *B. distachyon* natural accessions were selected (Table S3.1) for the study of natural variability in ammonium tolerance. These inbred lines have been recently *de novo* assembled and annotated (Gordon *et al*., 2017; https://brachypan.jgi.doe.gov/). Seeds for the different accessions were obtained from different laboratories working on *B. distachyon*: Pilar Catalán (University of Zaragoza, Spain), Luis Mur (Aberystwyth University, UK), Ludmila Tyler (University of Massachusetts, USA), John P Vogel (University California, Berkeley, USA) and from the National Plant Germplasm System of the United States.

Seed treatment and germination

Brachypodium distachyon Bd21 seeds were sterilized in 100 % ethanol for 1 min, rinsed three times with deionised water and incubated in deionised water for 2 h. Then, seeds were placed on trays filled with a perlite:vermiculite (1:1, v:v) mixture moistened with deionised water. After 4 days of stratification at 4°C in the dark, the trays were transferred to a growth chamber. Eleven days after sowing seedlings were transferred to 4.5-L hydroponic tanks (10 plants/tank).

The methodology described by Tyler *et al.* (2016) was adopted later since it gained higher and more uniform germination rates. Seeds were peeled by removing the lemma, washed for 4 min in a solution containing 15 % bleach plus 0.1 % Triton-X 100 and thoroughly rinsed with sterile deionised water. To synchronise germination, seeds were placed in Petri dishes on damp paper towels and stratified in the dark at 4°C for 7 days (Figure 4.1A). After stratification, the plates covered with aluminum foil were transferred into a growing chamber for 3 days (Figure 4.1B). Germinated seeds (Figure 4.1C) were then sowed on trays filled with perlite:vermiculite (1:1, v:v) misted with deionised water. After 7 days, seedlings with a uniform appearance (Figure 4.1D) were finally transferred to hydroponic tanks filled with 4.5-L of nutrient solution (10-12 plants/tank, Figure 4.2).

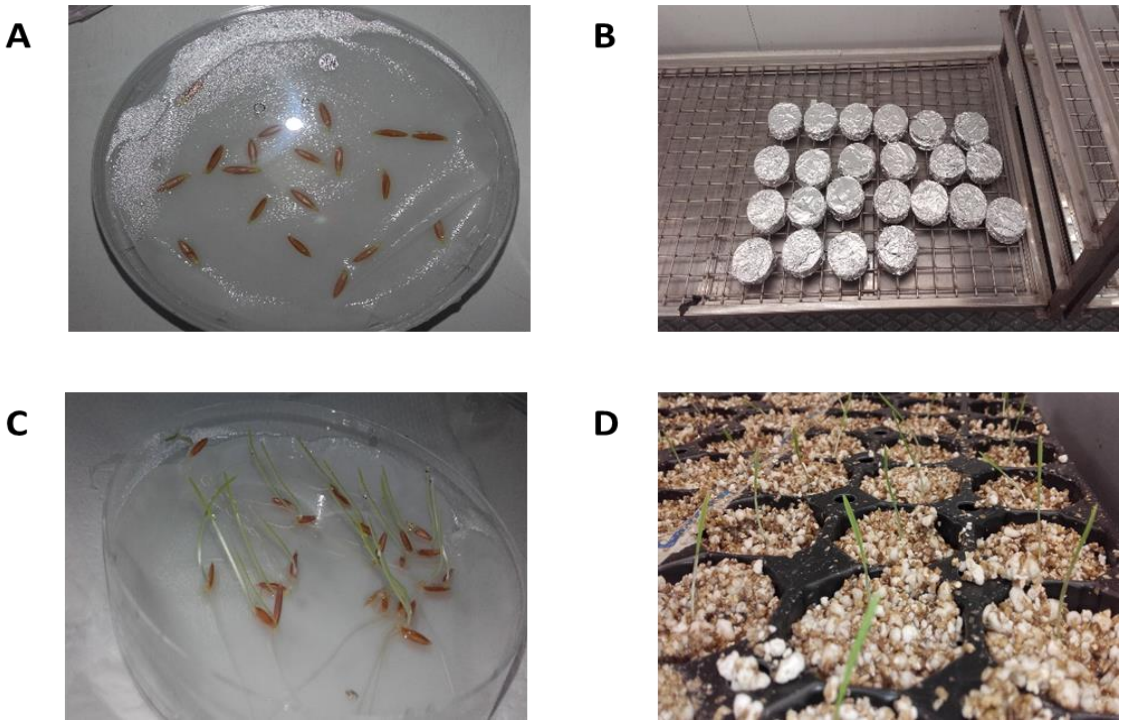

Figure 4.1. Germination of *Brachypodium distachyon* seeds. (A) Seed stratification, (B-D) seed germination.

Nutrient solution

The basic nutrient solution (Rigaud and Puppo, 1975) contained:

1.15 mM	K_2HPO_4
0.85 mM	$MgSO_4$
0.70 mM	$CaSO_4$
2.68 mM	KCl
0.50 mM	$CaCO_3$
0.07 mM	NaFeEDTA
16.5 µM	Na_2MoO_4
3.70 µM	$FeCl_3$
3.50 µM	$ZnSO_4$
16.2 µM	H_3BO_3
0.47 µM	$MnSO_4$
0.12 µM	$CuSO_4$
0.21 µM	$AlCl_3$
0.126 µM	$NiCl_2$
0.06 µM	KI, pH 6.8.

The nitrogen source was supplied as $(NH_4)_2SO_4$ for ammonium-fed plants and as $Ca(NO_3)_2$ for nitrate-fed ones. Each N source was supplied at 1 or 2.5 mM of total N. To compare both N sources within each concentration, NO_3^--fed plants were supplied with extra $CaSO_4$ to balance the SO_4^{2-} supplied with the NH_4^+. The pH of the solution was checked every 2 days and the nutrient solution replaced every 4 days.

The interaction between nitrogen and Fe nutrition was studied supplying different Fe(III)EDTA-treatments to the base nutrient solutions either with ammonium or nitrate. Fe(III)EDTA-treatment consisted of free-NaFe(III)-EDTA or 0.01 mM NaFe(III)-EDTA for deficiency (D) or moderate Fe deficiency (MD), respectively 0.1 mM NaFe(III)-EDTA for Fe control conditions, and 2.5 mM NaFe(III)-EDTA for Fe toxicity (T). During the first 7 days in hydroponic culture, treatments of Fe deficiency were grown in the same nutritional regime with optimal Fe supply (0.1 mM NaFe(III)-EDTA). At 7^{th} day, Fe control plants were kept under the same conditions, but Fe was removed for deficiency treatments (D) or supplied at 0.01 mM for moderate deficiency (MD). For Fe toxicity treatment the plants were provided with 2.5 mM Fe since the transfer of seedlings to hydroponic tanks. To maintain constant the pH and the concentration of mineral elements of the hydroponic medium, the nutrient solution was replaced three times on 7^{th}, 11^{th} and 15^{th} days. After each renewal of nutrient solution the stability of pH in the nutrient solution was checked.

Hydroponic system and controlled environmental

The tanks used for the hydroponic systems consisted of 4.5-L plastic containers with lid (29.7x19.2x12.4 cm, Tatay). Plastic containers were wrapped with black plastic in order to prevent the path of the light. The container lid was adapted in order to prevent the adjacent roots from intertwining each other and to facilitate the individual harvesting of roots (Figure 4.2). Several holes (10-12) were performed and uniformly distributed on the lid and individual plastic alveoli (Projar/Herkupak, Hercu Pack® HP 104/5R) were stuck on the back on the lid keeping the hole in middle of the alveolus. The aeration in the hydroponic system was settled connecting silicone 0.5-cm width tubes from the tank to the power diaphragm air pump (Mistral 400), to keep the dissolved oxygen in the nutrient solution with 20 cm length diffuser bars (Soloacuarios HJS-3802A). Seven-day-old seedlings were transplanted to the hydroponic system, and shoots were kept upright and protected in the holds by a small amount of hydrophobic cotton wrapping the plant neck (Figure 4.2).

Plants were grown under controlled environmental conditions (60/70 % of relative humidity, 23 °C day (14 h) with a light intensity of 350 µmol m^{-2} s^{-1} and 18 ºC night (10 h)) in growth chambers of Phytothron and Greenhouse Service of the Advanced Research Facilities (SGIKER) at the University of the Basque Country (UPV/EHU, Faculty of Science and Technology, Leioa-Bizkaia).

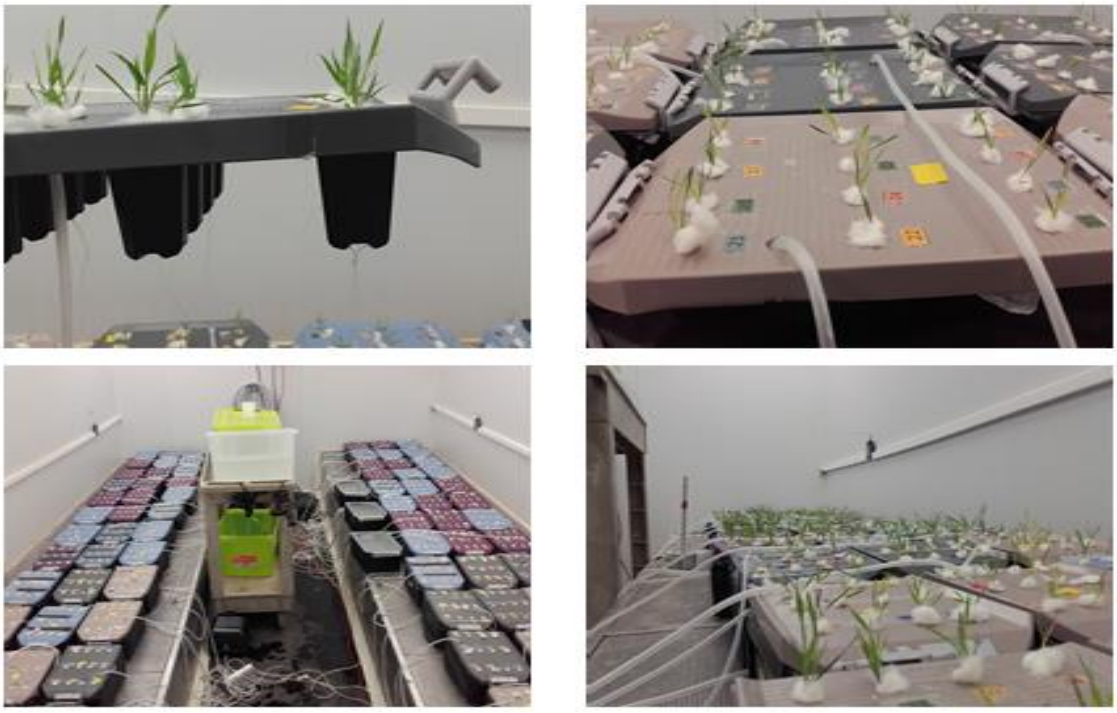

Figure 4.2. Hydroponic systems for *Brachypodium distachyon* cultivation

Harvesting of plants and conservation

Plants were harvested at 19th or 24th days, between 10 and 12 a.m., this is two hours after the onset of the photoperiod. Shoots and roots were separated and individually weighed. Plants grown within the same tank for the same accession were pooled, immediately frozen in liquid nitrogen, homogenized in a Tissue Lyser (Retsch MM 400) and stored at -80 °C until use or until being lyophilized.

Metabolites extraction

Metabolites were extracted using different solvents: acetone extraction, ethanol extraction, HCl-extraction, methanol:water:chloroform extraction and water extraction.

Acetone extraction: approximately, 20 mg of frozen fresh weight (FW) were extracted by adding 1.8 ml 80 % aqueous acetone, centrifuged at 13,200 rpm for 20 min at 4º, recovered supernatant and 5 fold-diluted with acetone 80 %.

Ethanol extraction: Approximately, 20 mg of frozen FW were extracted in 3 phases: 250 µl 80 % ethanol, 10 mM HEPES/KOH pH 6, incubated 20 min at 80 ºC, centrifuged 13,200 rpm for 5 min at 4º and supernatant recovered. The process was replicated with 150 µl 80 % ethanol, 10 mM HEPES/KOH, pH 6, and 250 µl 50 % ethanol in 10 mM HEPES/KOH pH 6. Supernatants from each step were pooled.

HCl-extraction: Approximately, 100 mg of frozen FW was homogenized in 1.5 ml 1 M HCl and incubated on ice for 10 min. Subsequently, extracts were centrifuged at 20,000 *g* and 4°C for 10 min, supernatants were neutralized using NaOH.

Methanol:water:chloroform extraction: Approximately, 150 and 200 mg of frozen FW for leaf and root material, respectively, were extracted in 1.8 ml of methanol:water:chloroform (4:4:10, v:v:v). After centrifugation, the upper layer (methanol:water) was recovered, vacuum dried and the pellet was resuspended in 1 ml of ultrapure water, that was finally filtered through a 0.22 µm polyethersulfone membrane filter.

Water extraction: approximately, 20 mg of frozen FW were extracted by adding 650 µl of milli-Q water, homogenized at 27 Hertz for one minute, heated at 80 °C for 5 min and centrifuged at 13,200 rpm for 20 min at 4º and the supernatant recovered.

Chlorophyll quantification

Chlorophylls extraction was performed either with acetone (chapter 1) or ethanol (chapter 2 and 3).

Following the acetone extraction, chlorophyll content was immediately quantified spectrophotometrically in 1-cm light path cuvettes at 663 and 645 nm (Power Wave x 340, BioTek Instruments) using the following formula (Arnon, 1949):

$$\text{Chl a } (\mu g\ ml^{-1}) = 12.7\ A_{663} - 2.69\ A_{645}$$

$$\text{Chl b } (\mu g\ ml^{-1}) = 22.9\ A_{645} - 4.86 A_{663}$$

Following the ethanol extraction, immediately 50 µl aliquots of ethanol extraction were mixed with 120 µl 98 % ethanol in 96-well microplates. Plates were measured for absorbance (OD) in a 96-well microplate reader (SAFAS MP96) at 645 and 665 nm. Chlorophyll content was adapted to microplates with a final volume of 170 µl per well from previously described Arnon (1949), using the following formula:

$$\text{Chl a } (\mu g\ well^{-1}) = 5.21\ A_{665} - 2.07\ A_{645},$$

$$\text{Chl b } (\mu g\ well^{-1}) = 9.29\ A_{645} - 2.74 A_{665}$$

Total chlorophyll (a + b) content was expressed as µg mg^{-1} FW

Ammonium quantification

Ammonium content was obtained following either water extraction (Chapter 1 and 2) or ethanol extraction (Chapter 3).

Aliquots of 50 µl of water or ethanol extractions or ammonium standard (0-0.5 mM $(NH_4)_2SO_4$) were mixed with 100 µl of 0.33 M sodium phenolate (pH 13), 50 µl of 0.76 mM sodium nitroprusside and 100 µl of sodium hypochloride (diluted solution of 2 % commercial bleach, v/v). Microplates were incubated for 30 min at room temperature and OD determined at 635 nm in a 96-well microplate reader (Power wave x 340, BioTek Instruments or SAFAS MP96). Ammonium content was expressed as µmol g^{-1} FW.

Nitrate quantification

Nitrate was determined as described by Tschoep *et al.* (2009). Aliquots of 5 µl of ethanol extraction or nitrate standard (0. 0.4, 0.8 and 1.4 mM KNO_3) were mixed with 95 µl assay mix.

Assay mix:

10	µl	1 M potassium phosphate buffer, pH 7.5
0.5	µl	50 mM NADPH in 50 mM NaOH
1	µl	5 U ml^{-1} nitrate reductase (NR) in 0.1 M phosphate buffer
83.5	µl	H_2O MilliQ

The reaction was formed by incubating the microplates at 25 °C for 30 min, then 15 µl 0.25 mM phenazine methosulfate, mixed, protected from light and incubated at 25 ºC for 20 min. Afterwards, nitrite was detected with the addition of 60 µl 1 % w/v sulphanilamide in 3 M phosphoric acid, 60 µl 0.02 % w/v NNEDA (N (1-Naphtyl) ethylendiamine dihydrochloride). Microplates were incubated for 10 min at 25ºC and OD determined at 540 nm in a 96-well microplate reader and (Power wave x 340, BioTek Instruments or SAFAS MP96). Nitrate content was expressed as µmol g^{-1} FW.

Amino acids

Total free amino acids quantification

Quantification of total free amino acids was performed either from water extraction (chapter 2) or from ethanol extraction (chapter 3)

In chapter 2, total free amino acids were determined by the ninhydrin method (Yemm *et al.,* 1955). Aliquots of 10 µl of water extraction or standard (0-5 mM L-glutamine) were mixed with 90 µl of milli-Q water, 50 µl of 25.5 µM KCN (pH 5.4) and 50 µl of 0.168 M ninhydrin diluted in

ethylene glycolmonomethyl ether. The samples were mixed, stirred, and incubated at 100 °C for 15 min. Finally, 500 µl of 50 % (v/v) isopropanol were added and stirred and OD was determined at 570 nm (Power wave x 340, BioTek Instruments).

In chapter 3, total free amino acids were assayed as described by Bantan-Polak *et al.,* (2001). 2 µl aliquots of ethanol extraction or Na-glutamate standard (0, 100, 200, 400, 800 µM in 70 % ethanol/HEPES KOH 10 mM) were mixed with 15 µl 0.1 M borate buffer pH 8, 90 µl fluorescamine in acetonitrile and 100 µl H_20 milliQ. Plates were incubated for 5 min at room temperature and fluorescence determined at 405 nm excitation, 485 nm emission in a 96-well microplate reader (SAFAS XENIUS XMA).

Total free amino acid content was expressed as µmol Glu or Gln g^{-1} FW.

Individual amino acid quantification

From the HCl-extraction the internal standards norvaline and homoglutamic acids were added. Samples were then derivatized with 1 mM fluorescein isothiocyanate (FITC) in acetone at room temperature for 15 h in 20 mM borate buffer (pH 10). The content of free amino acids was determined using a Beckman Coulter capillary electrophoresis SYSTEM PA-800 (Beckman Coulter Inc., USA) coupled to a laser induced florescence detector (argon laser at 488 nm), as described in Takizawa and Nakamura (1998), with minor modifications. Individual free amino acid content was expressed as µmol g^{-1} FW. The determination of Individual amino acid was carried out at the Natural Sciences Department of the Public University of Navarra in Pamplona (Spain).

Glutamate quantification

To determine glutamate enzymatically 15 µl aliquots of ethanol extraction or standard (ranging from 0 to 0.5 mM Na-glutamate) were mixed with 185 µl of assay mix.

Assay mix:

20	µl	1 M Tricine KOH pH 8.5
10	µl	10 mM methylthiazolyldiphenyl tetrazolium bromide (protected from light)
10	µl	30 mM NAD^+
5	µl	10 % Triton X-100
2	µl	50 mM ADP
5	µl	2.5 mM phenazine ethosulfate
133	µl	H_2O MilliQ

After reading the absorbance at 570 nm for 10 min, one unit of glutamate dehydrogenase was added, and the OD was read until curve reaction stabilized. Content of glutamate was expressed in µmol g^{-1} FW.

Organic acids quantification

Organic acids were extracted from 150 and 200 mg of frozen FW leaf and root, respectively, in 1.8 ml of methanol:water:chloroform (4:4:10). After centrifugation, the upper layer was recovered, vacuum dried and the pellet resuspended in 1 ml of ultrapure water that was finally filtered through a 0.22-µm polyethersulfone (PES) membrane filter. Separation and quantification of the different organic acid were performed by ion chromatography (Dionex ICS-5000, Thermo Scientific) in the Service of the Advanced Research Facilities (SGIker) at the University of the Basque Country (UPV/EHU, Faculty of Science and Technology, Leioa-Bizkaia). Contents of phosphoenolpyruvate, pyruvate, oxaloacetate, malate, citrate, isocitrate, 2-oxoglutarate, fumarate (chapter 1) were expressed in nmol mg^{-1} FW.

Citrate and malate enzymatic quantification

To determine citrate 10 µl aliquots of ethanolic extracts were mixed with 100 µl assay mix.

Assay mix:

5	µl	1M Tricine/KOH pH 8,
1	µl	50 mM NADH in 50 mM NaOH
0.05	µl	200 mM $ZnSO_4$
0.15	µl	1000 U ml^{-1} malate dehydrogenase in 100 mM Tricine
93.8	µl	H_2O milliQ

After reading the absorbance at 340 nm for 10 min, 0.014 units of citrate lyase were added, and the OD was read until curve reaction stabilized. The ΔOD due to the addition of citrate lyase was determined for the calculation of citrate content.

To determine malate 10 µl aliquots of ethanolic extracts were mixed with 90 µl assay mix.

Assay mix:

69	µl	0.1 M Tricine /KOH pH 9
10	µl	30 mM NAD^+
10	µl	20 mM Na-glutamate
1	µl	200 U ml^{-1} glutamate:oxoglutarate aminotransferase

After reading the absorbance at 340 nm for 15 min, 2 units of malate dehydrogenase were added, and the OD was read until curve reaction stabilized (Nunes-Nesi *et al.,* 2007). Content of

citrate and malate were expressed in nmol mg^{-1} FW. The ΔOD due to the addition of malate dehydrogenase was determined for the calculation of malate.

Soluble sugars quantification: glucose, fructose and sucrose

Soluble sugars, glucose, fructose and sucrose, were determined as described by Jelitto *et al.,* (1992). Aliquots of 50 µl of ethanol extraction were mixed with 160 µl of assay mix.

Assay mix:

193.7	µl	0.1 M HEPES/KOH, 3 mM $MgCl_2$, pH 7
6	µl	100 mM ATP
6	µl	45 mM $NADP^+$
1	µl	700 U ml^{-1} Glucose-6-phosphate dehydrogenase (G6PDH grade II)

Plates were incubated at 37 ºC in a 96-well microplate reader (SAFAS MP96) and NADPH evolution was monitored at 340 nm (one reading every 30 s) until OD1 was stabilized, and then added successively the following enzymes:

1 µl Hexokinase (900 U ml^{-1} solution in 0.1 M HEPES/KOH 0, 3 mM $MgCl_2$, pH 7)

Waiting until OD2 is stabilized, and adding of

1 µl Phosphoglucose isomerase (1000 U ml^{-1} solution in 0.1 M HEPES/KOH 0, 3 mM $MgCl_2$, pH 7),

Waiting until OD3 is stabilized and adding of

1 µl Invertase (300 mg in 3 ml 0.1 M buffer)

Then when stabilized OD4 was recorded evolution of NAD(P)H. Content of glucose, fructose and sucrose were expressed in eq µmol glucose g^{-1} FW. For glucose determination, ΔOD due to the difference between the absorbance before and after applying hexokinase was calculated. For fructose determination, ΔOD due to the difference between the absorbance before and after applying phosphoglucose isomerase was calculated. For sucrose determination, ΔOD due to the difference between the absorbance before and after applying invertase was calculated.

Starch

Starch was determined from the pellet obtained from the ethanolic extraction by adding 400 µl 0.1 M NaOH and heating at 95 ºC for 30 min, as described by Hendriks *et al.* (2003). The re-suspended pellet was acidified to pH 4.9 with 80 µl 0.5 M HCl / 0.1 M sodium-acetate, mixed and the suspension was digested overnight at 37 ºC with 100 µl of starch degradation enzymatic buffer (210 units amyloglucosidase and 150 units α-amylase in 12.5 ml of 50 mM acetate buffer

for 1 microplate). The glucose content of the supernatant was then used to assess the starch content of the sample, according to the glucose determination above stated.

Total glutathione extraction and determination

Total glutathione (oxidized (GSSG) and reduced (GSH)) were extracted using approximately 20 mg of FW in 400 µl of 5 % metaphosphoric acid. To determine total glutathione pool (GSH + GSSG) 10 µl aliquots of extracts or standard (0, 3.12, 6.25, 12.5, 25, 50 µM GSSG) were mixed with 150 µl assay mix (Griffith, 1980).

Assay mix:

31.59	µl	Phosphate buffer (add 0.5 M KH_2P_4 to 0.5 M K_2HPO_4 until pH 7)
1.46	µl	0.5 M EDTA pH 7
4.19	µl	Glutathione reductase in 4.12 µl buffer 1X (5.2 ml phosphate buffer, 0.24 ml EDTA, 18.56 ml H_2O milliQ)
4.19	µl	DTNB (5.5' Dithio-2-nitro benzoic acid) 1.5 mg ml^{-1} in Ethanol 99 % (prepared fresh just before the assay)
112.76	µl	H_2O milliQ

After 5-min incubation, 5 µl of 2mM NADPH were added and TNB (5- thionitrobenzoic acid) evolution absorbance at 415 nm was measured every 30 s for 30 min in a 96-well microplate reader (SAFAS MP96). Total glutathione was expressed

$$\text{Total glutathione (GSSG + GSH)} = \frac{[\Delta OD\ at\ 415/min - (y - intercept)]\ x\ sample\ dilution\ x\ 2}{slope}$$

Total glutathione is expressed as eq nmol GSSG g^{-1} FW

Phytosidopheres determination

The concentration of nicotianamine, mugenic acid (MA) and analogous chelators: 2´-deoxymugineic acid, deoxydistichonic acid A, distichonic acid A, avenic acid and 3-hydroxymugineic acid were measured by HPLC (Kawai *et al*., 1988) in the Experimental Station Aula Dei, CSIC (Zaragoza).

Mineral elements: extraction and quantification

Lyophilized leaf and root samples (10 mg DW) were extracted with HNO_3 by microwave-assisted digestion (Mars6, Vertex, Spain). Nitrogen (N), carbon (C) and sulphur (S) contents were determined with an elemental analyser Flash EA1112 (Thermo Fisher Scientific Inc., Waltham, MA, USA). Quantification of inorganic elements (Fe, Zn, Mg, Ca, P, K and Na) was performed by optical emission spectrophotometer with inductively coupled plasma ICP-OES (Horiba Jobin Yvon, Activa). The determination of mineral elements were carried out at the Central Analysis

Service of the Advanced Research Facilities (SGIKER) at the University of the Basque Country (UPV/EHU, Faculty of Science and Technology, Leioa-Bizkaia).

Soluble proteins extraction and enzymatic activity determination

Soluble proteins were extracted using three protocols, referred as "ethanolic extraction" used in the chapter 3, "extraction buffer 1" in the chapter 1, and "extraction buffer 2" in the chapter 3.

Ethanolic extraction: Approximately, 20 mg of frozen FW were extracted in 3 phases: 250 µl 80 % ethanol, 10 mM HEPES/KOH pH 6, incubated 20 min at 80 ºC, centrifuged 13,200 rpm for 5 min at 4º and supernatant recovered. The process was replicated with 150 µl 80 % ethanol, 10 mM HEPES/KOH, pH 6, and 250 µl 50 % ethanol in 10 mM HEPES/KOH pH 6. Supernatants from each step were pooled.

Extraction buffer 1: 40 mg of frozen FW with 20-30 mg polyvinylpyrrolidone (PVPP) were extracted with 800 µl of extraction buffer containing 10 % Glycerol, 0.05% BSA, 0.1% Triton X-100, 50 mM HEPES-KOH pH 7.5, 10 mM $MgCl_2$, 1 mM EDTA Na_2, 1 mM EGTA, 10 mM DTT, 1 mM PMSF, 1 mM delta-aminocapronic acid, 5 µM leupeptin, 1 mM benzamidine). Afterwards, it was homogenized twice for 60 s at 27 Hertz and centrifuged at 13,200 rpm and 4 ºC for 20 min. The supernatant was used for enzyme activities determination and soluble protein content (Chapter 1).

Extraction buffer 2: 20 mg of frozen FW with 20 mg of polyvinylpyrrolidone (PVPP) were extracted with 500 µl of extraction buffer (289.5 µl H_2O milliQ, 100 µl glycerol 99%, 50 µl pre-extraction buffer 10X, 50 µl 10 % Triton-X 100, 5 µl leupeptin 2 mM , 0.5 µl DTT 500 mM). After mixed vigorously, it was centrifuged at 2500 rpm and 4 ºC for 10 min. The supernatant was used for enzymatic activities performed in the high throughput metabolic phenotyping platform (HiTe Platform) in the National Institute of Agricultural Research (INRA), Aquitaine-University of Bordeaux.

Soluble proteins quantification

The content of soluble protein was measured according to Bradford assay (Bradford, 1976) adjusting the volumes for microplate reader in each case. Aliquots of 10 µl of enzymatic extract (extraction buffer 1, chapter 1), or 3 µl of ·ethanolic extraction (chapter 3) or bovine serum albumin standard (0-0.5-1-2-3-4-5-6 µg ml^{-1}) were mixed with 240 µl and 180 respectively, of 5-fold diluted Bradford base dye-binding assay (Bio-Rad, Hercules, CA, USA). Plates were incubated

for 5 or 10 min at room temperature and OD determined at 595 nm in a 96-well microplate reader (Power wave x 340, BioTek Instruments, SAFAS MP96).

Soluble proteins content was expressed in mg BSA g^{-1} FW.

Enzymatic activities

NADP(H)- glutamate dehydrogenase

In chapter 1, to determine glutamate deshydrogenase (NAD(P)(H)-GDH, EC 1.4.1.2, EC 1.4.1.4) activity in the aminating sense 20 µl aliquots of enzymatic extraction (buffer 1) were mixed with 280 µl assay mix.

Assay mix:

28	µl	1 M Tricine KOH, pH 8
0.28	µl	1 M $CaCl_2$
5.6	µl	2.5 M $(NH_4)_2SO_4$
28	µl	2.5 M NADH or NADPH
28	µl	130 mM α-Ketoglutaric acid disodium salt dihydrate
190.2	µl	H_2O milliQ

Microplates were incubated at 25 °C during 20 min in a 96-well microplate reader (Power wave x 340, BioTek Instruments) and NAD(P)H evolution was monitored at 340 nm. Activity was expressed in µmol NAD(P)H g^{-1} FW h^{-1}

To determine NAD-GDH (EC 1.4.1.2) activity in the aminating sense 2 µl aliquots of enzymatic extraction (buffer 2) or standard (0, 50, 100, 200 µM NAD^+) were mixed with 18 µL of assay mix.

Assay mix:

4	µl	Assay buffer (Tricine/KOH 0.5 M pH 8, $CaCl_2$ 5 mM, NH_4 acetate 3.2 M, Triton X100 0.25 %)
2	µl	150 mM α-Ketoglutaric acid disodium salt dihydrate
0.04	µl	60 mM NADH in 60 mM of NaOH
11.96	µl	H_2O milliQ

After incubating at 25 °C for 20 min, the reaction was stopped with 20 µl of 0.5 M HCl in 100 mM Tricine/KOH pH 9, incubated at 90 ºC for 10 min and 20 µl 0.5 M NaOH. After mixed, 45 µl of determination mix and 5 µl of 4 mM PES (Phenazine ethosulfate) were added and reduced MTT (3-(4,5-dimethylthiazol-2-yl)-2,5-diphenyltetrazolium bromide) evolution were monitored at 570 nm. For blanks α-Ketoglutaric (acid disodium salt dehydrate) was substituted by water (Gibon *et al.,* 2004). Activity was expressed in µmol NADH g^{-1} FW h^{-1}

Determination mix

10	µl	1 M Tricine/KOH pH 9 buffer
10	µl	10 mM MTT (3-(4,5-dimethylthiazol-2-yl)-2,5-diphenyltetrazolium bromide)
4	µl	200 mM EDTA
2	µl	50 % Ethanol
1	µl	2000 U ml^{-1} alcohol dehydrogenase (in 200 mM Tricine/KOH, pH 9, 10 mM $MgCl_2$)
18	µl	H_2O milliQ

Glutamine synthetase

In chapter 1, glutamine synthase (GS, EC 6.3.1.2) activity was determined in the semibiosynthetic reaction, according to O'Neal and Joy (1973). Aliquots of 50 µl of enzymatic extraction (buffer 1) or standard (0-4 nmol μl^{-1} γ-glutamilhydroxamate), were mixed with 100 µl assay mix, and incubated for 30 min. Afterwards, 150 µl of "stopping mix" (0.37 M $FeCl_3$, 0.2 M trichloroacetic acid, 0.67 N HCl) were added, centrifuged for 10 min and 200 µl of supernatant was transferred to a new microplate. The OD was read at 540 nm in a 96-well microplate (Power wave x 340, BioTek Instruments). GS activity was expressed in µmol γ-glutamilhydroxamate g^{-1} FW h^{-1}.

Assay mix:

5	µl	1 M Tris-HCl pH 7.6
2	µl	1 M $MgSO_4$
10	µl	0.8 M Na-glutamate
1	µl	0.6 M Hydroxylamine
0.8	µl	0.5 M EDTA
6.66	µl	120 mM ATP
47.54	µl	H_2O milliQ

In chapter 3, to determine glutamine synthetase activity 5-µl aliquots of enzymatic extraction (buffer 2), were mixed with 95 µl of assay mix. Microplates were incubated at 25 °C during 20 min in a 96-well microplate reader (SAFAS MP96) and NADH evolution was monitored at 340 nm. For blanks L-glutamate was substituted by water (Gibon *et al.,* 2004).

Assay mix:

20	µl	Assay buffer 5X ($MgCl_2$ 100 mM, HEPES/KOH 0.5 M pH 7.5, $NaVO_3$ 2 mM, 5',5'- Diadenosine pentaphosphate 0.4 mM , NH_4Cl 20 mM, EDTA 10 mM, Triton-X 100 0.25%)
10	µl	99 % Glycerol
2	µl	50 mM Phospho(enol)pyruvic acid trisodium salt hydrate
5	µl	100 mM ATP
2	µl	50 $U.ml^{-1}$ Pyruvate kinase
1	µl	60 mM NADH in 60 mM NaOH
1	µl	Lactate dehydrogenase (60 U ml^{-1} in 200 mM HEPES/KOH pH 7.5, 10 mM $MgCl_2$)
45	µl	L-glutamate 100 mM pH (7.5)
9	µl	H_2O milliQ

NADH-dependent glutamate synthase

To determine NADH-dependent glutamate synthase (NADH-GOGAT, EC 1.4.1.14) activity (chapter 1) 20 µl aliquots enzymatic extraction (buffer 1) were mixed with 280 µl assay mix. Microplates were incubated at 25 °C during 20 min in a 96-well microplate reader (Power wave x 340, BioTek Instruments) and NADH evolution was monitored at 340 nm. Activity was expressed in µmol NADH g^{-1} FW h^{-1}

Assay mix:

28	µl	1 M Tricine KOH pH 8.6
22.4	µl	2.5 mM NADH
1.4	µl	1 M Dithiothreitol (DTT)
2.15	µl	0.13 M α-Ketoglutaric acid disodium salt dihydrate
28	µl	30 mM Gln
198.05	µl	H_2O milliQ

Phosphoenolpyruvate carboxylase

In chapter 1, to determine phosphoenolpyruvate carboxylase (PEPC, EC 4.1.1.31) activity 20 µl aliquots of enzymatic extraction (buffer 1) were mixed with 280 µl assay mix. Microplates were incubated at 25 °C during 20 min in a 96-well microplate reader (Power wave x 340, BioTek Instruments) and NADH evolution was monitored at 340 nm. Activity was expressed in µmol NADH g^{-1} FW h^{-1}

Assay mix:

28	µl	1 M Tricine KOH pH 8
1.4	µl	1M $MgCl_2$
5.6	µl	0.1 M $NaHCO_3$
5.6	µl	0.25 M NaF
5.6	µl	0.15 M Phosphoenolpyruvic acid trisodium salt hydrate
0.21	µl	10 kU malate dehydrogenase in 1.18 ml $(NH_4)_2SO_4$
28	µl	2.5 mM NADH
205.59	µl	H_2O milliQ

In chapter 3, phosphoenolpyruvate carboxylase activity was determined using 5 µl of aliquots of enzymatic extraction buffer 2, mixed with 95 µl of assay mix. Plates were incubated at 25 °C during 20 min in a 96-well microplate reader (SAFAS MP96) and NADH evolution was monitored at 340 nm. For blanks phosphoenolpyruvate was substituted by water (Bénard and Gibon, 2016)

Assay mix:

20	µl	Assay buffer (0.5M Tricine/KOH pH8, 100 mM $MgCl_2$, 50 mM $NaHCO_3$, 0.25% Triton X-100)
10	µl	100 U ml^{-1} Malate dehydrogenase in 200 mM tricine/KOH pH8, 10mM $MgCl_2$
4	µl	50 mM Phosphoenolpyruvic acid trisodium salt hydrate
1	µl	60 mM NADH in 60 mM NaOH
60	µl	H_20 milliQ

NAD-dependent malate dehydrogenase

In chapter 1, to determine NAD-dependent malate dehydrogenase (NAD-MDH, EC 1.1.1.37) activity 20 µl aliquots of enzymatic extraction buffer 1 were mixed with 280 µl assay mix. Plates were incubated at 25 °C during 20 min in a 96-well microplate reader (Power wave x 340, BioTek Instruments) and NADH evolution was monitored at 340 nm. Activity was expressed in mol NADH g^{-1} FW h^{-1}

Assay mix:

28	µl	1 M HEPES pH 7.5
1.4	µl	1 M $MgSO_4$
2.8	µl	0.2 M Oxaloacetate (OAA, fresh prepared)
28	µl	2 mM NADH
219	µl	H_2O milliQ

In chapter 3, to determine NAD-MDH activity 5 µL of aliquots of enzymatic extraction (buffer 2) were mixed with 95 µL of assay mix. Plates were incubated at 25 °C during 20 min in a 96-well microplate reader (SAFAS MP96) and NADH evolution was monitored at 340 nm. For blanks oxaloacetate was substituted by water. Activity was expressed in mmol NADH g^{-1} FW h^{-1}

Assay mix:

20	µL	Reaction buffer: 0.5 mM Tricine-KOH pH 8, 0.25% Triton X-100, 0.5 mM EDTA)
2	µL	60 mM NADH in 60 mM NaOH
22.5	µL	5 mM Oxaloacetate (fresh prepared)
50.5	µL	H_2O milliQ

NAD-dependent malic enzyme

To determine NAD-dependent malic enzyme (NAD-ME, EC 1.1.1.38) activity 20 µl of aliquots of enzymatic extraction (buffer 1) were mixed with 280 µl of assay mix. Plates were incubated at 25 °C during 20 min in a 96-well microplate reader (Power wave x 340, BioTek Instruments) and NADH evolution was monitored at 340 nm. Activity was expressed in µmol NADH g^{-1} FW h^{-1}

Assay mix:

14	µl	1 M KOH pH 8
0.112	µl	1 M EDTA
1.4	µl	1 M DTT
2.8	µl	0.5 M Malate
1.12	µl	1 M $MnCl_2$
2.8	µl	10 mM Coenzyme A (CoA)
28	µl	20 mM NAD
28	µl	2.5 µM NADH
201.77	µl	H_2O milliQ

NADP-dependent malic enzyme

To determine NADP-dependent malate dehydrogenase (NADP-ME, EC 1.1.1.40) activity 20 µl of aliquots of enzymatic extraction (buffer 1) were mixed with 280 µl of assay mix. Plates were incubated at 25 °C during 20 min in a 96-well microplate reader (Power wave x 340, BioTek Instruments) and NAD(P)H evolution was monitored at 340 nm. Activity was expressed in µmol NADPH g^{-1} FW h^{-1}

Assay mix:

28	µl	1 M Tris-HCl, pH 7
2.8	µl	1 M $MgCl_2$
28	µl	5 mM NADP
5.6	µl	0.5 M Malate
215	µl	H_2O milliQ

NADP-dependent isocitrate dehydrogenase

In chapter 1, to determine NADP-dependent isocitrate dehydrogenase (NADP-ICDH, EC 1.1.1.42) activity 20 µl aliquots of enzymatic extraction (buffer 1) were mixed with 280 µl assay mix. Plates were incubated at 25 °C during 20 min in a 96-well microplate reader (Power wave x 340, BioTek Instruments) and NAD(P)H evolution was monitored at 340 nm. Activity was expressed in µmol NADPH g^{-1} FW h^{-1}

Assay mix:

28	µl	1 MTricine KOH pH 8
28	µl	1 M NADP
1.4	µl	1 M $MgCl_2$
28	µl	50 mM Isocitrate
194.6	µl	H_2O milliQ

In chapter 3, to determine NADP-dependent isocitrate dehydrogenase (EC 1.1.1.42) activity 5 µl of aliquots of enzymatic extraction (buffer 2) were mixed with 95 µl of assay mix. Plates were incubated at 25 °C during 20 min in a 96-well microplate reader (SAFAS MP96) and NADPH evolution was monitored at 340 nm. For blanks isocitrate was substituted by water. Activity was expressed in µmol NADPH g^{-1} FW h^{-1}

Assay mix:

20	µl	Assay buffer (0.5 M Tricine/KOH pH 8, 40 mM $MgCl_2$, 0.25 % Triton X-100)
50	µl	20 mM $NADP^+$
10	µl	20 mM Isocitrate (adjusted to pH 8.5 with NaOH)
15	µl	H_2O milliQ

Aspartate aminotransferase

To determine aspartate aminotransferase (AAT, EC 2.6.1.1) activity 20 µl of aliquots of enzymatic extraction (buffer 1) were mixed with 280 µl assay mix. Plates were incubated at 25 °C during 20 min in a 96-well microplate reader (Power wave x 340, BioTek Instruments) and NADH evolution was monitored at 340 nm. Activity was expressed in µmol NADH g^{-1} FW h^{-1}

Assay mix:

56	µl	0.25 M Mes-Bicine-MOPS (MBM) pH 8
1.4	µl	1 M $MgCl_2$
28	µl	100 mM Aspartic acid
6.46	µl	130 µM Pyridoxal phosphate
28	µl	3 mM NADH
0.25	µl	10 kU Malate dehydrogenase enzyme in $(NH_4)_2SO_4$
159.9	µl	H_2O milliQ

Pyruvate kinase

To determine pyruvate kinase (PK, EC 2.7.1.40) activity 5 µl of aliquots of enzymatic extraction (buffer 2) were mixed with 95 µl of assay mix. Plates were incubated at 25 °C during 20 min in a 96-well microplate reader (SAFAS MP96) and NADH evolution was monitored at 340 nm. For blanks phosphoenolpyruvate was substituted by water. Activity was expressed in µmol NADH g^{-1} FW h^{-1}

Assay mix:

20	µl	Assay buffer (0.5 M Tricine/KOH pH 8, 0.5 M KCl, 50 mM $MgCl_2$, 2 mM EDTA, 0.25 % Triton-X-100)
10	µl	50 mM Phosphoenolpyruvic acid trisodium salt hydrate
5	µl	20 mM ADP
0.79	µl	60 mM NADH in 60 mM NaOH
1	µl	60 U ml^{-1} Lactate dehydrogenase in 200 mM Hepes/KOH pH 7.5, 10 mM $MgCl_2$
58.16	µl	H_2O milliQ

Citrate synthase

To determine citrate synthase (CS, EC 2.3.3.1) total activity 5 µl of aliquots of enzymatic extraction (buffer 2) were mixed with 87 µl of assay mix. After incubating at 25 °C during 5 min, 4 µl of 2 mM DTNB (5, 5'-dithiobis(2-nitrobenzoic acid) in 99 % ethanol and 4 µl of 10 mM acetyl-CoA were added. TNB (5-thionitrobenzoic acid) evolution was monitored at 418 nm in a 96-well microplate reader (SAFAS MP96). For blanks acetyl-CoA was substituted by water. Activity was expressed in µmol NADH g^{-1} FW h^{-1}

Assay mix:

2	µl	500 mM Tricine/KOH, pH 8
4	µl	5 mM Oxalacetate (fresh prepeared)
63	µl	H_2O milliQ

To determine citrate synthase mitochondrial activity (CSm) 5 µl of aliquots of enzymatic extraction (buffer 2) were mixed with 87 µl of assay mix. After incubating at 25 °C during 5 min, 4 µl of 2 mM DTNB (5, 5'-dithiobis (2-nitrobenzoic acid) in 99 % ethanol and 4 µl of 5 mM oxaloacetate were added. TNB evolution was monitored at 418 nm in a 96-well microplate reader (SAFAS MP96). For blanks acetyl-CoA was substituted by water. Activity was expressed in µmol NADH g^{-1} FW h^{-1}

Assay mix:

20	µl	500 mM Tricine/KOH, pH 8
4	µl	2 mM DTNB
63	µl	H_2O milliQ

Hexokinases

To determine fructokinase (FK, EC 2.7.1.3) and glucokinase (GK, EC 2.7.1.1) activities, 2 µl aliquots of enzymatic extraction (buffer 2) or standard (0, 20, 50, 100 µM glucose-6-phosphate or frutose-6-phosphate) were mixed with 18 µl of assay mix.

Assay mix:

4	µl	Assay buffer (0.5 M Tricine/KOH pH 8, 25 mM $MgCl_2$, 0.25 % Triton X 100)
0.4	µl	100 mM ATP
0.5	µl	20 mM $NADP^+$
0.4	µl	50 U ml^{-1} Glucose-6-phosphate dehydrogenase (G6PDH grade II) in 200 mM Tricine/KOH pH 8, 10 mM $MgCl_2$
0.2	µl	1 U ml^{-1} phosphoglucoisomerase (fructokinase assay)
0.2	µl	2 mM glucose (glucokinase) or fructose (fructokinase)
12.3	µl	H_2O milliQ

After incubating at 25 °C for 20 min, the reaction was stopped with 20 µl of 0.5 M NaOH, incubated 95 ºC for 5 min. Then, 20 µl of 0.5 M HCl in 100 mM Tricine/KOH pH 9 was added. After being mixed, 45 µl of determination mix and 5 µl of 4 mM PES (Phenazine ethosulfate) were added and reduced MTT (3-(4,5-dimethylthiazol-2-yl)-2,5-diphenyltetrazolium bromide) evolution were monitored at 570 nm. For blanks ATP was substituted by water (Gibon *et al.,* 2004). Activity was expressed in µmol NADPH g^{-1} FW h^{-1}

Determination mix

10	µl	Tricine/KOH, pH 9
10	µl	2 mM MTT (3-(4,5-dimethylthiazol-2-yl)-2,5-diphenyltetrazolium bromide)
4	µl	200 mM EDTA
2	µl	205 mM G6P
0.5	µl	5 U ml^{-1} glucose-6-phosphate-dehydrogenase (G6PDH grade I)
18.5	µl	H_2O milliQ

RNA extraction and gene expression analysis

RNA extraction was carried out from 25 mg of frozen FW leaf or root powder with the Nucleospin RNA plant kit (Macherey-Nagel) that includes DNAse treatment. One µg of RNA was retrotranscribed into cDNA (PrimeScriptTM RT; Takara Bio Inc.) and gene expression was determined from 2 µL of cDNA diluted 1:10 in a 15 µL reaction volume using SYBR Premix ExTaqTM (Takara Bio Inc.) in a Step One Plus Real Time PCR System (Applied Biosystems). The PCR program was 95 °C for 5 min followed by 40 cycles of 94 °C for 15 s and 60 °C for 1 min and a melting curve (40–95 °C with one fluorescence read every 0.3 °C). ACT3 and SamDC were used as housekeeping genes to normalize gene expression. Absence of genomic DNA contamination was checked in all RNA samples. Primers used and their efficiency, calculated with serial cDNA dilution, are described as following (Table 4.1, also included in supplementary information, Table S1.1).

Table 4.1. *Brachypodium distachyon* Bd21 genes encoding for GLN, AS and GDH enzymes. The primers used for qPCR expression together with their efficiencies (E) are shown. *BdSamDC* and *BdACT3* are the genes that served as reference for relative gene expression quantification.

Name	Locus name	Gene symbol	Forward	Reverse	E
BdGLN1;1	Bradi3g59970	LOC100845598	aagctgcccaagtggaactacg	tccttgaagatagcctgtgggtag	1.76
BdGLN1;2	Bradi1g69530	LOC100824429	tcgtcgagtacttgtgggttgg	ccattcacggtccttgctttgc	1.80
BdGLN1;3	Bradi1g11450	LOC100837122	caagccatcttcagggatccattc	tgcatagcagtcacacataaccag	1.92
BdGLN2	Bradi5g24550	LOC100842712	tcgcttcacaagtgccatggtatg	agaggccagttcacatctctctgg	1.76
BdASN1	Bradi1g65540	LOC100830770	tgccgaagcatatcctctac	tttcatcatctcatcggtgac	1.93
BdASN2	Bradi2g21050	LOC100830419	tctcttgtctggtggacttg	tcaggagaacccttcaaacc	2.02
BdASN3	Bradi4g45010	LOC100839462	cagtgttcaggatggcattg	gcgacttgatcttgcgtgac	2.05
BdGDH1	Bradi1g05680	LOC100831066	agtttcatggttactcgcctgctg	tcccagagatcctccaaggtcaac	1.89
BdGDH2	Bradi5g17330	LOC100828452	acatgggaactaatgcacagacc	agtggcagcatccctacctaatg	1.91
BdNADP-GDH	Bradi2g41130	LOC100833076	cgatgccgatctacgtcaaagc	tgaaccacctcctggatagactg	1.95
BdSamDC	Bradi5g14640	LOC100821874	tgctaatctgctccaatggc	gacgcagctgaccacctaga	2.04
BdACT3	Bradi4g41850	LOC100834364	cctgaagtccttttccagcc	agggcagtgatctccttgct	2.05

Phylogenetic analysis

Phylogenetic analysis for GS, GDH and AS genes was done using the programs included in the Phylogeny.fr tool (Dereeper *et al.,* 2008) as follows. Coding Sequences (CDs) multiple alignments were conducted with the Muscle algorithm and refined using G blocks. Phylogeny analysis was done using the bootstrapping procedure with the PhyML software. Finally, TreeDyn was used to visualize the tree.

Proteomics

The proteomic analysis was performed in the Proteomics Core Facility-SGIKER (member of ProteoRed-ISCIII) at the University of the Basque Country.

Protein extraction and digestion

Around 10 mg of dried root powdered material was resuspended in 0.4 ml 8 M urea, homogenized through vortex and disrupted by sonication. After centrifuged at 13,000 rpm, the supernatant was collected. Protein integrity was checked by SDS-PAGE. Then, 100 µl were precipitated with 2D CleanUp (GE Healthcare) according to the manufacturer's instructions, re-suspended in RapiGest 0.2 % (Waters) and protein concentration determined by Bradford (BCA assay; Thermo Fisher Scientific). Aliquots of each samples containing 75 µg of protein were heated (85 °C, 15 min), reduced with DTT (5 mM), alkylated with iodoacetamide (15 mM) and digested with trypsin (1.5 mg) overnight at 37 ° (Roche Diagnostics). RapiGest was inactivated twice by the addition of HCl at a final concentration of 0.5 % and incubation at 37 °C for 40 min. Samples were centrifuged at 16,000 *g* for 10 min, the supernatant was collected and 25 µg were desalted using C-18 Micro SpinColums (Harvard Apparatus). Finally, samples were dried down in a SpeedVac centrifuge (ThermoFisher Scientific).

Quantification of peptides by LC-MC/MS

Mass spectrometric analyses were performed on an EASY-nLC 1200 liquid chromatography system interfaced with a Q Exactive HF-X mass spectrometer (ThermoFisher Scientific) via a nanospray flex ion source. Dried peptides were dissolved in 0.1% formic acid and loaded onto an Acclaim PepMap100 pre-column (75 µm × 2 cm, ThermoFisher Scientific) connected to an Acclaim PepMap RSLC C18 (75 µm × 25 cm, ThermoFisher Scientific) analytical column. Peptides were eluted by a 150 min linear gradient from 2 % to 30 % acetonitrile in 0.1 % formic acid at a flow rate of 300 nl min^{-1}. The mass spectrometer was operated in positive ion mode. Full MS scans were acquired from m/z 375 to 1800 with a resolution of 60,000 at m/z 200. The 15 most intense ions were fragmented by higher energy C-trap dissociation with normalized collision energy of 28 and MS/MS spectra were recorded with a resolution of 15,000 at m/z 200. The maximum ion injection time was 60 ms for survey and MS/MS, whereas AGC target values were 3×10^6 and 5×10^5 respectively. In order to avoid repeat sequencing of peptides, dynamic exclusion was applied for 20 s. singly charged ions or ions with unassigned charge state were

also excluded from MS/MS. Data were acquired using Xcalibur software (ThermoFisher Scientific).

Proteomics data analysis

Acquired raw data files were processed with the MaxQuant (Cox and Mann, 2008) software (version 1.6.0.16) using the internal search engine Andromeda (Cox *et al*., 2011) and searched against the UniProt database restricted to *Brachypodium_distachyon* entries (release 2017_08). Carbamidomethylation (C) was set as fixed modification whereas Met oxidation and protein N-terminal acetylation were defined as variable modifications. Mass tolerance was set to 8 and 20 ppm at the MS and MS/MS level, respectively. Enzyme specificity was set to tryñ̃psin, allowing for a maximum of three missed cleavages. Match between runs option was enabled with 1.5 min match time window and 20 min alignment window to match identification across samples. The false discovery rate for peptides and proteins was set to 1 %. Normalized spectral protein label-free quantification (LFQ) intensities were calculated using the MaxLFQ algorithm.

MaxQuant output data was analysed with the Perseus module (version 1.6.0.7) (Tyanova *et al*., 2016). Proteins identified by site (identification based only on a modified peptide), reserve proteins (identified by a decoy database) and potential contaminants were filtered out. Proteins with 3 LFQ values in at least one group were used for quantification and missing LFQ intensity values were replaced with values from a normal distribution (width 0.3 and down shift 1.8), meant to simulate expression below the detection limit (Tyanova *et al*., 2016). Perseus program was used for comparison of media for the different treatments by running a *t*-student analysis. Significant and differential data were selected by a *p*-value lower than 0.05, and a fold change of < 0.67 (down accumulation) and >1.5 (up-accumulation) in linear scale. Functional classification of proteins identified was carried with Protein Analysis through Evolutionary Relationships (PANTHER v14.1 http://www.pantherdb.org), which is in compliance with gene ontology (GO) standards.

Genome wide association analysis

The SNP data set from 51 inbred sequenced lines was analyzed with the GWAS tool GAPIT (Genome Association and Prediction Integrated Tool-R package) (Lipka *et al*., 2012) for all measured phenotypes in each condition (ammonium or nitrate).The principal component (PC) matrix was generated automatically by setting GAPIT parameters PCA.total to 3 since three groups were observed in the VanRaden plot (Figure S4.1). These three match with those described by Gordon *et al.* (2017). The PC analysis and the kinship matrix were calculated from a SNP.fraction = 0.05. We used four models for GWAS analysis: 1) GLM, 2) MLM, 3) MLMM and

4) FarmCPU. A Bonferroni-corrected threshold probability based on individual tests was calculated to correct for multiple comparisons, using 0.05/N, where N is the number of individual trait-SNP combinations tested. Because SNPs with low MAF (Minor Allelic Frequency) can often result in false positive associations, SNPs were removed from the analysis if their minor allele frequency was less than 10 % across the panel. In total, 2 653 103 SNPs were distributed across the five chromosomes of *B. distachyon*. Wilson *et al.,* (2018) reported that the mean LD of 107 accessions including the panel of our study decays across all chromosomes ~113 kb. To limit false positives, we defined 20 kb up and downstream to find the genes associated in the reference genome Bd21 using JGI_Phytozome database 12 (https://phytozome.jgi.doe.gov/) and NCBI database (https://www.ncbi.nlm.nih.gov/)

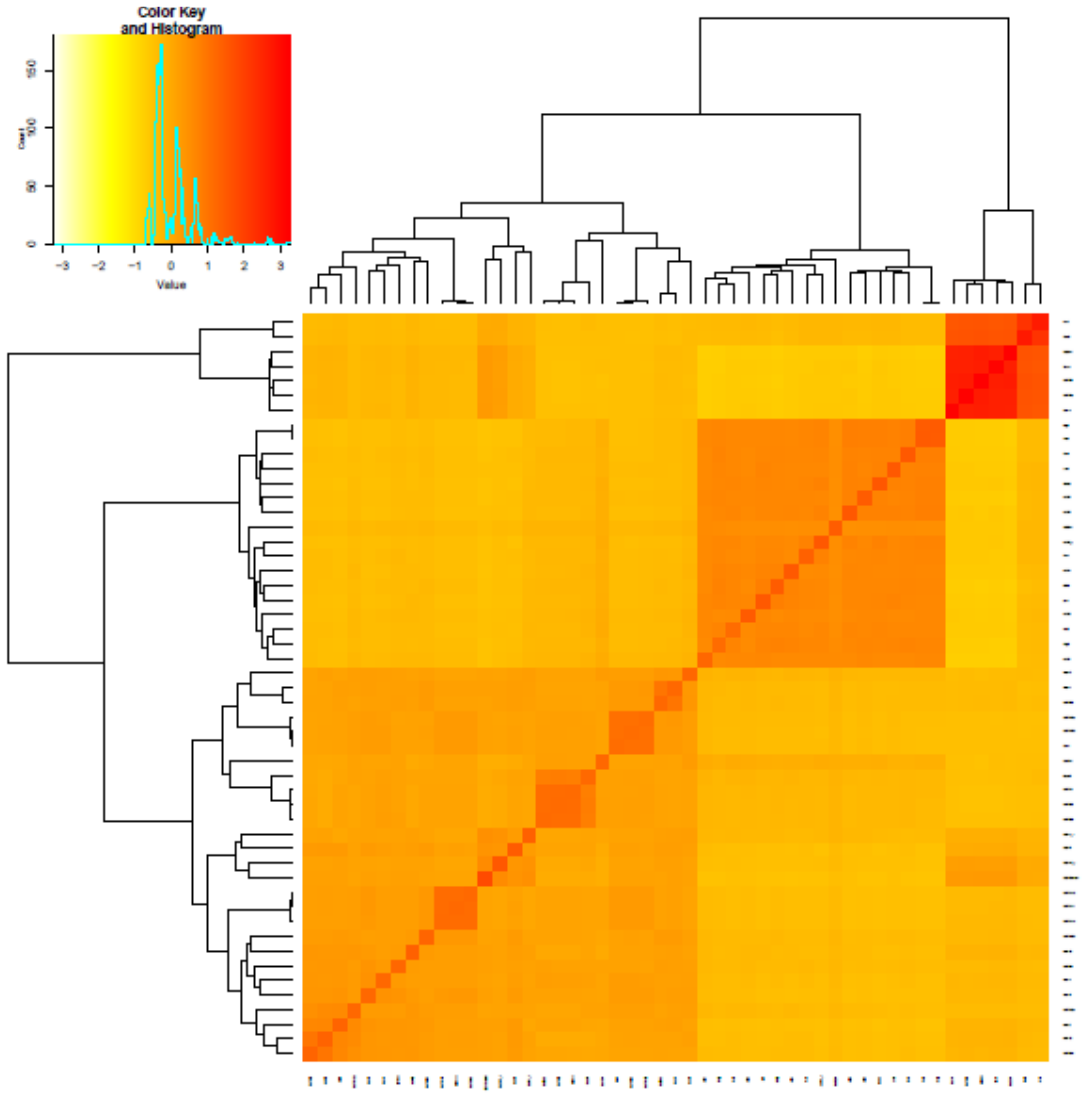

Figure 4.4 Kinship relationships among samples according to VanRaden method (VanRaden, 2008). Three main groups are generated.

BIBLIOGRAPHY

REFERENCES

Adu-Gyamfi, J. J., Ito, O., Yoneyama, T., Devi, G., and Katayama, K. (1997). Timing of N fertilization on N_2 fixation, N recovery and soil profile nitrate dynamics on sorghum/pigeonpea intercrops on Alfisols on the semi-arid tropics. *Nutrient Cycling in Agroecosystems*, *48*(3), 197-208.

Al-Kanani, T., MacKenzie, A. F., and Barthakur, N. N. (1991). Soil water and ammonia volatilization relationships with surface-applied nitrogen fertilizer solutions. *Soil Science Society of America Journal*, *55*(6), 1761-1766.

Alloush, G. A., Le Bot, J., Sanders, F. E., and Kirkby, E. A. (1990). Mineral nutrition of chickpea plants supplied with NO_3 or NH_4N: I. Ionic balance in relation to iron stress. *Journal of plant nutrition*, *13*(12), 1575-1590.

Angelovici, R., Lipka, A. E., Deason, N., Gonzalez-Jorge, S., Lin, H., Cepela, J., Buell, R., and DellaPenna, D. (2013). Genome-wide analysis of branched-chain amino acid levels in Arabidopsis seeds. *The Plant Cell*, *25*(12), 4827-4843.

Arias-Baldrich, C., de la Osa, C., Bosch, N., Ruiz-Ballesta, I., Monreal, J. A., andGarcía-Mauriño, S. (2017). Enzymatic activity, gene expression and posttranslational modifications of photosynthetic and non-photosynthetic phosphoenolpyruvate carboxylase in ammonium-stressed sorghum plants. *Journal of plant physiology*, *214*, 39-47.

Ariz, I., Artola, E., Asensio, A. C., Cruchaga, S., Aparicio-Tejo, P. M., and Moran, J. F. (2011). High irradiance increases NH_4^+ tolerance in *Pisum sativum*: higher carbon and energy availability improve ion balance but not N assimilation. *Journal of plant physiology*, *168*(10), 1009-1015.

Ariz, I., Asensio, A. C., Zamarreño, A. M., García-Mina, J. M., Aparicio-Tejo, P. M., and Moran, J. F. (2013). Changes in the C/N balance caused by increasing external ammonium concentrations are driven by carbon and energy availabilities during ammonium nutrition in pea plants: the key roles of asparagine synthetase and anaplerotic enzymes. *Physiologia Plantarum*, *148*(4), 522-537.

Arnon, D. I. (1949). Copper enzymes in isolated chloroplasts. Polyphenoloxidase in *Beta vulgaris*. *Plant physiology*, *24*(1), 1.

Arrivault, S., Senger, T., and Krämer, U. (2006). The *Arabidopsis* metal tolerance protein AtMTP3 maintains metal homeostasis by mediating Zn exclusion from the shoot under Fe deficiency and Zn oversupply. *The Plant Journal*, *46*(5), 861-879.

Atwell, S., Huang, Y. S., Vilhjálmsson, B. J., Willems, G., Horton, M., Li, Y., Meng, D., Platt, A., Tarone, A. M., Hu, T. T., Jiang, R., Muliyati, N. W., Zhang, X., Amer, M. A., Baxter, I., Brachi, B., Chory, J., Dean, C., Debieu, M., de Meaux, J., Ecker, J. R., Faure, N., Kniskern, J. M., Jones, J. D. G., Michael, T., Nemri, A., Roux, F., Salt, D. E., Tang C, Todesco M, Traw M.B., Weigel D, Marjoram P, Borevitz J.O., Bergelson J, and Nordborg M (2010) Genome-wide association study of 107 phenotypes in *Arabidopsis thaliana* inbred lines. *Nature*, *465*, 627-631.

Balkos, K. D., Britto, D. T., andKronzucker, H. J. (2010). Optimization of ammonium acquisition and metabolism by potassium in rice (*Oryza sativa* L. cv. IR-72). *Plant, Cell and Environment*, *33*(1), 23-34.

Bantan-Polak, T., Kassai, M., and Grant, K. B. (2001). A comparison of fluorescamine and naphthalene-2, 3-dicarboxaldehyde fluorogenic reagents for microplate-based detection of amino acids. *Analytical biochemistry*, *297*(2), 128-136.

Barhoumi, Z. (2017). Insights into the growth response and nitrogen accumulation and use efficiency of the Poaceae grass *Brachypodium distachyon* to high nitrogen availability. *Russian journal of plant physiology*, *64*(6), 839-844.

Becker, M., and Asch, F. (2005). Iron toxicity in rice—conditions and management concepts. *Journal of Plant Nutrition and Soil Science*, *168*(4), 558-573.

Belastegui-Macadam, X. M., Estavillo, J. M., García-Mina, J. M., González, A., Bastias, E., andGónzalez-Murua, C. (2007). Clover and ryegrass are tolerant species to ammonium nutrition. *Journal of plant physiology*, *164*(12), 1583-1594.

Bénard, C., and Gibon, Y. (2016). Measurement of Enzyme Activities and Optimization of Continuous and Discontinuous Assays. *Current protocols in plant biology*, *1*(2), 247-262.

Bernhard, A. (2010). The Nitrogen Cycle: Processes, Players, and Human Impact. Nature Education Knowledge, 3(10):25

Bittsánszky, A., Pilinszky, K., Gyulai, G., and Komives, T. (2015). Overcoming ammonium toxicity. *Plant Science*, *231*, 184-190.

Bloom, A. J., Burger, M., Asensio, J. S. R., and Cousins, A. B. (2010). Carbon dioxide enrichment inhibits nitrate assimilation in wheat and *Arabidopsis*. *Science*, *328*(5980), 899-903.

Bouain, N., Krouk, G., Lacombe, B., and Rouached, H. (2019). Getting to the root of plant mineral nutrition: combinatorial nutrient stresses reveal emergent properties. *Trends in plant science*.

Bouvierd'Yvoire, M., Bouchabke-Coussa, O., Voorend, W., Antelme, S., Cézard, L., Legée, F., Lebris, P., Legay, S., Whitehead, C., McQueen-Mason, S. J., Gomez, L. D., Jouanin, L., Lapierre, C., and Sibout, R. (2013). Disrupting the cinnamyl alcohol dehydrogenase 1 gene (Bd CAD 1) leads to altered lignification and improved saccharification in *Brachypodiumdistachyon*. *The Plant Journal*, *73*(3), 496-508.

Boyle, E. A., Li, Y. I., and Pritchard, J. K. (2017). An expanded view of complex traits: from polygenic to omnigenic. *Cell*, *169*(7), 1177-1186.

Bowles, T. M., Atallah, S. S., Campbell, E. E., Gaudin, A. C., Wieder, W. R., andGrandy, A. S. (2018). Addressing agricultural nitrogen losses in a changing climate. *Nature Sustainability*, *1*(8), 399-408.

Brachi, B., Morris, G. P., and Borevitz, J. O. (2011). Genome-wide association studies in plants: the missing heritability is in the field. *Genome biology*, *12*(10), 232.

Bradford, M. M. (1976). A rapid and sensitive method for the quantitation of microgram quantities of protein utilizing the principle of protein-dye binding. Analytical biochemistry, 72(1-2), 248-254.

Briat, J. F., Duc, C., Ravet, K., and Gaymard, F. (2010). Ferritins and iron storage in plants. *Biochimicaet Biophysica Acta (BBA)-General Subjects*, *1800*(8), 806-814.

Briat, J. F., Dubos, C., and Gaymard, F. (2015). Iron nutrition, biomass production, and plant product quality. *Trends in Plant Science*, *20*(1), 33-40.

Britto, D. T., Siddiqi, M. Y., Glass, A. D., and Kronzucker, H. J. (2001). Futile transmembrane NH_4^+ cycling: a cellular hypothesis to explain ammonium toxicity in plants. *Proceedings of the National Academy of Sciences*, *98*(7), 4255-4258.

Britto, D. T., and Kronzucker, H. J. (2002). NH_4^+ toxicity in higher plants: a critical review. *Journal of Plant Physiology*, *159*(6), 567-584.

Britto, D. T., and Kronzucker, H. J. (2013). Ecological significance and complexity of N-source preference in plants. *Annals of botany*, *112*(6), 957-963.

Brutnell, T. P., Bennetzen, J. L., and Vogel, J. P. (2015). *Brachypodium distachyon* and *Setariaviridis*: model genetic systems for the grasses. *Annual review of plant biology*, *66*, 465-485.

Bulgakov, V. P., Inyushkina, Y. V., and Fedoreyev, S. A. (2012). Rosmarinic acid and its derivatives: biotechnology and applications. *Critical reviews in biotechnology*, *32*(3), 203-217.

Burghardt, L. T., Young, N. D., and Tiffin, P. (2017). A guide to genome-wide association mapping in plants. *Current Protocols in Plant Biology*, *2*(1), 22-38.

Cameron, K. C., Di, H. J., and Moir, J. L. (2013). Nitrogen losses from the soil/plant system: a review. *Annals of Applied Biology*, *162*(2), 145-173.

Cassman, K. G., Dobermann, A., and Walters, D. T. (2002). Agroecosystems, nitrogen-use efficiency, and nitrogen management. *AMBIO: A Journal of the Human Environment*, *31*(2), 132-141.

Cao, P., Lu, C. C., and Yu, Z. (2018). Historical nitrogen fertilizer use in agricultural ecosystems of the contiguous United States during 1850–2015: application rate, timing, and fertilizer types. *Earth System Science Data Discussion*, *10*, 969.

Chaillou, S., and Lamaze, T. (2001). Ammoniacal nutrition of plants. *Nitrogen assimilation by plants. Ed. JF Morot-Gaudry*, 53-69.

Chao, D. Y., Silva, A., Baxter, I., Huang, Y. S., Nordborg, M., Danku, J., Lahner, B., Yakubova, E., and Salt, D. E. (2012). Genome-wide association studies identify heavy metal ATPase3 as the primary determinant of natural variation in leaf cadmium in *Arabidopsis thaliana*. *PLoS genetics*, *8*(9), e1002923.

Chen, G., Guo, S., Kronzucker, H. J., and Shi, W. (2013). Nitrogen use efficiency (NUE) in rice links to NH_4^+ toxicity and futile NH_4^+ cycling in roots. *Plant and Soil*, *369*(1-2), 351-363.

Chislock, M. F., Doster, E., Zitomer, R. A., and Wilson, A. E. (2013). Eutrophication: causes, consequences, and controls in aquatic ecosystems. *Nature Education Knowledge*, *4*(4), 10.

Coleto, I., Vega-Mas, I., Glauser, G., González-Moro, M. B., Marino, D., and Ariz, I. (2019). New Insights on *Arabidopsis thaliana* root adaption to ammonium nutrition by the use of a quantitative proteomic approach. *International journal of molecular sciences*, *20*(4), 814.

Coskun, D., Britto, D. T., and Kronzucker, H. J. (2017a). The nitrogen–potassium intersection: membranes, metabolism, and mechanism. *Plant, cell and environment*, *40*(10), 2029-2041.

Coskun, D., Britto, D. T., Shi, W., and Kronzucker, H. J. (2017b). Nitrogen transformations in modern agriculture and the role of biological nitrification inhibition. *Nature Plants*, *3*(6), 17074.

Couturier, J., Touraine, B., Briat, J. F., Gaymard, F., and Rouhier, N. (2013). The iron-sulfur cluster assembly machineries in plants: current knowledge and open questions. *Frontiers in plant science*, *4*, 259.

Cox, J., Neuhauser, N., Michalski, A., Scheltema, R. A., Olsen, J. V., and Mann, M. (2011). Andromeda: a peptide search engine integrated into the MaxQuant environment. *Journal of proteome research*, *10*(4), 1794-1805.

Cox, J., and Mann, M. (2008). MaxQuant enables high peptide identification rates, individualized ppb-range mass accuracies and proteome-wide protein quantification. *Nature biotechnology*, *26*(12), 1367.

Crawford, N. M., and Glass, A. D. (1998). Molecular and physiological aspects of nitrate uptake in plants. *Trends in plant science*, *3*(10), 389-395.

Cruz, C., Bio, A. F. M., Domínguez-Valdivia, M. D., Aparicio-Tejo, P. M., Lamsfus, C., and Martins-Louçao, M. A. (2006). How does glutamine synthetase activity determine plant tolerance to ammonium?. *Planta*, *223*(5), 1068-1080.

Cruz, C., Domínguez-Valdivia, M. D., Aparicio-Tejo, P. M., Lamsfus, C., Bio, A., Martins-Loução, M. A., and Moran, J. F. (2011). Intra-specific variation in pea responses to ammonium nutrition leads to different degrees of tolerance. *Environmental and Experimental Botany*, *70*(2-3), 233-243.

Cui, Y. N., Li, X. T., Yuan, J. Z., Wang, F. Z., Wang, S. M., and Ma, Q. (2019). Nitrate transporter NPF7. 3/NRT1. 5 plays an essential role in regulating phosphate deficiency responses in Arabidopsis. *Biochemical and biophysical research communications*, *508*(1), 314-319.

Dalmais, M., Antelme, S., Ho-Yue-Kuang, S., Wang, Y., Darracq, O., d'Yvoire, M. B., Cézard, L., Légée, F., Blondet, E., Oria, N., Troadec, C., Brunaud, V., Jouanin, L., Höfte, H., Bendahmane, A., Lapierre, C., and Sibout, R. (2013). A TILLING platform for functional genomics in *Brachypodium distachyon*. *PLoS One*, *8*(6), e65503.

David, L. C., Girin, T., Fleurisson, E., Phommabouth, E., Mahfoudhi, A., Citerne, S., Berquin, P., Daniel-Vedele, F., Krapp, A., and Ferrario-Méry, S. (2019). Developmental and physiological responses of Brachypodiumdistachyon to fluctuating nitrogen availability. *Scientific reports*, *9*(1), 3824.

De la Peña, M., González-Moro, M. B., and Marino, D. (2019). Providing carbon skeletons to sustain amide synthesis in roots underlines the suitability of *Brachypodium distachyon* for the study of ammonium stress in cereals. *AoB Plants*, *11*(3), plz029.

Dell'Acqua, M., Zuccolo, A., Tuna, M., Gianfranceschi, L., and Pè, M. E. (2014). Targeting environmental adaptation in the monocot model *Brachypodium distachyon*: a multi-faceted approach. *BMC genomics*, *15*(1), 801.

Dereeper, A., Guignon, V., Blanc, G., Audic, S., Buffet, S., Chevenet, F., Dufayard, J. –F., Guindon, S., Lefort, V., Lescot, M., Claverie, J. M., and Gascuel, O. (2008). Phylogeny. fr: robust phylogenetic analysis for the non-specialist. Nucleic acids research, 36(suppl_2), W465-W469.

Di, D. W., Sun, L., Zhang, X., Li, G., Kronzucker, H. J., and Shi, W. (2018). Involvement of auxin in the regulation of ammonium tolerance in rice (*Oryza sativa* L.). *Plant and soil*, *432*(1-2), 373-387.

Divte, P., Yadav, P., kumar Jain, P., Paul, S., and Singh, B. (2019). Ethylene regulation of root growth and phytosiderophore biosynthesis determines iron deficiency tolerance in wheat (*Triticum spp*). *Environmental and Experimental Botany*, *162*, 1-13.

Dodds, W. K., Bouska, W. W., Eitzmann, J. L., Pilger, T. J., Pitts, K. L., Riley, A. J., Schloesser, J. T., and Thornbrugh, D. J. (2008). Eutrophication of US freshwaters: analysis of potential economic damages.

Domínguez-Valdivia, M. D., Aparicio-Tejo, P. M., Lamsfus, C., Cruz, C., Martins-Loução, M. A., and Moran, J. F. (2008). Nitrogen nutrition and antioxidant metabolism in ammonium-tolerant and-sensitive plants. *Physiologia Plantarum*, *132*(3), 359-369.

Doubnerová, V., and Ryšlavá, H. (2011). What can enzymes of C4 photosynthesis do for C3 plants under stress?. *Plant Science*, *180*(4), 575-583.

Dubois, F., Tercé-Laforgue, T., Gonzalez-Moro, M. B., Estavillo, J. M., Sangwan, R., Gallais, A., and Hirel, B. (2003). Glutamate dehydrogenase in plants: is there a new story for an old enzyme?. *Plant Physiology and Biochemistry*, *41*(6-7), 565-576.

Esteban, R., Ariz, I., Cruz, C., and Moran, J. F. (2016). Mechanisms of ammonium toxicity and the quest for tolerance. Plant Science, 248, 92-101.

Ferraro, G., D'Angelo, M., Sulpice, R., Stitt, M., and Valle, E. M. (2015). Reduced levels of NADH-dependent glutamate dehydrogenase decrease the glutamate content of ripe tomato fruit but have no effect on green fruit or leaves. *Journal of experimental botany*, *66*(11), 3381-3389.

Fewtrell, L. (2004). Drinking-water nitrate, methemoglobinemia, and global burden of disease: a discussion. *Environmental health perspectives*, *112*(14), 1371-1374.

Fontaine, J. X., Tercé-Laforgue, T., Armengaud, P., Clément, G., Renou, J. P., Pelletier, S., Catterou, M., Azzopardi, M., Gibon, Y., Lea, P. J., Hirel, B., and Dubois, F. (2012). Characterization of a NADH-dependent glutamate dehydrogenase mutant of *Arabidopsis* demonstrates the key role of this enzyme in root carbon and nitrogen metabolism. *The Plant Cell*, *24*(10), 4044-4065.

Fulgenzi, F. R., Peralta, M. L., Mangano, S., Danna, C. H., Vallejo, A. J., Puigdomenech, P., and Santa-María, G. E. (2008). The ionic environment controls the contribution of the barley HvHAK1 transporter to potassium acquisition. *Plant physiology*, *147*(1), 252-262.

Fusari, C. M., Kooke, R., Lauxmann, M. A., Annunziata, M. G., Enke, B., Hoehne, M., Krohn, N., Becker, F. F. M., Schlereth, A., Sulpice, R., Stitt, M., and Keurentjes, J. J. B. (2017). Genome-wide association mapping reveals that specific and pleiotropic regulatory mechanisms fine-tune central metabolism and growth in Arabidopsis. *The Plant Cell*, *29*(10), 2349-2373.

Gahoonia, T.S., Claassen, N., and Jungk, A. 1992. Mobilization of phosphate in different soils by ryegrass supplied with ammonium or nitrate. *Plant Soil* 140, 241-248.

Gao, Y., Li, Y., Yang, X., Li, H., Shen, Q., and Guo, S. (2010). Ammonium nutrition increases water absorption in rice seedlings (*Oryza sativa* L.) under water stress. *Plant and Soil*, *331*(1-2), 193-201.

Gapper, C., and Dolan, L. (2006). Control of plant development by reactive oxygen species. *Plant physiology*, *141*(2), 341-345.

Garnett, T., Plett, D., Heuer, S., and Okamoto, M. (2015). Genetic approaches to enhancing nitrogen-use efficiency (NUE) in cereals: challenges and future directions. *Functional plant biology*, *42*(10), 921-941.

Gerendás, J., Zhu, Z., Bendixen, R., Ratcliffe, R. G., and Sattelmacher, B. (1997). Physiological and biochemical processes related to ammonium toxicity in higher plants. *ZeitschriftfürPflanzenernährung und Bodenkunde*, *160*(2), 239-251.

Gibon, Y., Blaesing, O. E., Hannemann, J., Carillo, P., Höhne, M., Hendriks, J. H., and Stitt, M. (2004). A robot-based platform to measure multiple enzyme activities in Arabidopsis using a set of cycling assays: comparison of changes of enzyme activities and transcript levels during diurnal cycles and in prolonged darkness. The Plant Cell, 16(12), 3304-3325.

Glass, A. D., Britto, D. T., Kaiser, B. N., Kinghorn, J. R., Kronzucker, H. J., Kumar, A., Okamoto, M., Rawat, S., Siddiqi, M. Y., Unkles, S. E., and Vidmar, J. J. (2002). The regulation of nitrate and ammonium transport systems in plants. *Journal of Experimental Botany*, *53*(370), 855-864.

Gondro, C., Van der Werf, J., and Hayes, B. J. (Eds.). (2013). *Genome-wide association studies and genomic prediction* (p. 566). New York, NY: Humana Press.

Goodall, A. J., Kumar, P., and Tobin, A. K. (2013). Identification and expression analyses of cytosolic glutamine synthetase genes in barley (*Hordeum vulgare* L.). *Plant and Cell Physiology*, *54*(4), 492-505.

Gordon, S. P., Contreras-Moreira, B., Woods, D. P., Des Marais, D. L., Burgess, D., Shu, S., Strirtt, C., Roulin, A. C., Schackwitz, W., Tyler, L., Marin, J., Lipzen, A., Dochy, N., Phillips, J., Barry, K., Geuten, K., Budak, H., Juenger, T. E., Amasino, R., Caicedo, A. L., Goodstein, D., Davidson, P., Mur, L. A. J., Figueroa, M., Freeling, M., Catalan, P., and Voger, J. P. (2017). Extensive gene content variation in the *Brachypodium distachyon* pan-genome correlates with population structure. *Nature communications*, *8*(1), 2184.

Gordon, A. J., and Kessler, W. (1990). Defoliation-Induced Stress in Nodules of White Clover: II. Immunological and enzymic measurements of key proteins. *Journal of Experimental Botany*, *41*(10), 1255-1262.

Griffith, O. W. (1980). Determination of glutathione and glutathione disulfide using glutathione reductase and 2-vinylpyridine. Analytical biochemistry, 106(1), 207-212.

Guan, M., de Bang, T. C., Pedersen, C., andSchjoerring, J. K. (2016). Cytosolic glutamine synthetase Gln1; 2 is the main isozyme contributing to GS1 activity and can be up-regulated to relieve ammonium toxicity. *Plant Physiology*, *171*(3), 1921-1933.

Hachiya, T., and Noguchi, K. (2011). Mutation of NRT1. 1 enhances ammonium/low pH-tolerance in *Arabiopsis thaliana*. *Plant signaling and behavior*, *6*(5), 706-708.

Han, M., Okamoto, M., Beatty, P. H., Rothstein, S. J., and Good, A. G. (2015). The genetics of nitrogen use efficiency in crop plants. *Annual Review of Genetics*, *49*, 269-289.

Handakumbura, P. P., and Hazen, S. P. (2012). Transcriptional regulation of grass secondary cell wall biosynthesis: playing catch-up with *Arabidopsis thaliana*. *Frontiers in plant science*, *3*, 74.

Hara, Y., Yokoyama, R., Osakabe, K., Toki, S., and Nishitani, K. (2014). Function of xyloglucan endotransglucosylase/hydrolases in rice. *Annals of botany*, *114*(6), 1309-1318.

Haydon, M. J., Kawachi, M., Wirtz, M., Hillmer, S., Hell, R., and Krämer, U. (2012). Vacuolar nicotianamine has critical and distinct roles under iron deficiency and for zinc sequestration in *Arabidopsis*. *The Plant Cell*, *24*(2), 724-737.

Hawkesford, M. J., and Griffiths, S. (2019). Exploiting genetic variation in nitrogen use efficiency for cereal crop improvement. *Current opinion in plant biology*, *49*, 35-42.

Hell, R., and Stephan, U. W. (2003). Iron uptake, trafficking and homeostasis in plants. *Planta*, *216*(4), 541-551.

Hendriks, J. H., Kolbe, A., Gibon, Y., Stitt, M., and Geigenberger, P. (2003). ADP-glucose pyrophosphorylase is activated by posttranslational redox-modification in response to light and to sugars in leaves of Arabidopsis and other plant species. *Plant Physiology*, *133*(2), 838-849.

Hessini, K., Hamed, K. B., Gandour, M., Mejri, M., Abdelly, C., and Cruz, C. (2013). Ammonium nutrition in the halophyte *Spartinaalterniflora* under salt stress: evidence for a priming effect of ammonium?. *Plant and soil*, *370*(1-2), 163-173.

Hindt, M. N., and Guerinot, M. L. (2012). Getting a sense for signals: regulation of the plant iron deficiency response. *Biochimicaet Biophysica Acta (BBA)-Molecular Cell Research*, *1823*(9), 1521-1530.

Hirschhorn, J. N., and Daly, M. J. (2005). Genome-wide association studies for common diseases and complex traits. *Nature reviews genetics*, *6*(2), 95.

Hsia, M. M., O'malley, R., Cartwright, A., Nieu, R., Gordon, S. P., Kelly, S., Williams, T. G., Wood, D. F., Zhao, Y., Bragg, J., Jordan, M., Pauly, M., Ecker, J. R., Gu, Y., and Vogel, J. P. (2017). Sequencing and functional validation of the JGI *Brachypodium distachyon* T-DNA collection. *The Plant Journal*, *91*(3), 361-370.

Huérfano, X., Fuertes-Mendizábal, T., Duñabeitia, M. K., González-Murua, C., Estavillo, J. M., and Menéndez, S. (2015). Splitting the application of 3, 4-dimethylpyrazole phosphate (DMPP): Influence on greenhouse gases emissions and wheat yield and quality under humid Mediterranean conditions. *European Journal of Agronomy*, *64*, 47-57.

Ingram, P. A., Zhu, J., Shariff, A., Davis, I. W., Benfey, P. N., and Elich, T. (2012). High-throughput imaging and analysis of root system architecture in *Brachypodium distachyon* under differential nutrient availability. *Philosophical Transactions of the Royal Society B: Biological Sciences*, *367*(1595), 1559-1569.

Irani, S., and Todd, C. D. (2016). Ureide metabolism under abiotic stress in *Arabidopsis thaliana*. *Journal of plant physiology*, *199*, 87-95.

Jaiswal, V., Gahlaut, V., Meher, P. K., Mir, R. R., Jaiswal, J. P., Rao, A. R., Balyan, H. S., and Gupta, P. K. (2016). Genome wide single locus single trait, multi-locus and multi-trait association mapping for some important agronomic traits in common wheat (*T. aestivum* L.). *PloS one*, *11*(7), e0159343.

Jelitto, T., Sonnewald, U., Willmitzer, L., Hajirezeai, M., and Stitt, M. (1992). Inorganic pyrophosphate content and metabolites in potato and tobacco plants expressing *E. coli*pyrophosphatase in their cytosol. *Planta*, *188*(2), 238-244.

Jian, S., Liao, Q., Song, H., Liu, Q., Lepo, J. E., Guan, C., Zhang, J., Ismail, A. M. and Zhang, Z. (2018). NRT1. 1-related NH_4^+ toxicity is associated with a disturbed balance between NH_4^+ uptake and assimilation. *Plant physiology*, *178*(4), 1473-1488.

Jia, Z., Giehl, R. F., Meyer, R. C., Altmann, T., and von Wirén, N. (2019). Natural variation of BSK3 tunes brassinosteroid signaling to regulate root foraging under low nitrogen. *Nature communications*, *10*(1), 2378.

Kabir, A. H., Khatun, M. A., Hossain, M. M., Haider, S. A., Alam, M. F., and Paul, N. K. (2016). Regulation of phytosiderophore release and antioxidant defense in roots driven by shoot-based auxin signaling confers tolerance to excess iron in wheat. *Frontiers in plant science*, *7*, 1684.

Kanter, D. R., andSearchinger, T. D. (2018). A technology-forcing approach to reduce nitrogen pollution. *Nature Sustainability*, *1*(10), 544.

Kawai, S., Takagi, S. I., and Sato, Y. (1988). Mugineic acid-family phytosiderophores in root-secretions of barley, corn and sorghum varieties. *Journal of Plant Nutrition*, *11*(6-11), 633-642.

Kellogg, E. A. (2015). *Brachypodium distachyon* as a genetic model system. *Annual Review of Genetics*, *49*, 1-20.

Khosla, R., Alley, M. M., and Davis, P. H. (2000). Nitrogen management in no-tillage grain sorghum production: I. Rate and time of application. *Agronomy Journal*, *92*(2), 321-328.

Kobayashi, T., Suzuki, M., Inoue, H., Itai, R. N., Takahashi, M., Nakanishi, H., Takahashi, M., Nakanishi, H., Mori, S., and Nishizawa, N. K. (2005). Expression of iron-acquisition-related genes in iron-deficient rice is co-ordinately induced by partially conserved iron-deficiency-responsive elements. *Journal of Experimental Botany*, *56*(415), 1305-1316.

Kobayashi, T., Nozoye, T., and Nishizawa, N. K. (2019). Iron transport and its regulation in plants. *Free Radical Biology and Medicine*, *133*, 11-20.

Kosegarten, H., and Englisch, G. (1994). Effect of various nitrogen forms on the pH in leaf apoplast and on iron chlorosis of Glycine max L. *ZeitschriftfürPflanzenernährung und Bodenkunde*, *157*(6), 401-405.

Kosegarten, H., Schwed, U., Wilson, G., and Mengel, K. (1998). Comparative investigation on the susceptibility of faba bean (*Viciafaba* L.) and sunflower (*Helianthus annuus* L.) to iron chlorosis. *Journal of plant nutrition*, *21*(7), 1511-1528.

Kosegarten, H. U., Hoffmann, B., and Mengel, K. (1999). Apoplastic pH and Fe^{3+} reduction in intact sunflower leaves. *Plant Physiology*, *121*(4), 1069-1079.

Kumar, C., Igbaria, A., D'autreaux, B., Planson, A. G., Junot, C., Godat, E., Bachawat, A., Delaunay-Moisan, A., and Toledano, M. B. (2011). Glutathione revisited: a vital function in iron metabolism and ancillary role in thiol-redox control. *The EMBO journal*, *30*(10), 2044-2056.

Kusano, M., Tabuchi, M., Fukushima, A., Funayama, K., Diaz, C., Kobayashi, M., Hayashi, N., Tsuchiya, Y. N., Takahashi, H., Kamata, A., and Yamaya, T. (2011). Metabolomics data reveal a crucial role of cytosolic glutamine synthetase 1; 1 in coordinating metabolic balance in rice. *The Plant Journal*, *66*(3), 456-466.

Labboun, S., Tercé-Laforgue, T., Roscher, A., Bedu, M., Restivo, F. M., Velanis, C. N., Skopelitis, D. S., Moshou, P. N., Roubelakis-Angelakis, K. A., Suziki, A., and Hirel, B. (2009). Resolving the role of plant glutamate dehydrogenase. I. In vivo real time nuclear magnetic resonance spectroscopy experiments. *Plant and cell physiology*, *50*(10), 1761-1773.

Lasa, B., Frechilla, S., Lamsfus, C., andAparicio-Tejo, P. M. (2001). The sensitivity to ammonium nutrition is related to nitrogen accumulation. *Scientia Horticulturae*, *91*(1-2), 143-152.

Lasa, B., Frechilla, S., Aparicio-Tejo, P. M., and Lamsfus, C. (2002). Role of glutamate dehydrogenase and phosphoenolpyruvate carboxylase activity in ammonium nutrition tolerance in roots. *Plant Physiology and Biochemistry*, *40*(11), 969-976.

Lassaletta, L., Billen, G., Grizzetti, B., Anglade, J., and Garnier, J. (2014). 50 year trends in nitrogen use efficiency of world cropping systems: the relationship between yield and nitrogen input to cropland. *Environmental Research Letters*, *9*(10), 105011.

Lea, P. J., Sodek, L., Parry, M. A., Shewry, P. R., and Halford, N. G. (2007). Asparagine in plants. *Annals of Applied Biology*, *150*(1), 1-26.

Li, B., Li, Q., Xiong, L., Kronzucker, H. J., Krämer, U., and Shi, W. (2012). Arabidopsis plastid AMOS1/EGY1 integrates abscisic acid signaling to regulate global gene expression response to ammonium stress. *Plant Physiology*, *160*(4), 2040-2051.

Li, B., Li, G., Kronzucker, H. J., Baluška, F., and Shi, W. (2014). Ammonium stress in *Arabidopsis*: signaling, genetic loci, and physiological targets. *Trends in Plant Science*, *19*(2), 107-114.

Li, G., Dong, G., Li, B., Li, Q., Kronzucker, H. J., and Shi, W. (2012). Isolation and characterization of a novel ammonium overly sensitive mutant, amos2, in *Arabidopsis thaliana*. *Planta*, *235*(2), 239-252.

Li, W., and Lan, P. (2017). The understanding of the plant iron deficiency responses in Strategy I plants and the role of ethylene in this process by omic approaches. *Frontiers in plant science*, *8*, 40.

Lindsay, W. L., and Schwab, A. P. (1982). The chemistry of iron in soils and its availability to plants. *Journal of Plant Nutrition*, *5*(4-7), 821-840.

Liu, X., Huang, M., Fan, B., Buckler, E. S., and Zhang, Z. (2016). Iterative usage of fixed and random effect models for powerful and efficient genome-wide association studies. *PLoS genetics*, *12*(2), e1005767.

Liu, Y., and von Wirén, N. (2017). Ammonium as a signal for physiological and morphological responses in plants. *Journal of Experimental Botany*, *68*(10), 2581-2592.

Liu, Y., Sun, J., Tian, Z., Hakeem, A., Wang, F., Jiang, D., Cao, W., Adkins, S. W., and Dai, T. (2017). Physiological responses of wheat (*Triticumaestivum* L.) germination to elevated ammonium concentrations: reserve mobilization, sugar utilization, and antioxidant metabolism. *Plant growth regulation*, *81*(2), 209-220.

Loqué, D., Ludewig, U., Yuan, L., and von Wirén, N. (2005). Tonoplast intrinsic proteins AtTIP2; 1 and AtTIP2; 3 facilitate NH3 transport into the vacuole. *Plant physiology*, *137*(2), 671-680.

Loulakakis, K. A., and Roubelakis-Angelakis, K. A. (1991). Plant NAD (H)-glutamate dehydrogenase consists of two subunit polypeptides and their participation in the seven isoenzymes occurs in an ordered ratio. *Plant physiology*, *97*(1), 104-111.

Luo, J. (2015). Metabolite-based genome-wide association studies in plants. *Current Opinion in Plant Biology*, *24*, 31-38.

Ma, J. F., Shinada, T., Matsuda, C., and Nomoto, K. (1995). Biosynthesis of phytosiderophores, mugineic acids, associated with methionine cycling. *Journal of Biological Chemistry*, *270*(28), 16549-16554.

Magalhäes, J. R., and Huber, D. M. (1989). Ammonium assimilation in different plant species as affected by nitrogen form and pH control in solution culture. *Fertilizer Research*, *21*(1), 1-6.

Marino, D., Ariz, I., Lasa, B., Santamaría, E., Fernández-Irigoyen, J., González-Murua, C., and Aparicio Tejo, P. M. (2016). Quantitative proteomics reveals the importance of nitrogen source to control glucosinolate metabolism in *Arabidopsis thaliana* and *Brassica oleracea*. *Journal of experimental botany*, *67*(11), 3313-3323.

Marschner, H. (2012). Marschner's mineral nutrition of higher plants. Vol. 89.Academic Press.

Masumoto, C., Miyazawa, S. I., Ohkawa, H., Fukuda, T., Taniguchi, Y., Murayama, S., Kusano, M., Saito, K., Fukuyama, H., and Miyao, M. (2010). Phosphoenolpyruvate carboxylase intrinsically located in the chloroplast of rice plays a crucial role in ammonium assimilation. *Proceedings of the National Academy of Sciences*, *107*(11), 5226-5231.

Matos, D. A., Whitney, I. P., Harrington, M. J., and Hazen, S. P. (2013). Cell walls and the developmental anatomy of the *Brachypodiumdistachyon* stem internode. *PLoS One*, *8*(11), e80640.

Matsuda, F., Nakabayashi, R., Yang, Z., Okazaki, Y., Yonemaru, J. I., Ebana, K., Yano, M., and Saito, K. (2015). Metabolome-genome-wide association study dissects genetic architecture for generating natural variation in rice secondary metabolism. *The Plant Journal*, *81*(1), 13-23.

Medici, A., Marshall-Colon, A., Ronzier, E., Szponarski, W., Wang, R., Gojon, A., Crawford, N. M., Ruffel, S., Coruzzi, G. M., and Krouk, G. (2015). AtNIGT1/HRS1 integrates nitrate and phosphate signals at the Arabidopsis root tip. *Nature communications*, *6*, 6274.

Mengel, K., and Geurtzen, G. (1988). Relationship between iron chlorosis and alkalinity in *Zea mays*. *PhysiologiaPlantarum*, *72*(3), 460-465.

Menz, J., Li, Z., Schulze, W. X., and Ludewig, U. (2016). Early nitrogen-deprivation responses in Arabidopsis roots reveal distinct differences on transcriptome and (phospho-) proteome levels between nitrate and ammonium nutrition. *The Plant Journal*, *88*(5), 717-734.

Miao, C., Yang, J., and Schnable, J. C. (2019). Optimising the identification of causal variants across varying genetic architectures in crops. *Plant biotechnology journal*, *17*(5), 893-905.

Miflin, B. J., and Lea, P. J. (1977). The pathway of nitrogen assimilation in plants. *Progress in phytochemistry*, *4*, 1-26.

Míka, V., Kuban, V., Klejdus, B., Odstrcilová, V., and Nerusil, P. (2005). Phenolic compounds as chemical markers of low taxonomic levels in the family Poaceae. *Plant Soil and Environment*, *51*(11), 506.

Miller, A. J., and Cramer, M. D. (2005). Root nitrogen acquisition and assimilation. In *Root physiology: from gene to function* (pp. 1-36). Springer, Dordrecht.

Miranda, R. D. S., Gomes-Filho, E., Prisco, J. T., and Alvarez-Pizarro, J. C. (2016). Ammonium improves tolerance to salinity stress in *Sorghum bicolor* plants. *Plant growth regulation*, *78*(1), 121-131.

Miranda, R. D. S., Mesquita, R. O., Costa, J. H., Alvarez-Pizarro, J. C., Prisco, J. T., and Gomes-Filho, E. (2017). Integrative control between proton pumps and SOS1 antiporters in roots is crucial for maintaining low Na^+ accumulation and salt tolerance in ammonium-supplied *Sorghum bicolor*. *Plant and Cell Physiology*, *58*(3), 522-536.

Monselise, E. B. I., and Kost, D. (1993). Different ammonium-ion uptake, metabolism and detoxification efficiencies in two Lemnaceae. *Planta*, *189*(2), 167-173.

Montaez, C. A. C., Fergus, P., Montaez, A. C., Hussain, A., Al-Jumeily, D., and Chalmers, C. (2018, July). Deep learning classification of polygenic obesity using genome wide association study SNPs. In *2018 International Joint Conference on Neural Networks (IJCNN)* (pp. 1-8). IEEE.

Navarro, J. A. R., Willcox, M., Burgueño, J., Romay, C., Swarts, K., Trachsel, S., Preciado, E., Terron, A., Delgado, H. V., Vidal, V., Ortega, A., Banda, A. E., Montiel, N. O. G., Ortiz-Monasterios, I., San Vicente, F., Espinoza, A. G., Atlin, G., Wenzl, P., Hearne, S., and Buckler E. S.

(2017). A study of allelic diversity underlying flowering-time adaptation in maize landraces. *Nature genetics*, *49*(3), 476.

Noctor, G., Mhamdi, A., Chaouch, S., Han, Y. I., Neukermans, J., Marquez-Garcia, B., Queval, G., and Foyer, C. H. (2012). Glutathione in plants: an integrated overview. *Plant, cell and environment*, *35*(2), 454-484.

Nunes-Nesi, A., Carrari, F., Gibon, Y., Sulpice, R., Lytovchenko, A., Fisahn, J., Graham, J., Ratcliffe, R. G., Sweetlove, L. J., and Fernie, A. R. (2007). Deficiency of mitochondrial fumarase activity in tomato plants impairs photosynthesis via an effect on stomatal function. *The Plant Journal*, *50*(6), 1093-1106.

Ohashi, M., Ishiyama, K., Kojima, S., Konishi, N., Nakano, K., Kanno, K., Hayakawa, T., and Yamaya, T. (2015). Asparagine synthetase1, but not asparagine synthetase2, is responsible for the biosynthesis of asparagine following the supply of ammonium to rice roots. *Plant and Cell Physiology*, *56*(4), 769-778.

Oliveira, I. C., and Coruzzi, G. M. (1999). Carbon and amino acids reciprocally modulate the expression of glutamine synthetase in *Arabidopsis*. *Plant physiology*, *121*(1), 301-310.

Onda, Y., Inoue, K., Sawada, Y., Shimizu, M., Takahagi, K., Uehara-Yamaguchi, Y., Hirai, M. Y., Garvin, D. F., and Mochida, K. (2019). Genetic Variation for Seed Metabolite Levels in *Brachypodium distachyon*. *International journal of molecular sciences*, *20*(9), 2348.

Paramasivam, S., and Alva, A. K. (1997). Leaching of nitrogen forms from controlled-release nitrogen fertilizers. *Communications in Soil Science and Plant Analysis*, *28*(17-18), 1663-1674.

Patterson, K., Cakmak, T., Cooper, A., Lager, I. D. A., Rasmusson, A. G., and Escobar, M. A. (2010). Distinct signalling pathways and transcriptome response signatures differentiate ammonium- and nitrate-supplied plants. *Plant, cell and environment*, *33*(9), 1486-1501.

Pelloux, J., Rusterucci, C., andMellerowicz, E. J. (2007). New insights into pectin methylesterase structure and function. *Trends in plant science*, *12*(6), 267-277.

Perea-García, A., Garcia-Molina, A., Andrés-Colás, N., Vera-Sirera, F., Pérez-Amador, M. A., Puig, S., and Peñarrubia, L. (2013). Arabidopsis copper transport protein COPT2 participates in the cross talk between iron deficiency responses and low-phosphate signaling. *Plant Physiology*, *162*(1), 180-194.

Pezeshki, S., and Petersen, M. (2018). Rosmarinic acid and related metabolites. In *Biotechnology of Natural Products* (pp. 25-60). Springer, Cham.

Podgorska, A., Gieczewska, K., Łukawska-Kuzma, K., Rasmusson, A. G., Gardeström, P., and SZAL, B. (2013). Long-term ammonium nutrition of *Arabidopsis* increases the extrachloroplastic NAD (P) H/NAD $(P)^+$ ratio and mitochondrial reactive oxygen species level in leaves but does not impair photosynthetic capacity. *Plant, cell and environment*, *36*(11), 2034-2045.

Podgórska, A., Burian, M., Gieczewska, K., Ostaszewska-Bugajska, M., Zebrowski, J., Solecka, D., and Szal, B. (2017a). Altered cell wall plasticity can restrict plant growth under ammonium nutrition. *Frontiers in plant science*, *8*, 1344.

Podgórska, A., Burian, M., Rychter, A. M., Rasmusson, A. G., and Szal, B. (2017b). Short-term ammonium supply induces cellular defence to prevent oxidative stress in *Arabidopsis* leaves. *Physiologiaplantarum*, *160*(1), 65-83.

Poiré, R., Chochois, V., Sirault, X. R., Vogel, J. P., Watt, M., and Furbank, R. T. (2014). Digital imaging approaches for phenotyping whole plant nitrogen and phosphorus response in *Brachypodium distachyon*. *Journal of integrative plant biology*, *56*(8), 781-796.

Prinsi, B., and Espen, L. (2018). Time-course of metabolic and proteomic responses to different nitrate/ammonium availabilities in roots and leaves of maize. *International journal of molecular sciences*, *19*(8), 2202.

Raun, W. R., and Johnson, G. V. (1999). Improving nitrogen use efficiency for cereal production. *Agronomy journal*, *91*(3), 357-363.

Rauh, B., Basten, C., and Buckler, E. (2002). Quantitative trait loci analysis of growth response to varying nitrogen sources in *Arabidopsis thaliana*. *Theoretical and Applied Genetics*, *104*(5), 743-750.

Raven, J. A. (1986). Biochemical disposal of excess H^+ in growing plants?. *New Phytologist*, *104*(2), 175-206.

Ricachenevsky, F. K., and Sperotto, R. A. (2014). There and back again, or always there? The evolution of rice combined strategy for Fe uptake. *Frontiers in plant science*, *5*, 189.

Rigaud, J., and Puppo, A. (1975). Indole-3-acetic acid catabolism by soybean bacteroids. *Microbiology*, *88*(2), 223-228.

Robinson, S. A., Slade, A. P., Fox, G. G., Phillips, R., Ratcliffe, R. G., and Stewart, G. R. (1991). The role of glutamate dehydrogenase in plant nitrogen metabolism. *Plant physiology*, *95*(2), 509-516.

Robertson, G. P., and Vitousek, P. M. (2009). Nitrogen in agriculture: balancing the cost of an essential resource. *Annual review of environment and resources*, *34*, 97-125.

Roosta, H. R., and Schjoerring, J. K. (2007). Effects of ammonium toxicity on nitrogen metabolism and elemental profile of cucumber plants. *Journal of Plant Nutrition*, *30*(11), 1933-1951.

Roosta, H. R., and Schjoerring, J. K. (2008). Root carbon enrichment alleviates ammonium toxicity in cucumber plants. *Journal of Plant Nutrition*, *31*(5), 941-958.

Rosas, U., Cibrian-Jaramillo, A., Ristova, D., Banta, J. A., Gifford, M. L., Fan, A. H., Zhou, R. W., Kim, G. J., Krouk, G., Birnbaum., K. D., Purugganan, M. D., and Coruzzi, G. M. (2013). Integration of responses within and across Arabidopsis natural accessions uncovers loci controlling root systems architecture. *Proceedings of the National Academy of Sciences*, *110*(37), 15133-15138.

Royo, B., Esteban, R., Buezo, J., Santamaría, E., Fernández-Irigoyen, J., Becker, D., and Moran, J. F. (2019). The proteome of *Medicagotruncatula* in response to ammonium and urea nutrition reveals the role of membrane proteins and enzymes of root lignification. *Environmental and Experimental Botany*, *162*, 168-180.

Ruser, R., and Schulz, R. (2015). The effect of nitrification inhibitors on the nitrous oxide (N_2O) release from agricultural soils—a review. Journal of Plant Nutrition and Soil Science, 178(2), 171-188.

Sánchez-Vallet, A., Hartmann, F. E., Marcel, T. C., and Croll, D. (2018). Nature's genetic screens: using genome-wide association studies for effector discovery. *Molecular plant pathology*, *19*(1), 3-6.

Sasaki, K., and Kojima, S. (2018). Identification of genomic regions regulating ammonium-dependent inhibition of primary root length in *Arabidopsis thaliana*. *Soil science and plant nutrition*, *64*(6), 746-751.

Sarasketa, A., González-Moro, M. B., González-Murua, C., and Marino, D. (2014). Exploring ammonium tolerance in a large panel of *Arabidopsis thaliana* natural accessions. *Journal of experimental botany*, *65*(20), 6023-6033.

Sarasketa, A., González-Moro, M. B., González-Murua, C., and Marino, D. (2016). Nitrogen source and external medium pH interaction differentially affects root and shoot metabolism in *Arabidopsis*. *Frontiers in plant science*, *7*, 29.

Sauter, M., Moffatt, B., Saechao, M. C., Hell, R., and Wirtz, M. (2013). Methionine salvage and S-adenosylmethionine: essential links between sulfur, ethylene and polyamine biosynthesis. *Biochemical Journal*, *451*(2), 145-154.

Scholthof, K. B. G., Irigoyen, S., Catalan, P., and Mandadi, K. K. (2018). *Brachypodium*: a monocot grass model genus for plant biology. *The Plant Cell*, *30*(8), 1673-1694.

Schortemeyer, M., Stamp, P., and Feil, B. O. Y. (1997). Ammonium tolerance and carbohydrate status in maize cultivars. *Annals of Botany*, *79*(1), 25-30.

Schubert, S., and Yan, F. (1997). Nitrate and ammonium nutrition of plants: effects on acid/base balance and adaptation of root cell plasmalemma H^+ ATPase. *ZeitschriftfürPflanzenernährung und Bodenkunde*, *160*(2), 275-281.

Serna, M. D., Borras, R., Legaz, F., and Primo-Millo, E. (1992). The influence of nitrogen concentration and ammonium/nitrate ratio on N-uptake, mineral composition and yield of citrus. *Plant and Soil*, *147*(1), 13-23.

Setién, I., Fuertes-Mendizabal, T., González, A., Aparicio-Tejo, P. M., González-Murua, C., González-Moro, M. B., and Estavillo, J. M. (2013). High irradiance improves ammonium tolerance in wheat plants by increasing N assimilation. *Journal of Plant Physiology*, *170*(8), 758-771.

Setién, I., Vega-Mas, I., Celestino, N., Calleja-Cervantes, M. E., González-Murua, C., Estavillo, J. M., and González-Moro, M. B. (2014). Root phosphoenolpyruvate carboxylase and NAD-malic enzymes activity increase the ammonium-assimilating capacity in tomato. *Journal of plant physiology*, *171*(5), 49-63.

Shaw, R. G., and Geyer, C. J. (2010). Inferring fitness landscapes. *Evolution: International Journal of Organic Evolution*, *64*(9), 2510-2520.

Shi, J., Yi, K., Liu, Y., Xie, L., Zhou, Z., Chen, Y., ...and Chen, J. (2015). Phosphoenolpyruvate carboxylase in Arabidopsis leaves plays a crucial role in carbon and nitrogen metabolism. *Plant physiology*, *167*(3), 671-681.

Shi, Y., Wang, Z., Meng, P., Tian, S., Zhang, X., and Yang, S. (2013). The glutamate carboxypeptidase AMP 1 mediates abscisic acid and abiotic stress responses in Arabidopsis. *New Phytologist*, *199*(1), 135-150.

Shi, J., Yi, K., Liu, Y., Xie, L., Zhou, Z., Chen, Y., Hu, Z., Zheng, T., Liu, R., Chen, Y., and Chen, J. (2015). Phosphoenolpyruvate carboxylase in *Arabidopsis* leaves plays a crucial role in carbon and nitrogen metabolism. *Plant physiology*, *167*(3), 671-681.

Sigurdarson, J. J., Svane, S., and Karring, H. (2018). The molecular processes of urea hydrolysis in relation to ammonia emissions from agriculture. *Reviews in Environmental Science and Bio/Technology*, *17*(2), 241-258.

Siqueira-Silva, A. I., Rios, C. O., and Pereira, E. G. (2019). Iron toxicity resistance strategies in tropical grasses: The role of apoplastic radicular barriers. *Journal of Environmental Sciences*, *78*, 257-266.

Skopelitis, D. S., Paranychianakis, N. V., Paschalidis, K. A., Pliakonis, E. D., Delis, I. D., Yakoumakis, D. I., Kouvarakis, A., Papadakis, A. K., Stephanou, E. G., and Roubelakis-Angelakis, K. A. (2006). Abiotic stress generates ROS that signal expression of anionic glutamate dehydrogenases to form glutamate for proline synthesis in tobacco and grapevine. *The Plant Cell*, *18*(10), 2767-2781.

Soltabayeva, A., Srivastava, S., Kurmanbayeva, A., Bekturova, A., Fluhr, R., and Sagi, M. (2018). Early senescence in older leaves of low nitrate-grown Atxdh1 uncovers a role for purine catabolism in N supply. *Plant physiology*, *178*(3), 1027-1044.

Swarbreck, S. M., Defoin-Platel, M., Hindle, M., Saqi, M., and Habash, D. Z. (2010). New perspectives on glutamine synthetase in grasses. *Journal of Experimental Botany*, *62*(4), 1511-1522.

Swarbreck, S. M., Wang, M., Wang, Y., Kindred, D., Sylvester-Bradley, R., Shi, W., Singh, V., Bentley, A. R., and Griffiths, H. (2019). A Roadmap for Lowering Crop Nitrogen Requirement. *Trends in plant science*.

Sweetlove, L. J., Beard, K. F., Nunes-Nesi, A., Fernie, A. R., andRatcliffe, R. G. (2010). Not just a circle: flux modes in the plant TCA cycle. *Trends in plant science*, *15*(8), 462-470.

Takizawa, K., and Nakamura, H. (1998). Separation and determination of fluorescein isothiocyanate-labeled amino acids by capillary electrophoresis with laser-induced fluorescence detection. *Analytical sciences*, 14, 925-928.

Taiz, L. (2013). Agriculture, plant physiology, and human population growth: past, present, and future. *Theoretical and Experimental Plant Physiology*, *25*(3), 167-181.

Tcherkez, G., Cornic, G., Bligny, R., Gout, E., and Ghashghaie, J. (2005). In vivo respiratory metabolism of illuminated leaves. *Plant Physiology*, *138*(3), 1596-1606.

Tenhaken, R. (2015). Cell wall remodeling under abiotic stress. *Frontiers in plant science*, *5*, 771.

Thomson, C. J., Marschner, H., and Römheld, V. (1993). Effect of nitrogen fertilizer form on pH of the bulk soil and rhizosphere, and on the growth, phosphorus, and micronutrient uptake of bean. *Journal of Plant Nutrition*, *16*(3), 493-506.

Touraine, B., Daniel-Vedele, F., and Forde, B. G. (2001). Nitrate uptake and its regulation. In *Plant nitrogen* (pp. 1-36). Springer, Berlin, Heidelberg.

Tschoep, H., Gibon, Y., Carillo, P., Armengaud, P., Szecowka, M., Nunes-Nesi, A., Fernie, A. R., Koehl, K., and Stitt, M. (2009). Adjustment of growth and central metabolism to a mild but sustained nitrogen-limitation in *Arabidopsis*. *Plant, cell and environment*, *32*(3), 300-318.

Tyanova, S., Temu, T., Sinitcyn, P., Carlson, A., Hein, M. Y., Geiger, T., Mann, M., and Cox, J. (2016). The Perseus computational platform for comprehensive analysis of (prote) omics data. *Nature methods*, *13*(9), 731.

Tyler, L., Lee, S. J., Young, N. D., Delulio, G. A., Benavente, E., Reagon, M., Sysopha J, Baldini RM, Troìa A, Hazen SP, and Caicedo, A. L. (2016). Population structure in the model grass *Brachypodiumdistachyon* is highly correlated with flowering differences across broad geographic areas. *The plant genome*, *9*(2).

Uauy, C., Distelfeld, A., Fahima, T., Blechl, A., and Dubcovsky, J. (2006). A NAC gene regulating senescence improves grain protein, zinc, and iron content in wheat. *Science*, *314*(5803), 1298-1301.

Van Beusichem, M. L., Kirkby, E. A., and Baas, R. (1988). Influence of nitrate and ammonium nutrition on the uptake, assimilation, and distribution of nutrients in *Ricinuscommunis*. *Plant Physiology*, *86*(3), 914-921.

VanRaden, P. M. (2008). Efficient methods to compute genomic predictions. *Journal of dairy science*, *91*(11), 4414-4423.

Vega-Mas, I., Marino, D., Sanchez-Zabala, J., Gonzalez-Murua, C., Estavillo, J. M., and González-Moro, M. B. (2015). CO_2 enrichment modulates ammonium nutrition in tomato adjusting carbon and nitrogen metabolism to stomatal conductance. *Plant Science*, *241*, 32-44.

Vega-Mas, I., Pérez-Delgado, C. M., Marino, D., Fuertes-Mendizábal, T., González-Murua, C., Márquez, A. J., Betti, M., Estavillo, J. M., and González-Moro, M. B. (2017). Elevated CO_2 induces root defensive mechanisms in tomato plants when dealing with ammonium toxicity. *Plant and Cell Physiology*, *58*(12), 2112-2125.

Vega-Mas, I., Cukier, C., Coleto, I., González-Murua, C., Limami, A. M., González-Moro, M. B., and Marino, D. (2019a). Isotopic labelling reveals the efficient adaptation of wheat root TCA cycle flux modes to match carbon demand under ammonium nutrition. *Scientific Reports*, *9*(1), 8925.

Vega-Mas, I., Rossi, M. T., Gupta, K. J., González-Murua, C., Ratcliffe, R. G., Estavillo, J. M., and González-Moro, M. B. (2019b). Tomato roots exhibit in vivo glutamate dehydrogenase aminating capacity in response to excess ammonium supply. *Journal of plant physiology*.

Vessey, J. K., Pawlowski, K., and Bergman, B. (2005). Root-based N 2-fixing symbioses: legumes, actinorhizal plants, *Parasponia* sp. and cycads. In *Root physiology: from gene to function* (pp. 51-78). Springer, Dordrecht.

Vogel, J. P. (Ed.). (2016). *Genetics and genomics of Brachypodium* (Vol. 18). Springer.

Vogel, J. P., Tuna, M., Budak, H., Huo, N., Gu, Y. Q., and Steinwand, M. A. (2009). Development of SSR markers and analysis of diversity in Turkish populations of *Brachypodium distachyon*. *BMC plant biology*, *9*(1), 88.

Wang, M. Y., Siddiqi, M. Y., Ruth, T. J., and Glass, A. D. (1993). Ammonium uptake by rice roots (II. Kinetics of $13NH_4^+$ influx across the plasmalemma). *Plant physiology*, *103*(4), 1259-1267.

Wang, Z. Q., Yuan, Y. Z., Ou, J. Q., Lin, Q. H., and Zhang, C. F. (2007). Glutamine synthetase and glutamate dehydrogenase contribute differentially to proline accumulation in leaves of wheat (*Triticum aestivum*) seedlings exposed to different salinity. *Journal of Plant Physiology*, *164*(6), 695-701.

Wang, M., Yan, J., Zhao, J., Song, W., Zhang, X., Xiao, Y., and Zheng, Y. (2012). Genome-wide association study (GWAS) of resistance to head smut in maize. *Plant science*, *196*, 125-131.

Wang, F., Gao, J., Liu, Y., Tian, Z., Muhammad, A., Zhang, Y., Jiang, D., Cao, W., and Dai, T. (2016a). Higher ammonium transamination capacity can alleviate glutamate inhibition on winter wheat (*Triticumaestivum* L.) root growth under high ammonium stress. *PloS one*, *11*(8), e0160997.

Wang, F., Gao, J., Tian, Z., Liu, Y., Abid, M., Jiang, D., Cao, W., and Dai, T. (2016b). Adaptation to rhizosphere acidification is a necessary prerequisite for wheat (*Triticumaestivum* L.) seedling resistance to ammonium stress. *Plant Physiology and Biochemistry*, *108*, 447-455.

Watanabe, A., Takagi, N., Hayashi, H., Chino, M., and Watanabe, A. (1997). Internal Gln/Glu ratio as a potential regulatory parameter for the expression of a cytosolic glutamine synthetase gene of radish in cultured cells. *Plant and cell physiology*, *38*(9), 1000-1026.

Wen, W., Li, D., Li, X., Gao, Y., Li, W., Li, H., Liu, J., Chen, W., Luo, J., and Yan, J. (2014). Metabolome-based genome-wide association study of maize kernel leads to novel biochemical insights. *Nature communications*, *5*, 3438.

Werner, A. K., Romeis, T., and Witte, C. P. (2010). Ureide catabolism in *Arabidopsis thaliana* and Escherichia coli. *Nature chemical biology*, *6*(1), 19.

Wilson, P. B., Streich, J. C., Murray, K. D., Eichten, S. R., Cheng, R., Aitkin, N. C., Spokas, K., Warthmann, N., and Borevitz, J. O. (2018). Population structure of the Brachypodium species complex and genome wide association of agronomic traits in response to climate. BioRxiv, 246074.

Xiao, C. N., and Wang, Y. (2015). NMR-Based Metabolomic Methods and Applications. In *Plant metabolomics* (pp. 275-301). Springer, Dordrecht.

Xu, G., Fan, X., and Miller, A. J. (2012). Plant nitrogen assimilation and use efficiency. *Annual review of plant biology*, *63*, 153-182.

Xuan, Y. H., Priatama, R. A., Huang, J., Je, B. I., Liu, J. M., Park, S. J., Piao, H. L., Son, D. Y., Lee, J. J., Park, S. H., Jung, K. H., Kim, T. H., Han, C., and Jung, K. H. (2013). *Indeterminate domain* 10 regulates ammonium-mediated gene expression in rice roots. *New Phytologist*, *197*(3), 791-804.

Yan, J., Su, P., Li, W., Xiao, G., Zhao, Y., Ma, X., Wang H., Nevo, E., and Kong, L. (2019). Genome-wide and evolutionary analysis of the class III peroxidase gene family in wheat and *Aegilopstauschii* reveals that some members are involved in stress responses. *BMC genomics*, *20*(1), 1-19.

Yano, K., Yamamoto, E., Aya, K., Takeuchi, H., Lo, P. C., Hu, L., Yamasaki, M., Yashida, S., Kitano, H., Hirano, K., and Matsuoka, M. (2016). Genome-wide association study using whole-genome sequencing rapidly identifies new genes influencing agronomic traits in rice. *Nature genetics*, *48*(8), 927.

Yordem, B. K., Conte, S. S., Ma, J. F., Yokosho, K., Vasques, K. A., Gopalsamy, S. N., and Walker, E. L. (2011). *Brachypodium distachyon* as a new model system for understanding iron homeostasis in grasses: phylogenetic and expression analysis of Yellow Stripe-Like (YSL) transporters. *Annals of botany*, *108*(5), 821-833.

Yoshino, M., and Murakami, K. (1980). AMP deaminase from spinach leaves purification and some regulatory properties. *ZeitschriftfürPflanzenphysiologie*, *99*(4), 331-338.

Zhang, Y., Lin, X., Zhang, Y., Zheng, S. J., and Du, S. (2005). Effects of nitrogen levels and nitrate/ammonium ratios on oxalate concentrations of different forms in edible parts of spinach. *Journal of Plant Nutrition*, *28*(11), 2011-2025.

Zhu, C. Q., Zhu, X. F., Hu, A. Y., Wang, C., Wang, B., Dong, X. Y., and Shen, R. F. (2016). Differential effects of nitrogen forms on cell wall phosphorus remobilization are mediated by nitric oxide, pectin content, and phosphate transporter expression. *Plant Physiology*, *171*(2), 1407-1417.

Zhu, C. Q., Zhang, J. H., Zhu, L. F., Abliz, B., Zhong, C., Bai, Z. G., Hu, W. J., Sajid, H., James, A. B., Cao, X. C., and Jin, Q. Y. (2018). NH_4^+ facilitates iron reutilization in the cell walls of rice (*Oryza sativa*) roots under iron-deficiency conditions. *Environmental and Experimental Botany*, *151*, 21-31.

Zhu, X. F., Dong, X. Y., Wu, Q., and Shen, R. F. (2019). Ammonium regulates Fe deficiency responses by enhancing nitric oxide signaling in *Arabidopsis thaliana*. *Planta*, 1-14.

Zou, C., Shen, J., Zhang, F., Guo, S., Rengel, Z., and Tang, C. (2001). Impact of nitrogen form on iron uptake and distribution in maize seedlings in solution culture. *Plant and soil*, *235*(2), 143-149.